Rational Design and Discovery of Natural Product-Inspired Chemical Entities Active against Multi-Faceted Inflammatory Targets

by

SANGEETHA MOHAN

10CC19J39004

A thesis submitted to the
Academy of Scientific and Innovative Research
for the award of the degree of
DOCTOR OF PHILOSOPHY
in
SCIENCE

Under the supervision of
Dr. Sasidhar B. S.

CSIR-National Institute for Interdisciplinary Science and Technology (NIIST), Thiruvananthapuram – 695 019

Academy of Scientific and Innovative Research
AcSIR Headquarters, CSIR-HRDC Campus
Sector 19, Kamla Nehru Nagar,
Ghaziabad, U.P. – 201 002, India

January 2025

राष्ट्रीय अंतर्विषयी विज्ञान तथा प्रौद्योगिकी संस्थान
वैज्ञानिक तथा औद्योगिक अनुसंधान परिषद् | विज्ञान तथा प्रौद्योगिकी मंत्रालय, भारत सरकार
इंडस्ट्रियल इस्टेट पी.ओ., पाप्पनंकोड, तिरुवनंतपुरम, भारत-695 019

CSIR-NATIONAL INSTITUTE FOR INTERDISCIPLINARY SCIENCE AND TECHNOLOGY (CSIR-NIIST)
Council of Scientific & Industrial Research | Ministry of Science and Technology, Govt. of India
Industrial Estate P.O., Pappanamcode, Thiruvananthapuram, India-695 019

Dr. Sasidhar B. S.
Principal Scientist & Associate Professor (AcSIR)
Chemical Sciences &Technology Division

Email: drsasidharbs@niist.res.in
Mobile: 9497260897

January 6th, 2025
Thiruvananthapuram

CERTIFICATE

This is to certify that the work incorporated in this Ph.D. thesis entitled, **"Rational Design and Discovery of Natural Product-Inspired Chemical Entities Active against Multi-Faceted Inflammatory Targets",** submitted by ***Ms. Sangeetha Mohan,*** to the Academy of Scientific and Innovative Research (AcSIR) in fulfilment of the requirements for the award of the Degree of ***Doctor of Philosophy in Science***, embodies original research work carried out by the student. We further certify that this work has not been submitted to any other University or Institution in part or full for the award of any degree or diploma. Research materials obtained from other sources and used in this research work has been duly acknowledged in the thesis. Images, illustrations, figures, tables etc., used in the thesis from other sources, have also been duly cited and acknowledged.

06/01/2025

Sangeetha Mohan

06/01/2025

Dr. Sasidhar B. S.
(Thesis Supervisor)

Tel : 91 471 2515226 | 2515234 | E-mail : director@niist.res.in | Website : http://niist.res.in

STATEMENTS OF ACADEMIC INTEGRITY

I, **Sangeetha Mohan**, a Ph.D. student of the Academy of Scientific and Innovative Research (AcSIR) with Registration No. 10CC19J39004 hereby undertake that, the thesis entitled **"Rational Design and Discovery of Natural Product-Inspired Chemical Entities Active against Multi-Faceted Inflammatory Targets"** has been prepared by me and that the document reports original work carried out by me and is free of any plagiarism in compliance with the UGC Regulations on *"Promotion of Academic Integrity and Prevention of Plagiarism in Higher Educational Institutions (2018)"* and the CSIR Guidelines for "*Ethics in Research and in Governance (2020)*".

6/01/2025

Sangeetha Mohan

January 6th, 2025
Thiruvananthapuram

It is hereby certified that the work done by the student, under my supervision, is plagiarism-free in accordance with the UGC Regulations on *"Promotion of Academic Integrity and Prevention of Plagiarism in Higher Educational Institutions (2018)"* and the CSIR Guidelines for "*Ethics in Research and in Governance (2020)*".

6/1/2025

Dr. Sasidhar B. S.

January 6th, 2025
Thiruvananthapuram

Acknowledgement

I extend my deepest gratitude to my research supervisor, Dr. Sasidhar B. S., for introducing me to this fascinating research field. His invaluable advice, unwavering patience, constant encouragement, and steadfast support have been instrumental throughout my research journey, culminating in the successful completion of this work. I am also sincerely thankful for the positive research environment he fostered, which, along with the essential facilities provided, greatly facilitated my progress.

I offer my sincere thanks to Dr. C. Anandharamakrishnan, Director, and Dr. A. Ajayaghosh, former Director of the CSIR-National Institute for Interdisciplinary Science and Technology (CSIR-NIIST), for providing the necessary facilities for carrying out this research.

I would like to express my deep sense of gratitude to Dr. Jayamurthy P. of the Agro-Processing and Technology Division (APTD), CSIR-NIIST, and Dr. Lekshmy Krishnan of the Chemical Sciences and Technology Division (CSTD), CSIR-NIIST, for their immense contributions to the biological aspects of my work. Their input was pivotal in shaping my thesis, and without them, this work would not have been complete.

My sincere gratitude goes to Dr. Naveen Vankadari, University of Melbourne, Australia, for his collaboration on the in silico work, which greatly influenced the direction of my thesis.

I would like to thank Dr. K. V. Radhakrishnan, Dr. P. Sujatha Devi, and Dr. R. Luxmi Varma, present and former Heads of the Chemical Sciences and Technology Division, for their consistent support and guidance.

I am deeply thankful to my Doctoral Advisory Committee (DAC) members—Dr. Jayamurthy P., Dr. A. Kumaran, Dr. Priya S., and Dr. Sridevi D.—for their invaluable help, suggestions, and encouragement throughout my Ph.D. journey.

I am grateful to Dr. Jayamurthy P., Dr. Karunakaran Venugopal, Dr. Suresh C. H., and Dr. Luxmi Varma, current and former AcSIR programme coordinators at CSIR-NIIST, for their support, guidance, and assistance in navigating all the academic procedures of AcSIR.

I would like to express my gratitude to Mrs. Saumini Mathew and Mrs. S. Viji for their prompt assistance and support in recording NMR spectra and conducting mass spectral analyses. I also thank Mr. Merin Santhosh and Ms. Aswathy C. Sreekumar for their assistance concerning the AcSIR programme.

I am extremely grateful to my seniors—Dr. Renjitha J., Dr. Ashitha K. T., Dr. Praveen Valmiki, and Dr. Basavaraja—for their valuable suggestions, constant help, support, and encouragement during my thesis work. I would also like to thank my lab mates—Mr. Mohan B., Mr. Ajay Krishna M. S., Ms. Athira C. S., Ms. Anjali S., Ms. Nithya M., Mr. Siddalingeshwar, Ms. Aiswarya, Ms. Sreelakshmi, Ms. Geethu Venugopal, Ms. Geethu, Mr. Lalshikanther Basha, Dr. Alan Sheeja D. B., Ms. Ancy, Mr. Michael, and Mr. Abraham—for their generous help, great support, care, and companionship. I am thankful to Ms. Keerthana and Ms. Sneha, M.Sc. project students, for their contributions to my thesis work.

My heartfelt appreciation goes to my wonderful room-mates, Ms. Ramees Jebin, Dr. Anjali Krishna P. K. and Ms. Athira C. S., who have been a constant source of support and companionship throughout our time together. A special thank you goes to Ms. Priyanka for the warmth and companionship she has shared with me throughout this journey.

I sincerely appreciate all my friends, along with the scientific and non-scientific personnel at CSIR-NIIST. I would like to express special thanks to the staff and students of the Chemical Sciences and Technology Division (CSTD).

I would like to offer my special thanks and appreciation to all my teachers for their help and blessings, especially Dr. Geetha Nazareth of St. Agnes College, Mangalore, for her continued support and encouragement.

I am forever indebted to my beloved parents, Mr. Mohanan A.C. and Mrs. Sreeja Mohan, and my brother, Mr. Anand Mohan, whose unyielding love, blessings, and constant support have been the foundation of my life. Their sacrifices and encouragement have been the cornerstone of my strength, equipping me with the determination and resilience needed to tackle any challenge and making it possible for me to reach this point. I also sincerely thank my partner, Mr. Nikhil Raj V., whose love, compassion, and relentless belief in me have consistently provided strength and inspiration. He has been a support system, helping me navigate tough times and motivating me to keep going. Collectively, my family has guided my path and made this achievement possible.

Finally, I sincerely thank the University Grants Commission (UGC), Government of India, for their financial assistance.

Above all, I bow before the Almighty for all the blessings.

Sangeetha Mohan

Contents

List of Figures

List of Schemes

List of Tables

List of Abbreviations

μg	:	Microgram
μL	:	Microlitre
μM	:	Micromolar
^{13}C NMR	:	Carbon-13 nuclear magnetic resonance
^{1}H NMR	:	Proton nuclear magnetic resonance
2D	:	Two dimensional
ALI	:	Acute lung injury
APCs	:	Antigen-presenting cells
ADME	:	Absorption, distribution, metabolism, and excretion
BSA	:	Bovine serum albumin
CON	:	Control
COPD	:	Chronic obstructive pulmonary disease
COX-1	:	Cyclooxygenase-1
COX-2	:	Cyclooxygenase-2
CFDA	:	Chinese Food and Drug Administration
CTLs	:	Cytotoxic T lymphocytes
CSA	:	Cajaninstilbene acid
CDCL3	:	Deuterated chloroform
$CuSO_4.5H_2O$	:	Copper sulfate penta hydrate
CuAAC	:	Copper-catalyzed azide–alkyne cycloaddition
CuI	:	Copper iodide
d	:	Doublet
dd	:	Doublet of doublet
DEPT-135	:	Distortionless Enhancement of Polarization Transfer
DMEM	:	Dulbecco's modified eagle medium
DMF	:	Dimethylformamide
DCM (CH_2Cl_2)	:	Dichloromethane
dsDNA	:	Double stranded DNA
eNOS	:	Neuronal Nitric Oxide Synthases
Equiv.	:	Equivalent

ELISA	:	Enzyme-linked immunosorbent assay
EGCG	:	Epigallocatechin-3-gallate
ESI	:	Electrospray ionization
FDA	:	Food and drug administration
g	:	Gram
hNF-kB	:	NF-Kb homodimer
HCl	:	Hydrochoric acid
		Hertz
HRMS	:	High resolution mass spectrometry
h	:	Hours
IBD	:	Inflammatory bowel disease
IκB	:	Inhibitor of nfκb
IKK	:	Iκb kinase
IL	:	Interleukin
IC_{50}	:	Half maximal inhibitory concentration
iNOS	:	Inducible nitric oxide synthase
IND	:	Indomethacin
IFN-γ	:	Interferon-gamma
J	:	Coupling constant
kCal	:	Kilocalorie
kDa	:	Kilodalton
K_2CO_3	:	Potassium carbonate
LD	:	Labdane dialdehyde
LPS	:	Lipopolysaccharide
LOX	:	Lipoxygenase
m	:	Multiplet
mg	:	Milligram
min	:	Minutes
ml	:	Millilitre
MCP-1	:	Macrophage chemoattractant protein-1
mCRPC	:	Metastatic castration-resistant prostate cancer
MHz	:	Mega hertz

MTT	:	3-[4,5-dimethylthiazol-2-yl]-2,5-diphenyl tetrazolium bromide
MHC	:	Major histocompatibility complex
MAPK	:	Mitogen-activated protein kinase
MCP-1	:	Monocyte chemotactic protein-1
NSAIDs	:	Non-steroidal anti-inflammatory drugs
NaH	:	Sodium hydride
NaN_3	:	Sodium azide
NaOH	:	Sodium hydroxide
Na_2SO_4	:	Sodium sulphate
NFκB	:	Nuclear factor kappa B
Nrf2	:	Nuclear factor erythroid 2-related factor 2
NMR	:	Nuclear magnetic resonance
nm	:	Nanometer
NO	:	Nitric oxide
NPs	:	Natural products
NPCEs	:	Novel phytochemical entities
NK	:	Natural killer cells
NOS	:	Nitric oxide synthases
$Pd(Ph_3P)_2Cl_2$	:	Palladium(II)bis(triphenylphosphine) dichloride
PAF	:	Platelet-activating factor
PMNs	:	Polymorphonuclear neutrophils
PBS	:	Phosphate buffered saline
PDB	:	Protein data bank
PVDF	:	Polyvinylidene difluoride
p-NF-κB	:	Phosphorylated NF-κb
PGE2	:	Prostaglandin E2
ROX	:	Rofecoxib
RASFs	:	Rheumatoid arthritis synovial fibroblasts
RHD	:	Rel homology domain
RA	:	Rheumatoid arthritis
ROS	:	Reactive oxygen species
rt	:	Room temperature

SD	:	Standard deviation
SAR	:	Structure-activity relationship
t	:	Triplet
TNF-α	:	Tumor necrosis factor-alpha
TGF-β	:	Transforming growth factor-beta (
TAK1	:	TGF-β-activated kinase 1
TLR4	:	Toll-like receptor 4
TLC	:	Thin layer chromatography
^{t}Butanol	:	Tertiary-Butanol
TEA	:	Triethylamine
TMS	:	Tetramethylsilane

Preface

Natural products continue to be a major alternative source for developing next-generation drugs. Plant-based natural products, in particular, have been well documented for their anti-inflammatory properties, due to their therapeutically potent phytoconstituents and semi-synthetic derivatives. *Curcuma amada* (mango ginger), a rhizomatous edible herb, belongs to the medicinally significant plant family called *Zingiberaceae*. Moreover, the extracts of *C. amada* rhizomes have been shown to have anti-inflammatory properties at various acute and chronic phases of inflammation. Therefore, in continuation of our dedicated efforts on medicinal chemistry activities (Drug design and discovery), in particular natural products-based, semi-synthetic modifications for therapeutically improved scaffolds, we have isolated the abundant marker compound, a labdane diterpenoid, *(E)*-labda-8(17),12-diene-15,16-dial (**1**), from the rhizomes of *C. amada*, to further explore the anti-inflammatory properties of the plant.

Inflammation is the natural immunological response of the body towards external stimuli such as microbial invasions or tissue injury. However, prolonged inflammation can lead to the pathogenesis of various inflammatory diseases such as atherosclerosis, cancer, Alzheimer's, inflammatory bowel disease, type II diabetes, etc. Steroidal drugs, though effective against inflammation, are often associated with irreversible side effects such as hypertension, osteoporosis, immunosuppression, glucose elevation, etc. Today, inflammation is mainly treated with non-steroidal anti-inflammatory drugs (NSAIDs) or anti-cytokine biologics. However, these therapies show clinical inefficacy due to their high cost and unwarranted side effects. Therefore, there is an unmet medical need to develop new, therapeutically improved and cost-effective drugs to treat inflammation and associated diseases. Semi-synthetic modification of therapeutically proven lead natural products is one of the most successful approaches to optimise its pharmacological properties and also to explore its vivid mode of action. Owing to this, our work is focused on the isolation of the abundant marker compound, a labdane diterpenoid, *(E)*-labda-8(17),12-diene-15,16-dial (**1**), from the rhizomes of *C. amada*, and has been synthetically transformed into biologically relevant heterocyclic hybrids by semi-synthesis and were evaluated for their biological potential against inflammation.

Chapter 1 delves into the concept of inflammation, its key mediators, and the urgent need for the discovery of novel anti-inflammatory agents. It underscores the value

of natural products as a source of potential therapeutic agents and the necessity of developing new compounds to address the limitations of current treatments. A major focus is semisynthesis, a versatile natural product research tool bridging the gap between initial discovery and the development of viable drugs. Through semisynthesis, natural compounds can be modified to enhance their drug-like properties and evaluate their biological efficacy. The chapter also reviews pivotal milestones in semisynthetic drug discovery, showcasing recent examples where modifications of natural products have led to the identification of new anti-inflammatory agents. Additionally, the anti-inflammatory potential of *Curcuma amada* is highlighted. The findings suggest that semisynthesis could play a crucial role in developing safer and more effective anti-inflammatory drugs, offering an innovative solution for chronic inflammatory diseases. **Chapter 2** outlines the materials and methods employed in the experiments described in the subsequent chapters.

In **Chapter 3,** we present rational designing and synthesis of novel phytochemical entities (NPCEs) through strategic linker-based molecular hybridization of aromatic or hetero-aromatic fragments with the labdane dialdehyde, isolated from the medicinally and nutritionally significant rhizomes of the plant *Curcuma amada*. One of the aldehyde groups of *(E)*-labda-8(17),12-diene-15,16-dial was selectively oxidised to give Zerumin A and was further converted to the corresponding propargyl ester by treating it with propargyl bromide. A new series of twenty-seven (27) novel aromatic/ hetero-aromatic appended analogues of labdane were synthesised by the reaction of propargyl ester with substituted aryl/hetero-aryl iodides by Sonogashira coupling. $Pd(Ph_3P)_2Cl_2$ and CuI were used as the catalyst and co-catalyst respectively, in dry DMF. All the synthesised derivatives were well characterized by IR, NMR and HRMS analyses and explored their potential towards multi-faceted inflammatory targets. Among the synthesised novel compounds, **5f** exhibited the highest anti-inflammatory potential by inhibiting the COX-2 enzyme (IC_{50} 17.67 μM), with a four-fold increased activity than the standard drug indomethacin (IC_{50} 67.16 μM). **5f** also significantly reduced the levels of LPS-induced NO, TNF-α, IL-6, and IL-1α, much better than the positive control. The *in silico* data well supported the *in vitro* studies. This infers the labdane derivative **5f** is a promising lead candidate as an anti-inflammatory agent for further exploring the therapeutic landscape.

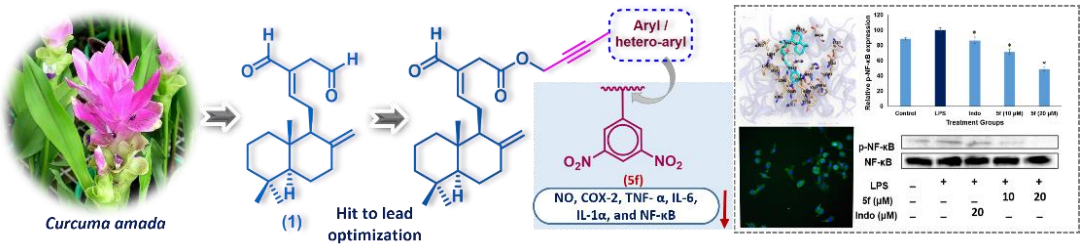

In **Chapter 4,** a ligand-based pharmacophoric approach was employed to design and synthesize thirty-three novel semi-synthetic labdane-appended triazolyl isatins to discover potential anti-inflammatory agents. The mono/di-propargylated esters of labdane dialdehyde were reacted with different isatin-azides *via* a highly regioselective CuAAC reaction to synthesize a series of thirty-three novel labdane conjugated mono/bis-triazolyl isatins. All the synthesized derivatives were evaluated for their anti-inflammatory potential. The anti-inflammatory efficacy of the derivatives was evaluated by their ability to inhibit the production of NO, TNF-α, and IL-6, in lipopolysaccharide-induced RAW264.7 macrophages. The initial screening revealed that compound **7a** ((1-(2-(2,3-dioxoindolin-1-yl)ethyl)-1H-1,2,3-triazol-4-yl)methyl (*E*)-3-formyl-5-((1S,4aS,8aS)-5,5,8a-trimethyl-2-methylenedecahydronaphthalen-1-yl)pent-3-enoate) exhibited an anti-inflammatory effect (NO inhibition, IC_{50} 3.13 μM), surpassing both the positive control indomethacin (NO inhibition, IC_{50} 7.31 μM) and the parent compound labdane dialdehyde. Notably, 7a reduced the levels of the pro-inflammatory cytokines TNF-α and IL-6, while increasing the levels of the anti-inflammatory cytokine IL-10. Mechanistic studies revealed that **7a** downregulated the expression of COX-2 and iNOS by inhibiting the NF-κB signalling pathway. *In silico* molecular modelling studies on NF-κB proteins provided insightful support for these findings, suggesting that **7a** is a promising candidate for development into a potent anti-inflammatory clinical agent.

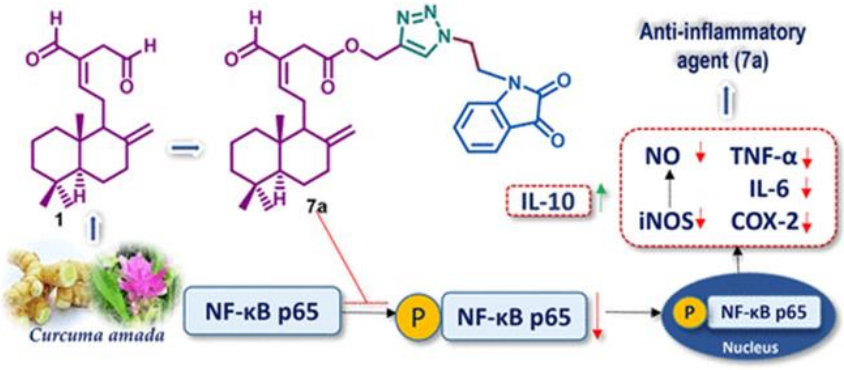

In **Chapter 5**, as part of the lead optimization process, we have modified the existing lead compound **7a** by incorporating different heterocyclic amides to the labdane template linked to heterocyclic amides of various pharmacologically active cyclic amines, to enhance the biological properties of the abundant bioactive compound. We have modified the existing lead compound **7a** by incorporating different heterocyclic amides to the labdane template. Zerumin A was reacted with chloroacetyl amides of various heterocyclic amines *via* a simple nucleophilic substitution, to give heterocyclic amide appended labdane derivatives. Triazole-incorporated labdane conjugates were obtained by the reaction of propargyl ester with various chloroacetyl azides through click chemistry. The products were confirmed by the application of spectroscopic methods and evaluated for their inflammatory potential. Among the synthesised derivatives, **9b** (NO inhibition, IC_{50} 1.46 μM) exhibited nearly 2-fold increased activity than indomethacin and the existing lead **7a** (NO inhibition, IC_{50} 3.13 μM). The levels of the pro-inflammatory cytokines TNF-α and IL-6 were reduced by **9b**, while the levels of the anti-inflammatory cytokine IL-10 increased. Studies investigating mechanisms found that **9b** reduced the expression of COX-2 and iNOS by inhibiting the NF-κB signaling pathway. Molecular modeling studies on NF-κB proteins provided valuable support for these results and indicated that the optimized lead **9b** is a potential candidate as a promising anti-inflammatory agent, however advanced studies are being progressed in our laboratory.

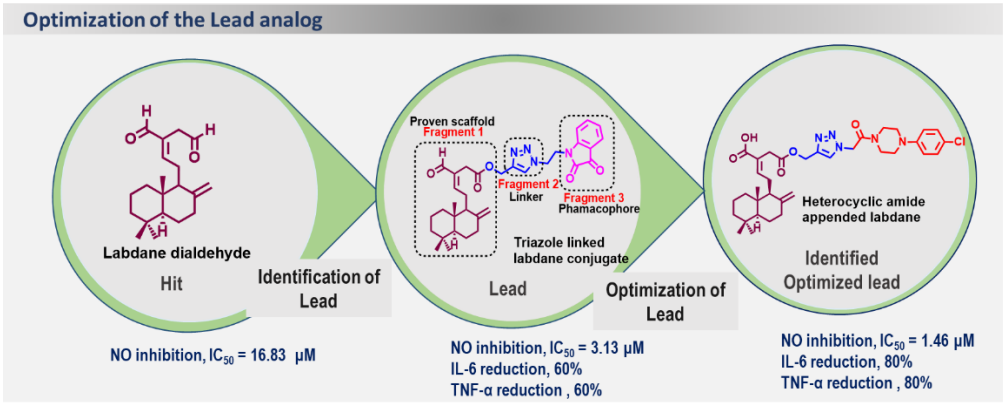

Chapter 1

Importance of Natural Products in Drug Discovery: Special Focus in the Area of Inflammation

1.1. Abstract

This chapter delves into the concept of inflammation, its key mediators, and the urgent need for the discovery of novel anti-inflammatory agents. It underscores the value of natural products as a source of potential therapeutic agents and the necessity of developing new compounds to address the limitations of current treatments. A major focus is semisynthesis, a versatile tool in natural product research that bridges the gap between initial discovery and the development of viable drugs. Through semisynthesis, natural compounds can be modified to enhance their drug-like properties and evaluate their biological efficacy. The chapter also reviews pivotal milestones in semisynthetic drug discovery, showcasing recent examples where modifications of natural products have led to the identification of new anti-inflammatory agents. Additionally, the anti-inflammatory potential of *Curcuma amada* is highlighted. The findings suggest that semisynthesis could play a crucial role in developing safer and more effective anti-inflammatory drugs, offering an innovative solution for chronic inflammatory diseases.

1.2. Inflammation

Inflammation is the natural immunological response of the body towards external stimuli such as microbial invasions or tissue injury.[1,2] Inflammation at the tissue level is characterized by redness, swelling, heat, pain, and diminished tissue function, driven by localized immune, vascular, and inflammatory cell responses to injury or infection. Key microcirculatory processes involved in inflammation include elevated vascular permeability, the recruitment and accumulation of leukocytes, and the release of inflammatory mediators.[3] While inflammation is essential for healing and defence, its prolonged or dysregulated state can lead to the pathogenesis of various inflammatory diseases, such as atherosclerosis,[4] cancer,[5] Alzheimer's,[6] inflammatory bowel disease,[7] type II diabetes,[8] etc.

Steroidal drugs, while effective in managing inflammation, are often associated with irreversible side effects such as hypertension, osteoporosis, immunosuppression, and elevated glucose levels.[9] These adverse effects significantly limit their long-term use, especially in patients requiring chronic treatment. Currently, inflammation is primarily treated with non-steroidal anti-inflammatory drugs (NSAIDs) or anti-cytokine biologics. NSAIDs, though widely used and cost-effective, are frequently linked to gastrointestinal complications, cardiovascular risks, and renal toxicity, particularly with prolonged use. On the other hand, anti-cytokine biologics, such as tumor necrosis factor-alpha (TNF-α) inhibitors and interleukin (IL) blockers, have revolutionized the treatment of inflammatory diseases by targeting specific molecular pathways. Despite their clinical advantages, these biologics come with significant limitations, including high treatment costs, the need for parenteral administration, and the potential for serious adverse effects, such as increased susceptibility to infections and malignancies. Furthermore, the clinical efficacy of these biologics is often constrained by these challenges, making them inaccessible or unsuitable for many patients.[10–13] Given these limitations, there is a pressing unmet medical need to develop novel, therapeutically effective, and cost-efficient drugs to treat inflammation and associated diseases. .[14]

The uncontrolled inflammatory response is characterised by the excessive release of pro-inflammatory mediators such as nitric oxide (NO), TNF-α, IL-6, IL-1α, and inflammatory enzymes such as cyclooxygenase-2 (COX-2) etc. Hence, the downregulation of these inflammatory factors, such as cytokines, chemokines and enzymes, can be an active therapy to control aberrant inflammation and tissue damage.[15]

1.3. Mediators of inflammation

Mediators of inflammation are a diverse group of molecules that regulate and orchestrate the inflammatory response. These molecules are produced by a variety of cells, including immune cells such as macrophages, neutrophils, and T cells, as well as endothelial cells and fibroblasts .[16,17] Key mediators of inflammation include:

1.3.1 Cytokines

Cytokines are small, secreted proteins (typically less than 40 kDa) that play a vital role in regulating and modulating immune responses. Maintaining a balance between effective immune defense and minimizing tissue damage relies on precise control of the cytokine network. In the innate immune system, cytokines are predominantly produced by phagocytes and natural killer (NK) cells, while in adaptive immunity, they are primarily secreted by antigen-presenting cells (APCs) and lymphocytes.

Cytokines and chemokines play pivotal roles in inflammation through various mechanisms, such as directing leukocyte migration to injury sites via chemotaxis, modulating immune cell activity, and promoting the proliferation and differentiation of both immune and non-immune cells. They operate within complex signalling networks to balance pro-inflammatory and anti-inflammatory responses, ensuring efficient pathogen clearance while minimal tissue damage.

Dysregulation of cytokine production can lead to excessive inflammation, autoimmune disorders, or immune suppression, highlighting their critical role inunderstanding and treating immune-related diseases.[18] Key cytokines driving and sustaining inflammatory responses include interleukin-1 (IL-1), interleukin-2 (IL-2), interleukin-6 (IL-6), interferon-gamma (IFN-γ), tumor necrosis factor-alpha (TNF-α), and transforming growth factor-beta (TGF-β). These molecules function through intricate signalling pathways to orchestrate immune responses while maintaining a delicate balance to prevent tissue damage.[15,16,19]

1.3.1.1. Interleukin-6 (IL-6)

IL-6 is a cytokine produced by various immune cells, including mononuclear phagocytes, T cells, B cells, and fibroblasts, as well as by certain non-immune cells. Initially recognized as a B-cell differentiation factor, IL-6 plays a pivotal role in the maturation of B cells into antibody-producing cells. Elevated levels of IL-6 are associated with polyclonal B-cell activation and chronic inflammation. Additionally, IL-6 is essential for T-cell activation and

differentiation, influencing Th2 and Treg phenotypes. It serves as a key mediator during the early stages of the acute-phase inflammatory response and remains elevated in chronic inflammatory conditions, promoting the survival and proliferation of lymphocytes and macrophages, thereby sustaining the inflammatory process. [17]

1.3.1.2. Interleukin-1 (IL-1) family

The IL-1 family of cytokines is produced and secreted by a variety of cell types, particularly monocytes and macrophages. Interleukin-1α (IL-1α) and interleukin-1β (IL-1β) were first identified in 1974 by Charles A. Dinarello and have been the focus of extensive research ever since. IL-1β, a key pro-inflammatory member of this family, plays a vital role in modulating inflammatory responses. It drives the expression and secretion of enzymes like inducible nitric oxide synthase (iNOS) and cyclooxygenase-2 (COX-2), which generate critical inflammatory mediators, including prostaglandin-E2, platelet-activating factor (PAF), and nitric oxide. Additionally, IL-1β stimulates the expression of adhesion molecules, promoting the recruitment of immune cells to sites of injury or infection, thereby amplifying the inflammatory response.[16]

1.3.1.3. Interleukin-2 (IL-2)

Interleukin-2 (IL-2) significantly enhances natural killer (NK) cell activity and stimulates the production of crucial inflammatory cytokines, including interleukin-1 (IL-1) and interferon-gamma (IFN-γ). Furthermore, IL-2 boosts the cytotoxic functions of macrophages. Its role extends to facilitating chronic inflammation by promoting the activation and proliferation of antigen-specific T and B lymphocytes. This multifaceted action underscores the importance of IL-2 in immune responses and its potential implications for therapeutic strategies in addressing inflammatory disorders.[15,19]

1.3.1.4. Tumor Necrosis Factor-Alpha (TNF-α)

Tumor necrosis factor-alpha (TNFα) was first identified in the 1970s as a serum factor induced by endotoxins, capable of causing necrosis in certain tumors both *in vivo* and *in vitro*. Following its discovery, TNFα was successfully isolated, and its gene was cloned. This powerful inflammatory mediator plays a central role in the innate immune system, coordinating a range of critical responses. TNFα drives the production of cytokines, activates adhesion molecule expression, and stimulates cell growth. It supports normal cell proliferation while exhibiting cytolytic and cytostatic effects on tumor cells, highlighting

its dual role in cellular processes. Additionally, TNFα demonstrates diverse functions, including inflammatory, antiviral, and immunoregulatory activities. Beyond its key role in inflammation, TNFα is involved in other physiological processes such as lipid metabolism, coagulation, insulin resistance, and endothelial function. Recognized as one of the most significant and versatile cytokines, TNFα is indispensable for the regulation of inflammatory and immune responses, with profound implications for health and disease.[19,20]

1.3.1.5. Interleukin-10 (IL-10)

Interleukin-10 (IL-10) is a critical anti-inflammatory cytokine that plays a central role in maintaining immune homeostasis by regulating inflammatory responses. It is produced by various immune cells, including macrophages, dendritic cells, neutrophils, B cells, natural killer (NK) cells, CD8+ T cells, and predominantly CD4+ T cells. IL-10 functions to suppress the production of pro-inflammatory cytokines, reduce antigen presentation, and inhibit phagocytic activity in innate immune cells, thereby preventing excessive immune activation and tissue damage. This cytokine is essential for balancing immune defence against pathogens while minimizing the risk of chronic inflammation and autoimmunity. Dysregulation of IL-10 is associated with inflammatory and autoimmune diseases, highlighting its significance as a therapeutic target for conditions like rheumatoid arthritis, inflammatory bowel disease, and other immune-related disorders.[21,22]

1.3.2. Chemokines

Pro-inflammatory chemokines are small proteins (8–12 kDa) that play a critical role in recruiting leukocytes to sites of infection or injury. These molecules are characterized by three to four conserved cysteine residues and are divided into four families based on the arrangement of their N-terminal cysteines:

1. **CXC Subfamily**: The first two cysteines are separated by a variable amino acid.
2. **CC Subfamily**: The cysteines are adjacent to each other.
3. **C Subfamily**: This group lacks the first and third cysteines, leaving only one conserved cysteine. It includes the lymphocyte-specific chemotactic peptide XCL1 (lymphotactin).
4. **CX3C Subfamily**: The two cysteines are separated by three variable amino acids. The sole human member, CX3CL1 (fractalkine), is unique for its mucin-like

glycosylated stalk, allowing it to function as either a soluble or membrane-bound chemokine.

Chemokines, primarily from the CXC and CC families, play a central role in inflammatory processes by recruiting effector leukocytes during infection, tissue injury, inflammation, and tumor development. They guide cell migration (chemotaxis) along chemokine gradients, regulate leukocyte localization *via* changes in chemokine receptor expression, and activate macrophages and polymorphonuclear neutrophils (PMNs). Additionally, they contribute to wound healing by promoting angiogenesis and stimulating fibrosis.In the central nervous system, chemokines drive astrocyte migration and microglial proliferation at injury sites, facilitating nociceptive pain signalling as a protective response to acute tissue damage.[15,16] **Table 1.1.** summarises the source and functions of the major cytokines and chemokines.

Table 1.1. Cytokines and chemokines important in inflammation

	Mediator	Source	Major Function
Cytokines			
	Interleukin-1 (IL-1)	Macrophages, dendritic cells, T and B cells	Stimulates activation of T and B lymphocytes Enhances the production of other cytokines and acute-phase proteins Induces adhesion molecules
	Interleukin-2 (IL-2)	Activated T cells, B cells	Stimulates the proliferation and activation of T and B cells, NK cells, and macrophages Promotes the production of pro-inflammatory cytokines

	Interleukin-6 (IL-6)	Macrophages, dendritic cells, B cells, activated T cells	Exerts diverse effects on T cells Myeloid cell development Controls the regulation of acute-phase proteins
	Interleukin-17 (IL-17)	TH17 cells, NK cells, NK T cells, macrophages	Recruits monocytes and neutrophils Stimulates the production of various cytokines, chemokines, and prostaglandins Increases allergic inflammatory responses
	Interleukin-10 (IL-10)	T cells	Suppresses cytokine production and the function of mononuclear cells Exhibits anti-inflammatory effects
	Interferon gamma (IFNγ)	T cells, NK cells, epithelial cells, fibroblasts	Increases major histocompatibility complex (MHC) expression Enhances cytotoxic T lymphocytes (CTLs), NK, and macrophage activity Stimulates production of IL-1 and TNFα
	Transforming growth factor-beta	Macrophages, megakaryocytes, chondrocytes	Suppresses cytokine production and activity

	(TGF-β)		Inhibits B-cell proliferation Promotes wound healing
	Tumor necrosis factor-alpha (TNF-α)	Macrophages, dendritic cells, lymphocytes, mast cells	Enhances MHC expression Stimulates macrophages Enhances the killing of tumor cells
Chemokines			
	Macrophage chemoattractant protein-1 (MCP-1) (CC family)	Endothelial cells, epithelial cells, fibroblasts, monocytes	Attract monocytes Activates macrophages and T cells Triggers histamine release
	RANTES (CC family)	T cells, endothelial cells, platelets	Attract macrophages
	Gro (α, β, γ MSGA) (CXC family)	Macrophages, fibroblasts	Attract PMNs, angiogenesis
	Interleukin 8 (IL-8) (CXC family)	Macrophages, lymphocytes	Chemotaxis Pro-inflammatory
	Fractalkine (CX3C family)	Endothelial cells, microglia macrophages	Attract T cells, monocytes, and PMNs in the brain

1.3.3. Cyclooxygenases (COX)

Cyclooxygenase (COX) is a critical enzyme that facilitates the conversion of polyunsaturated fatty acids and arachidonic acid into prostaglandin (PG) H2, a precursor that subsequently produces various prostanoids, including prostaglandins, prostacyclins, and thromboxanes, all of which play essential roles in physiological and inflammatory processes. COX exists in two main isoforms, COX-1 and COX-2. COX-1 is constitutively expressed in most tissues, producing baseline levels of prostaglandins to maintain normal physiological functions such as protecting the stomach lining and regulating blood

platelets. It is often referred to as a "housekeeping" enzyme due to its steady-state synthesis of prostaglandins that support homeostasis. On the other hand, COX-2 is an inducible isoform, primarily expressed in response to inflammatory stimuli or certain growth factors, with significant upregulation observed in activated macrophages and tissues undergoing inflammation or tumorigenesis. This distinction forms the basis for the development of COX-2 selective inhibitors. Traditional non-steroidal anti-inflammatory drugs (NSAIDs) inhibit both COX-1 and COX-2, reducing inflammation but causing side effects such as gastrointestinal ulceration and bleeding due to COX-1 inhibition. In contrast, COX-2 selective inhibitors, such as celecoxib and etoricoxib, were designed to provide anti-inflammatory, analgesic, and antipyretic benefits while minimizing gastrointestinal toxicity and platelet dysfunction. However, while these agents improve gastrointestinal tolerability, they are associated with increased cardiovascular risks, including hypertension, myocardial infarction, and stroke, likely due to an imbalance in prostacyclin and thromboxane levels. COX-2 inhibitors are primarily used for managing chronic inflammatory conditions such as rheumatoid arthritis and osteoarthritis and for acute pain relief, though their use requires caution, especially in patients with cardiovascular risk factors.[23–26]

1.3.4. Nitric oxide (NO), inducible nitric oxide synthase (iNOS), and inflammation

Free radicals are highly reactive molecules that can exert either beneficial or harmful effects depending on the environmental context. Among these, Nitric Oxide (NO) is a free radical that plays a significant role in inflammatory processes.[27] NO is synthesized from the guanidino group of L-arginine during its conversion to L-citrulline by Nitric Oxide Synthases (NOS). Under normal physiological conditions, NO is continuously produced by the constitutively expressed endothelial NOS (eNOS) and neuronal NOS (nNOS), where it has various beneficial effects. However, during inflammatory responses, NO is produced in significantly higher amounts through the activity of inducible NOS (iNOS). This enzyme is expressed in macrophages, neutrophils, granulocytes, and other cell types in response to pro-inflammatory signals.[28] The elevated production of NO under these conditions contributes to the propagation of inflammatory responses. Extensive research has investigated the role of NO in inflammatory and autoimmune conditions, demonstrating that its inhibition can have anti-inflammatory effects.[27,29,30]

1.4. NFκB signalling in inflammation

The nuclear factor kappa-light-chain-enhancer of activated B cells (NF-κB) is a nuclear transcription factor found in nearly all mammalian cell types, where it performs a broad range of biological functions. First discovered in 1986 by Sen and Baltimore through its interaction with a specific site in the enhancer region of the κ light chain gene in B cells, NF-κB has since become a key area of study.[31] It plays an essential role in regulating critical processes such as cell proliferation, metastasis, DNA damage repair, apoptosis, and immune responses by activating various target genes. Consequently, NF-κB is closely associated with the progression of many diseases, including inflammation, cancer, and autoimmune disorders.[32]

The NF-κB superfamily in humans includes five transcription factors: NF-*κ*B1 (p50), NF-*κ*B2 (p52), RelA (p65), RelB, and ReL (c-Rel). Each of these proteins possesses a conserved N-terminal region known as the Rel Homology Domain (RHD), which is crucial for their ability to bind DNA, form dimers, and localize to the nucleus. While most NF-κB proteins can form both homodimers and heterodimers to regulate gene transcription, RelB is unique in that it exclusively forms heterodimers. Among these, the heterodimer formed by NF-κB1 (p50) and RelA (p65) is the most prevalent.[32,33]

The activity of NF-κB dimers is controlled by the inhibitory protein IκB. In its inactive form, NF-κB remains sequestered in the cytoplasm, bound to IκB. Upon activation by external signals, IκB is phosphorylated by IκB kinase (IKK) and subsequently degraded by the proteasome. This releases NF-κB, which is then phosphorylated and translocates to the nucleus. Within the nucleus, phosphorylated NF-κB (p-NF-κB) binds to specific DNA promoter regions, initiating the transcription of pro-inflammatory mediators such as cytokines (e.g., TNF-α and IL-6) and enzymes (e.g., COX-2 and iNOS) (**Figure 1.1)**.[34]

NF-κB plays a pivotal role in the development of various inflammatory diseases, including rheumatoid arthritis (RA), inflammatory bowel disease (IBD), multiple sclerosis, atherosclerosis, systemic lupus erythematosus, type I diabetes, chronic obstructive pulmonary disease (COPD), and asthma. Its role varies depending on the cellular context and the disease state, making it a complex but critical therapeutic target. Consequently, inhibiting the NF-κB signaling pathway is a promising approach for treating inflammation and its related complications.[35,36]

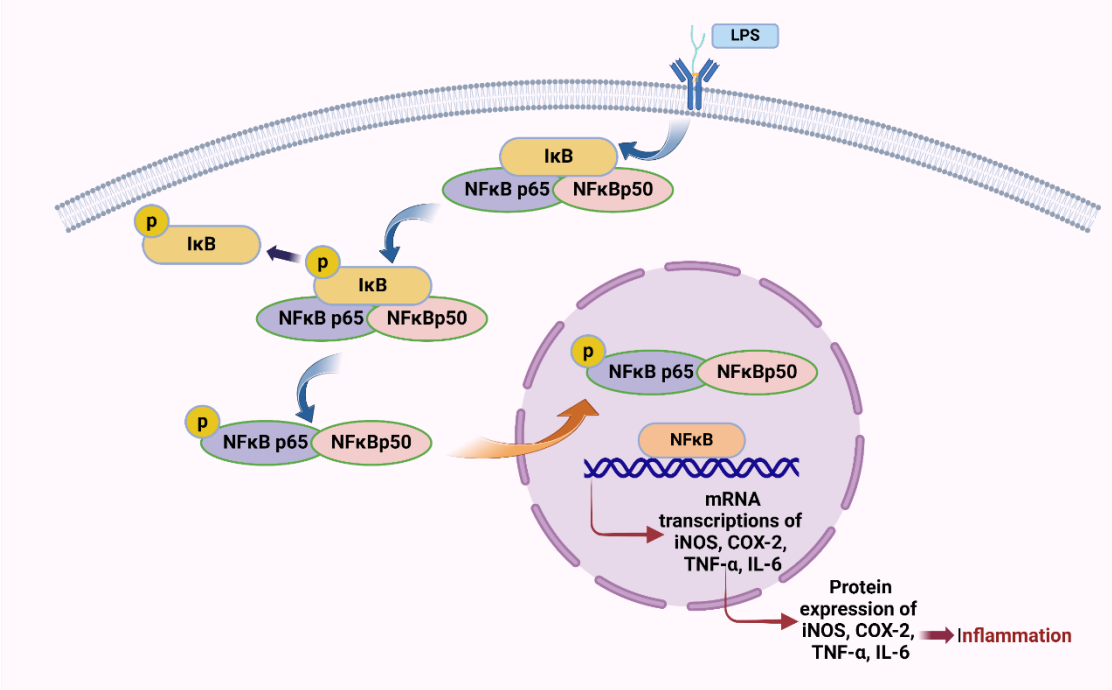

Figure 1.1. NFκB Signalling Pathway

1.5. Natural Products: a continuing source of drug leads

Throughout history, humans have turned to nature to fulfill essential needs, including the development of medicines for treating various illnesses. Plants, in particular, have been the foundation of many traditional medical systems. Historical records from around 2600 BCE document the use of approximately 1,000 plant-based substances in Mesopotamia. Among these were oils extracted from *Cedrus* species (cedar) and *Cupressus sempervirens* (cypress), *Glycyrrhiza glabra* (licorice), *Commiphora* species (myrrh), and *Papaver somniferum* (poppy juice). Remarkably, many of these remedies are still employed today to treat conditions such as parasitic infections, inflammation, and other ailments[37,38]

Natural products (NPs) are chemical compounds or substances naturally synthesized by living organisms. Primarily referring to secondary metabolites, these compounds are structurally diverse and exhibit unique pharmacological properties, making them a valuable source for discovering novel drugs.[39,40]

The emergence of combinatorial chemistry has led many pharmaceutical industries to move away from the traditional method of drug discovery from natural sources. Combinatorial chemistry refers to a set of innovative techniques used to synthesize large chemical libraries. Along with high-throughput screening, these techniques have opened new pathways for drug discovery by facilitating the identification of active lead compounds against various biological targets. While there are claims that combinatorial chemistry

generates large collections of novel drug leads, the decline in the number of new chemical entities (NCEs) discovered through this method is evident, with very few approved NCEs reported in the public domain.[40,41]

Despite the rise of combinatorial chemistry, NPs continue to contribute significantly to the discovery of new clinical candidates and drugs. A recent review by Newman and Cragg highlighted this contribution by examining the total number of natural product-derived drugs out of the total drugs marketed between 1981 and 2019. During this period, 1,881 drugs were approved and marketed. Of these, approximately 24.6% (463) were synthetic, 18.9% (356) were derived from natural products, and 18.4% (346) were vaccines. In addition, 11.5% (217) and 11% (207) of the drugs were either synthetic or total synthesis mimics of natural products. Notably, 3.8% (71) of these 1,881 drugs were unaltered natural products (**Figure 1.2**).

The review also pointed out that 60% of the total small molecule drugs discovered between 1981 and 2019 were based on natural products, with 2% of them being anti-inflammatory agents. This statistic underscores the significant potential for discovering novel anti-inflammatory agents from natural product sources, emphasizing the continued relevance of natural products in modern drug discovery.[40]

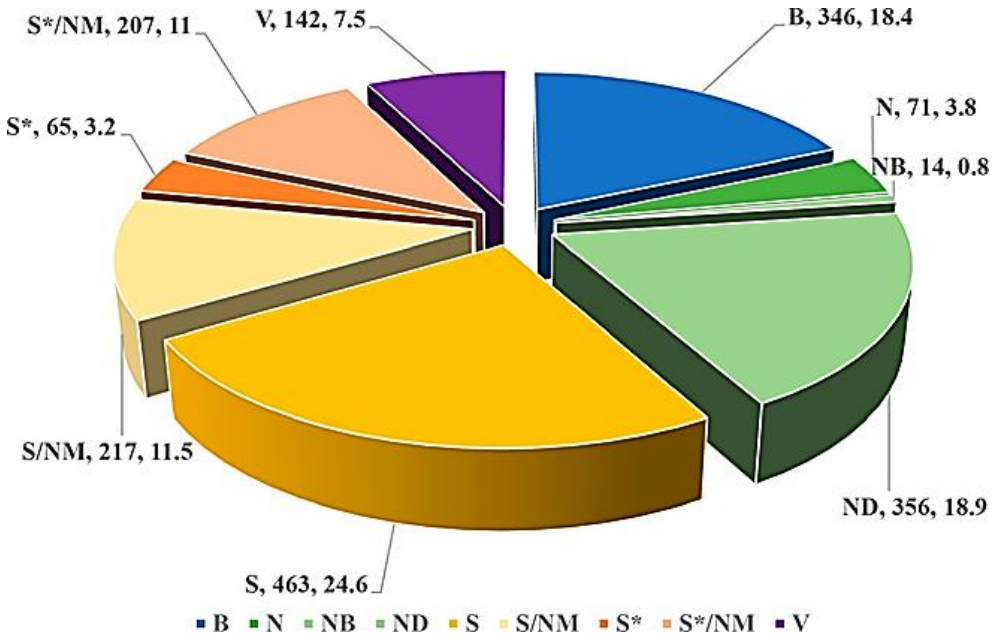

Figure 1.2. New drugs approved in between 1981-2019.[40] Abbreviations:, B: Biological; usually a large (>50 residues) peptide or protein either isolated from an organism/cell line or produced by biotechnological means in a surrogate host, N: Natural product, NB: Natural product "Botanical" (in general these have been recently approved), ND: Derived from a natural product and is usually a semisynthetic modification, NM: Mimic of natural products, S: Synthetic drug, often found by random screening/modification of an existing agent, S*: Made by total synthesis, but the pharmacophore is/was from a natural product, V: Vaccine.

1.6. Plant-based natural products as drugs

Natural products continue to be a major alternative source for the development of next-generation drugs.[40] Medicinal plants, in particular, continue to serve as a promising reservoir of bioactive compounds for addressing various health conditions. With over 150,000 plant species studied to date, numerous have yielded valuable therapeutic agents, underscoring the increasing prominence of plant-derived compounds in modern drug discovery and pharmaceutical development. .[42]

The history of natural product-based drug discovery has deep roots, with its origins dating back centuries. The first plant-derived new molecular entity (NME) was morphine, which Friedrich Wilhelm Sertürner successfully isolated as crystalline alkaloids from the seeds of *Papaver somniferum L.* (opium poppy) of the *Papaveraceae* family. His pioneering work between 1803 and 1817 marked a significant milestone in pharmaceutical

research. Morphine became widely used as an analgesic starting in 1827, long before receiving FDA approval in 1938.[43]

Quinine, another ground-breaking drug, was isolated in 1820 by Pierre Joseph Pelletier and Joseph Caventou from the bark of *Cinchona officinalis* (quina-quina), belonging to the *Rubiaceae* family. This plant, a rich source of medicinal alkaloids, was traditionally used by indigenous populations of the Amazon region to treat shivering and fevers linked to malaria. Quinine's isolation heralded the development of the first antimalarial drug and remains a landmark in medicinal history.[44]

Another revolutionary antimalarial discovery was artemisinin, isolated in 1972 from *Artemisia annua* (sweet wormwood) of the *Asteraceae* family. Tu Youyou's work on artemisinin, a unique sesquiterpene, earned her the Nobel Prize in 2015 for its transformative role in malaria treatment. Artemisinin remains a cornerstone in malaria management today.

The journey to isolate Taxol (paclitaxel) from *Taxus brevifolia* (Pacific yew) began in 1962, culminating in its FDA approval in 1992 for ovarian cancer and 1994 for breast cancer therapy. Taxol has since become a key therapeutic agent in cancer treatment and a benchmark for natural product-based anti-cancer drugs.[44]

Reports show that many life-saving and anti-cancer drugs are directly derived from natural sources with little to no modification. Examples of FDA-approved drugs of plant origin include reserpine, vinblastine, vincristine, noscapine, digoxin, colchicine etc. [37] (**Figure 1.3**).

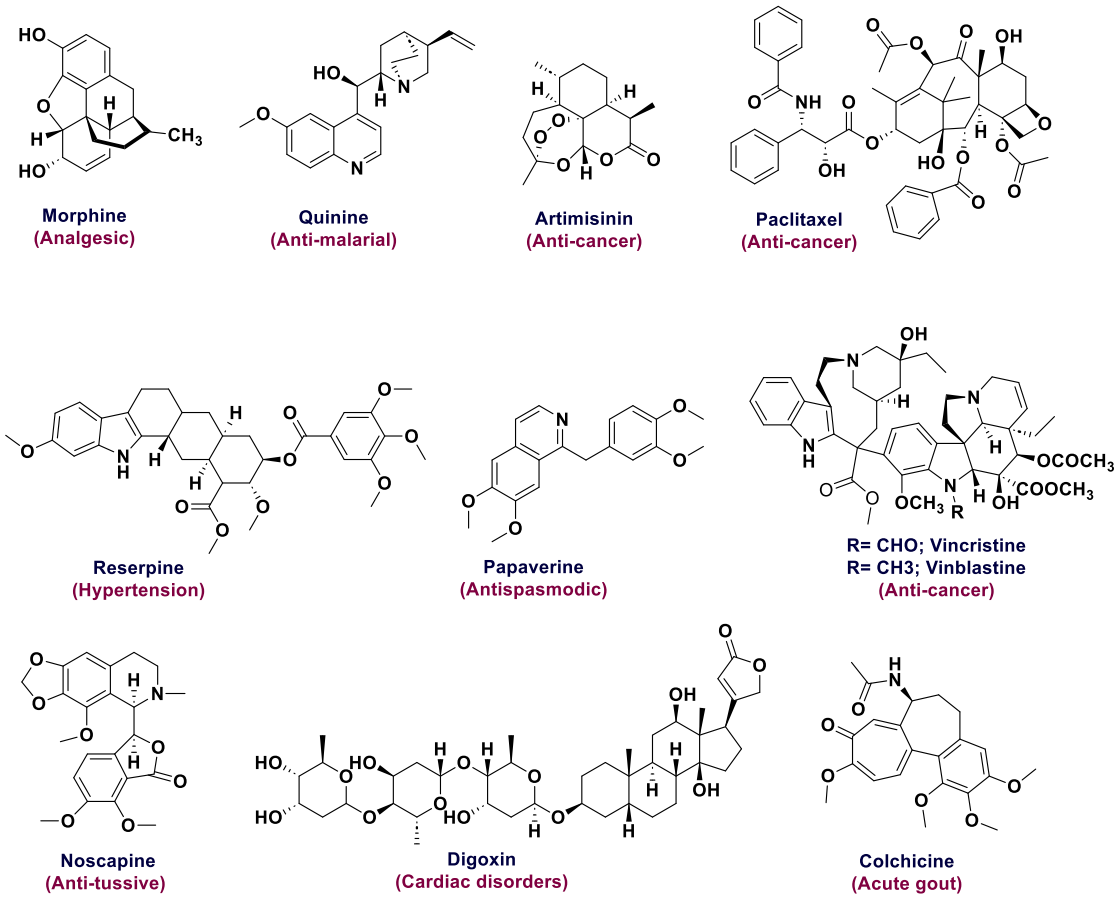

Figure 1.3. FDA-approved drugs derived from plant sources

1.6.1. Plant-derived bioactives as anti-inflammatory agents

Plant-based natural products have been well extensively documented for their anti-inflammatory properties, owing to their therapeutically potent phytoconstituents and their semisynthetic derivatives.[42,45] Curcumin, a polyphenol from *Curcuma longa*, exhibits anti-inflammatory, antioxidant, and anti-cancer activities by interacting with various molecular targets. Its anti-inflammatory effect is partially attributed to the suppression of NF-κB, a key transcription factor involved in immune responses. Epigallocatechin-3-gallate (EGCG), the most abundant catechin in green tea (*Camellia sinensis*), modulates the IL-1β signaling pathway by inhibiting the upstream kinase TGF-β-activated kinase 1 (TAK1). This results in decreased production of pro-inflammatory mediators such as IL-6, IL-8, COX-2, and MMP-2 in human rheumatoid arthritis synovial fibroblasts (RASFs). EGCG has been shown to prevent the progression of various inflammatory diseases, including rheumatoid arthritis, infections, atherosclerosis, and allergies. Quercetin, a flavonoid found in fruits, vegetables, tea, and wine, demonstrates significant anti-inflammatory effects by inhibiting pro-inflammatory molecules like cytokines and COX-2. It also modulates

various signalling pathways, such as NF-κB, which regulate immune and inflammatory responses. Quercetin has potential benefits in managing conditions like arthritis, cardiovascular diseases, and allergies due to its ability to reduce oxidative stress and inflammation. Resveratrol, a polyphenolic stilbene found in grapes, peanuts, and mulberries, exerts its anti-inflammatory effects by regulating targets such as COX-1/2, leukotriene A4 hydrolase, estrogen receptors, and death-associated protein kinase 1. Berberine, an isoquinoline alkaloid found in medicinal herbs like *Berberis aristata* and *Coptis chinensis*, reduces inflammation by modulating immune cell balance, decreasing IL-6 and IL-17, while increasing IL-10 and TGF-β, and inhibiting the NF-κB pathway, which is essential in treating chronic respiratory diseases like asthma and Chronic obstructive pulmonary disease (COPD). Salicin, a naturally occurring compound found in willow trees (*Salix* species), exhibits anti-inflammatory properties by suppressing the production of pro-inflammatory mediators, particularly prostaglandins, which are central to inflammation and pain. A notable derivative of salicin is acetylsalicylic acid (aspirin), a groundbreaking anti-inflammatory drug. Aspirin, synthesized from salicin, has become one of the most widely used and enduring therapeutic agents in medical history.[46] These plant-derived compounds (**Figure 1.4**) highlight the diverse mechanisms by which natural products can mitigate inflammation and related diseases.[47–52]

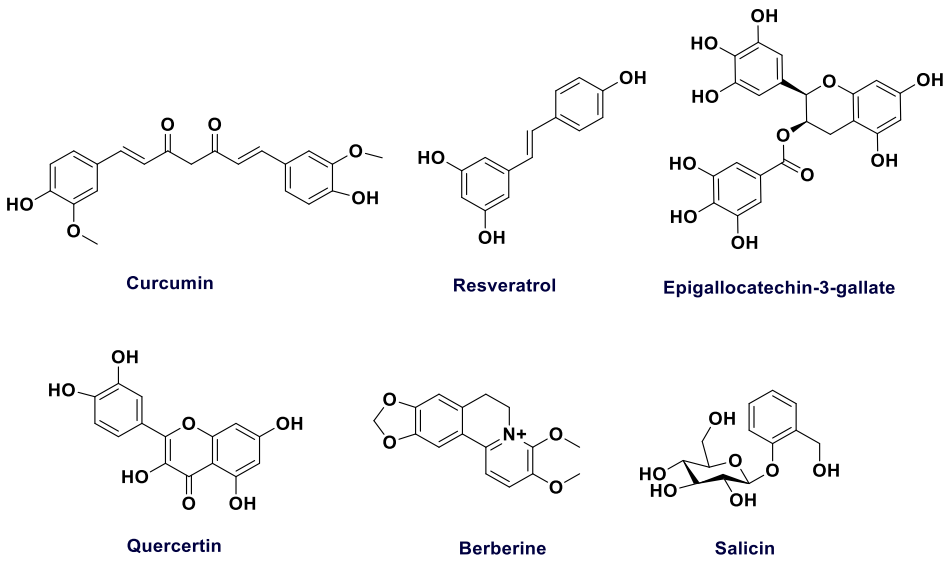

Figure 1.4. Plant based anti-inflammatory clinical candidates

1.7. *Zingiberaceae* family

The *Zingiberaceae* family, commonly referred to as the ginger family, is the largest family within the order Zingiberales. It comprises flowering plants renowned for their medicinal

and nutritional properties. This family is predominantly distributed across tropical and subtropical regions, including Asia, Africa, the Americas, and especially India and Southeast Asia. The *Zingiberaceae* family includes approximately 53 genera and 1,600 species, with the highest concentration found in the Indo-Malayan region of Asia. In India, the family encompasses around 20 genera and 200 species.

Members of the *Zingiberaceae* family are typically annual or perennial herbs with rhizomatous roots. The family is a valuable source of food, spices, dyes, perfumes, cosmetics, and medicines. Medicinally significant genera within *Zingiberaceae* include *Alpinia*, *Amomum*, *Curcuma*, *Elettaria*, *Hedychium*, *Kaempferia*, *Zingiber*, and *Costus*. Numerous species from this family are known for their nutraceutical and medicinal properties, being rich in volatile oils and oleoresins, which are often exported. The most notable species of the Zingiberaceae family, *Curcuma longa*, *Curcuma amada*, and *Zingiber officinale*, are well-known for their extensive medicinal properties. In this context, our research emphasizes the phytochemical analysis and biological assessment of *Curcuma amada*, a species within the genus *Curcuma*. Below is a concise overview of the *Curcuma* genus.[53,54]

1.8. The genus *Curcuma*

The genus *Curcuma*, belonging to the family *Zingiberaceae*, comprises over 120 species of perennial rhizomatous herbs native to tropical and subtropical regions, including Asia, Australia, and South America. Renowned for their therapeutic properties, species from this genus are also utilized as spices, perfumes, cosmetics, ornamental plants, and flavoring and coloring agents. The genus was first described by Carl Linnaeus in 1753. The name "Curcuma" is derived from the Arabic word "kurkum," meaning saffron, highlighting its historical association with vibrant coloring and medicinal value.

While more than 700 compounds have been isolated from the *Curcuma* genus, only a limited number have been thoroughly explored for their pharmaceutical potential. Curcumin, a compound predominantly found in *Curcuma longa* (turmeric), is the most extensively studied. It has been used for centuries in traditional medicine and is reported to have a wide range of therapeutic properties, including anti-inflammatory, anticancer, antiproliferative, gastrointestinal, hypoglycemic, antihyperlipidemic, neuroprotective, hepatoprotective, diuretic, carminative, hypotensive, antioxidant, insecticidal, antimicrobial, antiviral, anti-rheumatic, and antivenomous effects.

The biological activity of the *Curcuma* genus is largely attributed to its non-volatile curcuminoids and volatile terpenoids. Essential oils derived from *Curcuma* species also exhibit diverse pharmacological properties. Among the species, *C. longa*, *C. xanthorrhiza*, *C. aromatic*a, *C. malabarica*, *C. zedoaria*, *C. amada*, *C. caesia*, *C. leucorrhiza*, *C. angustifolia*, *C. flaviflora* are the most researched and hold significant medicinal value. India, being the largest producer of commercially important *Curcuma* species, plays a pivotal role in their cultivation and study.

Despite its vast potential, several *Curcuma* species remain underexplored, particularly in terms of their pharmaceutical applications against inflammation. To address this, we have focused on *Curcuma amada*, which offer promising opportunities for isolating bioactive compounds and conducting biological studies. The genus *Curcuma*, therefore, serves as a rich resource for novel drug discovery and lead identification[55–60]

1.9. *Curcuma amada* Roxb.

Curcuma amada is a rhizomatous aromatic herb characterized by a leafy tuft and a height ranging from 60 to 90 cm. The plant features long, petiolate leaves and produces flowers that are white or pale yellow, arranged in spikes at the center of the leaf tuft, typically blooming between November and April. Morphologically and phylogenetically similar to ginger (*Zingiber officinale*), it is commonly referred to as mango ginger due to the distinctive raw mango-like aroma of its rhizomes, reminiscent of *Mangifera indica*. This unique fragrance is attributed to the presence of volatile compounds such as 3-carene, myrcene, β-ocimene, and α-pinene. As a result, mango ginger is widely utilized as a flavouring agent in various culinary applications, including dishes, candies, sauces, pickles, and salads.[14] The taxonomical hierarchy of mango ginger is as follows.[61]

Kingdom	:	Plantae
Sub-kingdom	:	Phanerogamae
Division	:	Spermatophyta
Subdivision	:	Angiospermae
Class	:	Monocotyledonae
Series	:	Epigynae
Order	:	Zingiberales
Family	:	*Zingiberaceae*
Genus	:	*Curcuma*

Various extracts, preparations and bio-actives from many species of its genus *Curcuma* have been well explored for their anti-inflammatory properties.[62] The rhizomes of *Curcuma amada* impart a distinctive raw mango flavour, which makes them popular in culinary dishes. Furthermore, the rhizomes, being the storehouse of bioactives, are widely used as coolants, astringents, appetizers and nutraceuticals.[55,63,64] Due to its wide popularity in traditional medicine and food preparations, it is the second-largest cultivated *Curcuma* species after *C. longa*.[63,65] Rhizomes of the plant are a rich source of bioactive phytochemicals and essential oils with various pharmacological properties such as anti-microbial, anti-tubercular, anti-oxidant, analgesic, hepatoprotective, anti-cancer, anti-inflammatory properties etc.[59,61,66,67] Around 130 phytochemicals are reported to be isolated from the rhizomes[68] and possess various biological properties such as anti-inflammatory, anti-microbial, hepatoprotective, anti-cancer, analgesic properties etc.[61,66,67] (**Figure 1.5.** represents the flower and rhizomes of *Curcuma amada*)

Mango ginger contains several significant bioactive compounds, including flavonoids, terpenoids, diterpene dialdehyde, difurocumenonol, amadannulen, tannins, steroids, alkaloids, glycosides, and amaldehyde. The rhizomes are particularly rich in curcumin, bis-demethoxycurcumin, and demethoxycurcumin. The important phytoconstituents isolated from *C. amada* are represented in **Figure 1.7** and **Figure 1.8**. Essential oils from mango ginger leaves primarily consist of furanosesquiterpenoids, such as epi-curzerenone, curzeronone, curzerene, and furanogermenone. Additionally, the essential oil extracted from the roots contains isosorbide and hexadecenoic acid. Known for its bitter, aromatic, cooling, astringent, and carminative properties, the rhizome of *Curcuma amada* is considered a potent stomachic. It is traditionally used to enhance blood quality when combined with other medicines and is applied topically to treat contusions and sprains The important volatile constituents present in the essential oil of *C. amada* are given below in **Figure 1.6**.[69–73]

Moreover, the extracts of *C. amada* rhizomes have been reported to have anti-inflammatory properties at various acute and chronic phases of inflammation.[74,75] However, there haven't been many reports on the detailed exploration of the anti-inflammatory properties of *C. amada* or its bioactive natural products or semi-synthetic derivatives. (*E*)-labda-8(17),12-diene-15,16-dial is the abundant marker compound, a labdane-type diterpenoid, isolated from the chloroform extract of *Curcuma amada* rhizomes. Many labdane diterpenoids and their derivatives, such as angrographolide, sclareol, forskolin, and others have been proven to have substantial anti-inflammatory effects.[19] Therefore, as part

of our ongoing dedicated research program on natural product-based[20–22] semi-synthetic modifications to explore the biologically relevant chemical space,[23,24] our primary objective was to isolate the abundant marker compounds from *C. amada* and rationally modify it to generate a library of novel anti-inflammatory scaffolds.

Figure 1.5. Flower and rhizomes of *Curcuma amada*

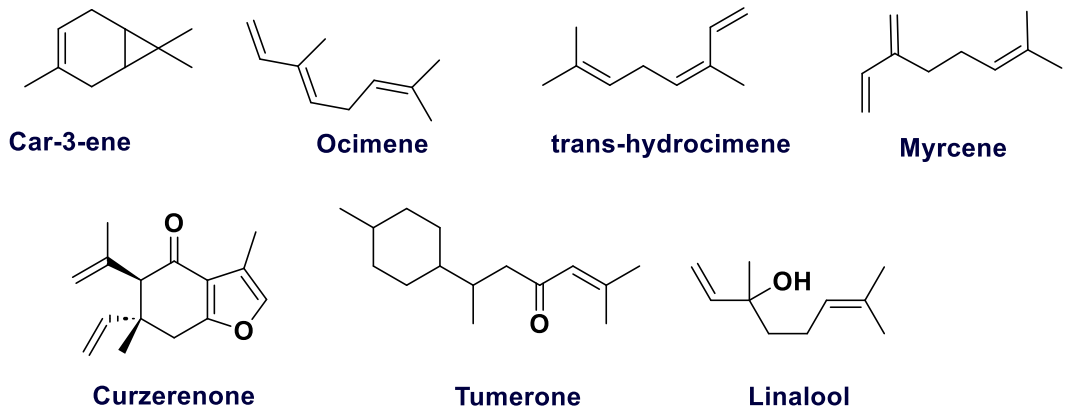

Figure 1.6. Volatile constituents of *C. amada*

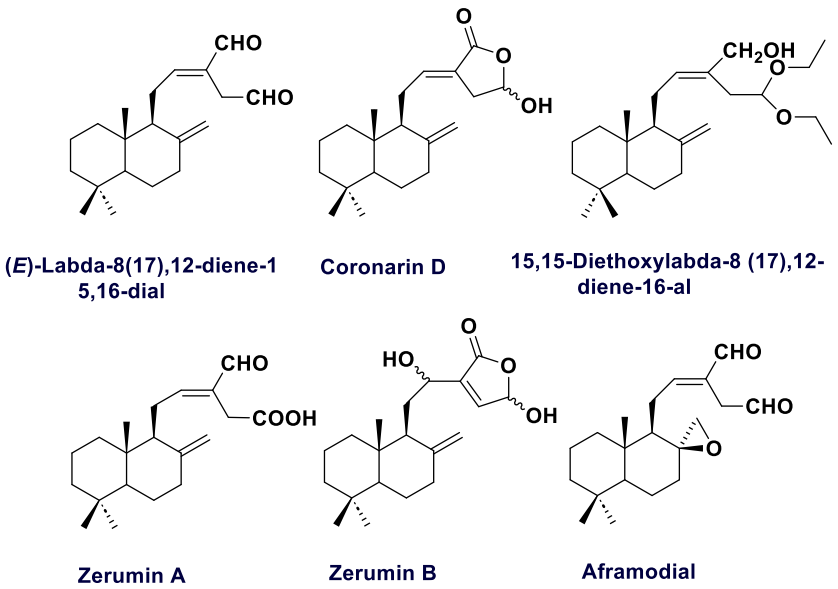

Figure 1.7. Labdane diterpenes isolated from *C. amada* rhizomes

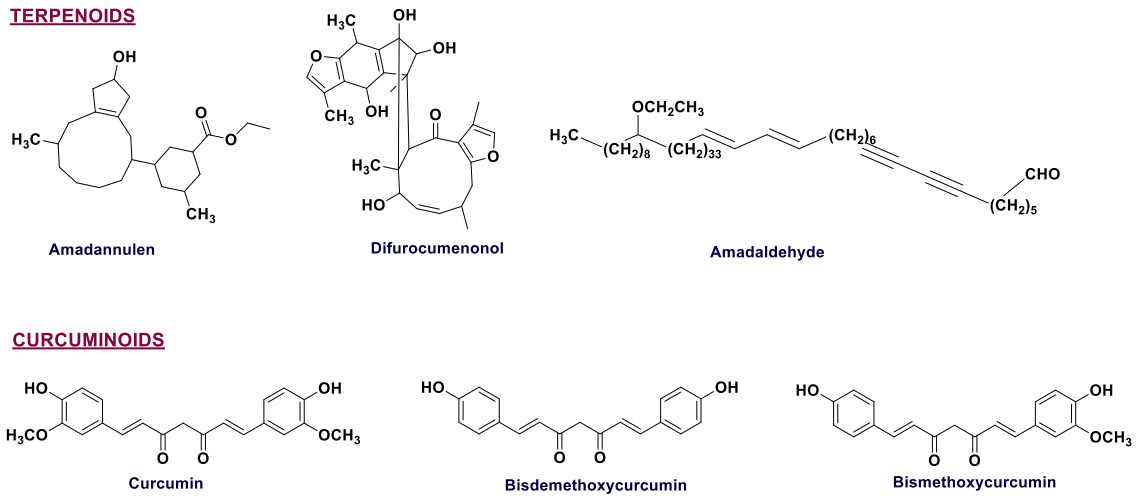

Figure 1.8. Terpenoids and curcuminoids from *C. amada*

1.10. Semisynthetic modification of natural products: a key strategy in drug development

Natural products (NPs) have a long-standing history of success in drug discovery, renowned for their unparalleled structural diversity. However, the development of NPs into new therapeutic agents faces several challenges. Common issues include poor solubility, metabolic instability, and a limited understanding of their precise mechanisms of action, all of which can hinder the advancement of related treatments. Additionally, many NPs have complex and "heavy" structures that often violate Lipinski's rules, reducing their potential for effective gastrointestinal absorption and complicating oral drug formulation. Furthermore, the intellectual property rights associated with unmodified NPs are frequently ambiguous, adding another layer of complexity. To address these challenges, structural modifications of NPs are often necessary to improve their properties and facilitate the development of successful drug candidates.

Semisynthetic modification of therapeutically validated natural product (NP) leads remains one of the most effective strategies to optimize their pharmacological properties and investigate their diverse mechanisms of action. This process involves the chemical alteration of naturally derived compounds, enabling improvements in their pharmacokinetic, physicochemical, and biochemical profiles. By merging the inherent structural complexity and diversity of NPs with the precision of synthetic chemistry, semisynthesis facilitates the enhancement of key drug properties, including pharmacodynamics and bioavailability.[76]

Even minor structural remodelling, such as the transfiguration of a single functional group, can significantly enhance a compound's physicochemical and pharmacokinetic characteristics. Structural modifications also simplify complex molecules, improving their drug-like properties. For instance, optimizing ligand efficiency (LE) by selectively removing redundant functional groups can enhance molecular binding while minimizing undesirable interactions. Most natural products predominantly consist of sp^3-hybridized carbons, which form tetrahedral geometries, creating flexible chains or cyclic structures. The presence of sp^3 centers is particularly significant in enhancing the efficacy of compounds such as the anti-cancer agent epothilone B and the immunosuppressant tacrolimus. However, notable exceptions exist, such as camptothecin, an anti-cancer drug with a fused and conjugated aromatic structure composed primarily of sp^2-hybridized carbons. Moreover, the introduction of nitrogen into molecular frameworks offers significant advantages, including increased nucleophilicity, the ability to form three- or five-valence bonds, and improved linking capabilities, thereby expanding the potential for diverse functional modifications. Unnecessary chiral centers, which do not influence a compound's biological activity, can complicate synthesis and drive-up costs. This challenge is evident in the transition from the structurally complex morphine to the streamlined design of fentanyl. Ultimately, tailored structural modifications are essential to fully harness privileged structural motifs for a wide range of biological and therapeutic applications. This versatile approach underscores the importance of semisynthesis in transforming NPs into more effective and reliable therapeutic agents, showcasing its enduring role in modern drug discovery and development.[38, 39]

Selective modifications of bioactive natural products serve multiple critical purposes, including:

1. **Enhancing activity and selectivity**: optimizing the molecular structure to increase potency and improve specificity for biological targets.
2. **Structural Simplification**: simplifying complex molecular structures to enhance the practicality and efficiency of synthesis while also improving the absorption and bioavailability of natural products.
3. **Improving physicochemical properties**: refining solubility, permeability, and other physical or chemical traits to enhance drug performance.
4. **Boosting metabolic and chemical stability**: enhancing resistance to degradation by metabolic enzymes or chemical processes, thereby prolonging the compound's effectiveness.

5. **Modulating pharmacokinetics (ADME)**: adjusting absorption, distribution, metabolism, and excretion parameters for optimal therapeutic outcomes.
6. **Reducing toxicity and adverse reactions**: eliminating or mitigating side effects and toxicological issues to ensure safety.
7. **Achieving novelty and intellectual property**: introducing unique modifications to secure patents and create new opportunities in drug development.

1.10.1. Overview of biologically significant natural products, their semisynthetic modifications, and therapeutic importance

1.10.1.1. Halichondrin B to eribulin

Halichondrin B, a polyether macrolide derived from the marine sponge *Halichondria okadai*, exhibits strong growth-inhibitory activity against a variety of cancer cell lines. However, its clinical development as an antitumor agent faced significant challenges due to its limited natural availability and intricate structure. To overcome these challenges, researchers analyzed the anticancer activities of intermediates generated during its total synthesis. Kishi et al., from Harvard University, reported the first successful total synthesis in 1992.[79] This investigation revealed that the compound's bioactivity was primarily attributed to its right-half macrolactone fragment. Through the synthesis of 180 target compounds, eribulin emerged as the optimal candidate, formulated as a mesylate salt for clinical use. The development of eribulin involved a significant simplification of halichondrin B, achieving approximately a 35% reduction in molecular weight and halving the number of synthetic steps required. The US Food and Drug Administration (FDA) approved eribulin in 2010 to treat patients with metastatic breast cancer (**Figure 1.9)**.[80]

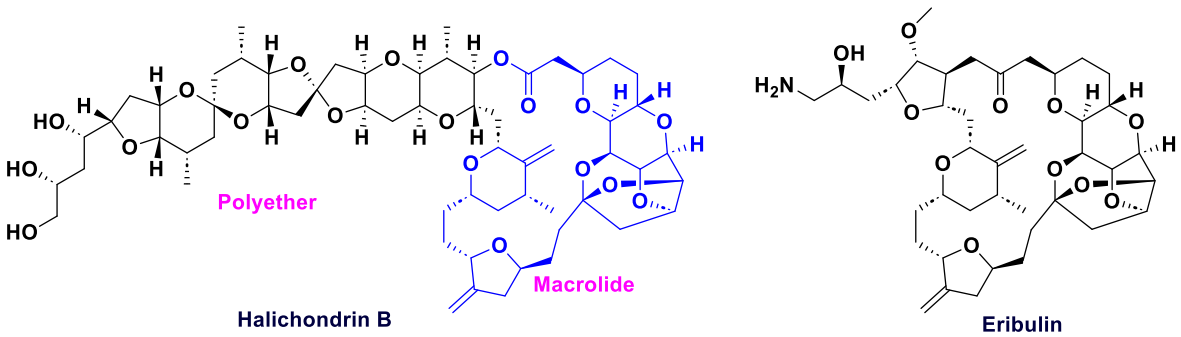

Figure 1.9. Halichondrin B and its semisynthetic derivative eribulin

1.10.1.2. Paclitaxel to cabazitaxel

Paclitaxel is the active compound isolated from the bark of the rare Pacific yew tree (*Taxus brevifolia*). Its initial extraction yielded extremely low quantities. The escalating demand for paclitaxel for clinical applications raised concerns regarding the potential environmental impact associated with the overharvesting of this limited resource. Consequently, research efforts were directed toward identifying more sustainable alternatives, leading to the discovery of docetaxel, a semisynthetic derivative synthesized from 10-deacetylbaccatin III. This precursor is renewable and can be derived from the leaves of the more abundant European yew tree (*Taxus baccata*). Docetaxel provides enhanced water solubility in comparison to paclitaxel and has been extensively utilized alongside paclitaxel within a significant class of chemotherapeutic agents. Over the past two decades, these agents have been employed, either alone or in combination, to treat a broad spectrum of solid tumors. However, the emergence of multidrug resistance (MDR) proteins has resulted in an increasing affinity for taxane-based drugs, thereby rendering numerous tumor cells resistant to treatment. To address this challenge, structural modifications were implemented to docetaxel, specifically substituting the hydroxyl groups at the C-7 and C-10 positions with methoxy groups. This modification facilitated the development of cabazitaxel, which demonstrated a noteworthy enhancement in *in vitro* potency against both docetaxel-sensitive and docetaxel-resistant cell lines, without a corresponding increase in toxicity at the maximum tolerated dose. The greater lipophilicity of cabazitaxel (logP of 3.9 compared to 3.2 for docetaxel) improves its ability to penetrate cell membranes *via* passive influx, thereby increasing its efficacy against resistant cancer cells. In a Phase III clinical study, cabazitaxel, in conjunction with prednisone, exhibited a statistically significant improvement in overall survival rates when compared to mitoxantrone plus prednisone in patients diagnosed with metastatic castration-resistant prostate cancer (mCRPC) who had previously undergone docetaxel therapy. In 2010, cabazitaxel garnered FDA approval for the treatment of patients with hormone-refractory metastatic prostate cancer (**Figure 1.10)**.[77,81,82]

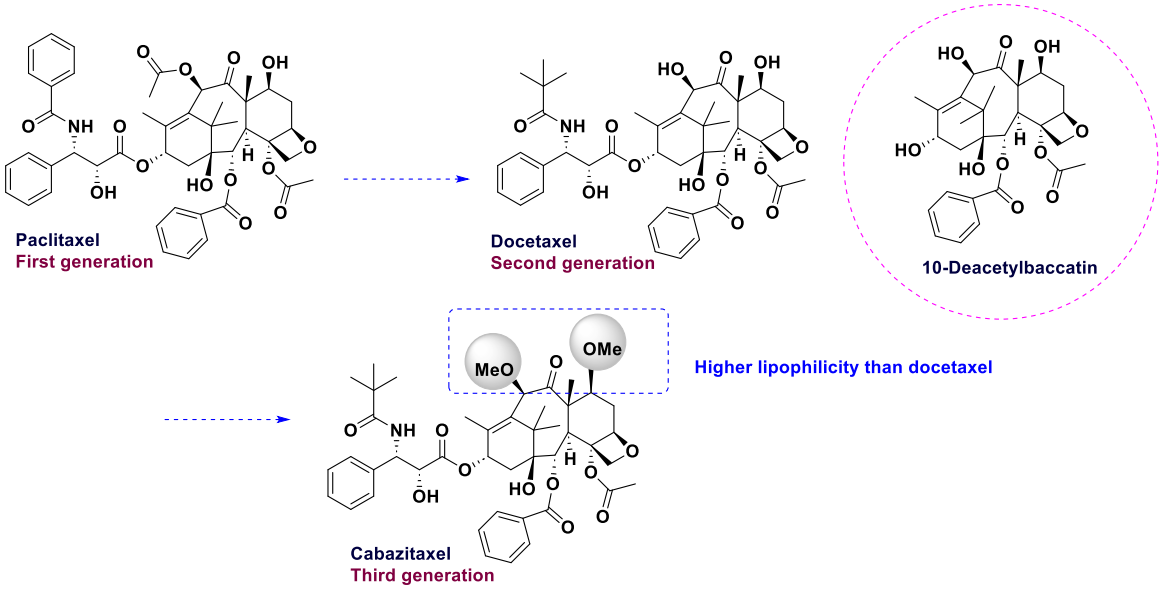

Figure 1.10. Semisynthetic modifications of paclitaxel

1.10.1.3. Myriocin to fingolimod

Myriocin, a natural compound isolated from the fungus *Isaria sinclairii*, exhibits immuno-modulating activity both *in vitro* and *in vivo*, demonstrating a potency that is ten times greater than that of cephalosporin A. The compound contains three chiral carbon atoms and features a trans double bond. Furthermore, myriocin is characterized as a zwitterion at pH 7.4 owing to the presence of amino and carboxyl groups, which adversely affects its *in vivo* absorption. This relatively complex amino acid, possessing three successive asymmetric, has been shown to exhibit strong immunosuppressive activity *in vitro*; however, it also induces considerable toxicity *in vivo*. The objective behind modifying myriocin was to simplify its structure by reducing the number of chiral centers, thereby enhancing its strength, selectivity, and pharmacokinetic properties. Consequently, the chemical structure of myriocin was refined into a non-chiral symmetric framework of 2-substituted-2-aminopropane-1,3-diol. This extensive chemical modification and subsequent pharmacological evaluation, notably utilizing a skin allograft model *in vivo*, culminated in the discovery of a highly effective immunosuppressant termed fingolimod. Fingolimod is a chiral and stereochemically inert linear compound. In 2010, the United States Food and Drug Administration (FDA) approved fingolimod as the first oral disease-modifying therapy aimed at reducing relapses and decelerating the progression of disability in patients suffering from relapsing forms of multiple sclerosis. As a prodrug, one of the hydroxyl groups in fingolimod undergoes phosphorylation by sphingosine kinases within the cells,

resulting in the formation of the active metabolite, fingolimod-1-phosphate, which has been established as a new molecular entity(**Figure 1.11)**.[83]

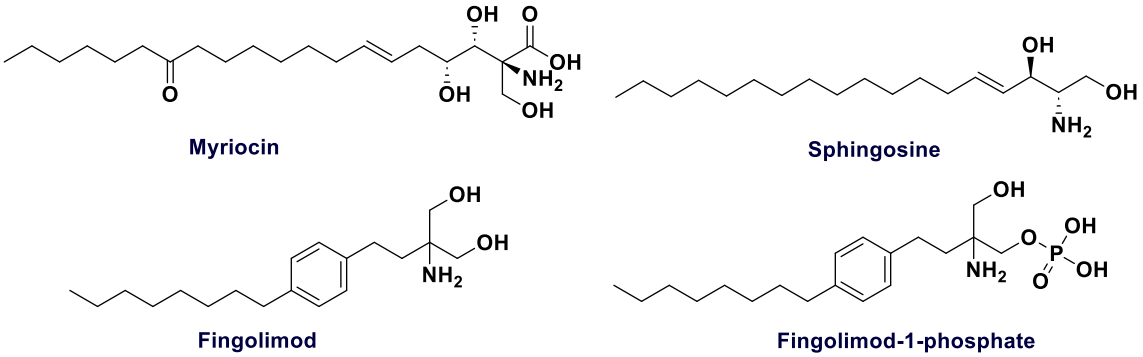

Figure 1.11. Semisynthetic modification of myriocin to fingolimod

1.10.1.4. Epothilone B to ixabepilone

Epothilone B, derived from the myxobacterium *Sorangium cellulosum*, has shown significant antineoplastic activity against various tumor cell lines *in vitro*. Like taxanes, it induces tumor cell death by stabilizing microtubules, which leads to cell division arrest and subsequent apoptosis. However, its clinical application is limited by poor metabolic stability and unfavorable pharmacokinetic properties. Research has shown that the lactone group within the compound is prone to hydrolysis. To address this issue, the lactone oxygen was replaced with nitrogen, resulting in the lactam compound ixabepilone. This single-atom modification has enhanced the metabolic stability of ixabepilone by making it resistant to hydrolysis mediated by esterases. Additionally, this alteration has improved water solubility, allowing for a formulation that requires a reduced amount of the undesirable solubilizing agent cremophor. The U.S. Food and Drug Administration (FDA) approved ixabepilone in October 2007 for the treatment of certain advanced breast cancers (**Figure 1.12)**.[84]

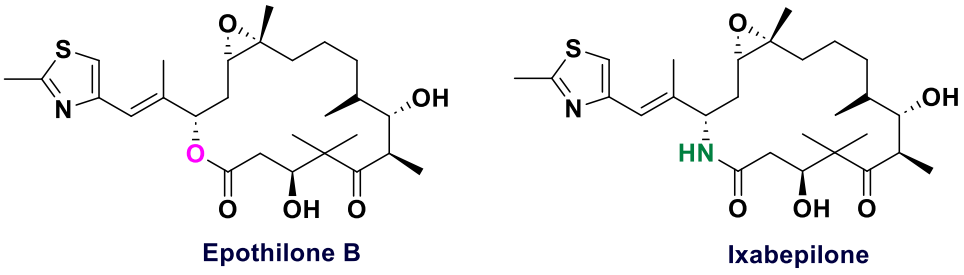

Figure 1.12. Epothilone B and its semisynthetic derivative ixabepilone

1.10.1.5. Semisynthetic modifications of artemisinin

Artemisinin, a sesquiterpene lactone peroxide, is derived from qinghao (*Artemisia annua*) and is renowned for its potent antimalarial properties, particularly against *Plasmodium falciparum*. However, its poor solubility in both water and oil limits its use in oral formulations, complicating treatment for severe malaria cases. To address these challenges, water soluble sodium artesunate and oil-soluble artemether were introduced in China in 1987. These derivatives exhibit improved solubility, making them suitable for intravenous and intramuscular administration, respectively, which is critical for severe malaria management. To further optimize therapeutic profiles, artemisone was developed. This derivative is highly crystalline and easily purifiable, ensuring better stability, bioavailability, and scalability for pharmaceutical applications. Artemisone represents an advanced version of artemisinin derivatives, tailored to meet stringent drug development requirements (**Figure 1.13)**.[85]

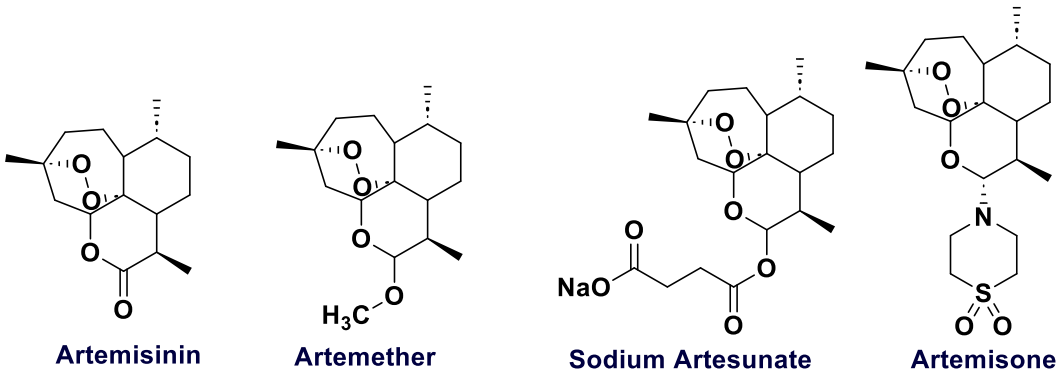

Figure 1.13. Artemisinin and its analogues

1.10.1.6. Indirubin to meisoindigo

Chronic granulocytic leukemia has been treated with the Angelica-Aloe Pill (Danggui Luhui Wan), a traditional Chinese medicine. Through extensive analysis, processed Indigofera tinctoria (Qingdai) was identified as the active ingredient in this six-component pill. This led to the discovery of indirubin, which was found to possess antileukemic properties. Animal studies showed that indirubin inhibits the formation of transplantable malignancies. Indirubin is clinically used for the oral treatment of chronic granulocytic leukemia. However, its limited bioavailability and harmful gastrointestinal effects hinder its widespread use. To optimize its anticancer activity, solubility, and *in vivo* effects, several N-alkyl substituted indirubins were developed. Among these compounds, meisoindigo emerged as the most promising candidate, demonstrating superior activity and favorable

physicochemical properties. It was successfully tested as a treatment for chronic myeloid leukemia and received approval from the Chinese Food and Drug Administration (CFDA) in 1984 (**Figure 1.14)**.

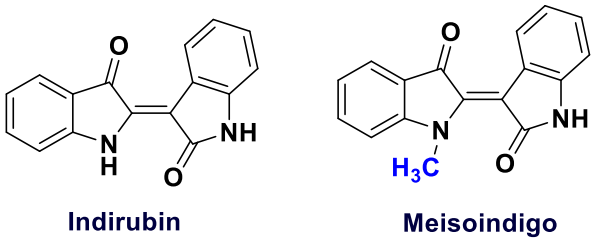

Figure 1.14. Indirubin and its methylated derivative meisoindigo

1.10.1.7. Multiple opioids from morphine

Opioid alkaloids are some of the earliest medicinal compounds known to humanity. Morphine, the primary active component of opium, was first isolated in 1806 and named after Morpheus, the Greek god of dreams. While highly effective as a pain reliever, morphine has significant drawbacks, including poor oral bioavailability, a high potential for addiction, tolerance development, and the risk of respiratory depression. These limitations have driven efforts to modify its structure to improve its therapeutic profile.

Semisynthetic opioids like naloxone, oxycodone, and buprenorphine have been developed from morphine to address these issues. Oxycodone, a μ-opioid receptor agonist similar to morphine, has been utilized in clinical practice since 1917. It is produced by modifying morphine through phenolic O-methylation to create codeine, followed by oxidation and hydrogenation to form oxycodone. Oxycodone produces oxymorphone, which has a stronger analgesic effect than morphine, making it a commonly prescribed painkiller.

Buprenorphine, another semisynthetic opioid, is valued for its strong analgesic properties and is frequently used in pain management and addiction therapy. Naloxone, in contrast, serves as an opioid antagonist and is critical for reversing opioid overdoses (**Figure 1.15)**.[77]

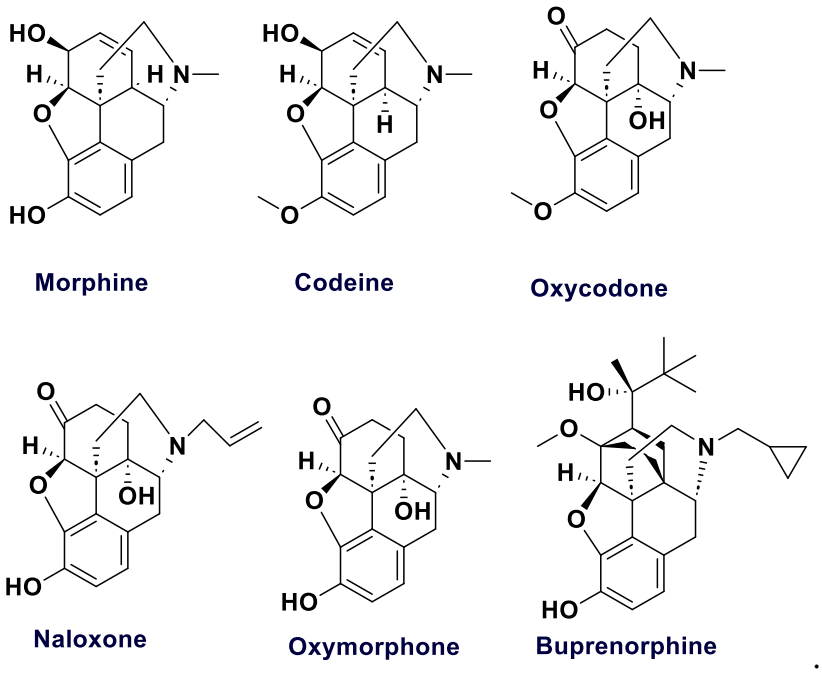

Figure 1.15. Morphine and its semisynthetic derivatives

1.10.1.8. Orlistat from lipstatin

Lipstatin, a natural compound extracted from *Streptomyces toxytricini*, is a potent inhibitor of pancreatic lipase, an enzyme critical for the absorption of dietary triglycerides. Through hydrogenation, lipstatin is converted into orlistat, a more stable derivative that has been widely utilized as a pharmacological treatment for obesity (**Figure 1.16)**. [86].

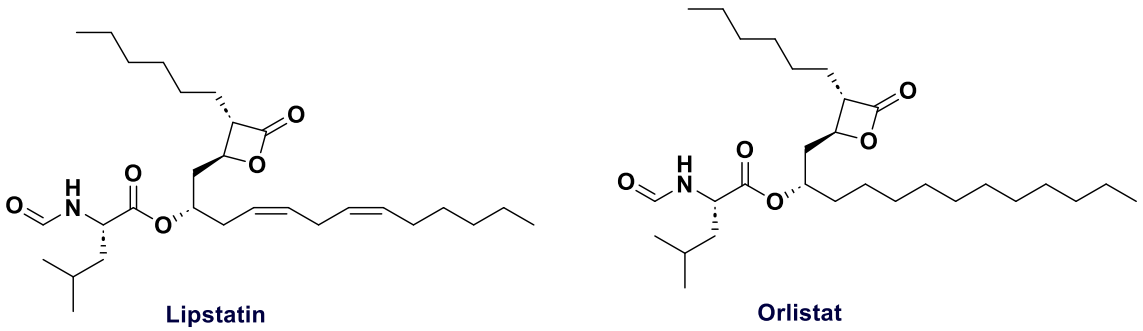

Figure 1.16. Semisynthetic modification of lipstatin to orlistat

1.10.2. Semisynthetic modifications of some of the natural products leading to the discovery of anti-inflammatory agents in recent reports

1.10.2.1. Synthesis of bakuchiol derivatives as effective anti-inflammatory agents

Bakuchiol, a prenylated phenolic monoterpene derived from the fruit of *Psoralea corylifolia* L. (Buguzhi), has a long history of therapeutic use against tumors, viral infections, inflammation, and bacterial infections. In 2022, Du et al., synthesized 30 bakuchiol derivatives to explore potential novel anti-inflammatory agents. The anti-inflammatory effects of these compounds were assessed in lipopolysaccharide (LPS)-stimulated RAW264.7 cells by measuring levels of nitric oxide (NO), interleukin-6 (IL-6), and tumor necrosis factor-α (TNF-α). Notably, a pyrrolidine amide derivative exhibited significantly greater anti-inflammatory activity than bakuchiol and the standard drug celecoxib. Mechanistic studies indicated that this compound effectively inhibited the release of pro-inflammatory cytokines by activating the nuclear factor erythroid 2-related factor 2 (Nrf2)/heme oxygenase-1 (HO-1) pathway while suppressing the nuclear factor-κB (NF-κB)/mitogen-activated protein kinase (MAPK) pathway. Additionally, *in vivo* experiments in zebrafish demonstrated its ability to reduce NO and reactive oxygen species (ROS) production in a dose-dependent manner. These findings underscore the potential of the pyrrolidine amide derivative of bakuchiol as a promising candidate for the development of new anti-inflammatory drugs (**Figure 1.17)**.[87]

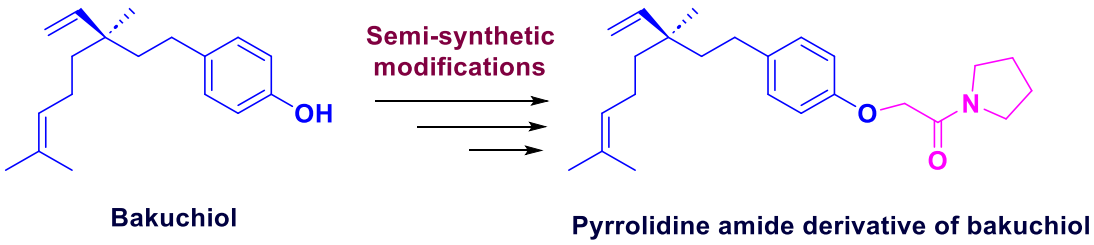

Figure 1.17. Semisynthetic modification of bakuchiol

1.10.2.2. Coixol derivatives as effective anti-inflammatory agents

Coixol, a derivative of 2-benzoxazolinone extracted from *Coix lachryma-jobi L.*, has demonstrated significant anti-inflammatory properties while exhibiting low cytotoxicity. In 2020, Cui et al., designed and synthesized a series of derivatives by hybridizing coixol with cinnamic acid in an effort to develop new anti-inflammatory agents. The anti-inflammatory potential of these derivatives was evaluated by assessing their ability to

inhibit LPS-induced overproduction of nitric oxide (NO) in RAW264.7 macrophages. Notably, the furan derivatives showed markedly greater activity compared to both coixol and the reference drug celecoxib. Mechanistic studies indicated that these compounds suppressed the expression of key pro-inflammatory mediators, including induced nitric oxide synthase (iNOS), tumor necrosis factor-alpha (TNF-α), interleukin-6 (IL-6), and interleukin-1β (IL-1β), through the inhibition of the nuclear factor-kappa B (NF-κB) signaling pathway. Moreover, *in vivo* studies conducted using a xylene-induced ear edema model in mice confirmed their anti-inflammatory efficacy. These preliminary *in vitro* and *in vivo* findings underscore the potential of these derivatives as promising candidates for the development of new anti-inflammatory drugs (**Figure 1.18)**.[88]

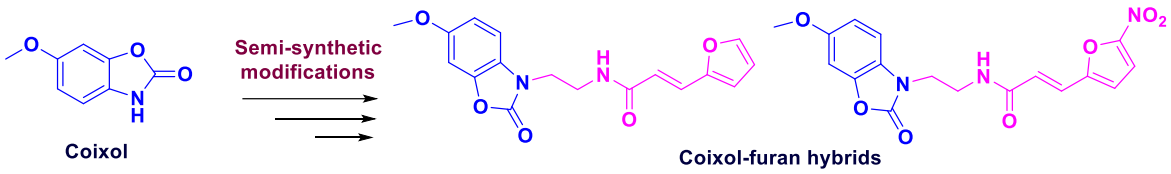

Figure 1.18. Semisynthetic modification of coixol

1.10.2.3. Cajaninstilbene acid derivatives as effective anti-inflammatory agents

Cajaninstilbene acid (CSA), an active compound extracted from pigeon pea leaves (*Cajanus cajan*), exhibits notable anti-inflammatory properties. In 2016, Chen et al., investigated the anti-inflammatory effects of CSA and its synthesized derivatives through both *in vitro* and *in vivo* models. *In vitro* studies using macrophage cell models revealed that these compounds showed comparable or superior inhibitory effects on the release of inflammatory mediators and cytokines (NO, TNF-α, and IL-6) compared to indomethacin. Notably, derivatives with halogen substituents on the phenyl B ring demonstrated enhanced anti-inflammatory activity. *In vivo* evaluation using transgenic zebrafish larvae confirmed that CSA and its fluoro-substituted derivative significantly reduced neutrophil production and migration, as well as primitive macrophage accumulation, in injured larvae. Mechanistic studies suggested that the anti-inflammatory effects of CSA and its fluoro-substituted derivative were mediated through suppression of NF-κB and MAPK pathway activation. These findings highlight the potential of CSA and its derivatives as promising candidates for anti-inflammatory drug development (**Figure 1.19)**.[89]

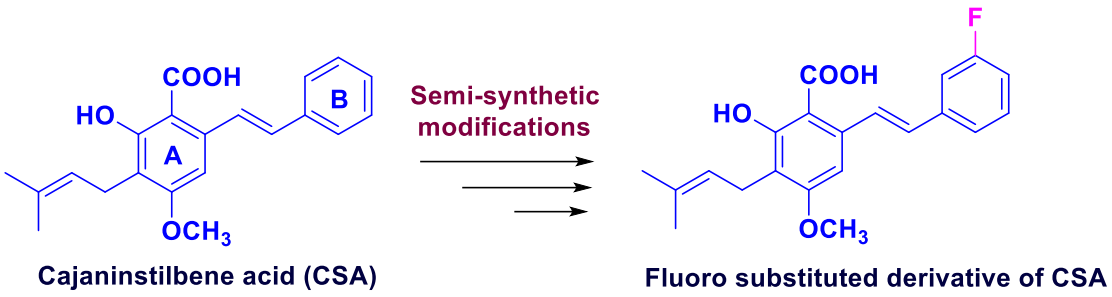

Figure 1.19. Semisynthetic modification of CSA

1.10.2.4. Pyxinol Derivatives as novel anti-inflammatory agents

Pyxinol, the primary metabolite of 20S-protopanaxadiol (a key intestinal metabolite of ginsenosides, the bioactive constituents of ginseng derived from the roots of *Panax ginseng* Meyer), serves as a promising scaffold for the development of anti-inflammatory agents. In 2020, Sun et al., synthesized and evaluated pyxinol derivatives by modifying the C-3, C-12, and C-25 positions, in addition to selected stereoisomers, for their *in vitro* anti-inflammatory activities. A structure–activity relationship (SAR) analysis, focusing on the pyxinol skeleton, was conducted to assess the derivatives' ability to inhibit lipopolysaccharide (LPS)-induced nitric oxide (NO) synthesis. Preliminary findings revealed that the biological activity of these derivatives is highly influenced by the R/S stereochemistry of the pyxinol skeleton, with the hydroxy group at C-3 identified as a key modifiable position. Among the tested compounds, 3-oximinopyxinol demonstrated the most potent NO-inhibitory activity, comparable to that of steroidal drugs. Additionally, the `compound significantly reduced LPS-induced TNF-α and IL-6 production, as well as the expression of iNOS and COX-2, by modulating the NF-κB pathway. These results establish pyxinol as a compelling scaffold for anti-inflammatory drug discovery and development (**Figure 1.20**).[90]

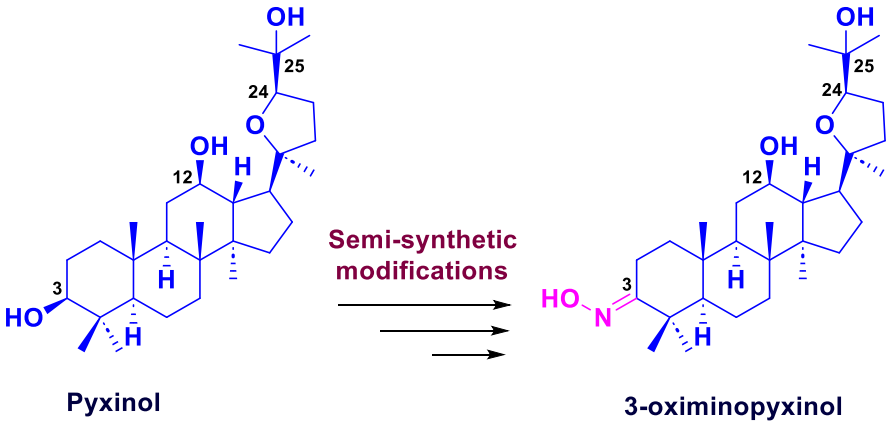

Figure 1.20. Semisynthetic modification of Pyxinol

1.10.2.5. Semisynthetic modifications of andrographolide

Andrographolide, a key component of *Andrographis paniculata*, a traditional Chinese medicine used for treating inflammation, has demonstrated a broad range of bioactivities. In 2018, Wang et al., synthesized two series of andrographolide derivatives, incorporating nitrogen-containing heterocycles, phenols, and aromatic acids as bioisosteric replacements for the lactone ring. Among these derivatives, a phenolic compound showed the most potent NO inhibitory effect, with an IC_{50} of 3.38 ± 1.03 μM. The structure-activity relationship (SAR) analysis indicated that replacing the lactone ring with small-molecule phenols enhanced anti-inflammatory efficacy. Furthermore, this compound significantly reduced the levels of pro-inflammatory cytokines IL-1β and IL-6 without affecting cell viability. Overall, the anti-inflammatory mechanism of this compound is associated with the inhibition of COX-2, iNOS, and the NF-κB signaling pathway (**Figure 1.21**).[91]

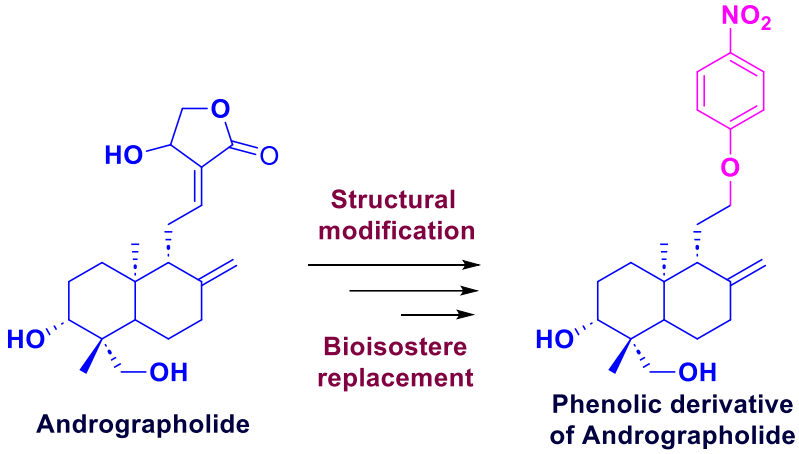

Figure 1.21. Semisynthetic modification of andrographolide

1.10.2.6. Unnatural estrane enantiomers as potent anti-inflammatory agents

Nicholson et al. identified a novel class of potent dissociated glucocorticoid receptor modulators by merging natural product frameworks with pharmaceutical lead compounds. This approach led to the development of unnatural estrane enantiomers, which demonstrated significant efficacy in suppressing the release of pro-inflammatory cytokines like IL-6 and TNF-α, highlighting their potential in advancing anti-inflammatory therapeutic strategies(**Figure 1.22**).[92]

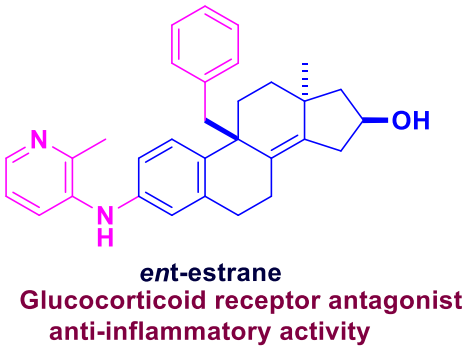

Figure 1.22. *ent*-strane

1.10.2.7. Novel resveratrol-based flavonol derivatives

In 2019, Chen et al., developed and synthesized a series of thirty-seven novel resveratrol-based flavonol derivatives to identify potential anti-inflammatory agents. Their structure-activity relationship (SAR) studies confirmed that introducing a hydroxyl group into the flavonoid structure enhances anti-inflammatory activity. They identified the most promising compound, which exhibited both high activity and low toxicity. Mechanistic investigations revealed that this compound inhibited TLR4 protein expression, thereby preventing the activation of the NF-κB signaling pathway. Its *in vivo* anti-inflammatory potential was validated in a mouse model of LPS-induced acute lung injury (ALI), where it effectively reduced pulmonary inflammation. These findings highlight a promising scaffold for designing more efficient inhibitors to regulate acute lung injury (**Figure 1.23**).[93]

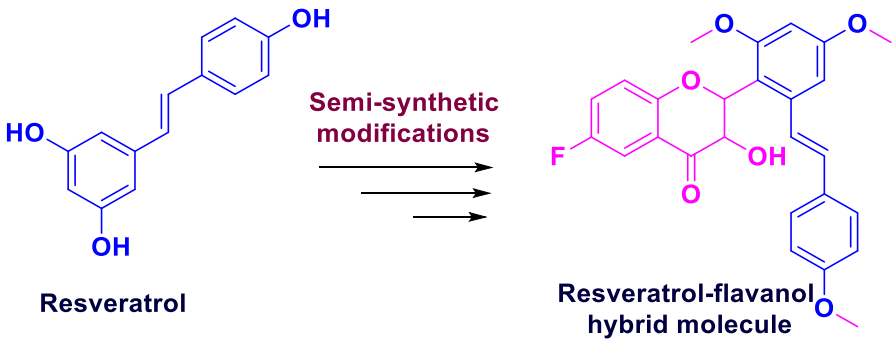

Figure 1.23. Semisynthetic modification of resveratrol

1.10.2.8. Betulin derivatives as effective anti-inflammatory agents

Betulin, a pharmacologically active triterpenoid found in the bark of birch trees (*Betula* sp. L.), along with its derivative betulinic acid, shares structural similarities with anti-

inflammatory steroids. However, their potential anti-inflammatory properties have yet to be thoroughly explored. In 2015, Laavola and colleagues conducted a study investigating the anti-inflammatory effects of betulin, betulinic acid, and 16 semisynthetic derivatives of betulin, concentrating on their influence on inflammatory gene expression. Among their findings, they identified a novel pyrazole-appended derivative of betulin that exhibited broad-spectrum anti-inflammatory activity. This compound significantly suppressed key inflammatory mediators, including cytokines such as interleukin-6 (IL-6), monocyte chemotactic protein-1 (MCP-1), prostaglandin synthase-2 (COX-2), and inducible nitric oxide synthase (iNOS). Additionally, its *in vivo* efficacy was demonstrated by a marked reduction in carrageenan-induced paw inflammation in mice. These findings reveal for the first time the substantial anti-inflammatory properties of the pyrazole-fused betulin derivative and suggest considerable therapeutic potential for related compounds (**Figure 1.24)**.[94]

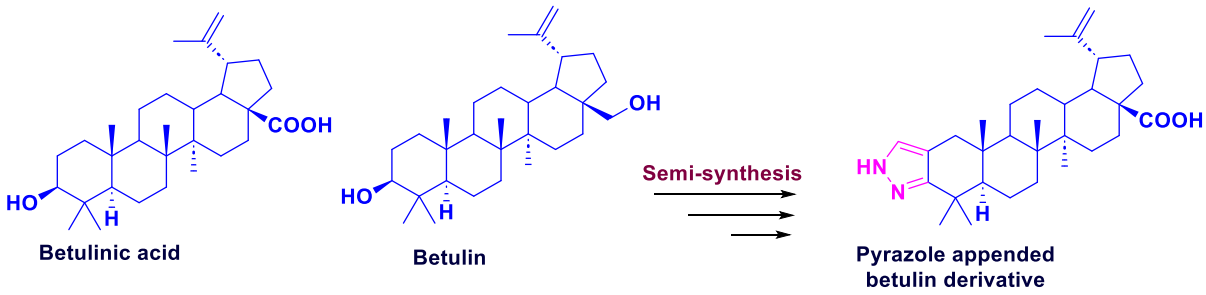

Figure 1.24. Betulinic acid, betulin and its semisynthetic modification

1.11. Conclusions and outline of the thesis

Natural products continue to serve as an invaluable source for next-generation drug development. Among these, plant-derived natural compounds are particularly notable for their potent anti-inflammatory properties. The semisynthetic modification of natural products has emerged as a transformative approach in drug discovery, bridging the gap between nature's vast chemical diversity and the therapeutic demands of modern medicine. These modifications not only enhance the efficacy and safety profiles of natural compounds but also expand their therapeutic potential, underscoring their pivotal role in addressing global health challenges. Inflammation is the body's natural defense mechanism against external stimuli, such as microbial infections or tissue injury. However, chronic inflammation is a key contributor to the onset of various diseases. The limitations of existing treatments highlight the urgent need for the development of novel, cost-effective, and therapeutically enhanced anti-inflammatory drugs. Addressing this challenge, our

research focuses on isolating abundant marker compounds from the rhizomes of Curcuma amada and transforming them into biologically significant heterocyclic hybrids through synthetic modification. These hybrids are subsequently evaluated for their potential anti-inflammatory activity. The major objectives of the thesis include:

- Isolation of abundant bioactive compounds from *Curcuma amada* rhizomes, followed by the semi-synthetic modifications to identify potential anti-inflammatory lead analogs
- Biological evaluation of the semisynthetic conjugates against multifaceted inflammatory targets
- Identification of potential hits, leads and optimization of the leads for the discovery of anti-inflammatory agents

The marker compound, (E)-labda-8(17), 12-diene-15, 16-dial, isolated from the rhizomes of *C. amada* was synthetically transformed into various heterocyclic appended labdane molecules *via* molecular hybridisation strategy. The isolates and synthetic derivatives were screened against multifaceted inflammatory targets. **Chapter 2** outlines the materials and methods employed in the experiments described in the subsequent chapters. In **Chapter 3,** we present rational designing and synthesis of novel phytochemical entities (NPCEs) through strategic linker-based molecular hybridization of aromatic or hetero-aromatic fragments with the labdane dialdehyde, isolated from the medicinally and nutritionally significant rhizomes of the plant *Curcuma amada*. The anti-inflammatory efficacy of the derivatives was evaluated. In **Chapter 4**, a ligand-based pharmacophoric approach was employed to design and synthesize thirty-three novel semi-synthetic labdane-appended triazolyl isatins to discover potential anti-inflammatory agents. In **Chapter 5**, as part of the lead optimization process, we have modified the existing lead compound by incorporating different heterocyclic amides into the labdane template, to enhance the biological properties of the abundant bioactive compound.

1.12. References

(1) Medzhitov, R. Origin and Physiological Roles of Inflammation. *Nature* **2008**, *454* (7203), 428–435. https://doi.org/10.1038/nature07201.

(2) Nathan, C.; Ding, A. Nonresolving Inflammation. *Cell* **2010**, *140* (6), 871–882. https://doi.org/10.1016/j.cell.2010.02.029.

(3) Chen, L.; Deng, H.; Cui, H.; Fang, J.; Zuo, Z.; Deng, J.; Li, Y.; Wang, X.; Zhao, L. Oncotarget 7204 Www.Impactjournals.Com/Oncotarget Inflammatory Responses and Inflammation-Associated Diseases in Organs. *Oncotarget* **2018**, *9* (6), 7204–7218.

(4) Alexander, R. W. Inflammation and Coronary Artery Disease. *N. Engl. J. Med.* **1994**, *331* (7), 468–469. https://doi.org/10.1056/nejm199408183310709.

(5) Crusz, S. M.; Balkwill, F. R. Inflammation and Cancer: Advances and New Agents. *Nat. Rev. Clin. Oncol.* **2015**, *12* (10), 584–596. https://doi.org/10.1038/nrclinonc.2015.105.

(6) Kokiko-Cochran, O. N.; Godbout, J. P. The Inflammatory Continuum of Traumatic Brain Injury and Alzheimer's Disease. *Front. Immunol.* **2018**, *9* (APR). https://doi.org/10.3389/fimmu.2018.00672.

(7) Bai, R.; Jie, X.; Yao, C.; Xie, Y. Discovery of Small-Molecule Candidates against Inflammatory Bowel Disease. *Eur. J. Med. Chem.* **2020**, *185*, 111805. https://doi.org/10.1016/j.ejmech.2019.111805.

(8) Donath, M. Y.; Shoelson, S. E. Type 2 Diabetes as an Inflammatory Disease. *Nat. Rev. Immunol.* **2011**, *11* (2), 98–107. https://doi.org/10.1038/nri2925.

(9) Cain, D. W.; Cidlowski, J. A. Immune Regulation by Glucocorticoids. *Nat. Rev. Immunol.* **2017**, *17* (4), 233–247. https://doi.org/10.1038/nri.2017.1.

(10) Bleumink, G. S.; Feenstra, J.; Sturkenboom, M. C. J. M.; Stricker, B. H. C. Nonsteroidal Anti-Inflammatory Drugs and Heart Failure. *Drugs* **2003**, *63* (6), 525–534. https://doi.org/10.2165/00003495-200363060-00001.

(11) Schmid, A. S.; Neri, D. Advances in Antibody Engineering for Rheumatic Diseases. *Nat. Rev. Rheumatol.* **2019**, *15* (4), 197–207. https://doi.org/10.1038/s41584-019-0188-8.

(12) Pereira-Leite, C.; Nunes, C.; Jamal, S. K.; Cuccovia, I. M.; Reis, S. Nonsteroidal Anti-Inflammatory Therapy: A Journey Toward Safety. *Med. Res. Rev.* **2017**, *37* (4), 802–859. https://doi.org/10.1002/med.21424.

(13) Mitlehner, W. Non-Steroidal Anti-Inflammatory Drugs. *Dtsch. Arztebl. Int.* **2022**,

119 (33–34), 566. https://doi.org/10.3238/arztebl.m2022.0183.

(14) Dinarello, C. A. Anti-Inflammatory Agents: Present and Future. *Cell* **2010**, *140* (6), 935–950. https://doi.org/10.1016/j.cell.2010.02.043.

(15) Germolec, D. R.; Shipkowski, K. A.; Frawley, R. P.; Evans, E. Markers of Inflammation. *Methods Mol. Biol.* **2018**, *1803*, 57–79. https://doi.org/10.1007/978-1-4939-8549-4_5.

(16) Turner, M. D.; Nedjai, B.; Hurst, T.; Pennington, D. J. Cytokines and Chemokines: At the Crossroads of Cell Signalling and Inflammatory Disease. *Biochim. Biophys. Acta - Mol. Cell Res.* **2014**, *1843* (11), 2563–2582. https://doi.org/10.1016/j.bbamcr.2014.05.014.

(17) Kany, S.; Vollrath, J. T.; Relja, B. Cytokines in Inflammatory Disease. *Int. J. Mol. Sci.* **2019**, *20* (23), 1–31.

(18) Ulloa, L.; Tracey, K. J. The ' Cytokine Profile ': A Code for Sepsis. **2005**, *11* (2). https://doi.org/10.1016/j.molmed.2004.12.007.

(19) Kany, S.; Vollrath, J. T.; Relja, B. Cytokines in Inflammatory Disease. *Int. J. Mol. Sci.* **2019**, *20* (23). https://doi.org/10.3390/ijms20236008.

(20) Mosser, D. M.; Edwards, J. P. Exploring the Full Spectrum of Macrophage Activation. *Nat. Rev. Immunol.* **2008**, *8* (12), 958–969. https://doi.org/10.1038/nri2448.

(21) Howes, A.; Gabryšová, L.; O'Garra, A. Role of IL-10 and the IL-10 Receptor in Immune Responses. *Ref. Modul. Biomed. Sci.* **2014**, *1*, 1–11. https://doi.org/10.1016/b978-0-12-801238-3.00014-3.

(22) Saraiva, M.; O'Garra, A. The Regulation of IL-10 Production by Immune Cells. *Nat. Rev. Immunol.* **2010**, *10* (3), 170–181. https://doi.org/10.1038/nri2711.

(23) Simmons, D. L.; Botting, R. M.; Hla, T. Cyclooxygenase Isozymes: The Biology of Prostaglandin Synthesis and Inhibition. *Pharmacol. Rev.* **2004**, *56* (3), 387–437. https://doi.org/10.1124/pr.56.3.3.

(24) Jin, K.; Qian, C.; Lin, J.; Liu, B. Cyclooxygenase-2-Prostaglandin E2 Pathway: A Key Player in Tumor-Associated Immune Cells. *Front. Oncol.* **2023**, *13* (January), 1–10. https://doi.org/10.3389/fonc.2023.1099811.

(25) Guan, F.; Wang, H.; Shan, Y.; Chen, Y.; Wang, M.; Wang, Q.; Yin, M.; Zhao, Y.; Feng, X.; Zhang, J. Inhibition of COX-2 and PGE2 in LPS-stimulated RAW264.7 Cells by Lonimacranthoide VI, a Chlorogenic Acid Ester Saponin. *Biomed Rep* **2014**, *2* (5), 760–764. https://doi.org/10.3892/br.2014.314.

(26) Luo, C.; He, M. L.; Bohlin, L. Is COX-2 a Perpetrator or a Protector? Selective COX-2 Inhibitors Remain Controversial. *Acta Pharmacol. Sin.* **2005**, *26* (8), 926–933. https://doi.org/10.1111/j.1745-7254.2005.00150.x.

(27) Bogdan, C. Nitric Oxide and the Immune Response - Nature Immunology. *Nat. Immunol.* **2001**, *2* (10), 907–916.

(28) Cinelli, M. A.; Do, H. T.; Miley, G. P.; Silverman, R. B. Inducible Nitric Oxide Synthase: Regulation, Structure, and Inhibition. *Med. Res. Rev.* **2020**, *40* (1), 158–189. https://doi.org/10.1002/med.21599.

(29) Papi, S.; Ahmadizar, F.; Hasanvand, A. The Role of Nitric Oxide in Inflammation and Oxidative Stress. *Immunopathol. Persa* **2019**, *5* (1), 3–6. https://doi.org/10.15171/ipp.2019.08.

(30) Paige, J.; Jaffrey, S. Pharmacologic Manipulation of Nitric Oxide Signaling: Targeting NOS Dimerization and Protein-Protein Interactions. *Curr. Top. Med. Chem.* **2006**, *7* (1), 97–114. https://doi.org/10.2174/156802607779318253.

(31) Sen, R.; Baltimore, D. Inducibility of κ Immunoglobulin Enhancer-Binding Protein NF-KB by a Posttranslational Mechanism. *Cell* **1986**, *47* (6), 921–928. https://doi.org/https://doi.org/10.1016/0092-8674(86)90807-X.

(32) MedComm - 2021 - Zhang - NF- B Signaling in Inflammation and Cancer.Pdf.

(33) Ghosh, S.; Hayden, M. S. New Regulators of NF-KB in Inflammation. *Nat. Rev. Immunol.* **2008**, *8* (11), 837–848. https://doi.org/10.1038/nri2423.

(34) Aggarwal, B. B. Nuclear Factor-KB: The Enemy Within. *Cancer Cell*. 2004, pp 203–208. https://doi.org/10.1016/j.ccr.2004.09.003.

(35) Liu, T.; Zhang, L.; Joo, D.; Sun, S. C. NF-KB Signaling in Inflammation. *Signal Transduct. Target. Ther.* **2017**, *2* (April). https://doi.org/10.1038/sigtrans.2017.23.

(36) Kong, P.; Cui, Z. Y.; Huang, X. F.; Zhang, D. D.; Guo, R. J.; Han, M. Inflammation and Atherosclerosis: Signaling Pathways and Therapeutic Intervention. *Signal Transduct. Target. Ther.* **2022**, *7* (1). https://doi.org/10.1038/s41392-022-00955-7.

(37) Cragg, G. M.; Newman, D. J. Natural Products: A Continuing Source of Novel Drug Leads. *Biochim. Biophys. Acta - Gen. Subj.* **2013**, *1830* (6), 3670–3695. https://doi.org/10.1016/j.bbagen.2013.02.008.

(38) Najmi, A.; Javed, S. A.; Al Bratty, M.; Alhazmi, H. A. Modern Approaches in the Discovery and Development of Plant-Based Natural Products and Their Analogues as Potential Therapeutic Agents. *Molecules* **2022**, *27* (2). https://doi.org/10.3390/molecules27020349.

(39) Newman, D. J.; Cragg, G. M.; Snader, K. M. Natural Products as Sources of New Drugs over the Period 1981-2002. *J. Nat. Prod.* **2003**, *66* (7), 1022–1037. https://doi.org/10.1021/np030096l.

(40) Newman, D. J.; Cragg, G. M. Natural Products as Sources of New Drugs over the Nearly Four Decades from 01/1981 to 09/2019. *J. Nat. Prod.* **2020**, *83* (3), 770–803. https://doi.org/10.1021/acs.jnatprod.9b01285.

(41) Cragg, G. M.; Grothaus, P. G.; Newman, D. J. Impact of Natural Products on Developing New Anti-Cancer Agents †. **2009**, 3012–3043.

(42) Reis Nunes, C.; Barreto Arantes, M.; Menezes de Faria Pereira, S.; Leandro da Cruz, L.; De Souza Passos, M.; Pereira de Moraes, L.; Curcino Vieira, I. J.; Barros de Oliveira, D. Plants as Sources of Anti-Inflammatory Agents. *Molecules* **2020**, *25* (3726), 1–22.

(43) Patridge, E.; Gareiss, P.; Kinch, M. S.; Hoyer, D. An Analysis of FDA-Approved Drugs: Natural Products and Their Derivatives. *Drug Discov. Today* **2016**, *21* (2), 204–207. https://doi.org/10.1016/j.drudis.2015.01.009.

(44) Cragg, G. M.; Newman, D. J. Natural Products: A Continuing Source of Novel Drug Leads. *Biochim. Biophys. Acta - Gen. Subj.* **2013**, *1830* (6), 3670–3695. https://doi.org/10.1016/j.bbagen.2013.02.008.

(45) M.C. Recio; I. Andujar; J.L. Rios. Anti-Inflammatory Agents from Plants: Progress and Potential. *Curr. Med. Chem.* **2012**, *19* (14), 2088–2103. https://doi.org/10.2174/092986712800229069.

(46) Dias, D. A.; Urban, S.; Roessner, U. A Historical Overview of Natural Products in Drug Discovery. *Metabolites* **2012**, *2* (2), 303–336. https://doi.org/10.3390/metabo2020303.

(47) Wang, R. X.; Zhou, M.; Ma, H. L.; Qiao, Y. B.; Li, Q. S. The Role of Chronic Inflammation in Various Diseases and Anti-Inflammatory Therapies Containing Natural Products. *ChemMedChem* **2021**, *16* (10), 1576–1592. https://doi.org/10.1002/cmdc.202000996.

(48) Wang, Y.; Zeng, K. Natural Products as a Crucial Source of Anti-Inflammatory Drugs: Recent Trends and Advancements. *Tradit. Med. Res.* **2019**, *4* (5), 257–268. https://doi.org/10.53388/tmr20190831133.

(49) R., F.; I., Z. Plant-Derived Anti-Inflammatory Compounds: Hopes and Disappointments Regarding the Translation of Preclinical Knowledge into Clinical Progress. *Mediators Inflamm.* **2014**, *2014*.

(50) Lahlou, M. The Success of Natural Products in Drug Discovery. *Pharmacol. & Pharm.* **2013**, *04* (03), 17–31. https://doi.org/10.4236/pp.2013.43a003.

(51) Shah, B. N.; Seth, A. K.; Maheshwari, K. M. A Review on Medicinal Plants as a Source of Anti-Inflammatory Agents. *Res. J. Med. Plant* **2011**, *5* (2), 101–115. https://doi.org/10.3923/rjmp.2011.101.115.

(52) Venkatesha, S. H.; Acharya, B.; Moudgil, K. D. Natural Products as Source of Anti-Inflammatory Drugs. *Inflamm. - From Mol. Cell. Mech. to Clin.* **2017**, 1661–1690. https://doi.org/10.1002/9783527692156.ch65.

(53) Zhou, Y. Q.; Liu, H.; He, M. X.; Wang, R.; Zeng, Q. Q.; Wang, Y.; Ye, W. C.; Zhang, Q. W. *A Review of the Botany, Phytochemical, and Pharmacological Properties of Galangal*; Elsevier Inc., 2018; Vol. 7. https://doi.org/10.1016/C2016-0-00380-7.

(54) Tamokou, J. de D.; Mbaveng, A. T.; Kuete, V. *Antimicrobial Activities of African Medicinal Spices and Vegetables*; 2017. https://doi.org/10.1016/B978-0-12-809286-6.00008-X.

(55) Al-Qudah, T. S.; Abu Malloh, S.; Nawaz, A.; Adnan Ayub, M.; Nisar, S.; Idrees Jilani, M.; Said Al-Qudah, T. Mango Ginger (Curcuma Amada Roxb.): A Phytochemical Mini Review. *Ijcbs* **2017**, *11* (September 2019), 51.

(56) Yuandani; Jantan, I.; Rohani, A. S.; Sumantri, I. B. Immunomodulatory Effects and Mechanisms of Curcuma Species and Their Bioactive Compounds: A Review. *Front. Pharmacol.* **2021**, *12* (April), 1–26. https://doi.org/10.3389/fphar.2021.643119.

(57) Azeez, T. B.; Lunghar, J. 6 - Antiinflammatory Effects of Turmeric (Curcuma Longa) and Ginger (Zingiber Officinale); Gopi, S., Amalraj, A., Kunnumakkara, A., Thomas, S. B. T.-I. and N. P., Eds.; Academic Press, 2021; pp 127–146. https://doi.org/https://doi.org/10.1016/B978-0-12-819218-4.00011-0.

(58) Rajkumari, S.; Sanatombi, K. Nutritional Value, Phytochemical Composition, and Biological Activities of Edible Curcuma Species: A Review. *Int. J. Food Prop.* **2018**, *20* (3), S2668–S2687. https://doi.org/10.1080/10942912.2017.1387556.

(59) Dosoky, N. S.; Setzer, W. N. Chemical Composition and Biological Activities of Essential Oils of Curcuma Species. *Nutrients*. 2018. https://doi.org/10.3390/nu10091196.

(60) Ewon, K.; Bhagya, A. S. A Review on Golden Species of Zingiberaceae Family around the World: Genus Curcuma. *African J. Agric. Res.* **2019**, *14* (9), 519–531.

https://doi.org/10.5897/ajar2018.13755.

(61) Policegoudra, R. S.; Aradhya, S. M.; Singh, L. Mango Ginger (Curcuma Amada Roxb.) - A Promising Spice for Phytochemicals and Biological Activities. *J. Biosci.* **2011**, *36* (4), 739–748. https://doi.org/10.1007/s12038-011-9106-1.

(62) Rahaman, M. M.; Rakib, A.; Mitra, S.; Tareq, A. M.; Emran, T. Bin; Shahid-Ud-daula, A. F. M.; Amin, M. N.; Simal-Gandara, J. The Genus Curcuma and Inflammation: Overview of the Pharmacological Perspectives. *Plants* **2021**, *10* (1), 1–19. https://doi.org/10.3390/plants10010063.

(63) Singh, S.; Singh, R.; Banerjee, S.; Negi, A. S.; Shanker, K. Determination of Anti-Tubercular Agent in Mango Ginger (Curcuma Amada Roxb.) by Reverse Phase HPLC-PDA-MS. *Food Chem.* **2012**, *131* (1), 375–379. https://doi.org/10.1016/j.foodchem.2011.08.054.

(64) Bhutia, P. H.; Viswavidyalaya, K.; Sharangi, A. B. Promising Curcuma Species Suitable for Hill Regions towards Maintaining Biodiversity. *J. Pharmacogn. Phytochem.* **2017**, *6* (6), 726–731.

(65) Syamkumar, S.; Sasikumar, B. Molecular Marker Based Genetic Diversity Analysis of Curcuma Species from India. *Sci. Hortic. (Amsterdam).* **2007**, *112* (2), 235–241. https://doi.org/https://doi.org/10.1016/j.scienta.2006.12.021.

(66) Ramachandran, C.; Quirin, K. W.; Escalon, E. A.; Lollett, I. V.; Melnick, S. J. Therapeutic Effect of Supercritical CO2 Extracts of Curcuma Species with Cancer Drugs in Rhabdomyosarcoma Cell Lines. *Phyther. Res.* **2015**, *29* (8), 1152–1160. https://doi.org/10.1002/ptr.5360.

(67) Singh, S.; Kumar, J. K.; Saikia, D.; Shanker, K.; Thakur, J. P.; Negi, A. S.; Banerjee, S. A Bioactive Labdane Diterpenoid from Curcuma Amada and Its Semisynthetic Analogues as Antitubercular Agents. *Eur. J. Med. Chem.* **2010**, *45* (9), 4379–4382. https://doi.org/10.1016/j.ejmech.2010.06.006.

(68) Jatoi, S. A.; Kikuchi, A.; Gilani, S. A.; Watanabe, K. N. Phytochemical, Pharmacological and Ethnobotanical Studies in Mango Ginger (Curcuma Amada Roxb.; Zingiberaceae). *Phyther. Res.* **2007**, *21* (6), 507–516. https://doi.org/https://doi.org/10.1002/ptr.2137.

(69) Policegoudra, R. S.; Abiraj, K.; Gowda, D. C.; Aradhya, S. M. Isolation and Characterization of Antioxidant and Antibacterial Compound from Mango Ginger (Curcuma Amada Roxb.) Rhizome. *J. Chromatogr. B* **2007**, *852* (1), 40–48. https://doi.org/https://doi.org/10.1016/j.jchromb.2006.12.036.

(70) Kumar, P. V.; T.Mangilal; Priya, A. S.; Jatoth, K.; Banu, R. F. Evaluation of Antipyretic Activity of Aqueous Extract of Curcuma Amada. *Int. J. Pharm. Phamaceutical Res.* **2015**, *3* (3).

(71) Anjusha, S.; Gangaprasad, A. Phytochemical and Antibacterial Analysis of Two Important Curcuma Species, Curcuma Aromatica Salisb. and Curcuma Xanthorrhiza Roxb.(Zingiberaceae). *J. Pharmacogn. Phytochem.* **2014**, *3* (3), 50–53.

(72) Sharma, G. J.; Chirangini, P.; Kishor, R. Gingers of Manipur: Diversity and Potentials as Bioresources. *Genet. Resour. Crop Evol.* **2011**, *58* (5), 753–767. https://doi.org/10.1007/s10722-011-9678-5.

(73) Pandey, A. K.; Chowdhury, A. R. Volatile Constituents of the Rhizome Oil of Curcuma Caesia Roxb. from Central India. *Flavour Fragr. J.* **2003**, *18* (5), 463–465. https://doi.org/10.1002/ffj.1255.

(74) Mujumdar, A. M.; Naik, D. G.; Dandge, C. N.; Puntambekar, H. M. Antiinflammatory Activity of Curcuma Amada Roxb. In Albino Rats. *Indian J. Pharmacol.* **2000**, *32* (6), 375–377.

(75) Nagavekar, N.; Singhal, R. S. Supercritical Fluid Extraction of Curcuma Longa and Curcuma Amada Oleoresin: Optimization of Extraction Conditions, Extract Profiling, and Comparison of Bioactivities. *Ind. Crops Prod.* **2019**, *134* (March), 134–145. https://doi.org/10.1016/j.indcrop.2019.03.061.

(76) DeCorte, B. L. Underexplored Opportunities for Natural Products in Drug Discovery. *J. Med. Chem.* **2016**, *59* (20), 9295–9304. https://doi.org/10.1021/acs.jmedchem.6b00473.

(77) Bennani, Y. L. Natural Products in Medicine: Transformational Outcome of Synthetic Chemistry. **2014**, No. c.

(78) Guo, Z. The Modi Fi Cation of Natural Products for Medical Use. **2016**. https://doi.org/10.1016/j.apsb.2016.06.003.

(79) Aicher, T. D.; Buszek, K. R.; Fang, F. G.; Forsyth, C. J.; Jung, S. H.; Kishi, Y.; Matelich, M. C.; Scola, P. M.; Spero, D. M.; Yoon, S. K. Total Synthesis of Halichondrin B and Norhalichondrin B. *J. Am. Chem. Soc.* **1992**, *114* (8), 3162–3164. https://doi.org/10.1021/ja00034a086.

(80) Swami, U.; Shah, U.; Goel, S. Eribulin in Cancer Treatment. *Mar. Drugs* **2015**, *13* (8), 5016–5058. https://doi.org/10.3390/md13085016.

(81) Nikolic, V. D.; Savic, I. M.; Savic, I. M.; Nikolic, L. B.; Stankovic, M. Z.; Marinkovic, V. D. Paclitaxel as an Anticancer Agent: Isolation, Activity, Synthesis

and Stability. *Cent. Eur. J. Med.* **2011**, *6* (5), 527–536. https://doi.org/10.2478/s11536-011-0074-5.

(82) Yao, H.; Liu, J.; Xu, S.; Zhu, Z.; Xu, J. Expert Opinion on Drug Discovery The Structural Modification of Natural Products for Novel Drug Discovery. **2016**, *0441* (December). https://doi.org/10.1080/17460441.2016.1272757.

(83) Chiba, K. Discovery of Fingolimod Based on the Chemical Modification of a Natural Product from the Fungus, Isaria Sinclairii. *J. Antibiot. (Tokyo).* **2020**, *73* (10), 666–678. https://doi.org/10.1038/s41429-020-0351-0.

(84) Chen, J.; Li, W.; Yao, H.; Xu, J. Insights into Drug Discovery from Natural Products through Structural Modification. *Fitoterapia* **2015**. https://doi.org/10.1016/j.fitote.2015.04.012.

(85) Haynes, R. K.; Fugmann, B.; Stetter, J.; Rieckmann, K.; Heilmann, H.; Chan, H.; Cheung, M.; Lam, W.; Wong, H.; Croft, S. L.; Vivas, L.; Rattray, L.; Stewart, L.; Peters, W.; Robinson, B. L.; Edstein, M. D.; Kotecka, B.; Kyle, D. E.; Beckermann, B.; Gerisch, M.; Radtke, M.; Schmuck, G.; Steinke, W.; Wollborn, U.; Schmeer, K.; Römer, A. Artemisone—A Highly Active Antimalarial Drug of the Artemisinin Class**. **2006**, 2082–2088. https://doi.org/10.1002/anie.200503071.

(86) Cragg, G. M.; Grothaus, P. G.; Newman, D. J. Impact of Natural Products on Developing New Anti-Cancer Agents. *Chem. Rev.* **2009**, *109* (7), 3012–3043. https://doi.org/10.1021/cr900019j.

(87) Ma, Q.; Bian, M.; Gong, G.; Bai, C.; Liu, C.; Wei, C.; Quan, Z. S.; Du, H. H. Synthesis and Evaluation of Bakuchiol Derivatives as Potent Anti-Inflammatory Agents in Vitro and in Vivo. *J. Nat. Prod.* **2022**, *85* (1), 15–24. https://doi.org/10.1021/acs.jnatprod.1c00377.

(88) Cui, E.; Qian, S.; Li, J.; Jiang, X.; Wang, H.; Du, S.; Du, L. Discovery of Coixol Derivatives as Potent Anti-Inflammatory Agents. *J. Nat. Prod.* **2023**, *86* (8), 1950–1959. https://doi.org/10.1021/acs.jnatprod.3c00309.

(89) Huang, M. Y.; Lin, J.; Lu, K.; Xu, H. G.; Geng, Z. Z.; Sun, P. H.; Chen, W. M. Anti-Inflammatory Effects of Cajaninstilbene Acid and Its Derivatives. *J. Agric. Food Chem.* **2016**, *64* (14), 2893–2900. https://doi.org/10.1021/acs.jafc.6b00227.

(90) Sun, Y.; Fang, X.; Gao, M.; Wang, C.; Gao, H.; Bi, W.; Tang, H.; Cui, Y.; Zhang, L.; Fan, H.; Yu, H.; Yang, G. Synthesis and Structure-Activity Relationship of Pyxinol Derivatives as Novel Anti-Inflammatory Agents. *ACS Med. Chem. Lett.* **2020**, *11* (4), 457–463. https://doi.org/10.1021/acsmedchemlett.9b00562.

(91) Wang, W.; Wu, Y.; Chen, X.; Zhang, P.; Li, H.; Chen, L. Synthesis of New Ent-Labdane Diterpene Derivatives from Andrographolide and Evaluation of Their Anti-Inflammatory Activities. *Eur. J. Med. Chem.* **2019**, *162*, 70–79. https://doi.org/10.1016/j.ejmech.2018.11.002.

(92) Nicholson, J. M.; Yang, D.; Koelblen, T.; Hu, E. L.; Coss, C. C.; Burris, T. P.; Hu, X.; Micalizio, G. C. Merging Natural Product Structures with Pharmaceutical Leads: Unnatural Enantiomers of Estranes as Glucocorticoid Receptor Modulators That Suppress TNF-α and IL-6 Release. *J. Med. Chem.* **2024**. https://doi.org/10.1021/acs.jmedchem.4c01007.

(93) Chen, L. Z.; Yao, L.; Jiao, M. M.; Shi, J. B.; Tan, Y.; Ruan, B. F.; Liu, X. H. Novel Resveratrol-Based Flavonol Derivatives: Synthesis and Anti-Inflammatory Activity in Vitro and in Vivo. *Eur. J. Med. Chem.* **2019**, *175*, 114–128. https://doi.org/10.1016/j.ejmech.2019.05.004.

(94) Laavola, M.; Haavikko, R.; Hämäläinen, M.; Leppänen, T.; Nieminen, R.; Alakurtti, S.; Moreira, V. M.; Yli-Kauhaluoma, J.; Moilanen, E. Betulin Derivatives Effectively Suppress Inflammation in Vitro and in Vivo. *J. Nat. Prod.* **2016**, *79* (2), 274–280. https://doi.org/10.1021/acs.jnatprod.5b00709.

Materials and Methods

2.1. Materials

All the chemicals and reagents, used for the isolation and semi-synthetic modifications of *E*-labda 8(17),12-diene -15,16-dial (**1**), were purchased from Sigma-Aldrich and Spectrochem, and were of commercial reagent grade. Solvents were purchased from Merck and were distilled before use. TLC plates (silica gel 60 F254) were used to monitor the purity of the isolated compounds and the reaction progress. The IR spectra were recorded on Bruker Alpha-T FT-IR spectrometer. ^{1}H and ^{13}C NMR spectra were recorded at 500 MHz and 125 MHz respectively, on Bruker ASCEND^{TM} spectrometer using $CDCl_3$ as the solvent and tetramethylsilane (TMS) as the internal standard. Chemical shift values are reported in δ scale, and coupling constants in Hertz. The solvent ($CDCl_3$) peak emerged as a singlet in ^{1}H NMR at 7.19 and as a triplet in ^{13}C NMR at 77.0. HRMS (ESI) mass spectra were acquired using a Thermo Scientific Exactive Orbitrap mass spectrometer. Labdane dialdehyde and its synthesized analogs were purified using column chromatography on silica gel (100-200 mesh) with a solvent system of hexane-ethyl acetate. For solvent removal, a Heidolph rotating evaporator was employed. Dulbecco's Modified Eagle's Medium (DMEM-high glucose) and 100 U/mL penicillin-streptomycin (100 µg/ml) mix, were procured from Himedia Pvt. Ltd. (Mumbai, India). Fetal bovine serum (FBS) was from Gibco (Grand Island, NY). 3-[4,5-dimethylthiazol-2-yl]-2,5-diphenyl tetrazolium bromide (MTT), Griess reagent and indomethacin were purchased from Sigma-Aldrich (U.S.A). IL-1α ELISA kit and COX-2 inhibitor screening kit (fluorometric) were purchased from Abcam. TNF-α, IL-6, and IL-10 ELISA kits were purchased from BD Biosciences. Absorbance and fluorescence were recorded using a microplate reader (BIOTEK- USA). No unexpected or unusually high safety hazards were encountered.

2.2. Methodology

2.2.1. Chemistry

2.2.1.1. Isolation of *E*-labda 8(17),12-diene -15,16-dial (1)

One kilogram of dried and powdered rhizomes of *C. amada* was extracted three times with chloroform. 50 g of crude extract was obtained after solvent removal, which was then subjected to column chromatography on silica gel (100-200 mesh). Different fractions of

approximately 100 ml volume were collected by gradient elution using different polarities of hexane and ethyl acetate mixture. The fractions collected in 5% of ethyl acetate-hexane were crystallized in hexane to obtain the pure compound **1** (*E*-labda 8(17),12-diene -15,16-dial, 15 g) as a white solid. The structure of compound **1** was confirmed by various spectroscopic and analytical methods *viz.* IR, ^{1}H NMR, ^{13}C NMR, and HRMS, as well as by comparing it with the literature.[1,2]

2.2.1.2. General procedure for the synthesis of Zerumin A (2)

To a stirred solution of *E*-labda 8(17),12-diene -15,16-dial (**1**) (1 g, 1 equiv.) in DMF, oxone (2.034 g, 2 equiv.) was added and stirred at room temperature until the completion of the reaction, monitored by TLC. 1N HCl was added to the reaction mixture to dissolve the salts. The compound was extracted with ethyl acetate, dried over anhydrous Na_2SO_4, and the solvent was removed under reduced pressure to afford compound **2** (1 g, 95 % yield).[3] The structure of the compound was confirmed by various spectroscopic analyses as well as by comparing it with the reported literature.

2.2.1.3. General procedure for the synthesis of prop-2-yn-1-yl (*E*)-3-formyl-5-((1S,4aS,8aS)-5,5,8a-trimethyl-2-methylenedecahydronaphthalen-1-yl)pent-3-enoate (3)

To a stirred solution of Zerumin A (1 g, 1 equiv.) in DMF at 0 ^{o}C, propargyl bromide (0.3736 g, 1 equiv.) was added dropwise. K_2CO_3 (0.6510 g, 1.5 equiv.) was added to the reaction mixture and stirred at room temperature till the reaction was complete, as indicated by TLC. The compound was extracted with ethyl acetate, washed with brine and dried over anhydrous Na_2SO_4. The solvent was removed under reduced pressure to afford compound **2** (1.083 g, 97% yield). The structure of the compound was confirmed by various spectroscopic analyses as well as by comparing it with the reported literature.[4]

2.2.2. Biology

2.2.2.1. Cell culture

Murine macrophage cell line RAW264.7 was procured from NCCS (Pune) and the cells were maintained in Dulbecco's Modified Eagle Medium (DMEM) supplemented with 10% Fetal bovine serum and 100 units/mL penicillin streptomycin mix. The cell cultures were maintained at 37 °C in 5% CO_2 in a humidified atmosphere.

2.2.2.2. MTT assay

To determine the non-cytotoxic concentration in RAW264.7, an MTT assay[5] was performed for 24 hours. RAW264.7 cells were cultured in a 96-well plate at a density of $1X10^4$ cells/well and after attaining 70% confluency, the cells were treated with various concentrations of compounds (upto 20 μM). After 24 hours of pretreatment, the pretreated media was decanted, washed and 100 μL of MTT (0.5 mg/mL) suspended in plain media, was added and incubated for 4 hours at 37 °C in a CO_2 incubator. The supernatant was decanted followed by the addition of dimethyl sulfoxide (DMSO) to each well. The plate was held on for 30 minutes in a plate shaker and the absorbance was recorded at 570 nm using a micro-plate reader (BIOTEK- USA). Percentage viability was calculated using the following equation:

$$\text{Percentage of viability} = \left[\frac{\text{Absorbance of sample}}{\text{Absorbance of control}}\right] X\ 100$$

2.2.2.3. Determination of nitric oxide (NO) production

Followed by pre-treatment with compounds of varying concentrations for 1h and co-incubated with lipopolysaccharide LPS (1 μg/mL) for an additional 23 h, the concentration of nitrite in the culture medium as a sign of nitric oxide production was quantified using the Griess method.[6] Briefly, 50 μL of Griess reagent (1% sulfanilamide and 0.1% naphthylethylenediamine dihydrochloride in 2.5% phosphoric acid), and an equal volume of cell supernatant after pretreatment was conflated and the plate was incubated for 10 min at room temperature. The absorbance was measured in a microplate reader (BIOTEK-USA) at 540 nm. The concentration of nitrite was quantified based on a sodium nitrite standard curve. Indomethacin was used as the positive control.

2.2.2.4. COX-2 inhibitory assay

The potential of compounds to inhibit the enzyme COX-2 was determined using a COX-inhibitor screening kit (ABCAM, ab283401, fluorometric) according to the manufacturer's instructions. The IC_{50} value of the compounds was determined from the concentration inhibition response curve.

2.2.2.5. Measurement of pro-inflammatory cytokines (TNF-α, IL-6, IL-1α and IL-10)

RAW264.7 cells, seeded in six-well plates (1×10^6 cells/well), were treated with compounds at 20 μM concentration and LPS (1 μg/mL) for a period of 24 h. The pre-treated cell-free culture supernatant was collected, and the concentrations of the cytokines levels (TNF-α, IL-6, IL-1α and IL-10) in the culture medium were determined using ELISA kits according to the manufacturer's instructions. Indomethacin was employed as the positive control. The natural compound was also expended for the comparative evaluation of these semi-synthetic molecules.

2.2.2.6. Western blotting

Raw 264.7 cells were seeded into a six-well plate at a density of $4x10^6$ cells per well. The cells were pre-treated with the test compounds (upto 20 μM) and the positive control indomethacin (upto 20 μM) for 2h and then coincubated with LPS (1 μg/mL) for a period of 24 h. The cells were harvested, lysed with 200 μL RIPA cell lysis buffer (Sigma, United States) and incubated at 4 ^oC for 30 minutes. The cell lysate was collected and centrifuged for 5 minutes at 4 ^oC and the concentration of total protein was measured by a BCA protein assay kit (Pierce, Thermo Fischer). Protein samples were resolved using 8−10% SDS-polyacrylamide gel electrophoresis and transferred to polyvinylidene difluoride (PVDF) membranes electrophoretically. The membranes were blocked with tris-buffered saline containing 0.1% Tween 20 (TBST) and 5% skimmed milk for 1 h at room temperature. Each blotted membrane was incubated with the specific primary antibody against COX-2, iNOS, NF-κB, p-NF-κB and β-actin (1:1000) overnight at 4 ^oC. The membranes were washed with TBST three times and incubated with HRP-conjugated secondary antibody (1:2000) for 2 h at room temperature. The membranes were then probed with ECL substrate (Thermo Fisher Scientific, Massachusetts, USA) in Chemidoc MP Imaging systems (BioRad, USA). Densitometric analysis of the obtained bands was performed using the Image lab software version 6.1 (BioRad, USA).

2.2.2.7. Immunofluorescence assay

Raw 264.7 cells were seeded at a density of $2x10^5$ cells into a 96 black well clear bottomed plate. The cells were pre-treated with test compounds (upto 20 μM) and the positive control indomethacin (upto 20 μM) for 2h and then coincubated with LPS (1 μg/mL) for a period of 24 h. After incubation, cells were washed twice with 200 μL of PBS and fixed with 4%

paraformaldehyde for 15 min. The cells were permeabilised with 0.5% Triton x -100 for 10 min and then blocked with 5% bovine serum albumin (BSA) in PBS for 1 h at room temperature. The cells were then incubated overnight with a primary antibody specific to NF-κb p65 (1:250) at 4 ^{o}C. The cells were washed with PBST and incubated with a secondary antibody labelled with Alexa flour 488 diluted to 1:400 in PBST at 37 ^{o}C for 2 h. After washing, the nuclei were stained with 4′,6-diamidino-2-phenylindole (DAPI), and the wells were washed with PBS. The fluorescent microscope (OLYMPUS, Japan) was used to capture the images, with excitation/emission wavelengths of 490 nm/540 nm for the Alexa Fluor-488 and 360 nm/450 nm for the DAPI.

2.2.2.8. Statistical analysis

All the experiments were completed in triplicates and the data are expressed as mean ± standard deviation (SD). Data were analysed by GraphPad software: Dotmatics, followed by a two-sample unpaired t-test. P value was determined.

2.3. References

(1) Facile Isolation of (E) -Labda-8 (17), 12-Diene-15 , 16-Dial from Curcuma Amada and Its Conversion to Other Biologically Active Compounds. **2014**, *53* (March), 319–324.

(2) Singh, S.; Kumar, J. K.; Saikia, D.; Shanker, K.; Thakur, J. P.; Negi, A. S.; Banerjee, S. A Bioactive Labdane Diterpenoid from Curcuma Amada and Its Semisynthetic Analogues as Antitubercular Agents. *Eur. J. Med. Chem.* **2010**, *45* (9), 4379–4382. https://doi.org/10.1016/j.ejmech.2010.06.006.

(3) Travis, B. R.; Sivakumar, M.; Hollist, G. O.; Borhan, B. Facile Oxidation of Aldehydes to Acids and Esters with Oxone. *Org. Lett.* **2003**, *5* (7), 1031–1034. https://doi.org/10.1021/ol0340078.

(4) Jalaja, R.; Leela, S. G.; Valmiki, P. K.; Salfeena, C. T. F.; Ashitha, K. T.; Krishna Rao, V. R. D.; Nair, M. S.; Gopalan, R. K.; Somappa, S. B. Discovery of Natural Product Derived Labdane Appended Triazoles as Potent Pancreatic Lipase Inhibitors. *ACS Med. Chem. Lett.* **2018**, *9* (7), 662–666. https://doi.org/10.1021/acsmedchemlett.8b00109.

(5) Wilson, A. P. Cytotoxicity and Viability Assays. *Anim. cell Cult. a Pract. approach* **2000**, *1*, 175–219.

(6) Bryan, N. S.; Grisham, M. B. Methods to Detect Nitric Oxide and Its Metabolites in Biological Samples. *Free Radic. Biol. Med.* **2007**, *43* (5), 645–657. https://doi.org/https://doi.org/10.1016/j.freeradbiomed.2007.04.026.

Linker-Based Pharmacophoric Design and Semisynthesis of Aryl/Heteroaryl Appended Labdane Conjugates

3.1. Abstract

Prolonged inflammation leads to the genesis of various inflammatory diseases such as atherosclerosis, cancer, inflammatory bowel disease, Alzheimer's, etc. The uncontrolled inflammatory response is characterized by the excessive release of pro-inflammatory mediators such as nitric oxide (NO), tumour necrosis factor-alpha (TNF-α), interleukin-6 (IL-6), interleukin-1alpha (IL-1α), and inflammatory enzymes such as cyclooxygenase-2 (COX-2). Hence, the downregulation of these inflammatory mediators is an active therapy to control aberrant inflammation and tissue damage. To address this, herein, we present the rational design and synthesis of novel phytochemical entities (NPCEs) through strategic linker-based molecular hybridization of aromatic/hetero-aromatic fragments with the labdane dialdehyde, isolated from the medicinally and nutritionally significant rhizomes of the plant *Curcuma amada*. To validate the anti-inflammatory potential, we employed a comprehensive *in vitro* study assessing its inhibitory effect on COX-2 enzyme and other inflammatory mediators *viz.* NO, TNF-α, IL-6 and IL-1α, in bacterial lipopolysaccharide-stimulated macrophages, and *in silico* molecular modelling studies targeting the inflammation regulator COX-2 enzyme. Among the synthesized novel compounds, **5f** exhibited the highest anti-inflammatory potential by inhibiting the COX-2 enzyme (IC_{50} 17.67 ± 0.89 μM), with a four-fold increased activity than the standard drug indomethacin (IC_{50} 67.16 ± 0.17 μM). **5f** also significantly reduced the levels of LPS-induced NO, TNF-α, IL-6, and IL-1α, much better than the positive control. Molecular mechanistic studies revealed that the **5f** suppressed the expression of COX-2 and pro-inflammatory cytokine release dose-dependently, which was associated with the inhibition of the NF-κB signalling pathway. This infers that the labdane derivative **5f** is a promising lead candidate as an anti-inflammatory agent to further explore its therapeutic landscape.

3.2. Introduction

Cyclooxygenases (COX), also known as prostaglandin-endoperoxide synthases, are crucial enzymes involved in the production of prostaglandins, which are the primary agents responsible for inflammation, pain, and elevated body temperature (hyperpyrexia). The human body generates two primary isoforms of cyclooxygenase proteins, specifically cyclooxygenase-1 (COX-1) and cyclooxygenase-2 (COX-2). COX-1 is a constitutive isoenzyme and plays a role in various physiological functions, such as protecting the gastrointestinal (GI) mucosa and maintaining renal balance. In contrast, COX-2 expression is typically triggered by inflammatory signals and facilitates the production of prostaglandins in inflammatory and cancer-related situations.[1,2] This suggests that targeted inhibition of COX-2 can be an active therapy to control aberrant inflammation and tissue damage.

Non-steroidal anti-inflammatory drugs (NSAIDs) constitute a chemically heterogeneous group of drugs which are commonly used for anti-inflammatory, analgesic, and antipyretic effects. NSAIDs are categorized into non-selective and COX-2-selective inhibitors (COXIBS) depending on their degree of selectivity for inhibiting COX. Nonetheless, irrespective of their selectivity, the primary adverse effects associated with NSAIDs include gastrointestinal issues, renal disturbances and cardiovascular events.[3] This indicates a pressing medical necessity for developing novel COX-2-targeting drugs that exhibit fewer side effects and enhanced efficacy.

Among the plant-based secondary metabolites, labdane diterpenoids have emerged as unique naturally occurring leads for contemporary drug development. Substantial evidence over the past decade highlights the significant role of labdane diterpenoids in modulating inflammatory diseases. Compounds such as andrographolide, andalusol, hedychenone, forkskolin and schlareol are notable representatives of this class, being extensively explored as potential anti-inflammatory agents (**Figure 3.3)**.[4–7] The anti-inflammatory properties of labdane diterpenoids are primarily attributed to their ability to inhibit nuclear factor-κB (NF-κB) signaling, regulate arachidonic acid (AA) metabolism, and suppress nitric oxide (NO) production.[7]

Molecular hybridization is a rational drug design approach that involves the synthesis of novel chemical entities by combining two or more pharmacophoric units from different bioactive compounds. In other words, molecular hybridization entails the integration of multiple known bioactive compounds into a single compound. Through this

approach, medicinal chemists aim to ensure that the resultant chemical entity preserves the desired attributes of the original templates and potentially exhibits dual or even multiple therapeutic effects.[8,9] In this study, we isolated the abundant bioactive marker compound (*E*)-labda-8(17),12-diene-15,16-dial (**1**), a labdane diterpenoid, from the rhizomes of *Curcuma amada*. Building on this scaffold, we rationally designed and synthesized a series of twenty-seven (27) novel phytochemical entities (NPCEs) by strategically incorporating aromatic and heteroaromatic fragments into the labdane template using a linker-based molecular hybridization approach (**Figure 3.3**). These compounds were subsequently evaluated for their potential to inhibit COX-2 and other multi-faceted inflammatory targets.

3.3. Review of literature

Most anti-inflammatory drugs in the market contain aromatic or hetero-aromatic cores. For instance, aspirin, diclofenac, and ibuprofen have simple aryl cores. Drugs like piroxicam, niflumic acid, tinoridine, and tiaprofenic acid feature pyridine and thiophene structures. There have been many reports that indicate semi-synthetic modifications of natural products, through the strategic inclusion of such relevant heterocyclic pharmacophores, can enhance the anti-inflammatory properties of these compounds.

Khan et al. have introduced a promising class of novel thiophene curcuminoids, aiming to enhance the efficacy of NSAIDs.[10] Additionally, Khan et al. synthesized, identified, and evaluated the anti-inflammatory activity of numerous new aromatic and heterocyclic aromatic curcuminoids *in vivo*.[11]Among the derivatives, a furan-curcuminoid derivative exhibited excellent anti-inflammatory effects by affecting the pro-inflammatory cytokines IL-1β and TNF-α production (**Figure 3.1**).

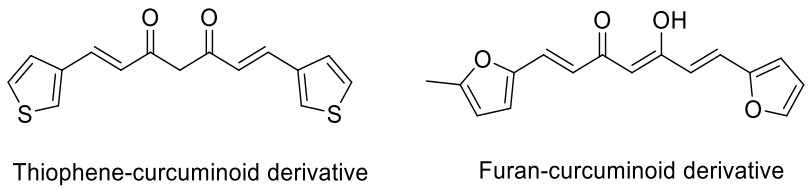

Figure 3.1. Heterocyclic curcuminoids as potential anti-inflammatory agents

Indole is an essential building block in the area of medicinal chemistry with a significant role in drug discovery. Indole derivatives have shown potential pharmacological activities, making them important chemical entities in drug design. The derivatives of

indole have been studied extensively for their potential use as anti-inflammatory, analgesic, and antipyretic agents.[12,13] Indomethacin, etodolac, acemethacin, and tenidap are a few examples of NSAIDs that contain indole nucleus that are effective COX-2 inhibitors. However, indomethacin, which is a non-selective COX-2 inhibitor, has been known to cause gastrointestinal side effects. In recent times, modified indomethacin-based compounds that act as selective inhibitors of COX-2 and other inflammatory mediators such as LOX, NO radical, ROS, and interleukins have been developed and extensively studied (**Figure 3.2**).

Kalgutkar et al. reported the conversion of the carboxylic acid group of indomethacin into amides and esters thus improving the selectivity and potency towards COX-2. Conversion of indomethacin into ester and amide derivatives provides a facile strategy for generating highly selective COX-2 inhibitors and eliminating the gastrointestinal side effects of the parent compound.[15,16]

Amir et al. demonstrated the synthesis of novel indomethacin-based derivatives by replacing the carboxylic acid group of indomethacin with various heterocycles. The findings have shown that these newly introduced heterocycles, such as 1,3,4-oxadiazoles, 1,2,4-triazoles, 1,3,4-thiadiazoles, and 1,2,4-triazine, exhibit a promising anti-inflammatory activity profile. Furthermore, the compounds have demonstrated a significant reduction in their ulcerogenic effect and lowered lipid peroxidation.[14]

In 2018 Bhat et al. reported novel indole hydrazide hybrids, synthesized in good yield by modifying the indomethacin core. The compounds demonstrated selective inhibition of COX-2 expression, while also maintaining gastric protective activity.[17]

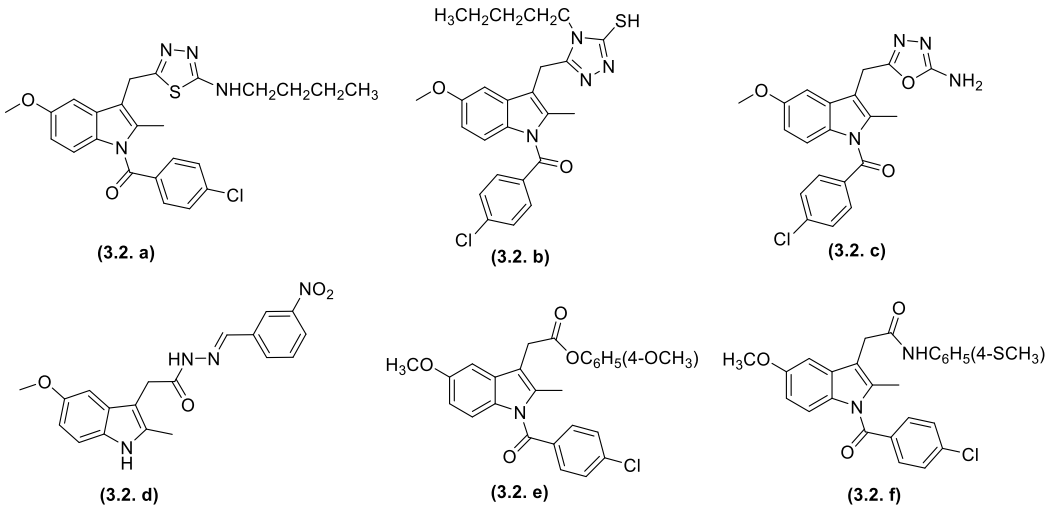

Figure 3.2. Indomethacin derivatives as selective COX-2 inhibitors

3.4. Aim and scope of the present study

Semi-synthetic modification of therapeutically validated natural product leads remains one of the most successful strategies to optimize their pharmacological properties and explore diverse modes of action.[18–20] Remodelling of the existing lead compound, sometimes by even a simple functional group transfiguration, can in turn result in the overall enhancement of its physico-chemical and pharmacokinetic properties.[19,20] Previously, we reported a series of novel labdane-appended scaffolds with promising anti-obesity and anti-hyperlipidemic activities.[21,22] These findings have inspired us to further focus on medicinal chemistry, particularly on natural product-based semi-synthetic modifications, for the development of therapeutically improved scaffolds. [23–29]

The extracts of *C. amada* rhizomes have been reported to be effective against various acute and chronic phases of inflammation.[30,31] However, detailed investigations into the anti-inflammatory properties of *C. amada* bioactive natural products or their semi-synthetic derivatives remain scarce. In this chapter, we describe the rational design and synthesis of twenty-seven novel phytochemical entities (NPCEs), achieved by strategically incorporating aromatic and heteroaromatic fragments into the labdane template through a linker-based molecular hybridization approach. These derivatives were then evaluated for their potential to target multiple inflammatory targets.

3.5. Design strategy for synthesis of aryl/hetero-aryl appended labdane conjugates

Many traditional anti-inflammatory drugs on the market, such as aspirin, diclofenac, and ibuprofen, feature a simple aryl-type core. Based on this, we hypothesized that conjugating an aryl core to the active labdane system *via* an alkyne linker could generate novel hybrid molecules with potent anti-inflammatory activity. This hypothesis guided the design and synthesis of compounds **5a–5h** (**Figure 3.4**). Additionally, data from DrugBank reveals that approximately 85% of bioactive compounds incorporate heterocyclic systems, which play a pivotal role in enhancing solubility, lipophilicity, polarity, and hydrogen-bonding capacity. These improvements often translate to better overall drug properties.[32] Heterocycles also form the core structure of many commonly used anti-inflammatory drugs, such as piroxicam, niflumic acid, tinoridine, and tiaprofenic acid, which frequently feature pyridine or thiophene moieties. This insight prompted the design and synthesis of compounds **5i–5l**, where the aryl core is replaced by pyridine and thiophene systems, maintaining the alkyne linker for molecular hybridization. Indole is a “privileged” nucleus

found in many bioactive natural products and synthetic and semi-synthetic drugs.[12,13] Indomethacin, etodolac, acemethacin, tenidap (**Figure 3.3**) etc., are a few examples of indole-based NSAIDs, which have been proven to be COX-2 inhibitors. The derivatives **5m-5za** were synthesised to include an indole core into the labdane system, where the nitrogen atom on the substituted indole rings was protected with *tert*-butyloxycarbonyl (boc), benzoyl and benzene sulfonyl groups. Indomethacin being a non-selective COX-2 inhibitor is known to cause various gastrointestinal side effects. Recent studies have highlighted the synthesis of modified indomethacin-based compounds as inhibitors of COX-2 and other inflammatory mediators, including LOX, NO radicals, ROS, and interleukins.[33] Derivatization of the carboxyl group at the third position of indomethacin has been shown to enhance its selectivity for COX-2, thereby improving both its anti-inflammatory efficacy and safety profile.[14–16] Building on this insight, we synthesized derivatives **5w–5y**, incorporating indomethacin-like fragments. In these compounds, the third position of the indole ring is functionalized with an active labdane moiety *via* an alkyne linker.

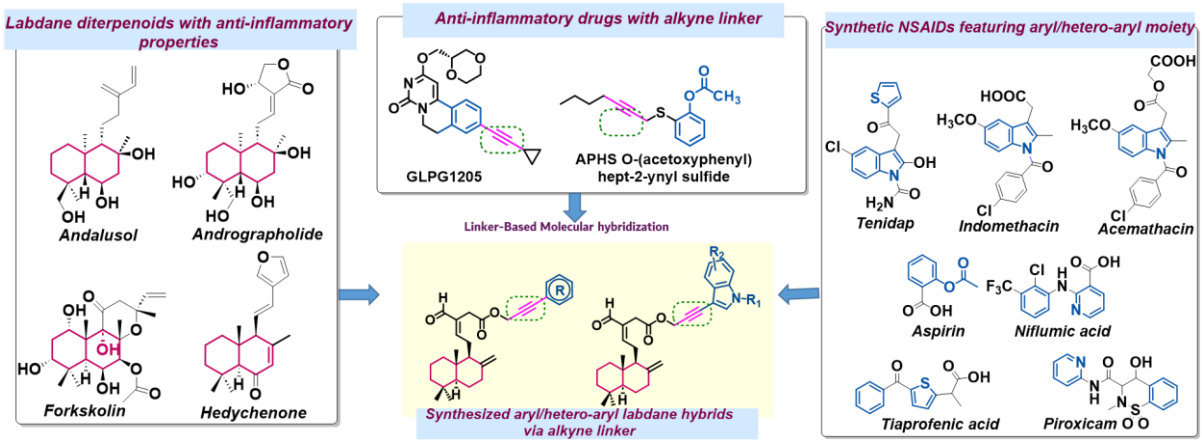

Figure 3.3. Rationale for the design and synthesis of aryl/hetero-aryl appended labdane conjugates

3.6. Results and discussion

To begin with, fresh rhizomes of *C. amada* were procured from CTCRI, Thiruvananthapuram, in January 2022. The marker compound, *(E)*-labda-8(17),12-diene-15,16-dial (**1**), was isolated from the chloroform extract of the rhizomes by adopting our

standard protocol,[21,22] as a colourless solid. The structure of the compound was confirmed by various spectroscopic and analytical data.

One of the aldehyde groups of *(E)*-labda-8(17),12-diene-15,16-dial (**1**) was selectively oxidised to give Zerumin A (**2**), by treating it with oxone in DMF at room temperature.[34] Zerumin A was further converted to the corresponding propargyl ester (**3**) by treating it with propargyl bromide. The structures of compounds **2** and **3** were confirmed by various spectroscopic, and analytical data and comparison with the reported literature.[21,35,36] A new series of twenty-seven novel aromatic/ hetero-aromatic appended analogues of labdane (**Scheme 3.1**) were synthesised by the reaction of propargyl ester (**3**) with substituted aryl/hetero-aryl iodides (**4**) by Sonogashira coupling.[37] $Pd(Ph_3P)_2Cl_2$ and CuI were used as the catalyst and co-catalyst respectively, in dry DMF (**Figure 3.4**). All the synthesised derivatives were well characterized by NMR and HRMS analyses.

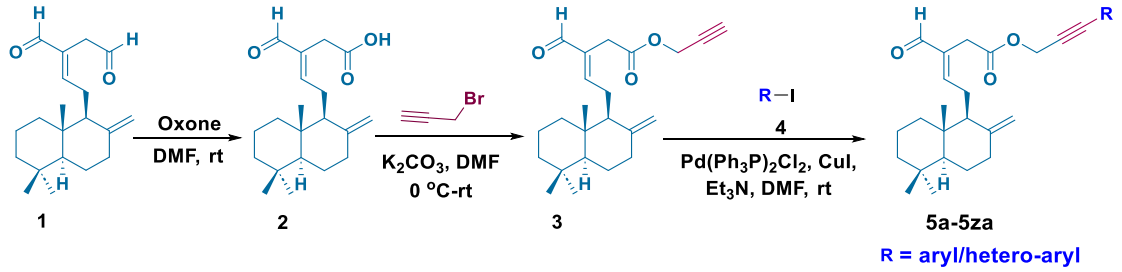

Scheme 3.1. Synthesis of aryl/hetero-aryl appended labdane derivatives **5a-5za** *via* Sonogashira coupling

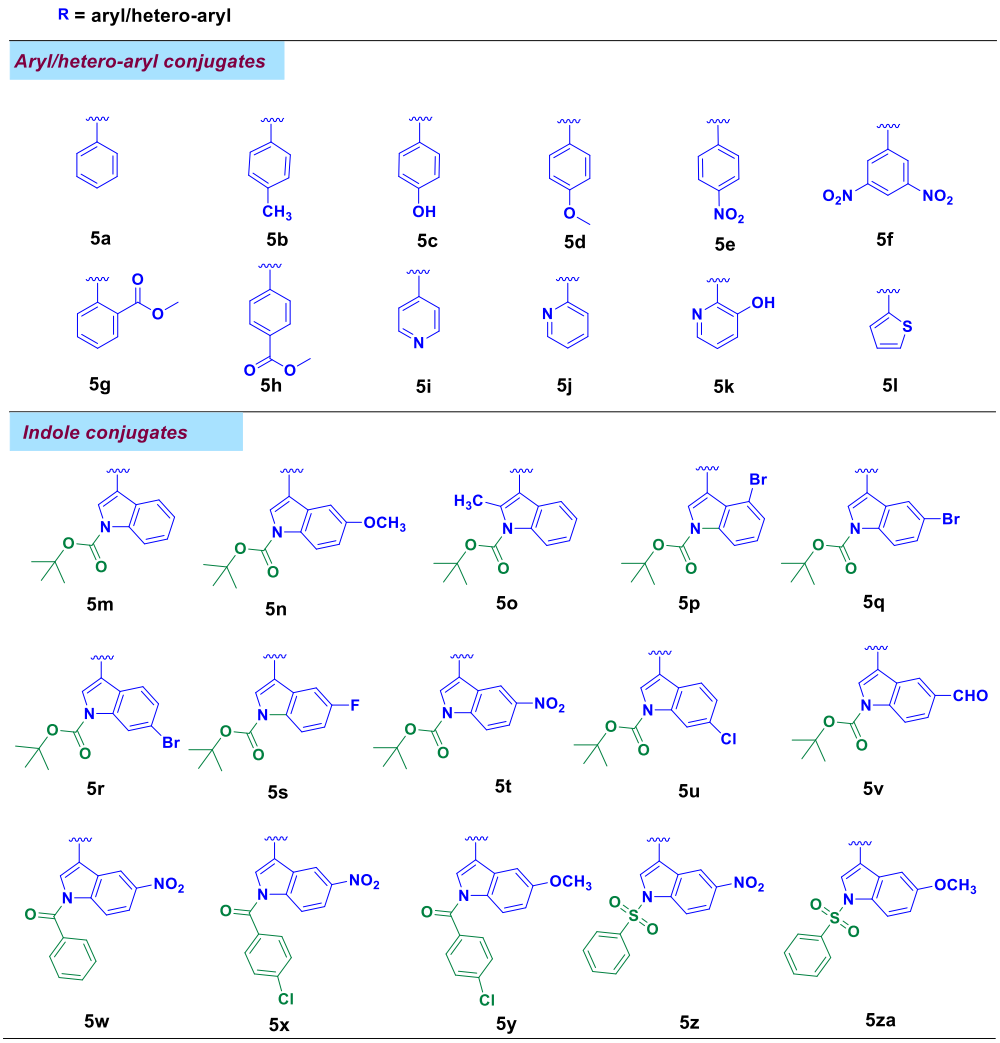

Figure 3.4. Diversity of aryl/hetero-aryl appended labdane derivatives

3.6.1. Spectral characterization aryl/hetero-aryl appended labdane derivatives

Spectral data leading to the structural characterization is exemplified using compound **5d** (**Figure 3.5**). The ^{1}H NMR spectrum (**Figure 3.6**) of the compound showed the aldehydic proton at δ 9.31 and two singlets at δ 4.78 and 4.34 attributed to the presence of exo-methylene group. Two doublets observed at δ 7.31 and 6.76 integrating two protons each, with J = 8.0 Hz indicated the presence of *p*-substituted aromatic protons. A singlet at δ 3.74 integrating for three protons indicated the presence of methoxy protons. The presence of aldehyde and ester carbonyl groups is confirmed by the presence of peaks at δ 193.4 and 169.5 in the ^{13}C NMR spectrum (**Figure 3.7**). The eight peaks between δ 159.9-107.9 confirmed the presence of aromatic and aliphatic double bonds. The two peaks at δ 86.69 and 81.36 correspond to that of the alkynes carbons. The mass spectrum of the compound showed the molecular ion peak at m/z 485.2681, which is $(M+Na)^{+}$ peak. From these data,

along with DEPT-135 and 2D spectra, the structure of the compound **5d** is confirmed as shown below.

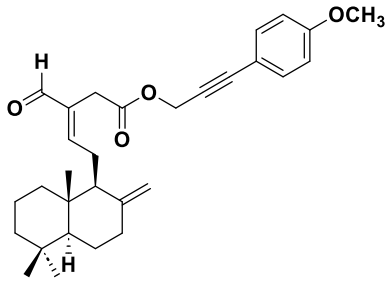

Figure 3.5. Compound **5d**

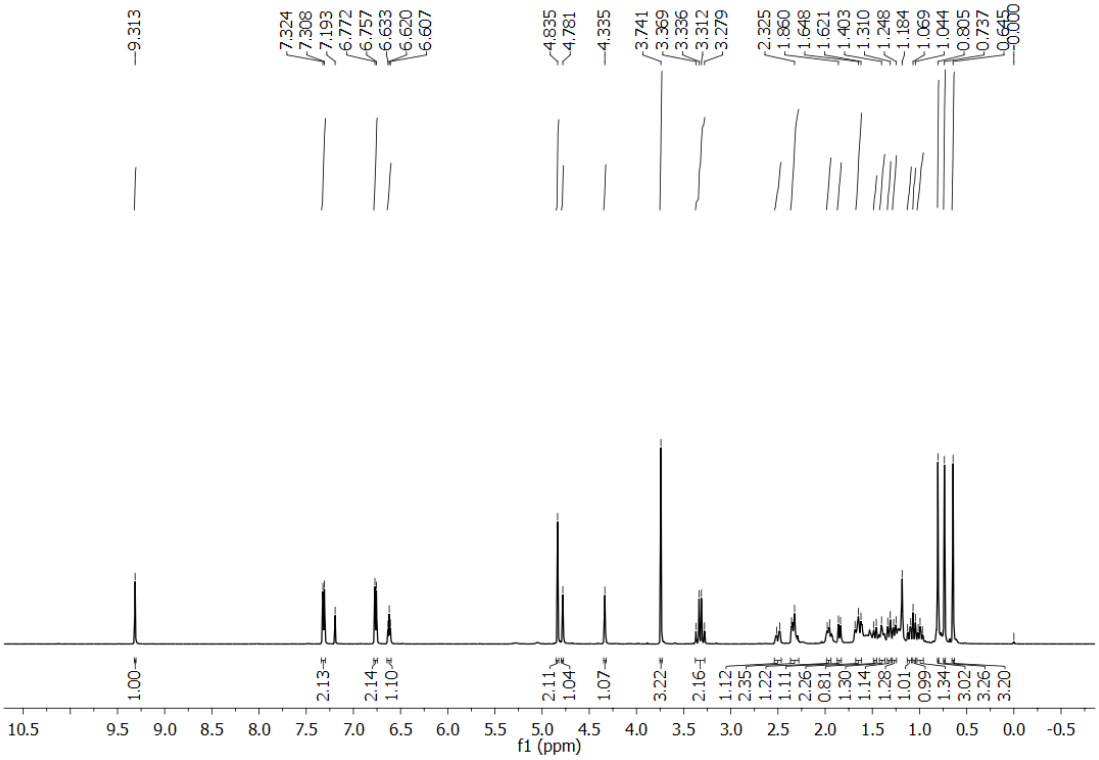

Figure 3.6. ^{1}H NMR spectrum of compound **5d** (500 MHz, $CDCl_3$)

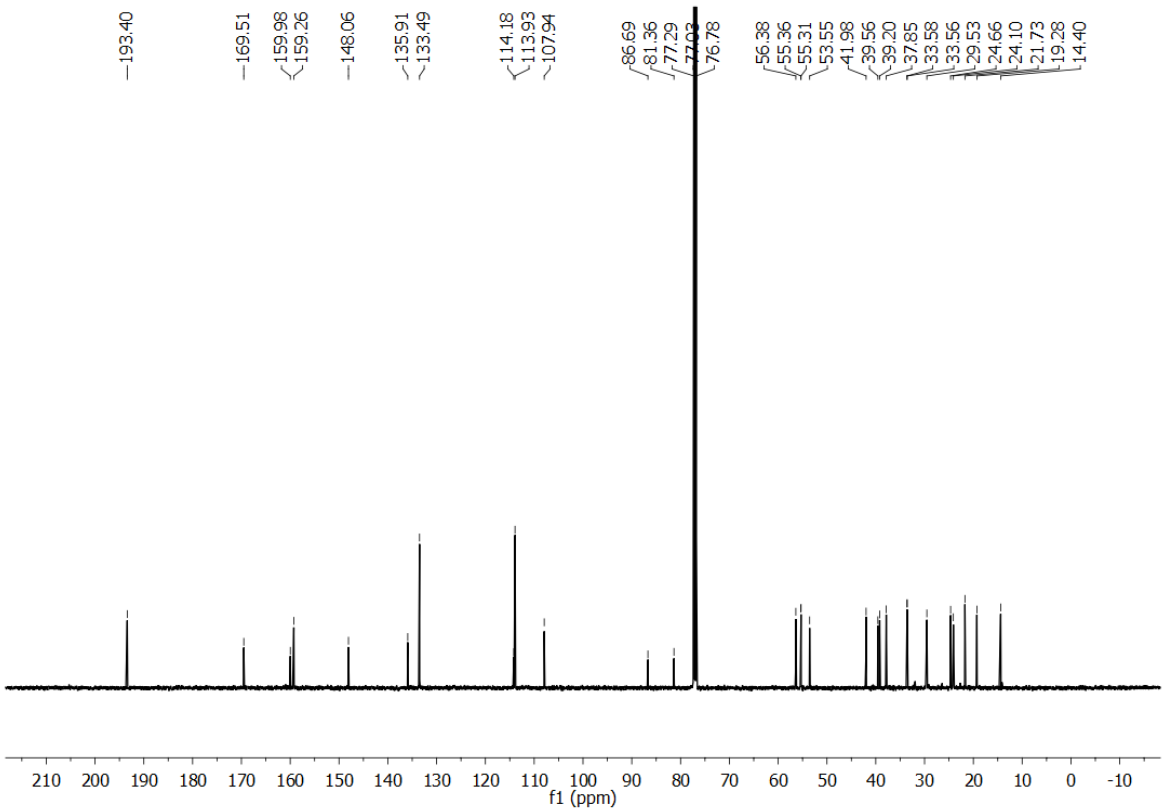

Figure 3.7. ^{13}C NMR spectrum of compound **5d** (125 MHz, $CDCl_3$)

3.6.2. Determination of *in vitro* cell viability by MTT assay

To determine the utmost effectual dose for an inflammatory response, the cytotoxic effect of all the semi-synthetic derivatives of labdane dialdehyde (**5a-5za**) was evaluated *via* the MTT assay.[38] The cytotoxicity assay showed a dose-dependent decrease in cell viability in RAW 264.7 cell lines upon pre-treatment with the semi-synthetic derivatives. All the compounds tested at 5, 10 and 20 µM concentrations for 24 h did not show marked cytotoxic effects in RAW 264.7 cell lines (**Table 3.1** and **Figure 3.8**). Thus, these concentrations were chosen for the evaluation of their anti-inflammatory potential

Table 3.1. Cytotoxicity of the test compounds in RAW264.7 cells (% Cell viability)

	5 µM	**10 µM**	**20 µM**
5a	104.73 ± 4.23	105.90 ± 4.76	92.37 ± 2.11
5b	106.06 ± 3.30	105.24 ± 5.78	97.12 ± 3.85
5c	107.62 ± 4.38	100.85 ± 3.04	92.53 ± 2.97
5d	107.56 ± 5.91	93.97 ± 4.69	95.89 ± 4.44
5e	112.51 ± 6.18	111.92 ± 6.27	109.19 ± 5.45
5f	103.23 ± 3.61	100.59 ± 3.52	96.05 ± 2.65
5g	116.67 ± 4.83	107.49 ± 5.37	97.73 ± 4.38
5h	101.92 ± 5.09	94.77 ± 4.73	91.33 ± 4.06
5i	100.15 ± 4.00	93.85 ± 4.69	94.22 ± 2.21
5j	103.78 ± 3.18	96.86 ± 4.84	93.76 ± 3.68
5k	103.30 ± 4.70	101.77 ± 4.93	95.53 ± 4.77
5l	109.31 ± 4.46	98.27 ± 4.91	94.07 ± 3.70
5m	130.60 ± 6.53	114.70 ± 4.01	94.68 ± 4.73
5n	115.27 ± 4.76	110.38 ± 2.51	102.33 ± 4.11
5o	117.23 ± 3.86	114.73 ± 4.16	102.07 ± 5.10
5p	113.24 ± 4.52	111.83 ± 3.59	97.97 ± 3.89
5q	113.89 ± 3.69	110.09 ± 5.05	109.91 ± 3.49
5r	106.02 ± 3.30	98.70 ± 4.93	93.10 ± 4.45
5s	130.61 ± 3.53	102.19 ± 3.10	99.11 ± 3.95
5t	103.52 ± 5.17	99.71 ± 4.98	94.48 ± 4.72
5u	115.83 ± 5.95	102.53 ± 3.12	99.45 ± 4.97
5v	109.60 ± 4.48	109.04 ± 4.45	105.61 ± 4.2
5w	119.49 ± 4.97	116.808 ± 5.25	109.12 ± 5.45
5x	119.10 ± 5.95	117.86 ± 5.89	102.62 ± 3.13
5y	118.10 ± 5.90	106.43 ± 5.32	99.72 ± 4.98
5z	97.19 ± 4.85	95.73 ± 4.68	95.85 ± 4.54
5za	113.98 ± 5.69	107.90 ± 3.39	101.02 ± 5.05
LD	110.10 ± 4.90	105.43 ± 5.02	100.72 ± 4.80

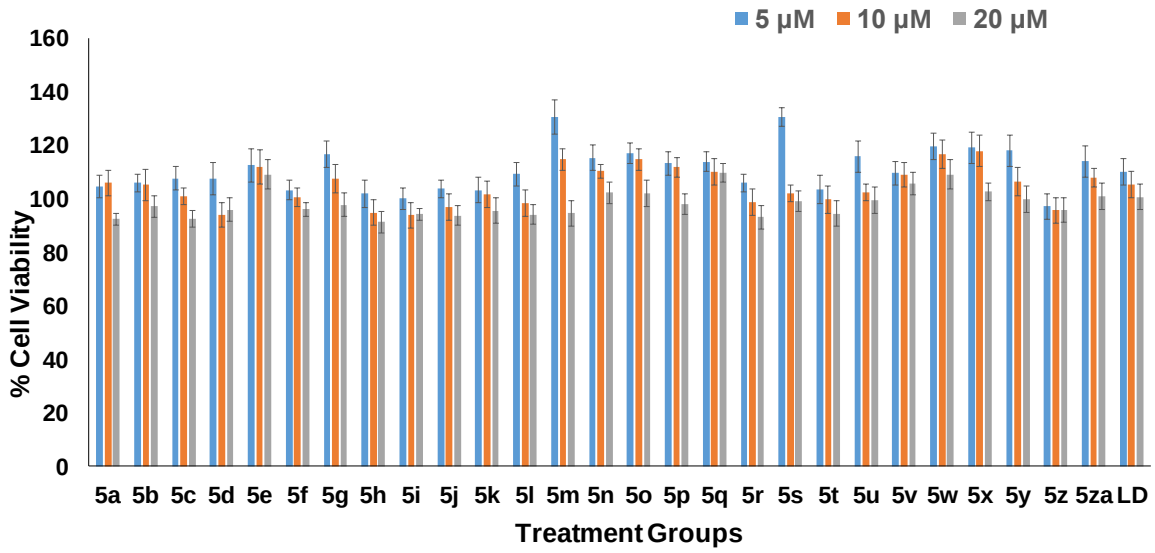

Figure 3.8. Effect of labdane dialdehyde (LD) and its semi-synthetic derivatives (**5a-5za**) on the cell viability in RAW264.7 cells. The viability of cells after pretreatment with different concentrations of compounds (5, 10 and 20 µM concentrations) for a period of 24 h, was determined by MTT assay.

3.6.3. Preliminary screening based on the inhibitory effect of labdane-conjugates on NO production

Nitric oxide is a membrane-permeable signalling molecule produced when lipopolysaccharide binds to the TLR-4 receptor and mounts a crucial defence in the contradiction of foreign infiltration. Conversely, the uninhibited generation of NO accelerates various chronic inflammatory ailments.[39] Hence it is critical to maintain the NO level using various anti-inflammatory mediators.[40] LPS-induced macrophages stimulate unrestricted release of nitric oxide by the degradation of L-arginine.[41] Based on the MTT assay, all the synthesised labdane derivatives were evaluated for their potential to inhibit nitric oxide at 5, 10 and 20 µM concentrations in LPS-induced RAW 264.7 cells. The parent compound labdane dialdehyde (1; LD), at 10 and 20 µM concentrations, was also included in the study for a comparative evaluation with the semi-synthetic derivatives. The anti-inflammatory drug, indomethacin (Indo) at 10 and 20 µM concentrations was used as the positive control. Nitrite concentration was assessed, as an indicator of NO production after 24 h of stimulus, through Griess assay.[42] Relative to the LPS-treated group, the parent compound (LD) exhibited a significant decrease in the production of NO, similar to that of the positive control. Among the twenty-seven tested labdane derivatives, twenty-two

derivatives (**5b-5h**, **5j-5l**, **5n-5p**, **5r-5z**) exhibited a significant decrease in NO production when compared to the positive control as well as the parent natural compound, in a dose-dependent manner. The decrease in NO production in the groups treated with these labdane derivatives rather than LD highlights the increased anti-inflammatory potential of the semi-synthetic derivatives over its parent natural product in murine macrophages (**Figure 3.9**). However, the compounds **5a**, **5i**, **5m**, **5q** and **5za** had no obvious NO inhibitory activity. Thus, the compounds **5b-5h**, **5j-5l**, **5n-5p** and **5r-5z** which demonstrated effective NO inhibition were selected for further evaluation of their anti-inflammatory potential.

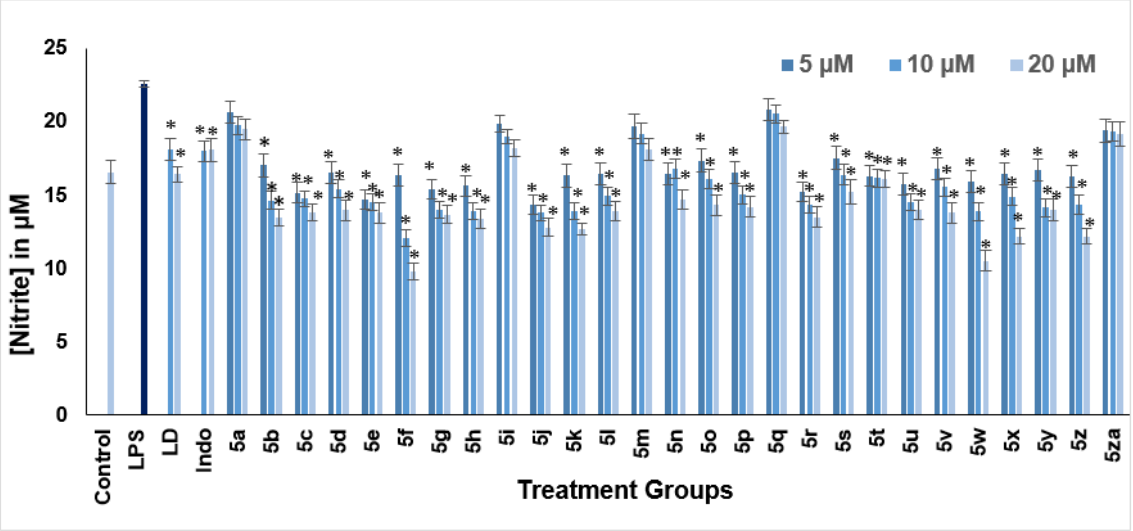

Figure 3.9. Effect of semi-synthetic derivatives of labdane dialdehyde on LPS induced NO production in RAW 264.7 cell lines. Cells were pre-treated with 5, 10 and 20 µM concentrations of compounds for 1 h before treatment with 1 µg/mL LPS. After 24 h of incubation, NO production was determined by the Griess test. Data are expressed as the mean ± SD (n = 3). *$p < 0.001$vs LPS group.

3.6.4. Structural activity relationship based on the inhibitory effect of labdane-conjugates on NO production

Based on the NO inhibitory effects of the labdane conjugates, a probable structure-activity relationship (SAR) has been established. Within the simple benzene series (**5a**–**5h**), nitro-substituted derivatives (**5e**, **5f**) exhibited the highest NO inhibition, with the di-nitro-substituted conjugate (**5f**) demonstrating superior activity compared to the mono-substituted derivative. In contrast, **5a**, with an unsubstituted benzene core, showed the least NO inhibition.

Among the simple heteroaromatic conjugates (**5i–5l**), the hydroxyl-substituted pyridine derivative (**5k**) displayed a pronounced inhibitory effect on NO production. For the indole derivatives (**5m–5za**), *N*-benzoyl and *N*-benzene sulfonyl-substituted derivatives exhibited strong NO inhibition, whereas *N*-boc-protected indole conjugates showed only moderate activity. Among the *N*-benzoyl and *N*-benzene sulfonyl-substituted conjugates, nitro-substituted derivatives (**5w**, **5x**) were more potent than the other derivatives.

Interestingly, no clear trend was observed based on the type of substitution on the indole ring, including halogens, electron-withdrawing groups, or electron-donating groups. Overall, among both simple aromatic/hetero-aromatic conjugates and indole conjugates, the nitro-substituted analogues were found to be more potent candidates of the series.

3.6.5. *In silico* molecular modelling studies on COX-2 enzyme

COX-2 is an inflammatory mediator and an inducible enzyme that catalyses the PGE2 synthesis. The activation of one of the mammalian transcription factors NF-κB by LPS and other cytokines is mediated by COX-2.[43] The inhibition of COX-2 regulates inflammatory homeostasis and hence it is identified as a molecular target in the prevention and treatment of inflammatory diseases. To understand the binding mode and mechanism of action of the selected compounds (**5b-5h**, **5j-5l**, **5n-5p**, **5r-5z**), interact with the target protein COX-2, we mapped the amino acid residues of COX-2 most likely involved in establishing the interaction with drugs (**Figure 3.16**). We found that the catalytic pocket or active site of COX-2 is well conserved, having a deep hydrophobic pocket. (**Figure 3.17**). Structural interactions showed that the amino acid residues A199, A202, T206, H207, F210, T212, L294, L295, Q383, H386, W387, H388, M391, L408, I444, H446, D450, and E454 make up the COX-2 active site. Furthermore, docking analysis revealed that the large catalytic pocket of COX-2 could accommodate both simple aromatic and hetero-aromatic derivatives. The head or labdane core of the compounds faces inward to the active site pocket and mostly occupies the inner pocket area made of amino acids A199, A202, Q203, T206, H207, F210, and W387 in COX-2. We calculated the overall buried interface and pocket volume between the COX-2 active site and labdane derivatives to be ~1400Å2 as calculated from the D3 pocket server (www.d3pharma.com/D3Pocket/), suggesting the ability of COX-2 to accommodate large targets. In addition, the docking studies of the semi-synthetic labdane derivatives to COX-2 showed that the binding affinity (delG) ranged from -10.35 kcal/mol for compound **5f** to -5.82 kcal/mol for compound **5g** among the

simple aromatic/ hetero-aromatic conjugates, while among the indole conjugates, the binding affinity (delG) ranged from -10.61 kcal/mol for compound **5x** to -5.78 kcal/mol for compound **5o** (**Table 3.1**).

The ligand in protein COX-2 (PDB:5KIR) is Rofecoxib (**ROX**).[44] Hence, the binding affinity of compounds was compared to that of **ROX**. For **ROX**, the binding affinity is about 8.2 kcal/mol, whereas for **5x**, the binding affinity is about -10.61 kcal/mol, followed by **5f** with a binding affinity of -10.35 kcal/mol. The compounds **5x** and **5f** can compete with the porphyrin and can effectively bind into the catalytic pocket of COX-2. Whereas in the crystal structure, **ROX** binds to an allosteric site. **5x**/**5f** can bind and compete for both allosteric and catalytic sites with good affinity (**Figure 3.10**).

Among the examined compounds, **5e**, **5f**, **5k**, **5w-5z** exhibited excellent binding affinity for COX-2 enzyme (**Table 3.2**). These findings further corroborate the high binding affinity of synthesised labdane-conjugates targeting COX-2 as potential inhibitors.

Table 3.2. Estimated binding free energy of the labdane-conjugates with COX-2 *in-silico*

Compound code	Del G Kcal/mol
Aryl/hetero-aryl conjugates	
5f	-10.35
5k	-9.28
5e	-8.78
5h	-8.47
5j	-7.65
5l	-7.43
5b	-6.80
5c	-6.61
5d	-6.45
5g	-5.82

Indole conjugates	
5x	-10.61
5w	-9.81
5z	-9.47
5y	-9.14
5t	-8.64
5s	-8.31
5p	-8.27
5r	-8.05
5u	-7.93
5v	-6.91
5n	-6.73
5o	-5.78
ROX	-8.2

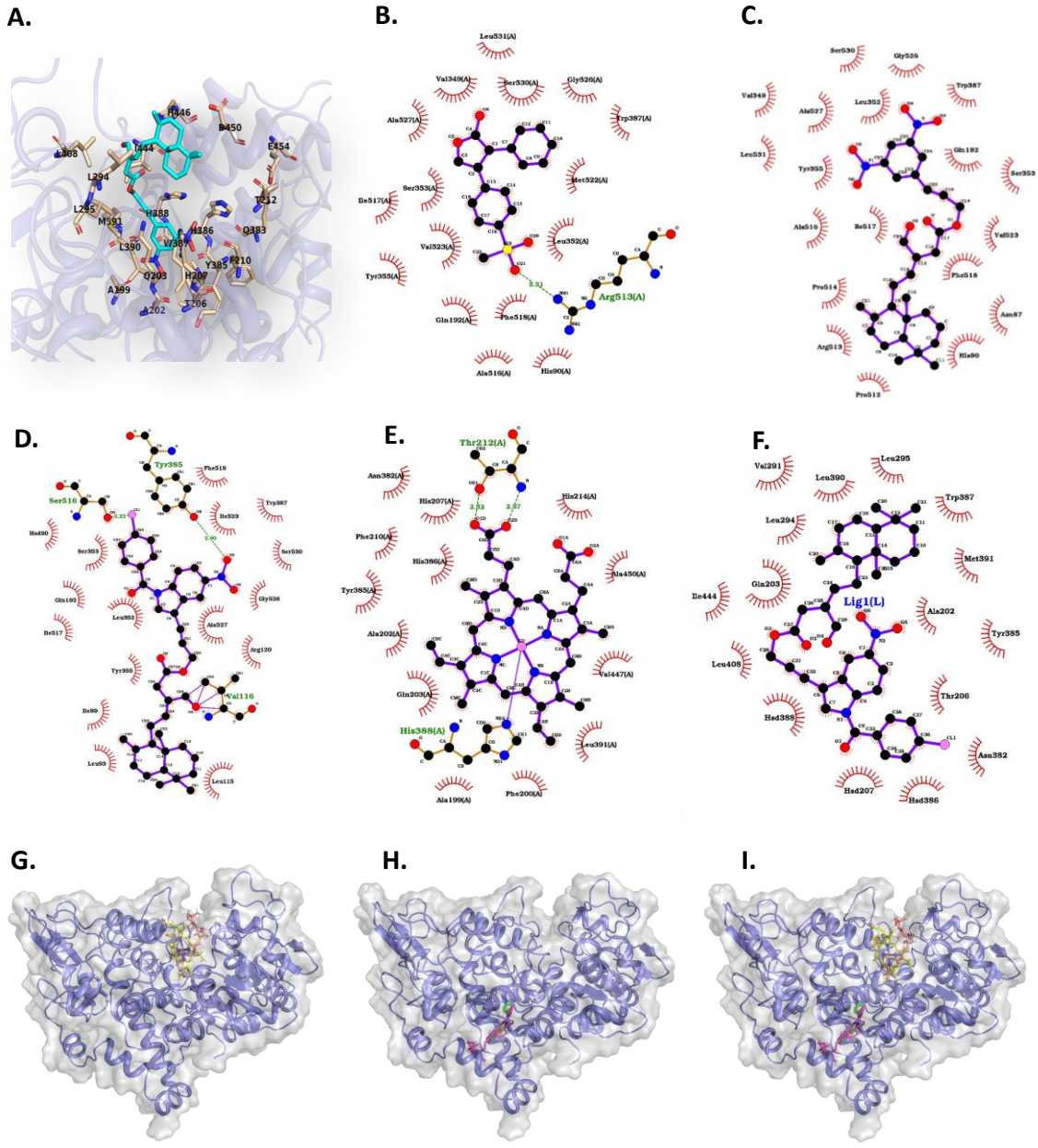

Figure 3.10. Molecular docking studies of compounds on COX-2 **(A)** The bound/docked compound **5f** (cyan) in COX-2 enzyme with the active site or catalytic pocket (shown in amino acid side chains). Ligplot view showing the COX-2 Interaction with (**B**) Rofecoxib (**ROX**) as derived from the crystal structure (PDB: 5KIR), (**C**) docked compound **5f** in the same **ROX** binding site (**D**) docked compound **5x** in the same ROX binding site (**E**) Protoporphyrin IX (**COH**) in the catalytic pocket (PDB: 5KIR) and (**F**) docked compound **5x** in **COH** binding site or catalytic pocket. (**G**) Superimposition of **COH** (yellow) and **5x** (Sand)(**H**) **ROX** (green) and **5x** (pink)and (**I**) all 3 molecules, where COX-2 is shown in the blue cartoon with grey surface, showing **5x** compound could effectively bind COX-2 in both sites and makes larger binding interface.

3.6.6. Evaluation of compounds for COX-2 enzyme inhibition

Based on the *in silico* molecular docking results on the COX-2 enzyme, the most promising seven active compounds **5e**, **5f**, **5k**, **5w-5z** were then investigated for the *in vitro* COX-2 inhibition at 20, 40 and 60 µM concentrations. Indomethacin (at 40 µM and 60 µM) was used as the positive control. The parent compound 1 (**LD**) (at 40 µM and 60 µM) was also included in the study for a comparison with the semi-synthetic derivatives. Among the screened derivatives, **5f** displayed the highest inhibition on COX-2, with an IC_{50} value of 17.67 ± 0.89 µM, which was nearly four-fold more active than the positive control indomethacin, followed by **5w** (IC_{50} 34.86 ± 2.32 µM). **5k**, **5x** and **5z** also exhibited excellent COX-2 inhibition potential better than that of the positive control. **Table 3.2** shows the IC_{50} values of the evaluated compounds. To our delight, the *in silico* results supported the *in vitro* investigations to a great extent. These seven derivatives (**5e**, **5f**, **5k**, and **5w-5z**) were again shortlisted for the next level of anti-inflammatory studies.

Table 3.3. Effect of labdane derivatives on COX-2 inhibition (IC_{50}) [a]

Compounds	IC_{50} (µM)
5e	84.27 ± 0.93
5f	17.67 ± 0.89
5k	52.5 ± 3.38
5w	34.86 ± 2.32
5x	50.58 ± 0.25
5y	101.25 ± 3.18
5z	42.68 ± 0.99
Indo	67.16 ± 0.17

[a]Half maximal inhibitory concentration (IC_{50}) values for COX-2 inhibition of selected labdane derivatives and the positive control indomethacin (indo). Data are expressed as the mean ± SD (n = 3).

3.6.7. Inhibitory effect of labdane-conjugates on pro-inflammatory cytokines production (TNF-α, IL-6 and IL-1α)

LPS-stimulated cells secrete excessive inflammatory markers comprising COX-2, a key enzyme involved in the production of PGE2, and the pro-inflammatory cytokines like TNF-α, IL-6 and IL-1α. The quantities of these cytokines specify the impact of inflammation in cellular models.[45] Hence, we further studied the effect of the seven selected (**5e**, **5f**, **5k**, **5w -5z**) compounds (at 20 μM concentration), on the quantity of TNF-α, IL-6 and IL-1α in the supernatant of LPS-stimulated RAW 264.7 cell lines *via* enzyme-linked immunosorbent assay (ELISA). LPS-treated groups exhibited remarkable increment in all three cytokine concentrations in RAW 264.7 cells when compared to control cells which implies the successful establishment of the cellular inflammatory model in murine macrophages. The LPS-induced upsurges were reversed by the treatment with natural compound LD and its semi-synthetic derivatives as this significantly reduced the level of cytokines. The level of IL-6 was found to be declined in the following order: LD > 5e > 5y > 5k > Indo > 5x > 5z > 5w > 5f. The results also demonstrated a reduction in IL-6 levels similar to the results obtained from COX-2 inhibition results. The levels of TNF-α and IL-1α were found to decline in a similar order as that of IL-6 and COX-2 (**Figure 3.11**).

In concordance with COX-2 inhibition results, the compound **5f** was observed with the most anti-inflammatory potential by inhibiting the production of pro-inflammatory cytokines in the cellular model. The other derivatives **5w**, **5z**, **5x** and **5k** also demonstrated a similar pattern of cytokine concentration in LPS co-treated cells better than the positive control indomethacin. The compounds **5e** and **5y** exhibited the release of pro-inflammatory cytokines which is at par with the positive control, indomethacin and better than that of the parent compound LD. Hence, this study indicates the anti-inflammatory potential of the semi-synthetic derivatives of LD superior over the parental compound.

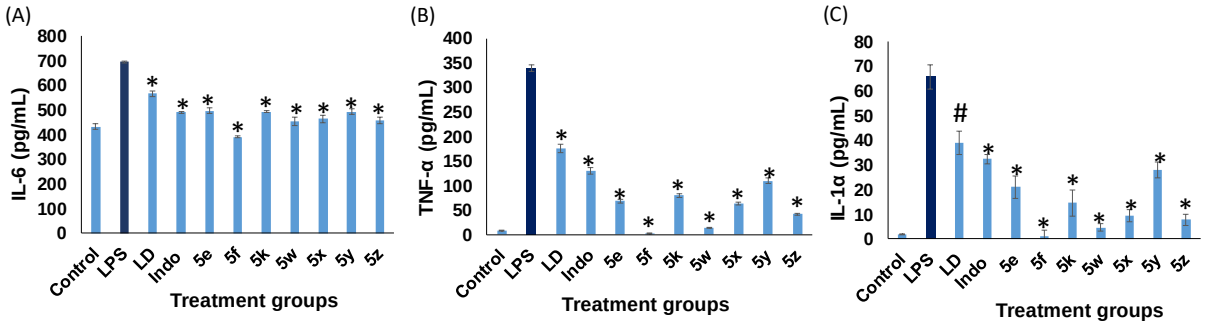

Figure 3.11. Effect of semi-synthetic derivatives of labdane dialdehyde on LPS induced cytokines production (**A**) IL-6, (**B**) TNF-α, (**C**) IL-1 α, in RAW 264.7 cell lines. Cells were pretreated with 20 µM concentration of compounds for 1 h, before treatment with 1 µg/mL LPS. After 24 h of incubation, cytokines production was determined by ELISA. Data are expressed as the mean ± SD (n = 3). *p < 0.001 vs LPS group, #p < 0.05 vs LPS group.

3.6.8. Dose-dependent studies of 5f on key pro-inflammatory cytokines (TNF-α and IL-6)

The most promising candidate **5f** was further assessed for its inhibitory effect on LPS-induced TNF-α and IL-6 release at different concentrations (1, 5 and 10 µM). As illustrated in **Figure 3.12,** compound **5f** markedly inhibited the TNF-α and IL-6 release in a dose-dependent manner, and hence confirmed to be a highly potent anti-inflammatory agent, outperforming the effects of the commercial drug indomethacin.

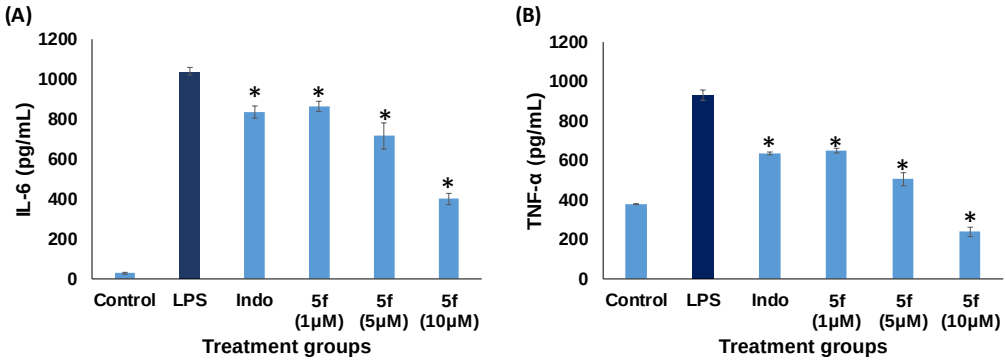

Figure 3.12. Effect of compound 5f on LPS induced cytokines production: (**A**) IL-6 and (**B**) TNF-α, in RAW 264.7 cell lines. Cells were pre-treated with various concentrations of compound 5f (1, 5 and 10 µM) and indomethacin (10 µM) for 1 h before treatment with 1 µg/mL LPS. After 24 h of incubation, cytokines production was determined by ELISA. Data are expressed as the mean ± SD (n = 3). *p < 0.001 vs LPS group.

3.6.9. Effect of 5f on COX-2 protein expression on LPS-stimulated RAW 264.7 cell lines

To explore the effect of **5f** on COX-2 protein expression, western blot analysis was performed, on LPS-stimulated RAW 264.7 cells at 10 and 20 µM concentrations. Indomethacin at 20 µM concentration was employed as the positive control. LPS stimulation significantly increased the expression of COX-2 protein, as depicted in the **Figure 3.13**. However, there was a significant decrease in COX-2 expression when pre-treated with the compound **5f**, in a dose-dependent manner, and was at par with indomethacin. The results confirm that **5f** exerts its anti-inflammatory effect by inhibiting the release of pro-inflammatory cytokines and nitric oxide *via* the down-regulation of COX-2 expression.

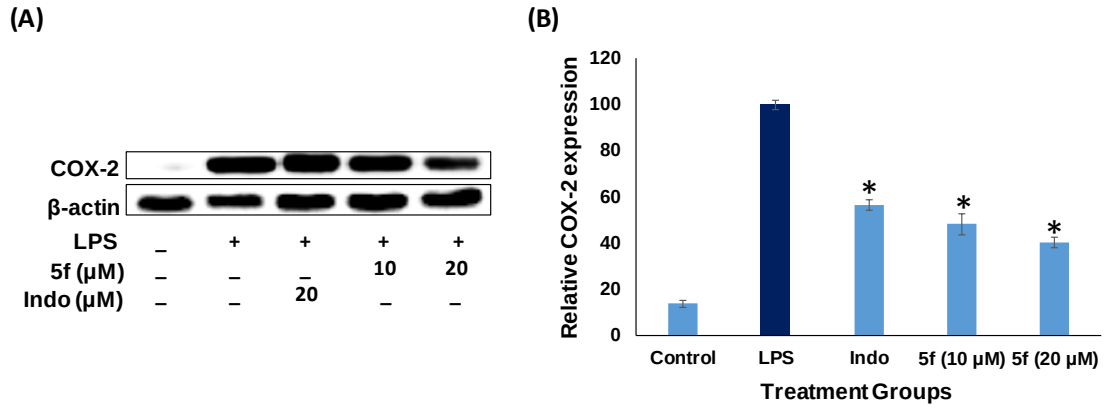

Figure 3.13. Effect of **5f** on COX-2 expression in LPS-stimulated RAW264.7 cells. Cells were pretreated with different concentrations of compound **5f** (10 and 20 µM) and indomethacin (20 µM) for 1h and then stimulated with or without 1 µg/mL of LPS for 24 h. COX-2 expression was detected by western blotting (A and B). Data are expressed as the mean ± SD (n = 3). *p < 0.001 vs LPS group.

3.6.10. Effect of 5f on NF-κB signalling pathway on LPS-stimulated RAW 264.7 cells *via* western blotting and immunofluorescence analysis

There have been extensive studies that point to the fact that the expression of the pro-inflammatory cytokines and enzymes such as COX-2 is transcriptionally mediated by the nuclear transcription factor, NF-κB.[46–48] NF-κB exists as an inactive dimer along with IκB in the cytoplasm of the cell. However, upon activation by external stimuli, NF-κB phosphorylates and translocate into the nuclei, where it promotes the expression of various pro-inflammatory mediators. Hence, down-regulating the expression of p-NF-κB is one of

the effective approaches to prevent inflammation. To establish the anti-inflammatory mechanism of **5f**, the effect on the NF-κB signalling pathway was investigated *via* western blotting and immunofluorescence assays. Indomethacin at 20 µM was chosen as the positive control. As depicted in **Figure 3.14**, LPS stimulation increased the expression of the p-NF-κB, on LPS-stimulated RAW 264.7 cells. Compound **5f** exhibited a significant reduction in NF-κB phosphorylation, in a dose-dependent manner and was comparable to positive control indomethacin. The confirmation of the anti-inflammatory mechanism of **5f** involving inhibition of the NF-κB signalling pathway was demonstrated by analysing the effect of the compound **5f** on the nuclear translocation of NF-κB by immunofluorescence assay. As shown in **Figure 3.15 A** compound **5f** markedly reduced the distribution of NF-κB in the nucleus in a dose-dependent manner signifying the suppression of phosphorylation and transport of NF-κB from the cytoplasm to the nucleus. The fluorescence intensity histogram extracted using cellSens software (OLYMPUS, Japan) demonstrated a significant increase in nuclear p65 in the cells treated with LPS. However, the cells co-treated with **5f** exhibited a significant reduction in nuclear p65 in a dose-dependent manner and was comparable to that of the positive control indomethacin (**Figure 3.15 B**). The results indicated that the compound **5f** inhibits the LPS-stimulated over-expression of pro-inflammatory mediators such as cytokines, NO and COX-2 by down-regulating the expression of the NF-κB signalling pathway.

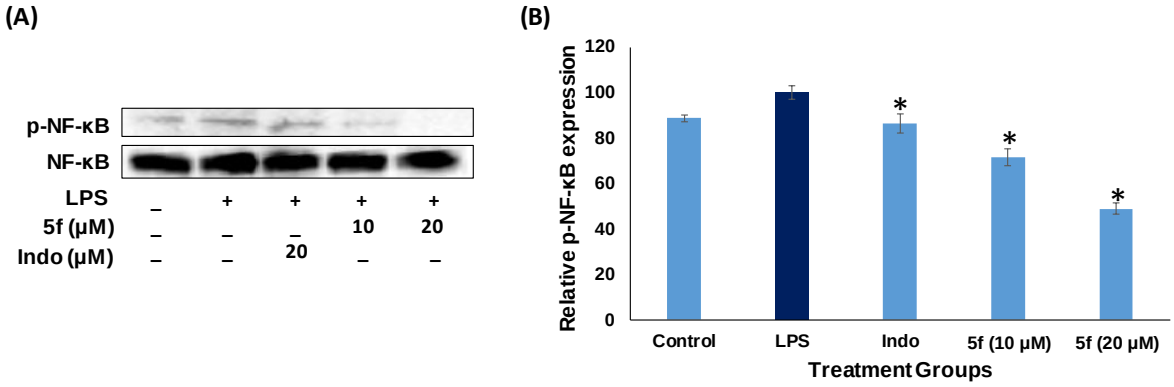

Figure 3.14. Effect of **5f** on NF-κB expression in LPS-stimulated RAW264.7 cells. Cells were pretreated with different concentrations of compound **5f** (10 and 20 µM) and indomethacin (20 µM) for 1h and then stimulated with or without 1 µg/mL of LPS for 24 h. NF-κB expression was detected by western blotting (**A** and **B**). Data are expressed as the mean ± SD (n = 3). *p < 0.001 vs LPS group.

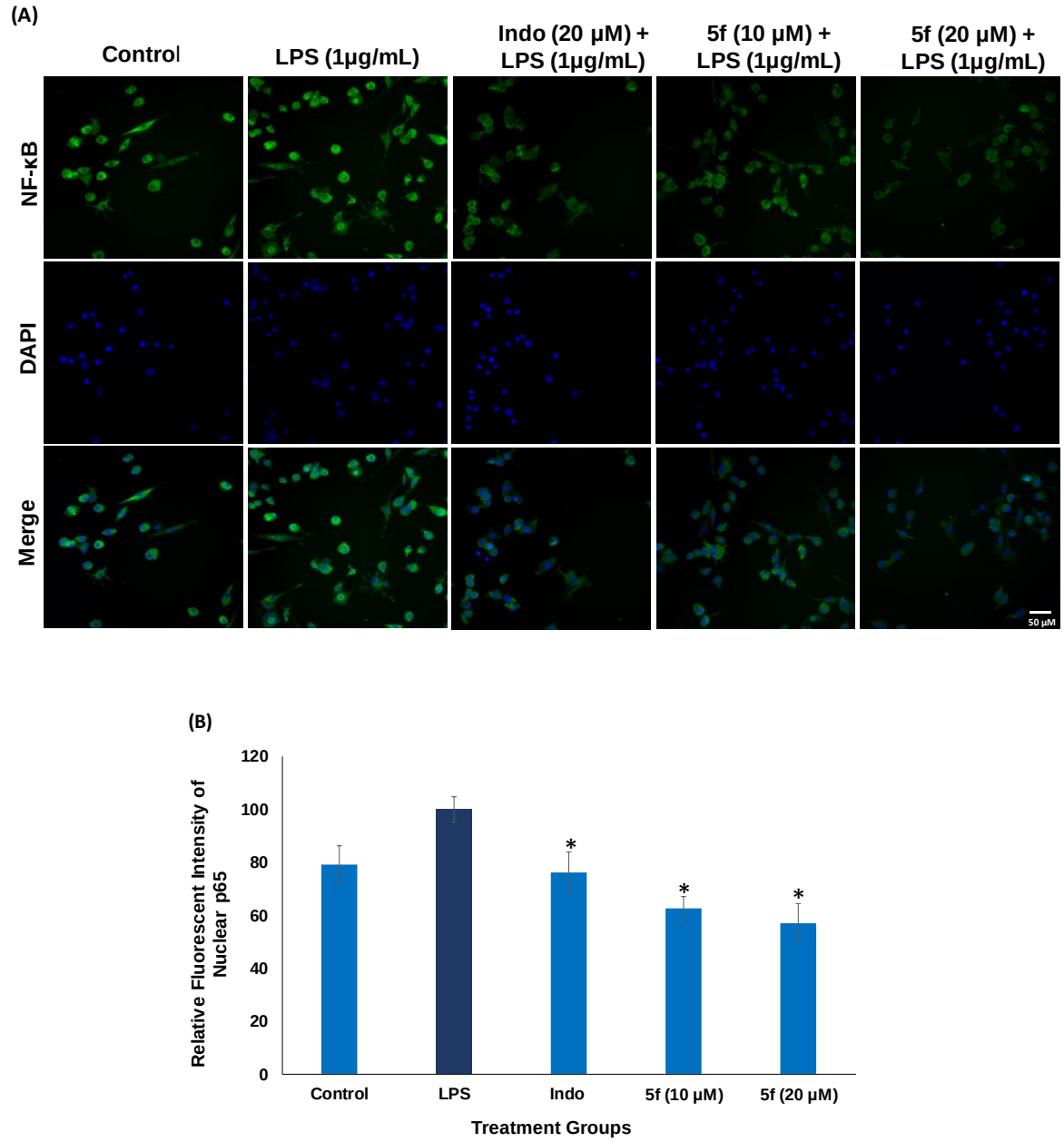

Figure 3.15. Effect of **5f** on NF-κB signalling pathway *via* immunofluorescence.
(A) Immunofluorescence staining detected the distribution of NF-κB-p65 in both the nuclei and cytoplasm by some colocalization of receptors (p65, Alexa Fluor 488, green) with the nuclei (DAPI, blue). Images were captured by fluorescent microscope (OLYMPUS, Japan). Scale = 50 µM. **(B)** Intensity histogram of NF-κB translocation. The fluorescence intensity was quantified using the cellSens software (OLYMPUS, Japan). Data are expressed as the mean ± SD (n = 3). *$p < 0.001$ vs LPS group.

3.7. Conclusions

In summary, this study explored the anti-inflammatory potential of the medicinally and nutritionally significant plant *Curcuma amada*. The abundant marker compound, (*E*)-labda-8(17),12-diene-15,16-dial, was isolated from its rhizomes, and a new series of 27 rationally designed labdane hybrids were synthesized. These hybrids were developed using a strategic linker-based molecular hybridization approach, incorporating aromatic and heteroaromatic fragments into the labdane template, and subsequently evaluated for their anti-inflammatory properties.

Among the labdane conjugates, compound **5f** demonstrated the highest anti-inflammatory potential, exhibiting a four-fold higher COX-2 inhibitory activity compared to the commercial drug indomethacin. Additionally, **5f** effectively inhibited the production of key inflammatory mediators, including NO, TNF-α, IL-6, and IL-1α, surpassing both the positive control and the parent natural compound (LD). Molecular mechanistic studies revealed that 5f modulates the NF-κB signaling pathway, thereby suppressing the expression of pro-inflammatory cytokines, NO, and COX-2. The in silico findings further supported these results, underscoring the compound's mechanism of action.

This is the first report detailing the anti-inflammatory properties of labdane dialdehyde and its semi-synthetic derivatives. The findings highlight the significant role of semi-synthetic modifications in enhancing the bioactivity of natural products and suggest that compound **5f** holds promise as a novel anti-inflammatory agent.

Furthermore, these extensive studies emphasize the medicinal relevance of C. amada, which can significantly enhance its economic value. Being a common edible plant native to India, scientific advancements related to *C. amada* can boost its export potential and elevate it to the status of a cash crop. This, in turn, may contribute to the socio-economic upliftment of the farmers cultivating it, adding considerable value to the agricultural sector.

3.8. Experimental section

3.8.1. Procedure for the synthesis of 4a-4o

Various substituted indoles were first iodinated at the third position by following the reported procedure (**Scheme 3.2**).[49]

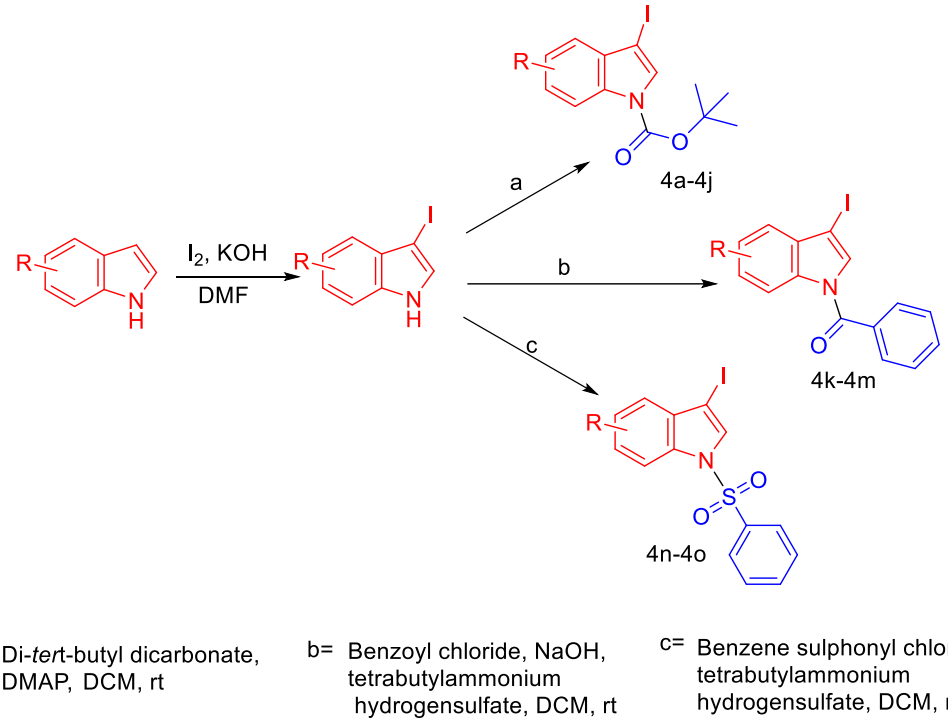

a= Di-*tert*-butyl dicarbonate, DMAP, DCM, rt

b= Benzoyl chloride, NaOH, tetrabutylammonium hydrogensulfate, DCM, rt

c= Benzene sulphonyl chloride, NaOH, tetrabutylammonium hydrogensulfate, DCM, rt

Scheme 3.2. Synthesis of *N*-protected iodoindoles (**4a-4o**)

3.8.1.1. Procedure for the synthesis of 4a-4j

To a solution of 3-iodoindole (1 equiv.) in DCM, a mixture of di-*tert*-butyl dicarbonate (1.5 equiv.) and 4-dimethyl aminopyridine (0.1 equiv.), dissolved in DCM, were added and stirred at room temperature for 30 minutes. 4ml of 0.1 N HCl was added to the reaction mixture and the combined organic layer was extracted with DCM, dried over anhydrous Na_2SO_4 and the solvent was removed under reduced pressure to afford the product **4a-4j.**

3.8.1.2. Procedure for the synthesis of 4k-4m

Benzoyl chloride (1.5 equiv.) was added to a stirred solution of 3-iodo-indole (1 equiv.), NaOH (2.5 equiv.) and tetrabutylammonium hydrogen sulfate (0.02 equiv.), in DCM. The reaction mixture was stirred at room temperature for 2 hours. The reaction mixture was diluted with water, extracted in DCM, dried over anhydrous Na_2SO_4 and the solvent was removed under reduced pressure to afford the product **4k-4m.**

3.8.1.3. Procedure for the synthesis of 4n-4o

A mixture of 3-iodoindole (1 equiv.), NaOH (2.5 equiv.) and tetrabutylammonium hydrogen sulfate (0.02 equiv.), was stirred in DCM at 0 ^{o}C. A solution of benzene sulfonyl chloride (1.5 equiv.) in DCM was added to the mixture and stirred at room temperature for 2 hours. The reaction mixture was diluted with water, extracted in DCM, dried over anhydrous Na_2SO_4 and the solvent was removed under reduced pressure. The product was purified by silica gel column chromatography, using ethyl acetate and hexane as the solvent system, to afford the pure products in good yields **4n-4o.**

3.8.2. General procedure for the synthesis of aryl/heteroaryl labdane derivatives (5a-5za)

To a stirred solution of compound 3 and aryl/ hetero-aryl iodides (4, 1.2 equiv.) in dry DMF, $Pd(Ph_3P)_2Cl_2$ (0.05 equiv.), CuI (0.02 equiv.) and triethyl amine (2 equiv.) were added. The reaction mixture was stirred at room temperature until the completion of the reaction, as indicated by TLC. The reaction was diluted with water, extracted with ethyl acetate, and dried over Na_2SO_4. The solvent was removed under reduced pressure and the product was purified by silica gel column chromatography, using ethyl acetate and hexane as the solvent system, to afford the pure products in good yields.[37]

3.8.3. Synthesis and characterisation of labdane conjugates 5a-5za

Synthesis of 3-phenylprop-2-yn-1-yl (*E*)-3-formyl-5-(5,5,8a-trimethyl-2-methylenedecahydronaphthalen-1-yl)pent-3-enoate (5a)

Compound **5a** was prepared by the reaction of compound **3** (31 mg) with iodobenzene in dry DMF as per the method described in the section **3.8.2.** Yield: 40% (15 mg).

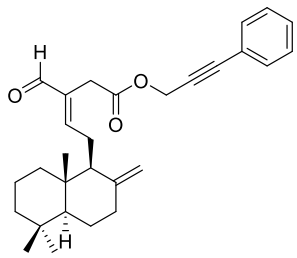

^{1}H NMR (500 MHz, $CDCl_3$) δ: 9.32 (s, 1H), 7.38 (d, *J* = 7Hz, 2H), 7.25-7.24 (m, 3H), 6.62 (t, *J* = 6.5Hz, 1H,), 4.85 (s, 2H), 4.78 (s, 1H), 4.34 (s, 1H), 3.33 (dd, J_1 = 16.5Hz, J_2 = 28.5Hz, 2H), 2.52-0.97 (m, 14H), 0.80 (s,3H), 0.74 (s,3H), 0.65 (s, 3H)

^{13}C NMR (125 MHz, $CDCl_3$) δ: 193.36, 169.47, 159.23, 148.07, 135.89, 131.94, 128.79, 128.30, 107.93, 86.65, 82.69, 56.39, 55.37, 53.36, 41.98,

39.57, 39.22, 37.85, 33.57, 29.52, 24.66, 24.10, 21.72, 19.27, 14.39

HRMS (ESI) m/z: $[M+Na]^+$ calcd for $C_{29}H_{36}O_3Na$ is 455.2562, found 455.2571

Synthesis of 3-(p-tolyl)prop-2-yn-1-yl (E)-3-formyl-5-((1S,8aS)-5,5,8a-trimethyl-2-methylenedecahydronaphthalen-1-yl)pent-3-enoate (5b)

Compound **5b** was prepared by the reaction of compound **3** (32 mg) with 4-iodotoluene in dry DMF as per the method described in the section **3.8.2.** Yield: 40% (16 mg).

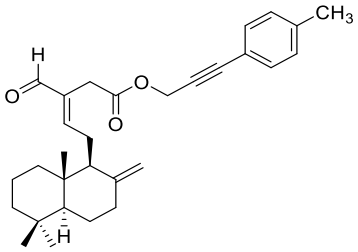

^{1}H NMR (500 MHz, $CDCl_3$) δ: 9.31 (s, 1H), 7.26 (d, *J* = 7.5Hz, 2H), 7.04 (d, *J* = 7.5Hz, 2H), 6.62 (t, *J* = 6.5 Hz, 1H), 4.84 (s, 2H), 4.78 (s, 1H), 4.33 (S, 1H), 3.32 (dd, J_1 = 16.5 Hz, J_2 = 29.5 Hz, 2H), 2.52-2.32 (m, 3H), 2.27 (s, 3H), 1.97-0.96 (m, 11H), 0.80 (s, 3H), 0.73 (s, 3H), 0.64 (s, 3H)

^{13}C NMR (125 MHz, $CDCl_3$) δ: 193.41, 169.50, 159.29, 148.06, 138.99, 135.89, 131.85, 129.06, 119.02, 107.95, 86.85, 81.99, 56.37, 55.35, 53.48, 41.98, 39.56, 39.20, 37.85, 33.58, 33.56, 29.52, 24.66, 24.10, 21.73, 21.52, 19.27, 14.40

HRMS (ESI) m/z : $[M+Na]^+$ calcd for $C_{30}H_{38}O_3Na$ is 469.2719, found 469.2724

Synthesis of 3-(4-hydroxyphenyl)prop-2-yn-1-yl (E)-3-formyl-5-((1S,4aS,8aS)-5,5,8a-trimethyl-2-methylenedecahydronaphthalen-1-yl)pent-3-enoate (5c)

Compound **5c** was prepared by the reaction of compound **3** (38 mg) with 4-iodophenol in dry DMF as per the method described in the section **3.8.2.** Yield: 36% (17 mg).

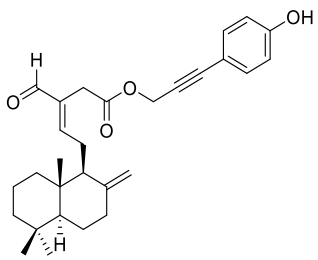

^{1}H NMR (500 MHz, $CDCl_3$) δ: 9.31 (s, 1H), 7.24 (d, *J* = 7.5Hz, 2H), 6.70 (d, *J* = 7.5 Hz, 2H), 6.63 (t, *J* = 6 Hz, 1H), 5.78 (bs, 1H), 4.83 (s, 2H), 4.78 (s, 1H), 4.33 (S, 1H), 3.32 (dd, J_1 = 16.5 Hz, J_2 = 27.5 Hz, 2H), 2.52-0.97 (m, 14H), 0.81 (s, 3H), 0.74 (s, 3H), 0.65 (s, 3H)

^{13}C NMR (125 MHz, $CDCl_3$) δ: 193.63, 169.67, 159.61, 156.49, 148.06, 135.86, 133.70, 115.47, 114.07, 107.93, 86.74, 81.14, 56.38, 55.37, 53.62, 41.98, 39.57, 39.21, 37.85, 33.57, 29.58, 24.70, 24.10, 21.73, 19.28, 14.40

HRMS (ESI) m/z: $[M+Na]^+$ calcd for $C_{29}H_{36}O_4Na$ is 471.2511, found 471.2517

Synthesis of 3-(4-methoxyphenyl)prop-2-yn-1-yl (E)-3-formyl-5-((1S,8aS)-5,5,8a-trimethyl-2-methylenedecahydronaphthalen-1-yl)pent-3-enoate (5d)

Compound **5d** was prepared by the reaction of compound **3** (61 mg) with 4-iodoanisole in dry DMF as per the method described in the section **3.8.2.** Yield: 32% (27 mg).

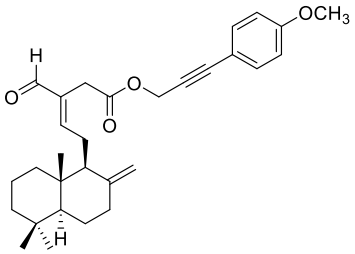

^{1}H NMR (500 MHz, $CDCl_3$) δ: 9.31 (s, 1H), 7.31 (d, 2H, *J* = 8Hz), 6.76 (d, *J* = 7.5Hz, 2H), 6.20 (t, *J* = 6.5 Hz, 1H), 4.84 (s, 2H), 4.78 (s, 1H), 4.34 (S, 1H), 3.74 (s, 3H), 3.32 (dd, J_1 = 16.5 Hz, J_2 = 28.5 Hz, 2H), 2.51-0.97 (m, 14H). 0.81 (s, 3H), 0.74 (s, 3H), 0.65 (s, 3H)

^{13}C NMR (125 MHz, $CDCl_3$) δ: 193.40, 169.51, 159.98, 159.26, 148.06, 135.91, 133.49, 114.18, 113.93, 107.94, 86.69, 81.36, 56.38, 55.36, 55.31, 53.55, 41.98, 39.56, 39.20, 37.85, 33.58, 33.56, 29.53, 24.66, 24.10, 21.73, 19.28, 14.40

HRMS (ESI) m/z: $[M+Na]^+$ calcd for $C_{30}H_{38}O_4Na$ is 485.2668, found 485.2681

Synthesis of 3-(4-nitrophenyl)prop-2-yn-1-yl (E)-3-formyl-5-((1S,8aS)-5,5,8a-trimethyl-2-methylenedecahydronaphthalen-1-yl)pent-3-enoate (5e)

Compound **5e** was prepared the reaction of compound **3** (30 mg) with 1-iodo-4-nitrobenzene in dry DMF as per the method described in the section **3.8.2.** Yield: 52% (21 mg).

^{1}H NMR (500 MHz, $CDCl_3$) δ: 9.32 (s, 1H), 8.12 (d, *J* = 8.5Hz, 2H,), 7.52 (d, *J* = 8.5Hz, 2H), 6.63 (t, *J* =

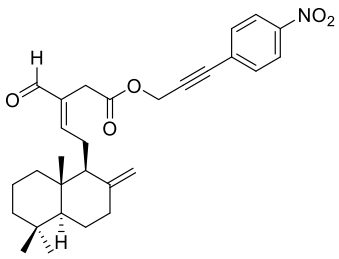

6.5 Hz, 1H), 4.87 (s, 2H), 4.78 (s, 1H), 4.34 (S, 1H), 3.34 (dd, J_1 = 16.5 Hz, J_2 = 20.5 Hz, 2H), 2.52-0.98 (m, 14H). 0.81 (s, 3H), 0.74 (s, 3H), 0.65 (s, 3H)

^{13}C NMR (125 MHz, $CDCl_3$) δ: 193.26, 169.35, 159.12, 148.10, 147.48, 135.79, 132.65, 128.96, 123.55, 107.89, 88.04, 84.59, 56.42, 55.41, 52.86, 41.98, 39.58, 39.27, 37.85, 33.55, 29.51, 24.66, 24.10, 21.70, 19.30, 14.41

HRMS (ESI) m/z: $[M+Na]^+$ calcd for $C_{29}H_{35}NO_2Na$ is 500.2413, found 500.2406

Synthesis of 3-(3,5-dinitrophenyl)prop-2-yn-1-yl (E)-3-formyl-5-((1S,8aS)-5,5,8a-trimethyl-2-methylenedecahydronaphthalen-1-yl)pent-3-enoate (5f)

Compound **5f** was prepared by the reaction of compound **3** (42 mg) with 1-iodo-3,5-dinitrobenzene in dry DMF as per the method described in the section **3.8.2.** Yield: 68% (42 mg).

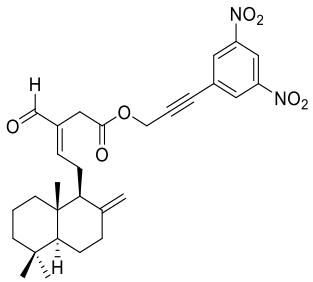

^{1}H NMR (500 MHz, $CDCl_3$) δ: 9.32 (s, 1H), 8.92 (s, 1H), 8.52 (s, 2H), 6.65 (t, J = 6.5 Hz, 1H), 4.85 (s, 2H), 4.79 (s, 1H), 4.34 (S, 1H), 3.34 (s, 2H), 2.52-0.99 (m, 14H), 0.82 (s, 3H), 0.74 (s, 3H), 0.66 (s, 3H)

^{13}C NMR (125 MHz, $CDCl_3$) δ: 193.31, 169.34, 159.25, 148.45, 148.16, 135.70, 131.60, 125.89, 118.59, 107.92, 88.82, 82.07, 56.40, 55.38, 52.50, 41.95, 39.58, 39.28, 37.84, 33.57, 29.53, 24.67, 24.08, 21.70, 19.30, 14.43

HRMS (ESI) m/z: $[M+Na]^+$ calcd for $C_{29}H_{34}N_2O_7Na$ is 545.2264, found 545.2272

Synthesis of methyl 2-(3-(((E)-3-formyl-5-((1S,8aS)-5,5,8a-trimethyl-2-methylenedecahydronaphthalen-1-yl)pent-3-enoyl)oxy)prop-1-yn-1-yl)benzoate (5g)

Compound **5g** was prepared by the reaction of compound **3** (30 mg) with methyl 2-iodobenzoate in dry DMF as per the method described in the section **3.8.2.** Yield: 39% (16 mg).

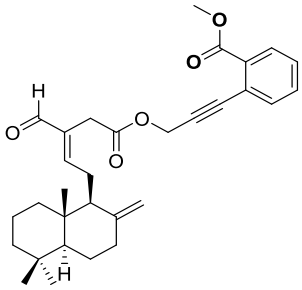

^{1}H NMR (500 MHz, $CDCl_3$) δ: 9.32 (s, 1H), 7.87 (d, *J* = 8Hz, 1H), 7.50 (d, *J* = 7.5Hz, 1H), 7.40 (t, *J* = 7Hz, 1H), 7.32 (t, *J* = 7.5 Hz, 1H), 6.62 (t, *J* = 6.5 Hz, 1H), 4.91 (s, 2H), 4.78 (s, 1H), 4.33 (S, 1H), 3.86 (s, 3H), 3.34 (dd, J_1 = 16.5 Hz, J_2 = 28 Hz, 2H), 2.52-1.96 (m, 14H), 0.80 (s, 3H), 0.73 (s, 3H), 0.64 (s, 3H)

^{13}C NMR (125 MHz, $CDCl_3$) δ: 193.34, 169.44, 166.42, 159.22, 148.07, 135.88, 134.47, 132.12, 131.71, 130.39, 128.42, 122.66, 107.93, 87.69, 85.24, 56.39, 55.37, 53.51, 52.20, 41.97, 39.56, 39.20, 37.85, 33.57, 33.56, 29.51, 24.65, 24.10, 21.72, 19.26, 14.38

HRMS (ESI) m/z: $[M+Na]^+$ calcd for $C_{31}H_{38}O_5Na$ is 513.2617, found 513.2623

Synthesis of methyl 4-(3-(((E)-3-formyl-5-((1S,8aS)-5,5,8a-trimethyl-2-methylenedecahydronaphthalen-1-yl)pent-3-enoyl)oxy)prop-1-yn-1-yl)benzoate (5h)

Compound **5h** was prepared by the reaction of compound **3** (35 mg) with methyl 4-iodobenzoate in dry DMF as per the method described in the section **3.8.2.** Yield: 54% (26 mg).

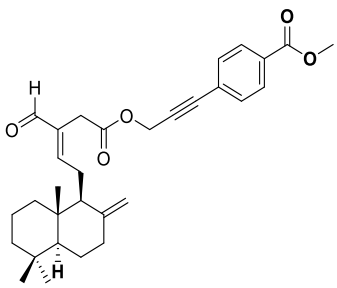

^{1}H NMR (500 MHz, $CDCl_3$) δ: 9.41 (s, 1H), 8.01 (d, *J* = 8Hz, 2H), 7.52 (d, *J* = 7.5Hz, 2H), 6.72 (t, *J* = 6.5 Hz, 1H), 4.95 (s, 2H), 4.87 (s, 1H), 4.42 (S, 1H), 3.94 (s, 3H), 3.42 (dd, J_1 = 16.5 Hz, J_2 = 24.5 Hz, 2H), 2.62-1.06 (m, 14H), 0.89 (s, 3H), 0.83 (s, 3H), 0.74 (s, 3H)

^{13}C NMR (125 MHz, $CDCl_3$) δ: 193.36, 169.42, 166.45, 159.27, 148.07, 135.82, 131.82, 130.06, 129.46, 126.77, 107.94, 85.78, 85.66, 56.38, 55.36, 53.14, 52.30, 41.96, 39.56, 39.22, 37.84, 33.57, 29.51, 24.66, 24.09, 21.72, 19.28, 14.41

HRMS (ESI) m/z: $[M+Na]^+$ calcd for $C_{31}H_{38}O_5$ is 513.2617, found 513.2631

Synthesis of 3-(pyridin-4-yl)prop-2-yn-1-yl (E)-3-formyl-5-((1S,4aS,8aS)-5,5,8a-trimethyl-2-methylenedecahydronaphthalen-1-yl)pent-3-enoate (5i)

Compound **5i** was prepared by the reaction of compound **3** (39 mg) with 4-iodopyridine in dry DMF as per the method described in the section **3.8.2.** Yield: 63% (30 mg).

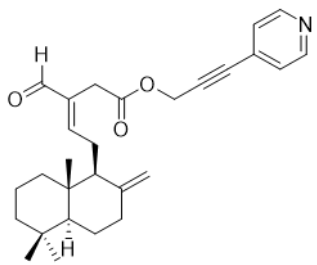

^{1}H NMR (500 MHz, $CDCl_3$) δ: 9.32 (s, 1H), 8.52 (s, 2H), 7.26 (s, 2H), 6.64 (t, *J* = 6Hz, 1H), 4.86 (s, 2H), 4.79 (s, 1H), 4.33 (S, 1H), 3.34 (dd, J_1 = 16.5 Hz, J_2 = 23.5 Hz, 2H), 2.52-0.97 (m, 14H). 0.81 (s, 3H), 0.74 (s, 3H), 0.65 (s, 3H)

^{13}C NMR (125 MHz, $CDCl_3$) δ: 193.30, 169.35, 159.21, 149.73, 148.09, 135.78, 130.38, 125.80, 107.92, 87.57, 83.89, 56.40, 55.39, 52.84, 41.97, 39.57, 39.25, 37.85, 33.57, 29.50, 24.66, 24.09, 21.72, 19.28, 14.42

HRMS (ESI) m/z: $[M+H]^+$ calcd for $C_{28}H_{36}NO_3$ is 434.2695, found 434.2682

Synthesis of 3-(pyridin-2-yl)prop-2-yn-1-yl (E)-3-formyl-5-(5,5,8a-trimethyl-2-methylenedecahydronaphthalen-1-yl)pent-3-enoate (5j)

Compound **5j** was prepared by the reaction of compound **3** (25 mg) with 2-iodopyridine in dry DMF as per the method described in the section **3.8.2.** Yield: 53% (16 mg).

^{1}H NMR (500 MHz, $CDCl_3$) δ: 9.31 (s, 1H), 8.52-8.51 (m, 1H), 7.61 (t, *J* = 7.5 Hz, 1H), 7.41 (d, *J* = 7.5 Hz, 1H), 7.22-7.20 (m, 1H), 6.63 (t, *J* = 6.5Hz, 1H),

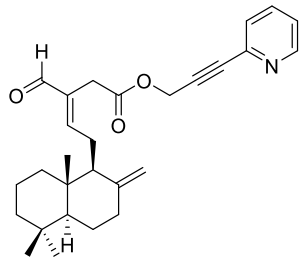

4.88 (s, 2H), 4.79 (s, 1H), 4.33 (s, 1H), 3.33 (dd, J_1 = 16.5Hz, J_2 = 28.5Hz, 2H), 2.53-0.97 (m, 14H), 0.81 (s, 3H), 0.74 (s,3H), 0.65 (s, 3H)

^{13}C NMR (125 MHz, $CDCl_3$) δ: 193.40, 169.39, 159.31, 149.87, 148.05, 142.20, 136.41, 135.79, 127.40, 123.40, 107.95, 85.54, 83.08, 56.38, 55.35, 52.95, 41.97, 39.57, 39.20, 37.84, 33.58, 33.56, 29.48, 24.65, 24.09, 21.73, 19.27, 14.41

HRMS (ESI) m/z: $[M+Na]^+$ calcd for $C_{28}H_{35}NO_3Na$ is 456.2515, found 456.2518

Synthesis of 3-(3-hydroxypyridin-2-yl)prop-2-yn-1-yl (E)-3-formyl-5-((1S,8aS)-5,5,8a-trimethyl-2-methylenedecahydronaphthalen-1-yl)pent-3-enoate (5k)

Compound **5k** was prepared by the reaction of compound **3** (50 mg) with 2-iodopyridin-3-ol in dry DMF as per the method described in the section **3.8.2.** Yield: 36% (23 mg).

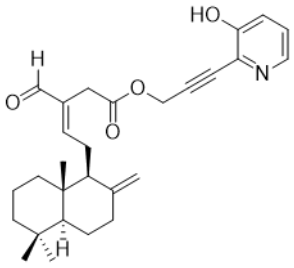

^{1}H NMR (500 MHz, $CDCl_3$) δ: 9.31 (s, 1H), 8.48 (s, 1H), 7.70 (d, J = 8Hz, 1H), 6.93 (s, 1H), 6.61 (t, J = 6.5 Hz, 1H), 5.20 (s, 2H), 4.74 (s, 1H), 4.28 (S, 1H), 3.34 (dd, J_1 = 16.5 Hz, J_2 = 22Hz, 2H), 2.47-0.91 (m, 14H), 0.80 (s, 3H), 0.73 (s, 3H), 0.60 (s, 3H)

^{13}C NMR (125 MHz, $CDCl_3$) δ: 193.36, 169.54, 159.26, 155.95, 148.04, 147.51, 145.91, 135.79, 119.52, 118.61, 107.95, 107.88, 58.94, 56.33, 55.34, 41.95, 39.53, 39.18, 37.82, 33.58, 33.55, 29.52, 24.62, 24.07, 21.73, 19.27, 14.36

HRMS (ESI) m/z : $[M+H]^+$ calcd for $C_{28}H_{36}NO_4$ is 450.2644, found 450.2645

3.8.3.12. Synthesis of 3-(thiophen-2-yl)prop-2-yn-1-yl (E)-3-formyl-5-((1S,8aS)-5,5,8a-trimethyl-2-methylenedecahydronaphthalen-1-yl)pent-3-enoate (5l)

Compound **5l** was prepared by the reaction of compound **3** (26 mg) with 2-iodothiophene in dry DMF as per the method described in the section **3.8.2.** Yield: 53% (17 mg).

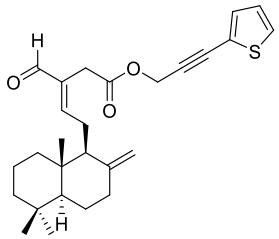

^{1}H NMR (500 MHz, $CDCl_3$) δ: 9.31 (s, 1H), 7.22-7.17 (m, 2H), 6.90 (m, 1H), 6.62 (t, *J* = 6.5Hz, 1H,), 4.86 (s, 2H), 4.78 (s, 1H), 4.33 (s, 1H), 3.33 (dd, J_1 = 16.5Hz, J_2 = 28.5Hz, 2H), 2.52-0.97 (m, 14H), 0.81 (s, 3H), 0.74 (s, 3H), 0.65 (s, 3H)

^{13}C NMR (125 MHz, $CDCl_3$) δ: 193.34, 169.43, 159.27, 148.06, 135.83, 133.05, 127.89, 126.97, 121.97, 107.93, 86.72, 80.02, 56.39, 55.37, 53.35, 41.99, 39.57, 39.22, 37.86, 33.58, 33.56, 29.49, 24.67, 24.10, 21.73, 19.28, 14.39

HRMS (ESI) m/z: $[M+Na]^+$ calcd for $C_{27}H_{34}O_3SNa$ is 461.2126, found 461.2135

Synthesis of *tert*-butyl 3-(3-(((E)-3-formyl-5-((1S,8aS)-5,5,8a-trimethyl-2-methylenedecahydronaphthalen-1-yl)pent-3-enoyl)oxy)prop-1-yn-1-yl)-1H-indole-1-carboxylate (5m)

Compound **5m** was prepared by the reaction of compound **3** (35 mg) with *tert*-butyl 3-iodo-1H-indole-1-carboxylate in dry DMF as per the method described in the section **3.8.2.** Yield: 32% (8 mg).

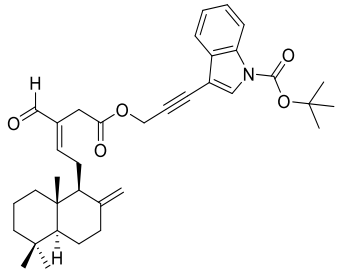

^{1}H NMR (500 MHz, $CDCl_3$) δ: 9.32 (s, 1H), 8.06 (d, *J* = 7.5 Hz, 1H), 7.71 (s, 1H), 7.59 (d, *J* = 8 Hz, 1H), 7.29 (t, *J* = 7.5 Hz, 1H), 7.22 (t, *J* = 7.5 Hz, 1H), 6.62 (t, *J* = 6.5 Hz, 1H), 4.92 (s, 2H), 4.77 (s, 1H), 4.33 (S, 1H), 3.34 (dd, J_1 =16.5 Hz, J_2 = 32 Hz, 2H), 2.52-1.64 (m, 6H), 1.60 (s, 9H), 1.43-0.934 (m, 8H), 0.78 (s, 3H), 0.71 (s, 3H), 0.61 (s, 3H)

^{13}C NMR (125 MHz, $CDCl_3$) δ: 193.35, 169.50, 159.25, 148.97, 148.06, 135.90, 134.57, 130.38, 129.80, 125.26, 123.30, 120.09, 115.24, 107.93, 102.31, 86.24, 84.45, 78.85, 56.38, 55.35, 53.54, 41.96, 39.54, 39.18, 37.84, 33.55, 33.53, 29.55, 28.14, 24.67, 24.08, 21.70, 19.22, 14.36;

HRMS (ESI) m/z: $[M+Na]^+$ calcd for $C_{36}H_{45}NO_5Na$ is 594.3195, found 594.3198

Synthesis of *tert*-butyl 3-(3-(((E)-3-formyl-5-((1S,8aS)-5,5,8a-trimethyl-2-methylenedecahydronaphthalen-1-yl)pent-3-enoyl)oxy)prop-1-yn-1-yl)-5-methoxy-1H-indole-1-carboxylate (5n)

Compound **5n** was prepared by the reaction of compound **3** (36 mg) with *tert*-butyl 3-iodo-5-methoxy-1H-indole-1-carboxylate in dry DMF as per the method described in the section **3.8.2.** Yield: 46% (28 mg).

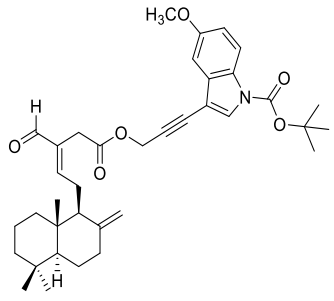

^{1}H NMR (500 MHz, $CDCl_3$) δ: 9.32 (s, 1H), 7.93 (d, *J* = 8Hz, 1H), 7.68 (s, 1H), 7.02 (s, 1H), 6.89 (d, *J* = 9Hz, 1H), 6.62 (t, *J* = 6.5 Hz, 1H), 4.92 (s, 2H), 4.77 (s, 1H), 4.32 (S, 1H), 3.82 (s, 3H), 3.34 (dd, J_1 =16.5 Hz, J_2 = 32 Hz, 2H), 2.52-1.64 (m, 6H), 1.53 (s, 9H), 1.44-0.94 (m, 8H), 0.78 (s, 3H), 0.71 (s, 3H), 0.62 (s, 3H)

^{13}C NMR (125 MHz, $CDCl_3$) δ: 193.34, 169.51, 159.23, 156.48, 148.91, 148.06, 135.91, 131.29, 130.29, 129.19, 116.06, 114.51, 107.92, 102.13, 102.06, 86.33, 84.30, 78.96, 56.37, 55.76, 55.34, 53.59, 41.95, 39.54, 39.18, 37.84, 33.55, 33.53, 29.57, 28.14, 24.67, 24.08, 21.70, 19.22, 14.36

HRMS (ESI) m/z : $[M+Na]^+$ calcd for $C_{37}H_{47}NO_6Na$ is 624.3301, found 624.3312

Synthesis of *tert*-butyl 3-(3-(((E)-3-formyl-5-((1S,8aS)-5,5,8a-trimethyl-2-methylenedecahydronaphthalen-1-yl)pent-3-enoyl)oxy)prop-1-yn-1-yl)-2-methyl-1H-indole-1-carboxylate (5o)

Compound **5o** (60 mg) was prepared by the reaction of compound **3** with *tert*-butyl 3-iodo-2-methyl-1H-indole-1-carboxylate in dry DMF as per the method described in the section **3.8.2.** Yield: 32% (32 mg).

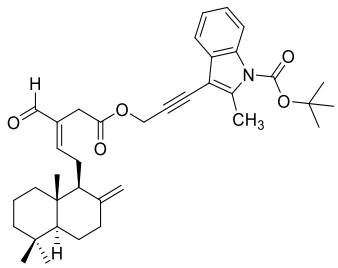

^{1}H NMR (500 MHz, $CDCl_3$) δ: 9.31 (s, 1H), 8.01-7.99 (m, 1H), 7.50-7.48 (m, 1H), 7.21-7.17 (2H, m), 6.62 (t, *J* = 6.5 Hz, 1H), 4.95 (s, 2H), 4.77 (s, 1H), 4.33 (S, 1H), 3.35 (dd, J_1 =16.5 Hz, J_2 = 34.5 Hz, 2H), 2.63 (s, 3H), 2.52-1.66 (m, 6H), 1.61 (s, 9H), 1.42-0.92 (m, 8H), 0.78 (s, 3H), 0.71 (s, 3H), 0.60 (s, 3H)

^{13}C NMR (125 MHz, $CDCl_3$) δ: 193.36, 169.51, 159.22, 150.05, 148.04, 142.65, 135.94, 135.28, 129.29, 124.30, 123.23, 119.10, 115.45, 107.94, 102.48, 88.18, 84.48, 79.44, 56.37, 55.35, 53.75, 41.95, 39.52, 39.16, 37.84, 33.55, 33.53, 29.59, 28.23, 24.67, 24.08, 21.69, 19.21, 15.84, 14.34

HRMS (ESI) m/z: $[M+Na]^+$ calcd for $C_{37}H_{47}NO_5Na$ is 608.3352, found 608.3371

Synthesis of *tert*-butyl 4-bromo-3-(3-(((E)-3-formyl-5-((1S,8aS)-5,5,8a-trimethyl-2-methylenedecahydronaphthalen-1-yl)pent-3-enoyl)oxy)prop-1-yn-1-yl)-1H-indole-1-carboxylate (5p)

Compound **5p** was prepared by the reaction of compound **3** (40 mg) with *tert*-butyl 4-bromo-3-iodo-1H-indole-1-carboxylate in dry DMF as per the method described in the section **3.8.2.** Yield: 29% (21 mg).

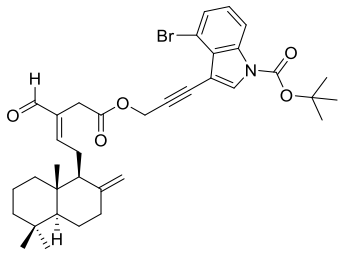

^{1}H NMR (500 MHz, $CDCl_3$) δ: 9.32 (s, 1H), 8.09 (d, *J* = 8Hz, 1H), 7.76 (s, 1H), 7.34 (d, *J* = 7.5 Hz, 1H), 7.10 (t, *J* = 8Hz, 1H), 6.62 (t, *J* = 6.5 Hz, 1H), 4.88 (s, 2H), 4.77 (s, 1H), 4.33 (S, 1H), 3.32 (dd, J_1 =16.5 Hz, J_2 = 32 Hz, 2H), 2.52-1.63 (m, 6H), 1.59 (s, 9H), 1.42-0.94 (m, 8H), 0.79 (s, 3H), 0.71 (s, 3H), 0.62 (s, 3H).

^{13}C NMR (125 MHz, $CDCl_3$) δ: 193.34, 169.50, 159.26, 148.37, 148.05, 135.91, 135.70, 131.87, 127.82, 125.99, 125.04, 115.16, 114.55, 107.92, 102.53, 87.37, 85.06, 79.42, 56.38, 55.35, 53.65,

41.95, 39.55, 39.18, 37.85, 33.54, 33.53, 29.49, 28.08, 24.69, 24.09, 21.70, 19.22, 14.34.

HRMS (ESI) m/z: $[M+Na]^+$ calcd for $C_{36}H_{44}NO_5$ is 672.2301, found 672.2294.

Synthesis of *tert*-butyl 5-bromo-3-(3-(((E)-3-formyl-5-((1S,8aS)-5,5,8a-trimethyl-2-methylenedecahydronaphthalen-1-yl)pent-3-enoyl)oxy)prop-1-yn-1-yl)-1H-indole-1-carboxylate (5q)

Compound **5q** (35 mg) was prepared by the reaction of compound **3** with *tert*-butyl 4-bromo-3-iodo-1H-indole-1-carboxylate in dry DMF as per the method described in the section **3.8.2.** Yield: 30% (19 mg).

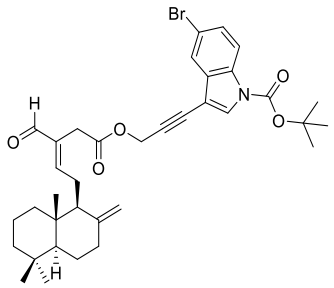

^{1}H NMR (500 MHz, $CDCl_3$) δ: 9.31 (s, 1H), 7.93 (d, *J* = 8.5 Hz, 1H), 7.71 (s, 1H), 7.69 (s, 1H), 7.37 (dd, J_1 = 1Hz, J_2 = 8.5Hz, 1H), 6.63 (t, *J* = 6.5 Hz, 1H), 4.90 (s, 2H), 4.78 (s, 1H), 4.33 (S, 1H), 3.35 (dd, J_1 =16.5 Hz, J_2 = 31 Hz, 2H), 2.52-1.64 (m, 6H), 1.59 (s, 9H), 1.46-0.92 (m, 8H), 0.78 (s, 3H), 0.71 (s, 3H), 0.61 (s, 3H)

^{13}C NMR (125 MHz, $CDCl_3$) δ: 193.33, 169.47, 159.25, 148.59, 148.05, 135.88, 133.33, 132.04, 130.64, 128.21, 122.82, 116.87, 116.73, 107.94, 101.68, 86.75, 84.96, 78.03, 56.36, 55.34, 53.38, 41.95, 39.53, 39.17, 37.84, 33.55, 33.53, 29.55, 28.10, 24.67, 24.08, 21.70, 19.23, 14.37

HRMS (ESI) m/z: $[M+Na]^+$ calcd for $C_{36}H_{44}BrNO_5$ is 672.2301, found 672.2312

Synthesis of *tert*-butyl 6-bromo-3-(3-(((E)-3-formyl-5-((1S,4aS,8aS)-5,5,8a-trimethyl-2-methylenedecahydronaphthalen-1-yl)pent-3-enoyl)oxy)prop-1-yn-1-yl)-1H-indole-1-carboxylate (5r)

Compound **5r** was prepared by the reaction of compound **3** (30 mg) with *tert*-butyl 6-bromo-3-iodo-1H-indole-1-carboxylate in dry DMF as per the method described in the section **3.8.2.** Yield: 24% (13 mg).

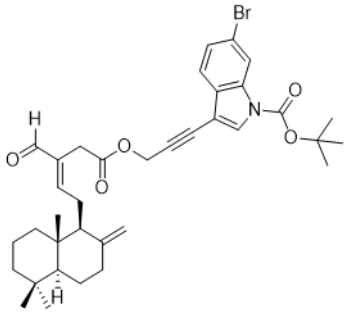

^{1}H NMR (500 MHz, $CDCl_3$) δ: 9.32 (s, 1H), 8.28 (s, 1H), 7.66 (s, 1H), 7.44 (d, *J* = 8Hz, 1H), 7.34 (d, *J* = 8.5 Hz, 1H), 6.62 (t, *J* = 6.5 Hz, 1H), 4.90 (s, 2H), 4.77 (s, 1H), 4.33 (S, 1H), 3.34 (dd, J_1 =16.5 Hz, J_2 = 29 Hz, 2H), 2.51-1.65 (m, 6H), 1.59 (s, 9H), 1.44-0.93 (m, 8H), 0.79 (s, 3H), 0.72 (s, 3H), 0.61 (s, 3H)

^{13}C NMR (125 MHz, $CDCl_3$) δ: 193.37, 169.49, 159.27, 148.55, 148.06, 135.86, 130.05, 129.21, 126.63, 121.24, 119.08, 118.50, 107.93, 102.28, 86.65, 85.06, 78.19, 56.37, 55.34, 53.42, 41.95, 39.54, 39.18, 37.84, 33.56, 33.54, 29.55, 28.07, 24.67, 24.08, 21.70, 19.24, 14.38

HRMS (ESI) m/z: $[M+Na]^+$ calcd for $C_{36}H_{44}BrNO_5$ is 672.2301, found 672.2312

Synthesis of *tert*-butyl 5-fluoro-3-(3-(((E)-3-formyl-5-((1S,8aS)-5,5,8a-trimethyl-2-methylenedecahydronaphthalen-1-yl)pent-3-enoyl)oxy)prop-1-yn-1-yl)-1H-indole-1-carboxylate (5s)

Compound **5s** was prepared by the reaction of compound **3** (51 mg) with *tert*-butyl 5-fluoro-3-iodo-1H-indole-1-carboxylate in dry DMF as per the method described in the section **3.8.2.** Yield: 30% (25 mg).

^{1}H NMR (500 MHz, $CDCl_3$) δ: 9.32 (s, 1H), 8.02-8.01 (m, 1H), 7.73 (s, 1H), 7.24 (dd, J_1 = 2.5Hz, J_2 = 8.5 Hz, 1H), 7.03-6.98 (m, 1H), 6.63 (t, *J* = 6.5 Hz, 1H), 4.90 (s, 2H), 4.77 (s, 1H), 4.33 (S, 1H), 3.34 (dd, J_1 =16.5 Hz, J_2 = 29.5 Hz, 2H), 2.52-1.64 (m, 6H), 1.59

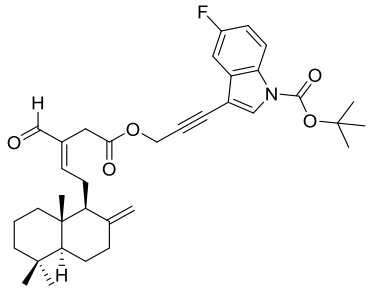

(s, 9H), 1.44-0.93 (m, 8H), 0.78 (s, 3H), 0.71 (s, 3H), 0.61 (s, 3H)

^{13}C NMR (125 MHz, CDCl$_3$) δ: 193.37, 169.48, 160.63, 159.28, 158.71, 148.70, 148.05, 135.87, 131.09, 116.39, 116.32, 113.31, 113.11, 107.94, 105.85, 105.66, 102.16, 102.13, 86.67, 84.75, 78.22, 56.37, 55.34, 53.43, 41.95, 39.53, 39.17, 37.84, 33.55, 33.53, 29.54, 28.10, 24.67, 24.07, 21.70, 19.21, 14.35

HRMS (ESI) m/z: $[M+Na]^+$ calcd for $C_{36}H_{44}FNO_5Na$ is 612.3101, found 612.3104

Synthesis of *tert*-butyl 3-(3-(((E)-3-formyl-5-((1S,8aS)-5,5,8a-trimethyl-2-methylenedecahydronaphthalen-1-yl)pent-3-enoyl)oxy)prop-1-yn-1-yl)-5-nitro-1H-indole-1-carboxylate (5t)

Compound **5t** (42 mg) was prepared by the reaction of compound **3** with *tert*-butyl 3-iodo-5-nitro-1H-indole-1-carboxylate in dry DMF as per the method described in the section **3.8.2.** Yield: 48% (35 mg).

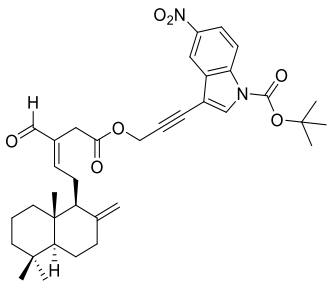

^{1}H NMR (500 MHz, CDCl$_3$) δ: 9.33 (s, 1H), 8.50 (s, 1H), 8.21-8.17(m, 2H), 7.83(s, 1H), 6.64 (t, J = 6.5 Hz, 1H), 4.91 (s, 2H), 4.77 (s, 1H), 4.33 (S, 1H), 3.36 (dd, J_1 =16.5 Hz, J_2 = 27 Hz, 2H), 2.52-1.66 (m, 6H), 1.62 (s, 9H), 1.44-0.94 (m, 8H), 0.78 (s, 3H), 0.71 (s, 3H), 0.61 (s, 3H)

^{13}C NMR (125 MHz, CDCl$_3$) δ: 193.40, 169.48, 159.29, 148.16, 148.05, 144.17, 137.56, 135.84, 132.24, 130.41, 120.53, 116.54, 115.68, 107.95, 103.36, 87.82, 85.98, 56.36, 55.33, 53.26, 41.93, 39.53, 39.18, 37.82, 33.55, 33.53, 29.55, 28.05, 24.67, 24.07, 21.70, 19.24, 14.36

HRMS (ESI) m/z: $[M+Na]^+$ calcd for $C_{36}H_{44}N_2O_7$ is 639.3046, found 639.3060

Synthesis of *tert*-butyl6-chloro-3-(3-(((E)-3-formyl-5-((1S,8aS)-5,5,8a-trimethyl-2-methylenedecahydronaphthalen-1-yl)pent-3-enoyl)oxy)prop-1-yn-1-yl)-1H-indole-1-carboxylate (5u)

Compound **5u** was prepared by the reaction of compound **3** (30 mg) with *tert*-butyl 6-chloro-3-iodo-1H-indole-1-carboxylate in dry DMF as per the method described in the section **3.8.2.** Yield: 25% (13 mg).

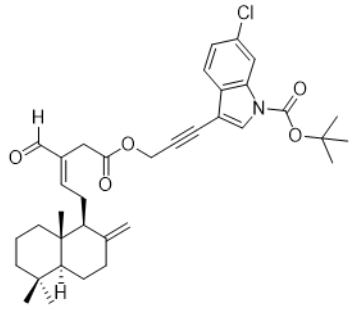

^{1}H NMR (500 MHz, $CDCl_3$) δ: 9.32 (s, 1H), 8.11 (s, 1H), 7.68 (s, 1H), 7.49 (d, *J* = 8.5 Hz, 1H), 7.21 (s, 1H)), 6.63 (t, *J* = 6.5 Hz, 1H), 4.90 (s, 2H), 4.77 (s, 1H), 4.31 (S, 1H), 3.34 (dd, J_1 =16.5 Hz, J_2 = 29.5 Hz, 2H), 2.52-1.67 (m, 6H), 1.60 (s, 9H), 1.44-0.94 (m, 8H), 0.79 (s, 3H), 0.72 (s, 3H), 0.62 (s, 3H)

^{13}C NMR (125 MHz, $CDCl_3$) δ: 192.30, 168.45, 158.15, 147.57, 147.06, 134.88, 133.89, 130.34, 129.13, 127.85, 122.94, 119.87, 114.60, 106.90, 101.27, 85.61, 84.02, 77.23, 55.39, 54.37, 52.40, 40.96, 38.54, 38.20, 36.84, 32.53, 28.54, 27.07, 23.66, 23.08, 20.68, 18.23, 13.36

HRMS (ESI) m/z: $[M+Na]^+$ calcd for $C_{36}H_{44}ClNO_5Na$ is 628.2806, found 628.2814

Synthesis of *tert*-butyl 5-formyl-3-(3-(((E)-3-formyl-5-((1S,8aS)-5,5,8a-trimethyl-2-methylenedecahydronaphthalen-1-yl)pent-3-enoyl)oxy)prop-1-yn-1-yl)-1H-indole-1-carboxylate (5v)

Compound **5v** was prepared by the reaction of compound **3** (50 mg) with *tert*-butyl 5-formyl-3-iodo-1H-indole-1-carboxylate in dry DMF as per the method described in the section **3.8.2.** Yield: 33% (28 mg).

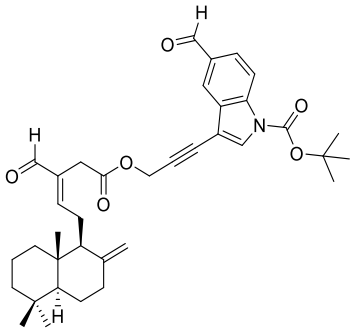

^{1}H NMR (500 MHz, $CDCl_3$) δ: 10.04 (s, 1H), 9.33 (s, 1H), 8.21 (d, *J* = 8.5Hz, 1H), 8.13 (s, 1H), 7.84 (d, *J* = 9 Hz, 1H), 7.79 (s, 1H)), 6.64 (t, *J* = 6.5 Hz, 1H), 4.91 (s, 2H), 4.77 (s, 1H), 4.33 (S, 1H), 3.35 (dd, J_1 = 16.5 Hz, J_2 = 27.5 Hz, 2H), 2.52-1.66 (m, 6H), 1.61 (s, 9H), 1.43-0.94 (m, 8H), 0.78 (s, 3H), 0.71 (s, 3H), 0.61 (s, 3H)

^{13}C NMR (125 MHz, $CDCl_3$) δ: 193.39, 192.03, 169.50, 159.28, 148.45, 148.05, 137.99, 135.86, 132.18, 131.26, 130.66, 125.82, 123.65, 115.87, 107.95, 103.16, 87.28, 85.49, 77.76, 56.37, 55.33, 53.36, 41.94, 39.53, 39.18, 37.83, 33.55, 33.53, 29.56, 28.08, 24.67, 24.07, 21.69, 19.23, 14.37

HRMS (ESI) m/z: $[M+Na]^+$ calcd for $C_{37}H_{45}NO_6$ is 622.3145, found 622.3134

Synthesis of 3-(1-benzoyl-5-nitro-1H-indol-3-yl)prop-2-yn-1-yl (E)-3-formyl-5-((1S,8aS)-5,5,8a-trimethyl-2-methylenedecahydronaphthalen-1-yl)pent-3-enoate (5w)

Compound **5w** was prepared by the reaction of compound **3** (35 mg) with (3-iodo-5-nitro-1H-indol-1-yl)(phenyl)methanone in dry DMF as per the method described in the section **3.8.2.** Yield: 21% (13 mg).

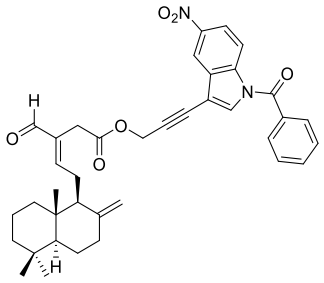

^{1}H NMR (500 MHz, $CDCl_3$) δ: 9.32 (s, 1H), 8.56 (d, *J* = 2 Hz, 1H), 8.43 (d, *J* = 9Hz, 1H), 8.260 (dd, J_1 = 2.5 Hz, J_2 = 9.5 Hz, 1H), 7.70-7.63 (m, 3H), 7.62 (s, 1H), 7.52 (t, *J* = 7.5 Hz, 2H), 6.64 (t, *J* = 6.5 Hz, 1H), 4.91 (s, 2H), 4.76 (s, 1H), 4.32 (S, 1H), 3.34 (dd, J_1 = 16.5 Hz, J_2 = 21.5 Hz, 2H), 2.51-0.95 (m, 14H), 0.79 (s, 3H), 0.71 (s, 3H), 0.61 (s, 3H)

^{13}C NMR (125 MHz, $CDCl_3$) δ: 193.42, 169.48, 167.99, 159.31, 148.07, 144.87, 138.31, 135.80, 133.55, 133.18, 132.64, 130.71, 129.47, 129.07,

121.13, 116.84, 116.50, 107.93, 104.29, 88.38, 56.36, 55.33, 53.17, 41.93, 39.53, 39.20, 37.82, 33.56, 33.54, 29.55, 24.66, 24.07, 21.71, 19.26, 14.37

HRMS (ESI) m/z: $[M+Na]^+$ calcd for $C_{38}H_{40}N_2O_6$ is 643.2784 found 643.2790

Synthesis of 3-(1-(4-chlorobenzoyl)-5-nitro-1H-indol-3-yl)prop-2-yn-1-yl (E)-3-formyl-5-((1S,8aS)-5,5,8a-trimethyl-2-methylenedecahydronaphthalen-1-yl)pent-3-enoate (5x)

Compound **5x** was prepared by the reaction of compound **3** (50 mg) with (4-chlorophenyl)(3-iodo-5-nitro-1H-indol-1-yl)methanone in dry DMF as per the method described in the section **3.8.2.** Yield: 24% (22 mg).

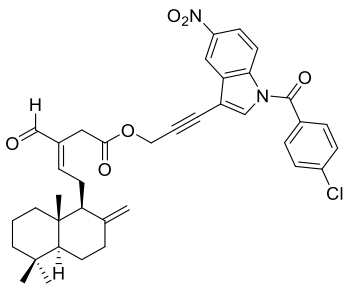

^{1}H NMR (500 MHz, $CDCl_3$) δ: 9.32 (s, 1H), 8.55 (s 1H), 8.40 (d, *J* = 9Hz, 1H), 8.260 (d, *J* = 9 Hz, 1H), 7.65 (d, *J* = 8.5 Hz, 2H), 7.57 (s, 1H), 7.50 (d, *J* = 8.5 Hz, 2H), 6.64 (t, *J* = 6.5 Hz, 1H), 4.91 (s, 2H), 4.76 (s, 1H), 4.33 (S, 1H), 3.34 (dd, J_1 =16.5 Hz, J_2 = 20 Hz, 2H), 2.51-0.95 (m, 14H), 0.79 (s, 3H), 0.72 (s, 3H), 0.61 (s, 3H)

^{13}C NMR (125 MHz, $CDCl_3$) δ: 193.32, 169.42, 166.84, 159.14, 148.08, 145.01, 139.82, 138.25, 135.83, 133.02, 130.97, 130.87, 130.69, 129.47, 121.23, 116.78, 116.53, 107.89, 104.72, 88.66, 76.53, 56.39, 55.38, 53.08, 41.96, 39.55, 39.23, 37.83, 33.54, 29.56, 24.66, 24.08, 21.69, 19.27, 14.37

HRMS (ESI) m/z: $[M+Na]^+$ calcd for $C_{38}H_{39}ClN_2O_6Na$ is 677.2394 found 677.2387

Synthesis of 3-(1-(4-chlorobenzoyl)-5-methoxy-1H-indol-3-yl)prop-2-yn-1-yl (E)-3-formyl-5-((1S,8aS)-5,5,8a-trimethyl-2-methylenedecahydronaphthalen-1-yl)pent-3-enoate (5y)

Compound **5y** was prepared by the reaction of compound 3 (50 mg) with (4-chlorophenyl)(3-iodo-5-methoxy-1H-indol-1-yl)methanonein dry DMF as per the method described in the section **3.8.2.** Yield: 38% (34 mg).

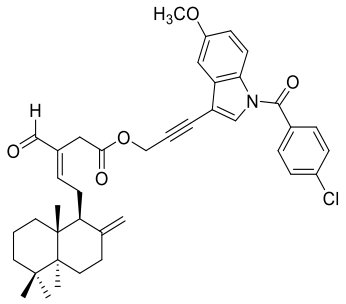

^{1}H NMR (500 MHz, $CDCl_3$) δ: 9.31 (s, 1H), 8.17 (d, *J* = 9Hz, 1H), 7.60 (d, *J* = 8.5 Hz, 2H), 7.45 (d, *J* = 8 Hz, 2H), 7.36 (s, 1H), 7.06 (s, 1H), 6.97-6.94 (m, 1H), 6.61 (t, *J* = 6.5 Hz, 1H), 4.90 (s, 2H), 4.76 (s, 1H), 4.32 (S, 1H), 3.85 (s, 3H), 3.33 (dd, J_1 =16.5 Hz, J_2 = 22.5 Hz, 2H), 2.51-0.94 (m, 14H), 0.79 (s, 3H), 0.72 (s, 3H), 0.61 (s, 3H)

^{13}C NMR (125 MHz, $CDCl_3$) δ: 193.27, 169.44, 166.76, 159.09, 157.44, 148.07, 138.72, 135.88, 132.18, 131.64, 131.21, 130.60, 129.92, 129.12, 117.33, 115.05, 107.88, 103.97, 102.35, 87.20, 78.30, 56.39, 55.79, 55.37, 53.37, 41.96, 39.55, 39.22, 37.84, 33.53, 29.56, 24.65, 24.09, 21.69, 19.25, 14.36

HRMS (ESI) m/z: $[M+Na]^+$ calcd for $C_{39}H_{42}ClNO_5Na$ is 662.2649 found 662.2661

Synthesis of 3-(5-nitro-1-(phenylsulfonyl)-1H-indol-3-yl)prop-2-yn-1-yl (E)-3-formyl-5-((1S,8aS)-5,5,8a-trimethyl-2-methylenedecahydronaphthalen-1-yl)pent-3-enoate (5z)

Compound **5z** was prepared by the reaction of compound 3 (54 mg) with 3-iodo-5-nitro-1-(phenylsulfonyl)-1H-indole in dry DMF as per the method described in the section **3.8.2.** Yield: 54% (54 mg).

^{1}H NMR (500 MHz, $CDCl_3$) δ: 9.32 (s, 1H), 8.45 (d, *J* = 2 Hz, 1H), 8.18 (dd, J_1 = 2 Hz, J_2 =

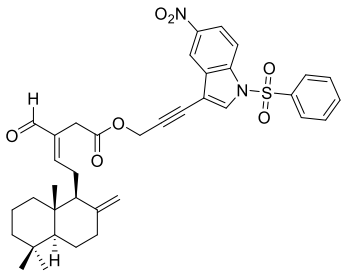

9 Hz, 1H), 8.01 (d, *J* = 9.5Hz, 1H), 7.85 (d, *J* = 8Hz, 2H), 7.82 (s, 1H), 7.56 (t, *J* = 7.5 Hz, 1H), 7.45 (t, *J* = 8Hz, 2H), 6.64 (t, *J* = 6.5 Hz, 1H), 4.91 (s, 2H), 4.76 (s, 1H), 4.33 (S, 1H), 3.34 (dd, J_1 =16.5 Hz, J_2 = 21.5 Hz, 2H), 2.52-0.94 (m, 14H), 0.76 (s, 3H), 0.70 (s, 3H), 0.61 (s, 3H)

^{13}C NMR (125 MHz, $CDCl_3$) δ: 193.34, 169.43, 159.21, 148.07, 144.69, 137.22, 136.79, 135.81, 134.95, 132.08, 130.72, 129.84, 127.02, 120.81, 117.14, 113.93, 107.92, 105.17, 88.81, 76.19, 56.37, 55.35, 53.08, 41.94, 39.54, 39.21, 37.82, 33.54, 33.52, 29.56, 24.67, 24.07, 21.69, 19.24, 14.37

HRMS (ESI) m/z: $[M+Na]^+$ calcd for $C_{37}H_{40}N_2O_7SNa$ is 679.2454, found 679.2459

Synthesis of 3-(5-methoxy-1-(phenylsulfonyl)-1H-indol-3-yl)prop-2-yn-1-yl (E)-3-formyl-5-((1S,8aS)-5,5,8a-trimethyl-2-methylenedecahydronaphthalen-1-yl)pent-3-enoate (5za)

Compound **5za** was prepared by the reaction of compound **3** (68 mg) with 3-iodo-5-methoxy-1-(phenylsulfonyl)-1H-indole in dry DMF as per the method described in the section **3.8.2.** Yield: 51% (62 mg).

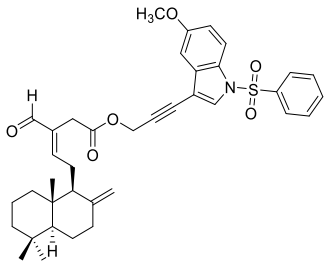

^{1}H NMR (500 MHz, $CDCl_3$) δ: 9.31 (s, 1H), 7.79-7.77 (m, 3H), 7.64 (s, 1H), 7.47 (t, *J* = 7.5 Hz, 1H), 7.36 (t, *J* = 8 Hz, 2H), 6.95 (d, *J* = 2.5 Hz, 1H), 6.88 (dd, J_1 = 2.5 Hz, J_2 = 9Hz, 1H), 6.61 (t, *J* = 6.5 Hz, 1H), 4.89 (s, 2H), 4.76 (s, 1H), 4.32 (S, 1H), 3.76 (s, 3H), 3.32 (dd, J_1 =16.5 Hz, J_2 = 24.5 Hz, 2H), 2.51-0.93 (m, 14H), 0.78 (s, 3H), 0.71 (s, 3H), 0.61 (s, 3H)

^{13}C NMR (125 MHz, $CDCl_3$) δ: 193.32, 169.46, 159.20, 157.05, 148.08, 137.81, 135.86, 134.12, 131.75, 130.28, 129.41, 128.71, 126.82, 115.23, 114.50, 107.91, 104.30, 102.42, 87.31, 77.98, 56.38, 55.74, 55.36, 53.39, 41.95, 39.55, 39.21, 37.84, 33.55, 33.53, 29.57, 24.67, 24.08, 21.70, 19.22, 14.38

HRMS (ESI) m/z: $[M+Na]^+$ calcd for $C_{38}H_{43}NO_6SNa$ is 664.2709, found 664.2708

3.8.4. Molecular modelling studies of aryl/hetero-aryl labdane derivatives with COX-2

We used structure-guided drug-binding analysis to screen our synthesized labdane derivatives for the potential target protein COX-2 (PDB:5KIR). The server SwissDock (http://swissdock.ch/) was primarily used for docking our novel compounds with COX-2 and then further validated using another server HADDOCK2.2 (https://haddock.science.uu.nl/) to obtain unbiased results. Both servers showed consistent docking results, indicating three positions where our compounds could potentially interact with COX-2 (**Figure 3.16** and **Figure 3.17**): a single true site (C1) and two false-positive sites (C2, C3). We assessed and corroborated these sites based on C-score (confidence score), Z-score (clash score), and based on known active site pockets. To select the best docking site and mode/orientation of the bound drug, we considered binding free energies and overall occupancy of the bound drug. The final best-fit model of individual drugs/ligands from **Scheme 3.1**, docked in COX-2 (**Figure 3.16**) was visualized in PyMol.

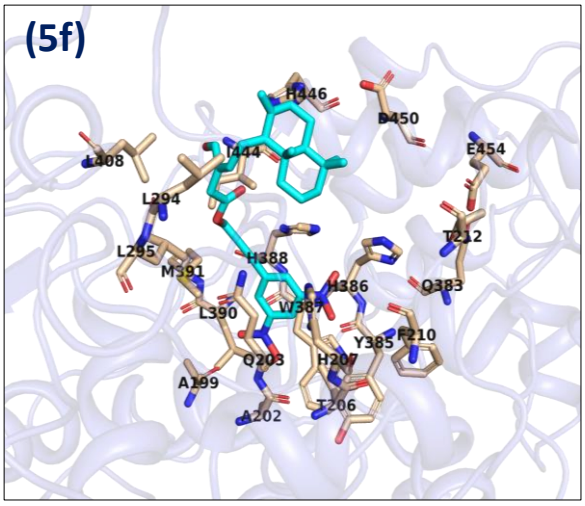
(5f)
H446
D450
E454
L408
I444
L294
T212
L295
M391
H388
H386
Q383
L390
W387
Y385
F210
Q203
H207
A199
T206
A202

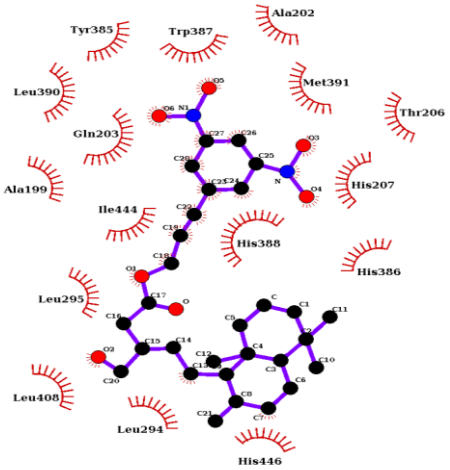
Ala202
Tyr385
Trp387
Leu390
Met391
Thr206
Gln203
Ala199
His207
Ile444
His388
His386
Leu295
Leu408
Leu294
His446

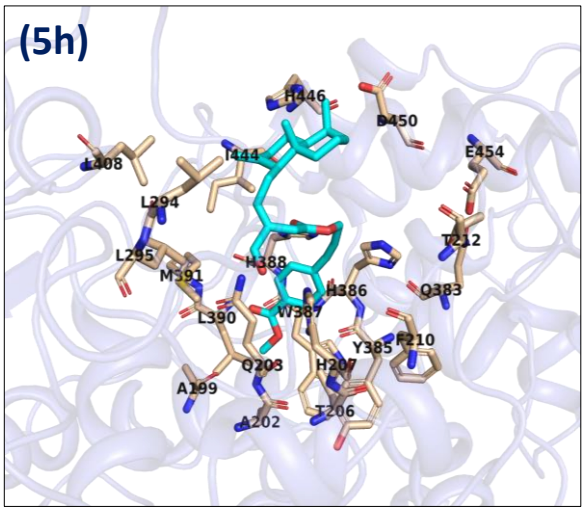
(5h)
H446
D450
E454
L408
I444
L294
T212
L295
M391
H388
H386
Q383
L390
W387
Y385
F210
Q203
H207
A199
T206
A202

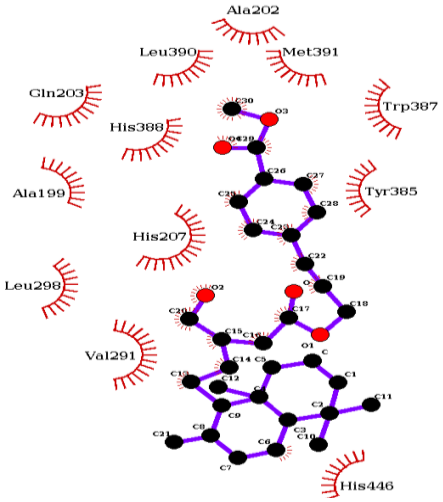
Ala202
Leu390
Met391
Gln203
His388
Trp387
Ala199
Tyr385
His207
Leu298
Val291
His446

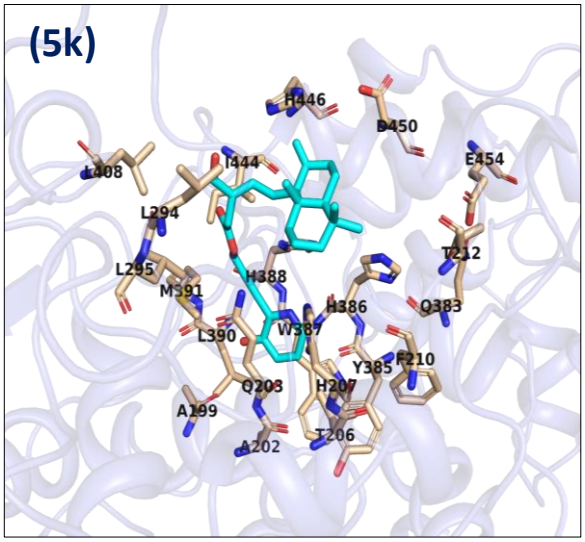
(5k)
H446
D450
E454
L408
I444
L294
T212
L295
M391
H388
H386
Q383
L390
W387
Y385
F210
Q203
H207
A199
T206
A202

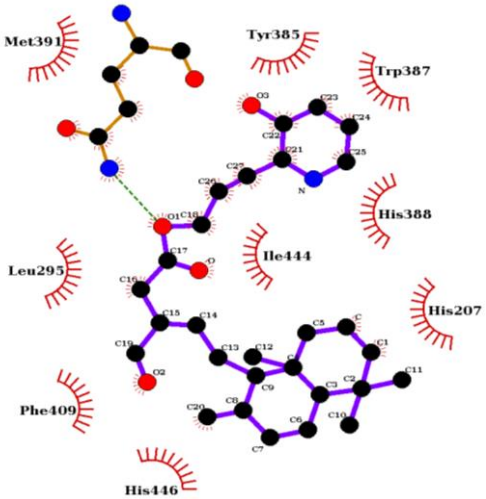
Met391
Tyr385
Trp387
His388
Ile444
Leu295
His207
Phe409
His446

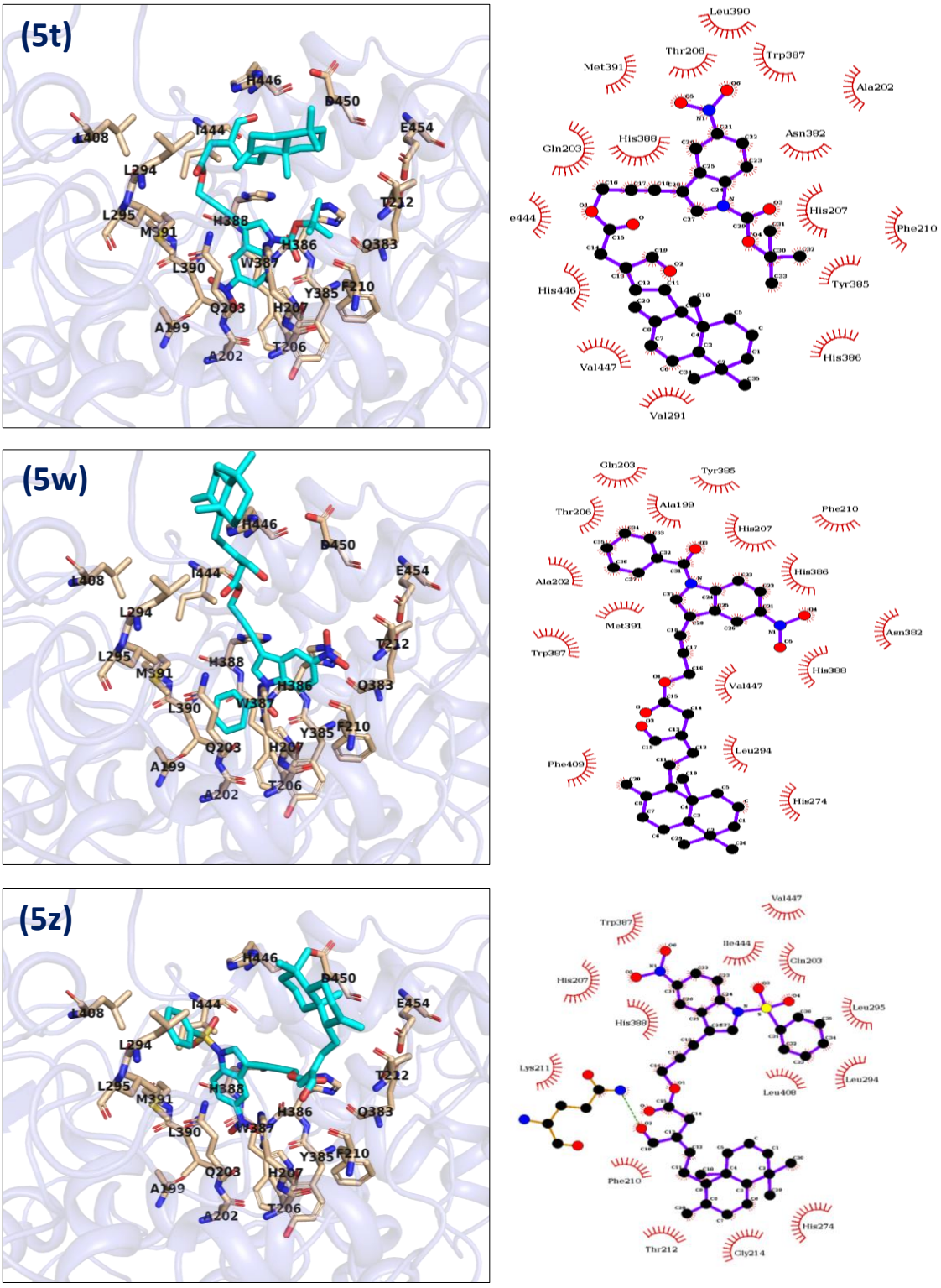

Figure 3.16. *In-silico* molecular modelling studies of the labdane conjugates with COX-2. Left panel showing the bound/docked compound (cyan) in COX-2 enzyme with the active site or catalytic pocket (shown in amino acid side chains). Right panel showing the interaction interphase of the bound compound and the respective position of the side chain amino acids of the COX-2.

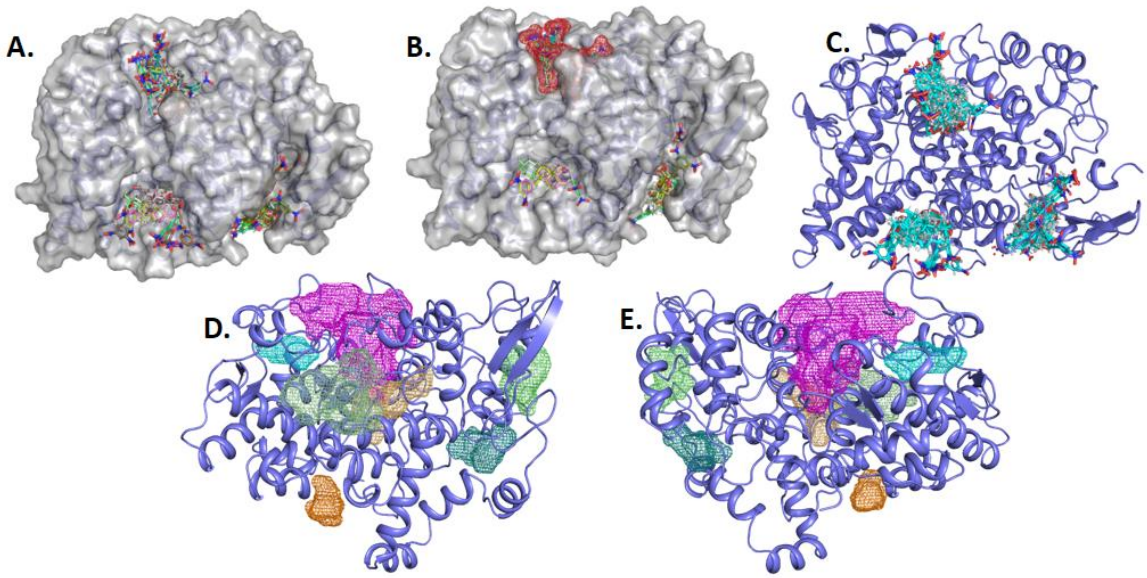

Figure 3.17. Overall COX-2, possible binding sites, and active sites. (**A-C**) Surface and cartoon diagram showing the most redundant drug/compound binding regions in the COX-2 as derived from the unbiased and templet free docking. The COX-2 catalytic site is shown in mesh. (**D** and **E**) Overall binding regions or pocket grove elucidated in the COX-2 enzyme (each pocket location coloured differently and the major catalytic pocket is show in the pink mesh).

3.9. References

(1) Jin, K.; Qian, C.; Lin, J.; Liu, B. Cyclooxygenase-2-Prostaglandin E2 Pathway: A Key Player in Tumor-Associated Immune Cells. *Front. Oncol.* **2023**, *13* (January), 1–10. https://doi.org/10.3389/fonc.2023.1099811.

(2) Simmons, D. L.; Botting, R. M.; Hla, T. Cyclooxygenase Isozymes: The Biology of Prostaglandin Synthesis and Inhibition. *Pharmacol. Rev.* **2004**, *56* (3), 387–437. https://doi.org/10.1124/pr.56.3.3.

(3) Harirforoosh, S.; Asghar, W.; Jamali, F. Adverse Effects of Nonsteroidal Antiinflammatory Drugs: An Update of Gastrointestinal, Cardiovascular and Renal Complications. *J. Pharm. Pharm. Sci.* **2013**, *16* (5), 821–847. https://doi.org/10.18433/j3vw2f.

(4) Yang, N.; Zou, C.; Luo, W.; Xu, D.; Wang, M.; Wang, Y.; Wu, G.; Shan, P.; Liang, G. Sclareol Attenuates Angiotensin II -induced Cardiac Remodeling and Inflammation via Inhibiting MAPK Signaling . *Phyther. Res.* **2022**, No. September, 1–14. https://doi.org/10.1002/ptr.7635.

(5) Chen, H.-W.; Lin, A.-H.; Chu, H.-C.; Li, C.-C.; Tsai, C.-W.; Chao, C.-Y.; Wang, C.-J.; Lii, C.-K.; Liu, K.-L. Inhibition of TNF-α-Induced Inflammation by Andrographolide via Down-Regulation of the PI3K/Akt Signaling Pathway. *J. Nat. Prod.* **2011**, *74* (11), 2408–2413. https://doi.org/10.1021/np200631v.

(6) De Las Heras, B.; Navarro, A.; Díaz-Guerra, M. J.; Bermejo, P.; Castrillo, A.; Boscá, L.; Villar, A. Inhibition of NOS-2 Expression in Macrophages through the Inactivation of NF-KB by Andalusol. *Br. J. Pharmacol.* **1999**, *128* (3), 605–612. https://doi.org/10.1038/sj.bjp.0702844.

(7) Tran, Q. T. N.; Wong, W. S. F.; Chai, C. L. L. Labdane Diterpenoids as Potential Anti-Inflammatory Agents. *Pharmacol. Res.* **2017**, *124*, 43–63. https://doi.org/10.1016/j.phrs.2017.07.019.

(8) Claudio Viegas-Junior; Eliezer J. Barreiro; Carlos Alberto Manssour Fraga. Molecular Hybridization: A Useful Tool in the Design of New Drug Prototypes. *Curr. Med. Chem.* **2007**, *14* (17), 1829–1852. https://doi.org/10.2174/092986707781058805.

(9) De Oliveira Pedrosa, M.; Marques Duarte Da Cruz, R.; De Oliveira Viana, J.; Olímpio De Moura, R.; Ishiki, H. M.; Filho, M. B.; Diniz, M. F. F. M.; Tullius Scotti, M.; Scotti, L.; Bezerra, F. J.; Junior, M. Current Topics in Medicinal Chemistry The

International Journal for In-Depth Reviews on Current Topics in Medicinal Chemistry Send Orders for Reprints to Reprints@benthamscience.Ae Hybrid Compounds as Direct Multitarget Ligands: A Review. *Curr. Top. Med. Chem.* **2017**, *17*, 1044–1079. https://doi.org/10.2174/1568026616666160927.

(10) Ahmed, M. M.; Khan, M. A.; Rainsford, K. D. Synthesis of Thiophene and NO-Curcuminoids for Antiinflammatory and Anti-Cancer Activities. *Molecules*. 2013, pp 1483–1501. https://doi.org/10.3390/molecules18021483.

(11) Samaan, N.; Zhong, Q.; Fernandez, J.; Chen, G.; Hussain, A. M.; Zheng, S.; Wang, G.; Chen, Q. H. Design, Synthesis, and Evaluation of Novel Heteroaromatic Analogs of Curcumin as Anti-Cancer Agents. *Eur. J. Med. Chem.* **2014**, *75*, 123–131. https://doi.org/10.1016/j.ejmech.2014.01.041.

(12) Kumari, A.; Singh, R. K. *Medicinal Chemistry of Indole Derivatives: Current to Future Therapeutic Prospectives*; Elsevier Inc., 2019; Vol. 89. https://doi.org/10.1016/j.bioorg.2019.103021.

(13) Sravanthi, T. V.; Manju, S. L. Indoles - A Promising Scaffold for Drug Development. *Eur. J. Pharm. Sci.* **2016**, *91*, 1–10. https://doi.org/10.1016/j.ejps.2016.05.025.

(14) Amir, M.; Kumar, S. Anti-Inflammatory and Gastro Sparing Activity of Some New Indomethacin Derivatives. *Arch. Pharm. (Weinheim).* **2005**, *338* (1), 24–31. https://doi.org/10.1002/ardp.200400891.

(15) Kalgutkar, A. S.; Crews, B. C.; Rowlinson, S. W.; Marnett, A. B.; Kozak, K. R.; Remmel, R. P.; Marnett, L. J. Biochemically Based Design of Cyclooxygenase-2 (COX-2) Inhibitors: Facile Conversion of Nonsteroidal Antiinflammatory Drugs to Potent and Highly Selective COX-2 Inhibitors. *Proc. Natl. Acad. Sci. U. S. A.* **2000**, *97* (2), 925–930. https://doi.org/10.1073/pnas.97.2.925.

(16) Kalgutkar, A. S.; Marnett, A. B.; Crews, B. C.; Remmel, R. P.; Marnett, L. J. Ester and Amide Derivatives of the Nonsteroidal Antiinflammatory Drug, Indomethacin, as Selective Cyclooxygenase-2 Inhibitors. *J. Med. Chem.* **2000**, *43* (15), 2860–2870. https://doi.org/10.1021/jm000004e.

(17) Bhat, M. A.; Mohamed, A. A. O.; Mohammad, R.; Ansari, M. A.; Abuelizz, H. A.; Bakheit, A. H.; Naglah, A. M. Indole Derivatives as Cyclooxygenase Inhibitors: Synthesis, Biological Evaluation and Docking Studies. *Molecules* **2018**, *23* (6). https://doi.org/10.3390/molecules23061250.

(18) DeCorte, B. L. Underexplored Opportunities for Natural Products in Drug Discovery. *J. Med. Chem.* **2016**, *59* (20), 9295–9304. https://doi.org/10.1021/acs.jmedchem.6b00473.

(19) Bennani, Y. L. Natural Products in Medicine: Transformational Outcome of Synthetic Chemistry. **2014**, No. c.

(20) Guo, Z. The Modi Fi Cation of Natural Products for Medical Use. **2016**. https://doi.org/10.1016/j.apsb.2016.06.003.

(21) Jalaja, R.; Leela, S. G.; Valmiki, P. K.; Salfeena, C. T. F.; Ashitha, K. T.; Krishna Rao, V. R. D.; Nair, M. S.; Gopalan, R. K.; Somappa, S. B. Discovery of Natural Product Derived Labdane Appended Triazoles as Potent Pancreatic Lipase Inhibitors. *ACS Med. Chem. Lett.* **2018**, *9* (7), 662–666. https://doi.org/10.1021/acsmedchemlett.8b00109.

(22) Jalaja, R.; Leela, S. G.; Mohan, S.; Nair, M. S.; Gopalan, R. K.; Somappa, S. B. Anti-Hyperlipidemic Potential of Natural Product Based Labdane-Pyrroles via Inhibition of Cholesterol and Triglycerides Synthesis. *Bioorg. Chem.* **2021**, *108*, 104664. https://doi.org/https://doi.org/10.1016/j.bioorg.2021.104664.

(23) Sasidhar, B. S.; Biradar, J. S. Synthesis of Some Bisindolyl Analogs for in Vitro Cytotoxic and DNA Cleavage Studies. *Med. Chem. Res.* **2013**, *22* (7), 3518–3526. https://doi.org/10.1007/s00044-012-0370-x.

(24) Lakshmi, S.; Renjitha, J.; B. Sasidhar, S.; Priya, S. Epoxyazadiradione Induced Apoptosis/Anoikis in Triple-Negative Breast Cancer Cells, MDA-MB-231, by Modulating Diverse Cellular Effects. *J. Biochem. Mol. Toxicol.* **2021**, *35* (6), 1–17. https://doi.org/10.1002/jbt.22756.

(25) Shilpa, G.; Renjitha, J.; Saranga, R.; Sajin, F. K.; Nair, M. S.; Joy, B.; Sasidhar, B. S.; Priya, S. Epoxyazadiradione Purified from the Azadirachta Indica Seed Induced Mitochondrial Apoptosis and Inhibition of NFκB Nuclear Translocation in Human Cervical Cancer Cells. *Phyther. Res.* **2017**, *31* (12), 1892–1902. https://doi.org/10.1002/ptr.5932.

(26) Anaga, N.; D, B.; Abraham, B.; Nisha, P.; Varughese, S.; Jayamurthy, P.; Somappa, S. B. Advanced Glycation End-Products (AGE) Trapping Agents: Design and Synthesis of Nature Inspired Indeno[2,1-c]Pyridinones. *Bioorg. Chem.* **2020**, *105*, 104375. https://doi.org/https://doi.org/10.1016/j.bioorg.2020.104375.

(27) Salfeena, C. T. F.; Jalaja, R.; Davis, R.; Suresh, E.; Somappa, S. B. Synthesis of

1,2,4-Trisubstituted-(1H)-Imidazoles through Cu(OTf)2-/I2-Catalyzed C–C Bond Cleavage of Chalcones and Benzylamines. *ACS Omega* **2018**, *3* (7), 8074–8082. https://doi.org/10.1021/acsomega.8b01017.

(28) Somappa, S. B.; Biradar, J. S.; Rajesab, P.; Rahber, S.; Sundar, M. A One-Pot Synthesis of Indole-Appended Heterocycles as Potent Anti-Inflammatory, Analgesic, and CNS Depressant Agents. *Monatshefte fur Chemie* **2015**, *146* (12), 2067–2078. https://doi.org/10.1007/s00706-015-1476-x.

(29) Praveen Kumar, V.; Renjitha, J.; Fathimath Salfeena, C. T.; Ashitha, K. T.; S. Keri, R.; Varughese, S.; Balappa Somappa, S. Antibacterial and Antitubercular Evaluation of Dihydronaphthalenone-Indole Hybrid Analogs. *Chem. Biol. Drug Des.* **2017**, *90* (5), 703–708. https://doi.org/10.1111/cbdd.12990.

(30) Mujumdar, A. M.; Naik, D. G.; Dandge, C. N.; Puntambekar, H. M. Antiinflammatory Activity of Curcuma Amada Roxb. In Albino Rats. *Indian J. Pharmacol.* **2000**, *32* (6), 375–377.

(31) Nagavekar, N.; Singhal, R. S. Supercritical Fluid Extraction of Curcuma Longa and Curcuma Amada Oleoresin: Optimization of Extraction Conditions, Extract Profiling, and Comparison of Bioactivities. *Ind. Crops Prod.* **2019**, *134* (March), 134–145. https://doi.org/10.1016/j.indcrop.2019.03.061.

(32) Jampilek, J. Heterocycles in Medicinal Chemistry. *Molecules* **2019**, *24* (21), 10–13. https://doi.org/10.3390/molecules24213839.

(33) Nisha, N.; Singh, S.; Sharma, N.; Chandra, R. The Indole Nucleus as a Selective COX-2 Inhibitor and Anti-Inflammatory Agent (2011-2022). *Org. Chem. Front.* **2022**, *9* (13), 3624–3639. https://doi.org/10.1039/d2qo00534d.

(34) Travis, B. R.; Sivakumar, M.; Hollist, G. O.; Borhan, B. Facile Oxidation of Aldehydes to Acids and Esters with Oxone. *Org. Lett.* **2003**, *5* (7), 1031–1034. https://doi.org/10.1021/ol0340078.

(35) Xu, H. X.; Dong, H.; Sim, K. Y. Labdane Diterpenes from Alpinia Zerumbet. *Phytochemistry* **1996**, *42* (1), 149–151. https://doi.org/10.1016/0031-9422(96)00887-4.

(36) Singh, S.; Kumar, J. K.; Saikia, D.; Shanker, K.; Thakur, J. P.; Negi, A. S.; Banerjee, S. A Bioactive Labdane Diterpenoid from Curcuma Amada and Its Semisynthetic Analogues as Antitubercular Agents. *Eur. J. Med. Chem.* **2010**, *45* (9), 4379–4382. https://doi.org/10.1016/j.ejmech.2010.06.006.

(37) Sonogashira, K.; Tohda, Y.; Hagihara, N. A Convenient Synthesis of Acetylenes : Catalytic Sutitutions of Acetyleyic Hydrogen With Broa E Es , Iodoare Es. *Tetrahedron Lett.* **1975**, No. 50, 4467–4470.

(38) Wilson, A. P. Cytotoxicity and Viability Assays. *Anim. cell Cult. a Pract. approach* **2000**, *1*, 175–219.

(39) Bengmark, S. Curcumin, an Atoxic Antioxidant and Natural NFκB, Cyclooxygenase-2, Lipooxygenase, and Inducible Nitric Oxide Synthase Inhibitor: A Shield against Acute and Chronic Diseases. *J. Parenter. Enter. Nutr.* **2006**, *30* (1), 45–51. https://doi.org/10.1177/014860710603000145.

(40) Kim, Y.; Park, W. Anti-Inflammatory Effect of Quercetin on RAW 264.7 Mouse Macrophages Induced with Polyinosinic-Polycytidylic Acid. *Molecules*. 2016. https://doi.org/10.3390/molecules21040450.

(41) S., V. A. E.; C., V. B. T. J.; Johan, K. Receptors, Mediators, and Mechanisms Involved in Bacterial Sepsis and Septic Shock. *Clin. Microbiol. Rev.* **2003**, *16* (3), 379–414. https://doi.org/10.1128/CMR.16.3.379-414.2003.

(42) Bryan, N. S.; Grisham, M. B. Methods to Detect Nitric Oxide and Its Metabolites in Biological Samples. *Free Radic. Biol. Med.* **2007**, *43* (5), 645–657. https://doi.org/https://doi.org/10.1016/j.freeradbiomed.2007.04.026.

(43) Guan, F.; Wang, H.; Shan, Y.; Chen, Y.; Wang, M.; Wang, Q.; Yin, M.; Zhao, Y.; Feng, X.; Zhang, J. Inhibition of COX-2 and PGE2 in LPS-stimulated RAW264.7 Cells by Lonimacranthoide VI, a Chlorogenic Acid Ester Saponin. *Biomed Rep* **2014**, *2* (5), 760–764. https://doi.org/10.3892/br.2014.314.

(44) Orlando, B. J.; Malkowski, M. G. Crystal Structure of Rofecoxib Bound to Human Cyclooxygenase-2. *Acta Crystallogr. Sect. Struct. Biol. Commun.* **2016**, *72* (10), 772–776. https://doi.org/10.1107/S2053230X16014230.

(45) Muniandy, K.; Gothai, S.; Badran, K. M. H.; Suresh Kumar, S.; Esa, N. M.; Arulselvan, P. Suppression of Proinflammatory Cytokines and Mediators in LPS-Induced RAW 264.7 Macrophages by Stem Extract of *Alternanthera Sessilis* via the Inhibition of the NF-*κ*B Pathway. *J. Immunol. Res.* **2018**, *2018*, 3430684. https://doi.org/10.1155/2018/3430684.

(46) Aggarwal, B. B. Nuclear Factor-KB: The Enemy Within. *Cancer Cell*. 2004, pp 203–208. https://doi.org/10.1016/j.ccr.2004.09.003.

(47) Ghosh, S.; Hayden, M. S. New Regulators of NF-KB in Inflammation. *Nat. Rev.*

Immunol. **2008**, *8* (11), 837–848. https://doi.org/10.1038/nri2423.

(48) Karin, M.; Ben-neriah, Y. Phosporilation Meets the Ubiquitination: The Control of NF- Kapp B Activity. *Annu. Rev. Immunol.* **2000**, *18*, 621–663.

(49) Mohan, B.; Salfeena, C. T. F.; Ashitha, K. T.; Krishnan, G. V.; Jesmina, A. R. S.; Varghese, A. M.; Patil, S. A.; Kumar, B. N. S. D.; Sasidhar, B. S. Functionalized Pyrimidines from Alkynes and Nitriles: Application towards the Synthesis of Marine Natural Product Meridianin Analogs. *ChemistrySelect* **2018**, *3* (23), 6394–6398. https://doi.org/10.1002/slct.201801126.

Ligand-Based Pharmacophoric Design and Semisynthesis of Triazole Linked Labdane Conjugates

4.1. Abstract

Inflammation-induced tissue damage plays a pivotal role in chronic conditions like cancer, Alzheimer's, and atherosclerosis. Given the limitations of existing anti-inflammatory drugs, including high costs and adverse effects, this research focuses on discovering innovative solutions. Utilizing a ligand-based pharmacophoric framework, thirty-three semi-synthetic labdane-appended triazolyl isatins were crafted through a linker-based molecular hybridization approach, aiming to uncover new anti-inflammatory agents. The anti-inflammatory properties of the derivatives were evaluated based on their ability to inhibit the production of NO, TNF-α, and IL-6, in lipopolysaccharide-induced RAW264.7 cells. Our initial screening revealed that compound **7a** demonstrated a superior dose-dependent anti-inflammatory effect compared to indomethacin and labdane dialdehyde. It significantly enhanced IL-10 levels, comparable to indomethacin. Mechanistic insights revealed that **7a** downregulates COX-2 and iNOS expression by inhibiting the NF-κB signaling cascade. Western blot analysis and immunofluorescence studies further validated that **7a** suppresses NF-κB nuclear translocation, confirming its role in modulating this critical pathway. *In silico* molecular modeling of NF-κB proteins aligned with our in vitro findings, underscoring the therapeutic potential of lead analogue **7a**. This study establishes a strong foundation for advancing **7a** into clinical development as a promising anti-inflammatory agent.

4.2. Introduction

NF-κB is the key transcription factor that induces the expression of major inflammation-related genes. It exists in the cellular cytoplasm as an inactive dimer with IκB. However, when activated by inflammatory stimuli, IKK kinase phosphorylates and degrades IκB, leading to the phosphorylation and activation of NF-κB. Phosphorylated NF-κB (p-NF-κB) translocates into the nucleus, where it interacts with the gene-promoting region on DNA leading to the transcription of a variety of pro-inflammatory mediators such as cytokines TNF-α, IL-6, and inflammatory enzymes COX-2 and iNOS. Therefore, the downregulation of the NF-κB signalling pathway can effectively combat inflammation and associated complications.[1,2]

Natural products, a class of small molecules inherently biologically relevant and evolutionarily pre-validated, remain a major source for drug discovery. However, evolutionary constraints limit the diversity of novel scaffolds available directly from nature. Notably, approximately 60% of small-molecule drugs discovered between 1989 and 2019 are natural product-based, with only 2% being anti-inflammatory agents.[4] Semi-synthetic modification of metabolites is a versatile tool to unlock their potential for precise interaction with a wide range of biomolecular targets, thus paving the way for the discovery of novel biologically relevant chemical spaces.[5]

Isatin (1*H*-indole-2,3-dione) and its derivatives exhibit a wide spectrum of biological properties, including anti-inflammatory, anti-cancer, anti-microbial, and anti-viral activities. It is an attractive scaffold to medicinal chemists, due to its vast scope for chemical modifications and can thus be employed as a precursor in drug synthesis.[6–8]

Triazoles are vital molecular frameworks in medicinal chemistry, renowned for their broad pharmacological potential. The triazole nucleus features prominently in drugs across various therapeutic categories, including antimicrobial, anti-inflammatory, analgesic, antiepileptic, antiviral, antineoplastic, and more. Their remarkable physicochemical properties, such as strong hydrogen-bonding affinity, enhanced dipole moment, π-stacking potential, and stability as bioisosteres for amides, make them invaluable in drug design. Specifically, 1,2,3-triazoles, in particular, are resistant to oxidative and reductive conditions as well as hydrolysis, making them exceptionally stable in biological systems compared to amide functionality.[9–13]

As part of our focused research on expanding biologically relevant chemical space through natural product-based semi-synthetic modifications,[14,15]we isolated (*E*)-labda-

8(17),12-diene-15,16-dial (**1**) from the chloroform extract of *C. amada.* This compound served as a scaffold for the rational design of a library of novel isatin-triazole-appended labdane conjugates, aimed at identifying promising anti-inflammatory agents. [14,15]

4.3. Review of literature

In the past decade, there have been extensive reports on the design and synthesis of various isatin-triazole hybrids, *via* molecular hybridization techniques, with diversified pharmacological effects[16] such as anti-cancer[17], anti-tubercular[18], anti-inflammatory properties[19,20] etc.

Boshra et al. employed a hybrid pharmacophore strategy to create and synthesize two new series of 2'-hydroxychalcone-triazole hybrid compounds. The majority of these compounds acted as selective inhibitors of COX-2. A series of the molecules demonstrated significant dual inhibition of both COX-2 and 15-LOX. Docking studies conducted on the COX-2 and 15-LOX active sites confirm their binding affinity and selectivity. These compounds show great potential as candidates for further development as anti-inflammatory agents (**Figure 4.1**).[19]

Sharma et al. developed novel isatin-triazole hybrids to evaluate their efficacy in inhibiting TNF-α induced expression of Intercellular Adhesion Molecule-1 (ICAM-1) on human endothelial cells. Structure-activity relationship (SAR) studies indicated that the presence of a bromo substituent at position 5 of the isatin moiety significantly enhanced the anti-inflammatory properties of the synthesized compounds (**Figure 4.1**).[20]

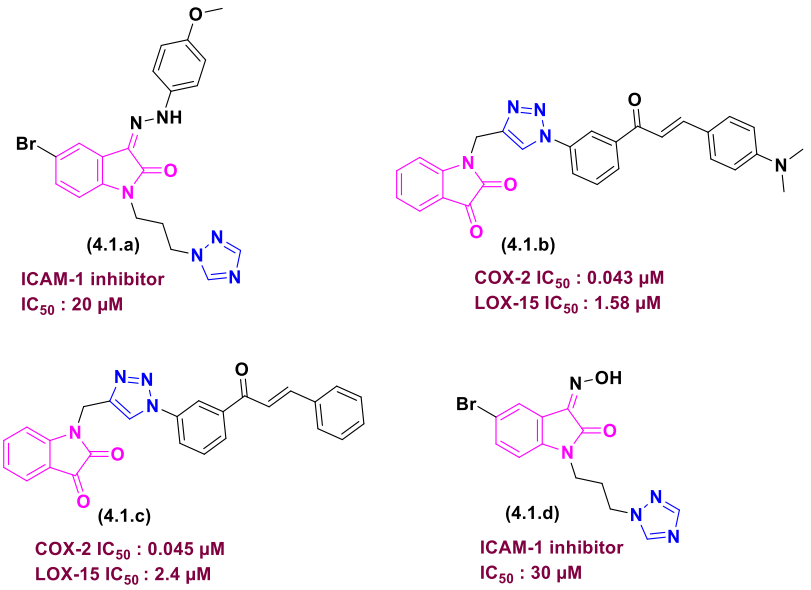

Figure 4.1. Isatin-triazole hybrids as anti-inflammatory agents

Considering the aforementioned findings and our growing interest towards the discovery of natural product-based new chemical entities, we have chosen the molecular hybridization technique to generate novel labdane appended 1,2,3-triazole tethered isatin hybrids with a broad spectrum of anti-inflammatory properties[19–25].

4.4. Aim and scope of the present study

In the second chapter, we reported the discovery of promising anti-inflammatory agents among aryl- and heteroaryl-appended labdanes, demonstrating the potential of semi-synthetic modifications to enhance the bioactivity of natural products. Inspired by these findings, we have extended our research to explore the semi-synthetic transformation of labdane dialdehyde isolated from *C. amada*. Our current objective is to generate a library of isatin-triazole-conjugated labdanes and systematically evaluate their activity against inflammatory mediators, including NO, TNF-α, IL-6, COX-2, and iNOS, which play pivotal roles in the NF-κB signaling pathway.

4.5. Design strategy for the synthesis of isatin-triazole appended labdane conjugates

The rationale for the designed hybrids is illustrated using a ligand-based molecular hybridization approach (**Figure 4.2**). This drug design strategy involves combining distinct

pharmacophoric subunits to create unique hybrid molecules with enhanced affinity, efficacy, modified selectivity profiles, multiple modes of action, and reduced side effects. [26,27]As shown in **Figure 4.2**, isatins and triazoles serve as critical cores in many anti-inflammatory agents. Thus, integrating these pharmacophores into labdane dialdehyde is anticipated to enrich its pharmacological properties, aiding the discovery of effective anti-inflammatory leads. Recent advancements in "Click chemistry"[9,28] and the significant contributions of natural product-derived triazoles[29] to chemical biology and drug design have inspired us to develop a diverse library of novel triazolyl-isatin-tethered labdanes using the copper-catalyzed alkyne-azide cycloaddition (CuAAC) reaction.

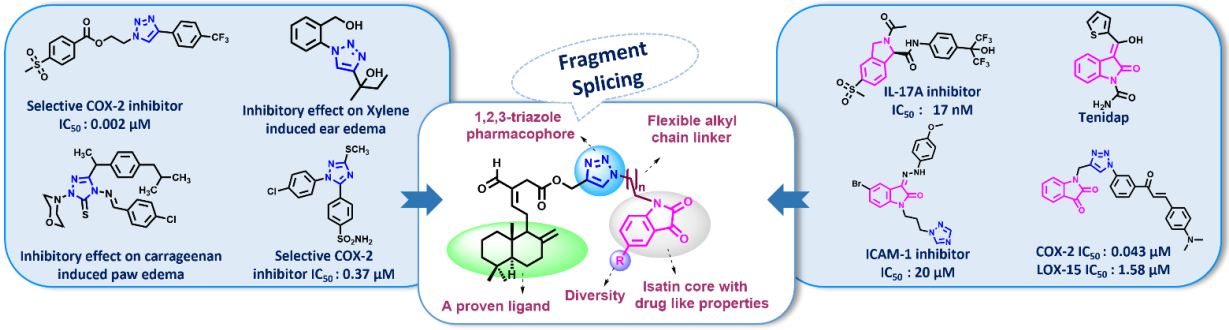

Figure 4.2. The rationale for the design and synthesis of triazolyl isatin appended labdane conjugates

4.6. Results and discussion

Fresh rhizomes of *Curcuma amada* were procured from CTCRI, Thiruvananthapuram, Kerala, in January 2023. The abundant and medicinally relevant marker compound (*E*)-labda-8(17),12-diene-15,16-dial (**1**) was isolated from the chloroform extract by our standard protocol. [14,15] We have synthesized a series of labdane appended mono-triazolyl-isatins as well as bis-triazolyl-isatins using variable alkyl chain linkers, which act as a spacer between the isatin core and the triazole moiety.

Scheme 4.1, outlines the synthesis of mono-triazolyl isatin appended labdane derivatives (**7a-7x**). One of the aldehyde groups of labdane dialdehyde (**1**) was selectively oxidized by using oxone to Zerumin A (**2**), which was further converted into its alkyne

intermediate (**3**) by treating it with propargyl bromide. Subsequently, substituted isatins (**4**) were alkylated with dibromoalkanes (with carbon chain length ranging from two to four) to give *N*-alkylated isatins (**5**), which were further treated with sodium azide to synthesize isatin-azides (**6**) with variable alkyl chain length. The propargylated ester of labdane dialdehyde (**3**) was reacted with different isatin-azides (**6**) in the presence of $CuSO_4.5H_2O$ and sodium ascorbate, *via* a highly regioselective CuAAC reaction, to generate exclusively the 1,4-disubstituted triazole appended labdane isatins (**7**), in good to excellent yields (**Figure 4.3**). All the synthesised derivatives were well characterized by NMR and HRMS analyses.

Scheme 4.2, describes the synthesis of bis-triazolyl isatin appended labdanes (**10a-i**). Both the aldehyde groups of labdane dialdehyde (**1)** were oxidized to furnish labdane diacid (**8**) by following the Pinnick oxidation protocol, which was further converted into the dipropargylated ester derivative (**9**) in good yield. Compound **9** was used as the substrate for the subsequent cycloaddition reaction with selected isatin azides (**6a-c**, **6e-h**, **6k**, **6n**), *via* click chemistry, to afford the desired bis-triazolyl isatin appended labdane hybrids (**10a-i**) in good to excellent yields (**Figure 4.3**). The structures of all the synthesized derivatives were confirmed by comprehensive analytical and spectroscopic techniques such as HRMS, ^{1}H NMR and ^{13}C NMR.

Scheme 4.1. Synthesis of mono-triazolyl isatin appended labdane derivatives **(7a-x)**

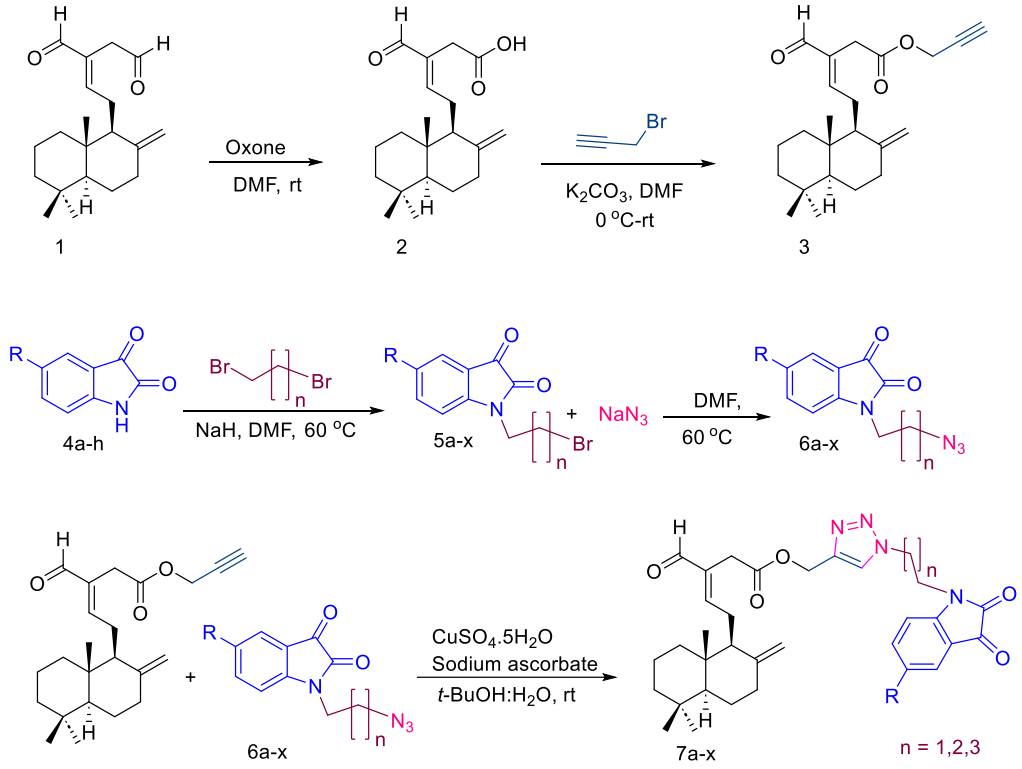

Scheme 4.2. Synthesis of bis-triazolyl isatin appended labdane derivatives **(10a-i)**

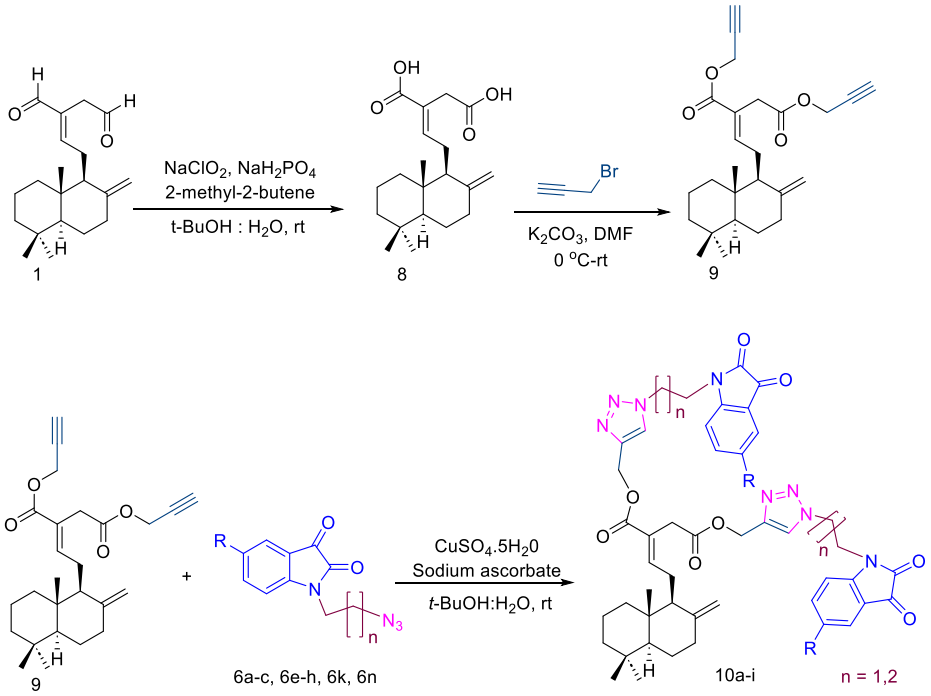

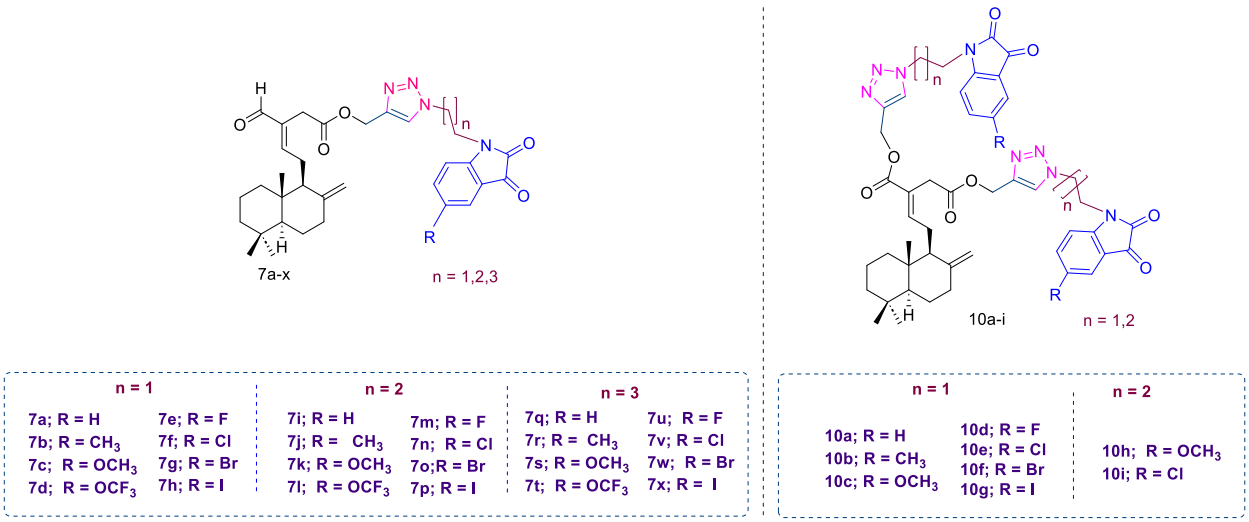

Figure 4.3. Synthesized library of mono/bis-triazolyl isatin appended labdane derivatives

4.6.1. Spectral characterization of triazolyl isatin appended labdane conjugates

4.6.1.1. Spectral characterization of mono-triazolyl isatin appended labdane conjugates

Spectral data leading to the structural characterization of mono-triazolyl isatin appended labdane conjugates is exemplified using compound **7c** (**Figure 4.4**). The peak at δ 9.21 in the ^{1}H NMR spectrum (**Figure 4.5**) indicated the presence of aldehyde proton. The two singlets at δ 4.77 and 4.28 attributed to the presence of exo-methylene group. The aromatic proton of the triazole ring resonated at δ 7.61. The peaks between δ 7.02-6.39 integrating for three protons corresponds to that of the isatin ring. Two triplets observed at δ 4.62 and 4.14, integrating two protons each, with a coupling constant *J* of 6.0 Hz, indicated the protons of the alkyl chain that connects the triazole and isatin nitrogens. The singlet at δ 5.02 integrating for two protons attributes to that of the methylene group attached to the oxygen atom. A singlet at δ 3.71, integrating for three protons, indicated the presence of a methoxy group. The presence of aldehyde and ester carbonyl groups was confirmed by peaks at δ 193.6 and 169.9 in the ^{13}C NMR spectrum (**Figure 4.6**). The two peaks at δ 182.7 and 158.7 correspond to that of the keto and amide carbons of the isatin core. The peaks between δ 159.3-107.9 confirmed the presence of aromatic and aliphatic double bonds. The mass spectrum of the compound showed the molecular ion peak at m/z 625.3002, which is $(M+Na)^{+}$ peak. From these data, along with DEPT-135 and 2D spectra, the structure of compound **7c** was confirmed as shown below.

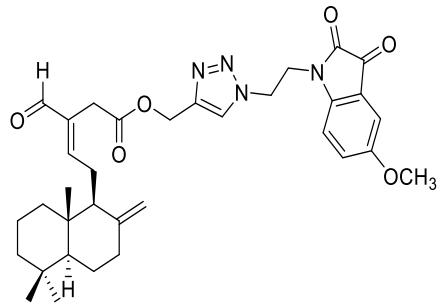

Figure 4.4. 7c

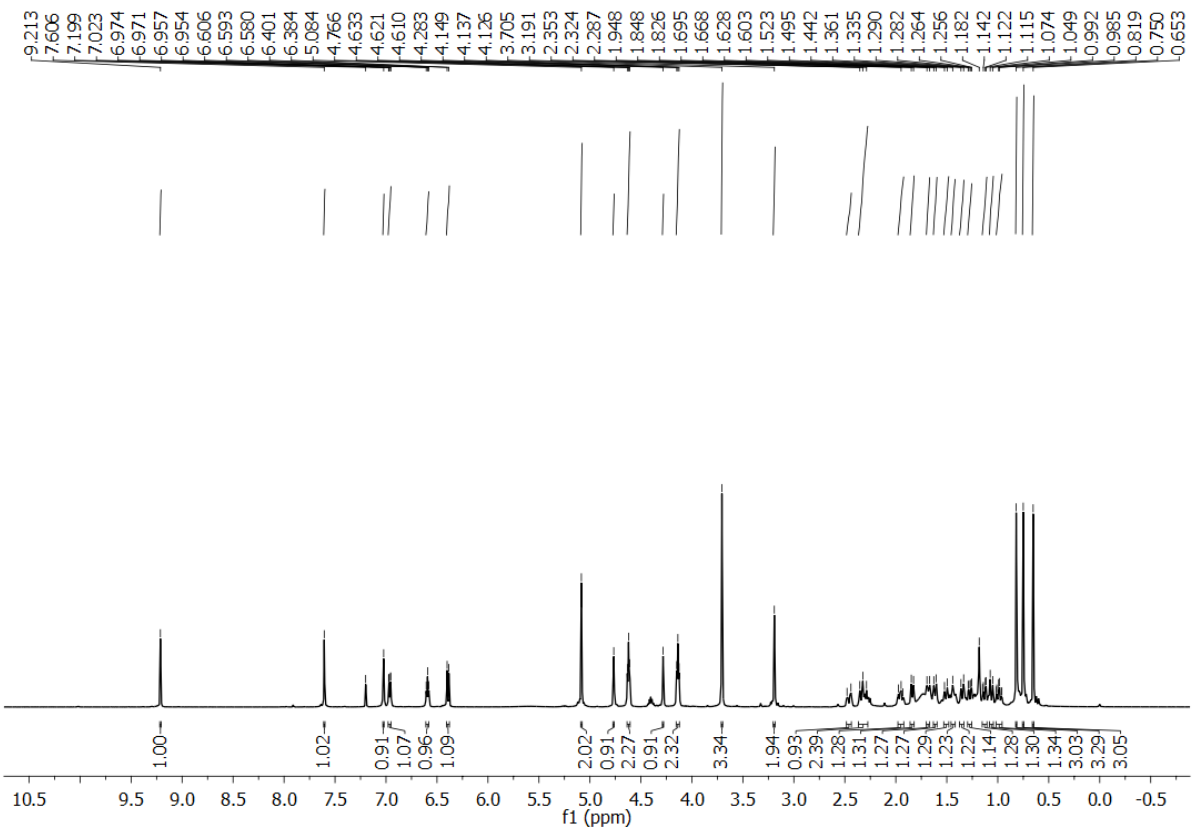

Figure 4.5. ^{1}H NMR (500 MHz, $CDCl_3$) Spectrum of compound **7c** (500 MHz, $CDCl_3$)

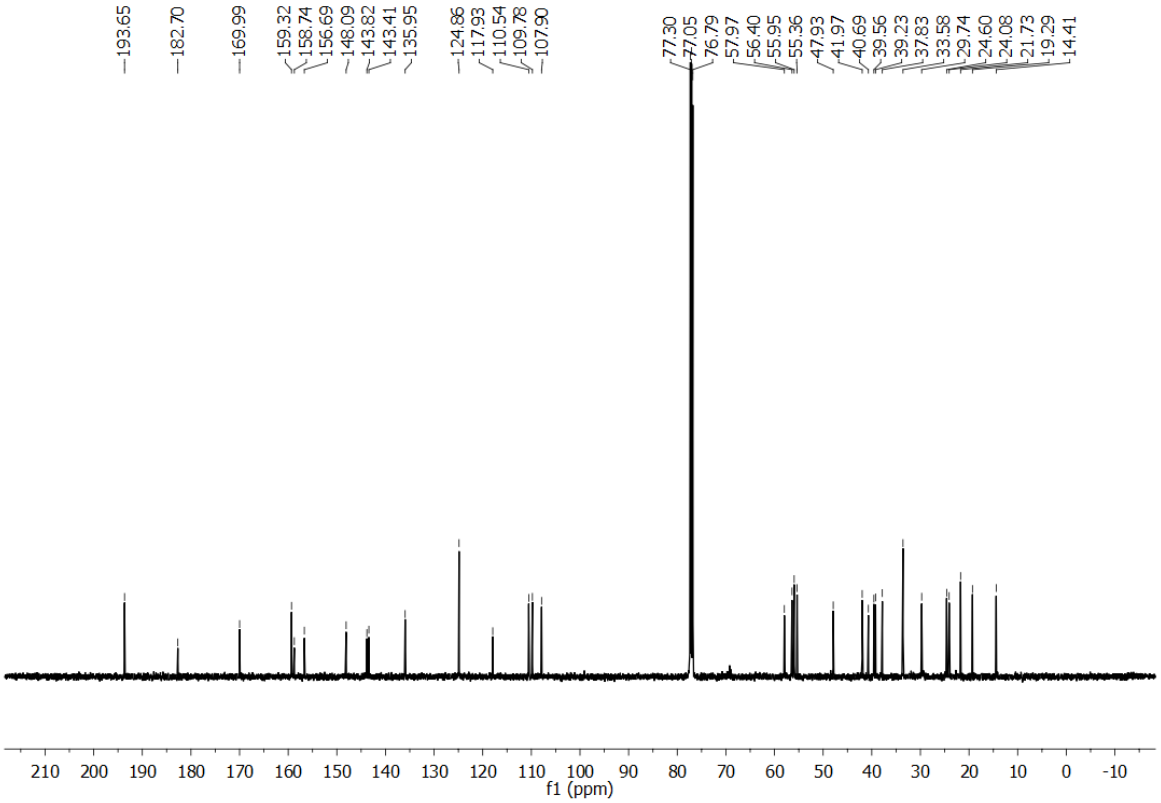

Figure 4.6. ^{13}C NMR (125 MHz, $CDCl_3$) of compound 7c (125 MHz, $CDCl_3$)

4.6.1.2. Spectral characterization bis-triazolyl isatin appended labdane conjugates

Spectral data leading to the structural elucidation bis-triazolyl isatin appended labdane conjugates is exemplified using compound **10c** (**Figure 4.7**). In the ^1H NMR spectrum (**Figure 4.8**), the two singlets at δ 4.71 and 4.25 attributed to the presence of exo-methylene group. The peaks between δ 7.69 and 6.41, integrating for eight protons, correspond to the aromatic protons of two isatin and two triazole cores. Additionally, the multiplets between δ 4.68 and 4.64, along with a singlet at δ 4.15 (both integrating for four protons each), indicate the protons of the two alkyl chains that connect the triazole and isatin nitrogens. The multiplet between δ 5.09- 5.03 integrating for four protons attributes to that of the methylene groups attached to the oxygen atoms. A singlet at δ 3.70, integrating for six protons, indicated the presence of two methoxy groups. In the ^{13}C NMR spectrum, the peak corresponding to the aldehyde carbon is absent, suggesting the formation of a bis-triazolyl isatin appended labdane conjugate (**Figure 4.9**). The peak at δ 183.0 corresponds to the carbonyl group of the isatin rings, while the two ester

carbonyl groups resonate at δ 170.4 and δ 166.4. Peaks between δ 158.7 and δ 107.7 confirm the presence of both aromatic and aliphatic double bonds. The mass spectrum of the compound indicates a molecular ion peak at m/z 925.3875, which represents the $(M+Na)^+$ peak. Combining these data with DEPT-135 and 2D spectra confirms the structure of compound **10c**, as illustrated below.

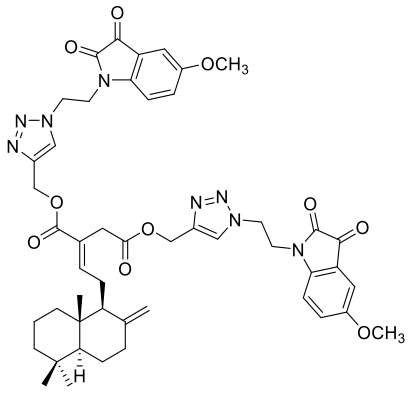

Figure 4.7. 10c

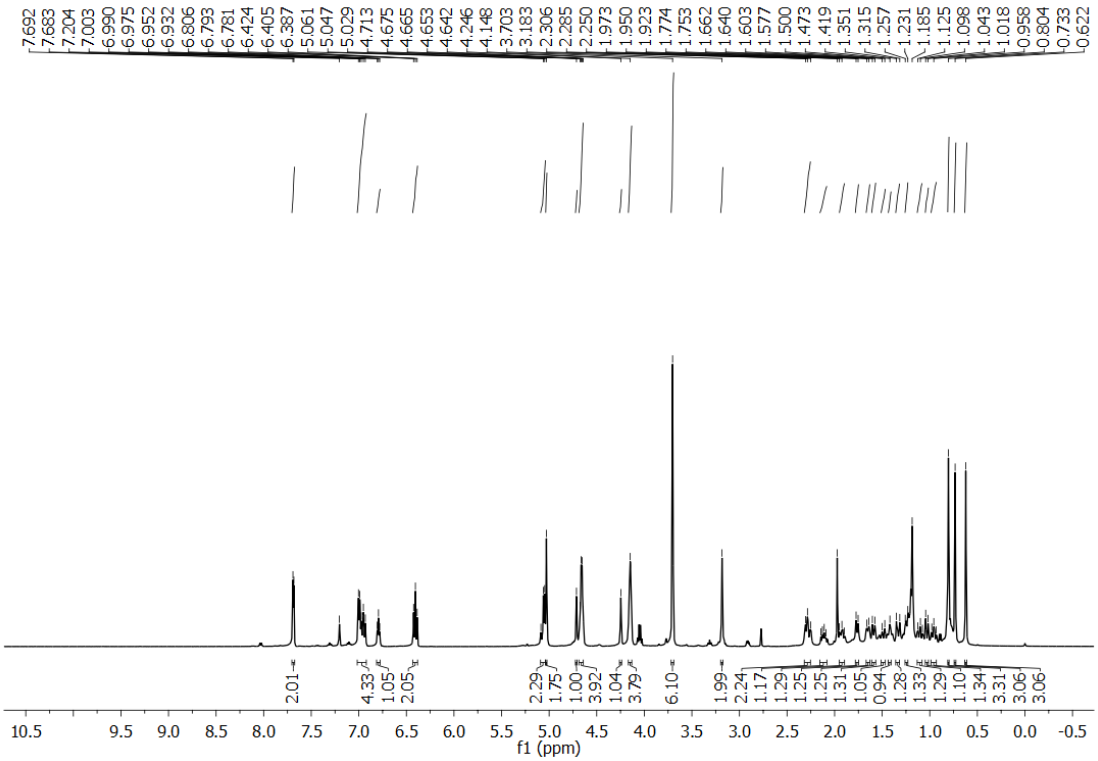

Figure 4.8. ^{1}H NMR (500 MHz, $CDCl_3$) of compound **10c** (500 MHz, $CDCl_3$)

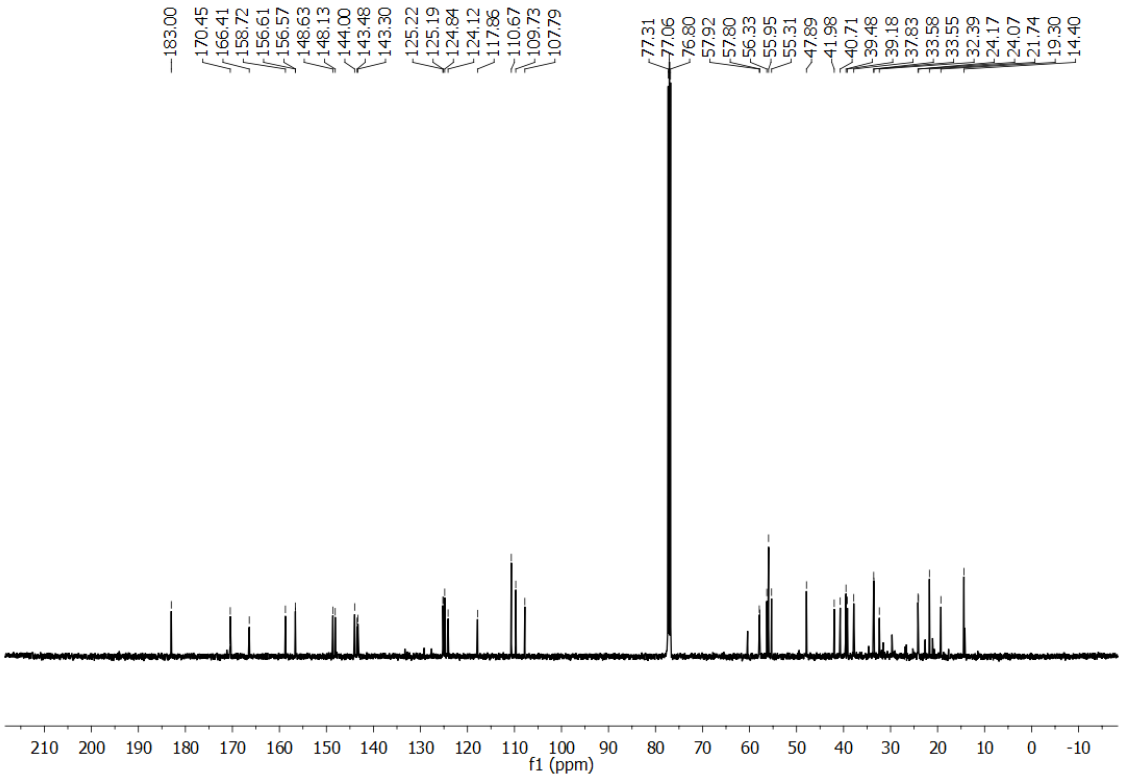

Figure 4.9. ^{13}C NMR (125 MHz, $CDCl_3$) of compound **10c** (125 MHz, $CDCl_3$)

4.6.2. Determination of *in vitro* cell viability by MTT assay

To avoid the cytotoxic interference in the anti-inflammatory effect, the intrinsic cytotoxicity of all the target compounds was determined by MTT assay. As shown in the **Figure 4.10**, none of the compounds showed significant cytotoxicity at test concentrations 1, 10 and 20 μM in RAW264.7 cell lines. Thus, these concentrations were considered to be safe for the cell based anti-inflammatory experiments.

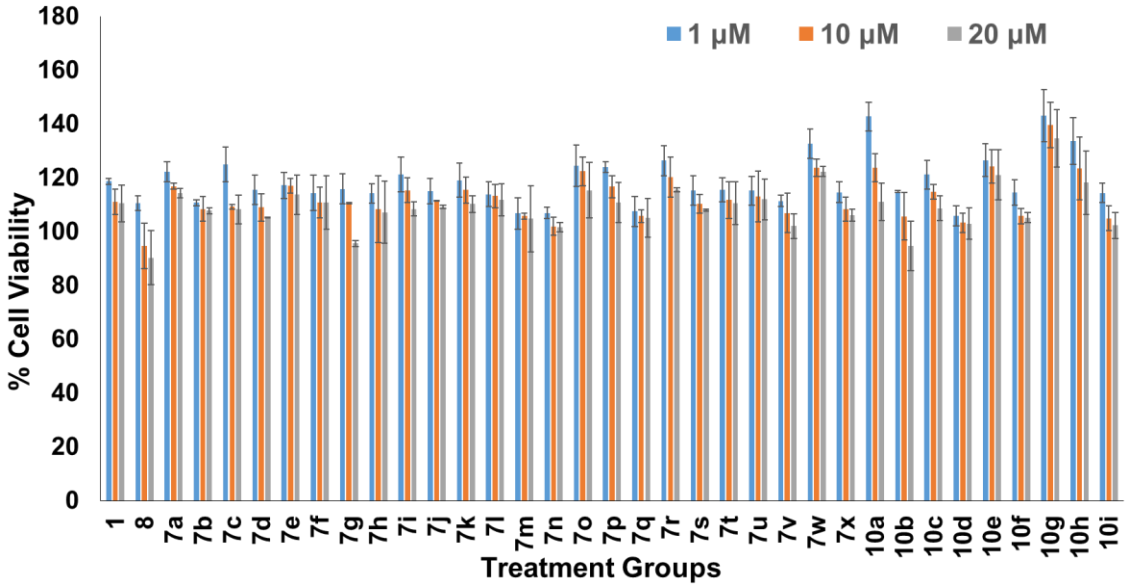

Figure 4.10. Effect of labdane dialdehyde (**1**), labdane diacid (**8**) and semi-synthetic derivatives (**7a-7x**, **10a-10i**) on cell viability in RAW264.7 cells. The viability of cells after pre-treatment with different concentrations of compounds (1, 10 and 20 µM concentrations) for a period of 24 h, was determined by MTT assay.

4.6.3. Effect of compounds on nitric oxide (NO) production *in vitro*

Elevated release of NO by activated macrophages leads to the initiation and progression of many inflammatory diseases.[42] Therefore, inhibition of NO production by the target compounds can be considered as the preliminary approach to evaluate its anti-inflammatory properties. All the synthesized thirty-three triazolyl-isatin derivatives of labdane dialdehyde (**7** & **10**), as well as the parent compound (**1**) and its diacid derivative (**8**), were evaluated for its potential to inhibit the production of NO in LPS-stimulated RAW 264.7 cells at 1, 10 and 20 µM concentrations. Indomethacin (IND) was chosen as the positive control. Griess method[43] was adopted to determine the nitrite concentration, which is an indicator of NO production, after 24 h LPS stimulation in RAW 264.7 cells. As observed in **Table 4.1**, five compounds specifically, **7a**, **7d**, **7m**, **7r** and **10a** significantly suppressed the production of NO better than the positive control indomethacin and the parent natural compound, labdane dialdehyde (**1**). Dialdehyde (**1**) exhibited better anti-inflammatory activity compared to that of its diacid derivative (**8**). Among all the tested groups, compound **7a** exhibited the most significant NO

inhibitory effect with an IC_{50} value of 3.13 ± 0.03 μM, and was much better than the positive control indomethacin (IC_{50} = 7.31 ± 0.12).

Table 4.1. Effect of Labdane Derivatives on NO Inhibition (IC_{50}) [a]

Compounds	IC_{50} (μM)
1	6.65 ± 0.09
8	15.45 ± 0.53
7a	3.13 ± 0.03
7b	5.04 ± 0.47
7c	4.53 ± 0.03
7d	3.83 ± 0.03
7e	5.54 ± 0.24
7f	28.25 ± 0.14
7g	5.46 ± 0.05
7h	6.20 ± 0.01
7i	14.55 ± 0.03
7j	4.76 ± 0.01
7k	5.54 ± 0.001
7l	5.87 ± 0.07
7m	3.87 ± 0.17
7n	15.25 ± 0.15
7o	60.28 ± 0.19
7p	6.12 ± 0.28
7q	21.27± 0.12
7r	3.95 ± 0.32
7s	5.48 ± 0.35
7t	4.88 ± 0.38
7u	4.68 ± 0.15
7v	7.10 ± 0.22
7w	6.58 ± 0.21

7x	5.07 ± 0.46
10a	3.72 ± 0.02
10b	5.04 ± 0.45
10c	7.54 ± 0.13
10d	4.80 ± 0.18
10e	14.55 ± 0.19
10f	6.00 ± 0.11
10g	31.06 ± 0.06
10h	5.72 ± 0.02
IND	7.31 ± 0.12

[a] Half maximal inhibitory concentration (IC_{50}) values for NO inhibition of labdane derivatives and the positive control indomethacin (IND). Data are expressed as the mean ± SD (n= 3).

4.6.4. Structural activity relationship based on the effect of compounds on NO inhibition

A probable structural activity relationship based on the effect of compounds on NO inhibition was drawn. Among the mono-triazolyl isatin labdane conjugates with alkyl chain length n = 1, compound **7a** incorporating a simple unsubstituted isatin core demonstrated a pronounced effect on NO inhibition. In contrast, the halogen substitutions at the fifth position of the isatin core (**7e-h**) resulted in reduced efficacy, among which a -Cl substituted derivative (**7f**) exhibited the least NO inhibition. The derivatives with $-OCF_3$, $-OCH_3$, and $-CH_3$ substitutions on isatin (**7b-d**) showed moderate NO inhibitory effect. On increasing the alkyl chain length to n = 2, the NO inhibitory potential of the unsubstituted isatin derivative (**7i**) decreased. However, the -F substituted derivative **7m** displayed an improved NO inhibitory effect. Other halogenated derivatives (**7n**, **7o, 7p**), displayed less inhibitory effect for NO. Derivatives **7j-l** with $-CH_3$, $-OCH_3$ and $-OCF_3$ substitutions showed a moderate effect on NO inhibition. Further increasing the alkyl chain length to n = 3, yet again decreased the activity of the unsubstituted isatin derivative (**7q**). Among the halogenated derivatives, -F and -I substituted derivatives (**7u** and **7x**) displayed better NO inhibitory effect than -Br and -Cl substituted derivatives (**7w**, **7v**). Moreover, increasing the chain length increased the NO inhibitory effect of the $-CH_3$ substituted conjugate (**7r**). Among the bis-triazolyl isatin conjugates of labdane, again a simple

unsubstituted isatin derivative (**10a**) demonstrated the highest NO inhibition potential. Overall, among all the mono/bis-triazolyl isatin appended labdane conjugates, analogues with simple isatin core without any substitution and with the shortest alkyl chain length (**7a** and **10a**) were found to be more potent candidates of the series. Interestingly, there was no particular trend based on the type of substitution on the isatin ring or based on alkyl chain length alone. However, we assume a synergistic effect of the alkyl chain length along with the substitution on the isatin core to be responsible for the NO inhibitory effect.

4.6.5. Effect of compounds on TNF-α and IL-6 production *in vitro*

TNF-α and IL-6 are the crucial cytokines which mediate different inflammatory mechanisms that impair organ integrity.[44] Therefore, we evaluated the potential of our thirty-three labdane derivatives to inhibit TNF-α and IL-6, using enzyme-linked immunosorbent assay (ELISA) at 20 μM concentration, in LPS-induced RAW264.7 cells. As displayed in **Figure 4.11**, the levels of the cytokines increased markedly with LPS exposure, whereas there was a marked reduction in pre-treatment with labdane dialdehyde (**1**) and all its semi-synthetic derivatives. Dialdehyde (**1**) exhibited better inhibition on TNF-α and IL-6, compared to that of its diacid derivative (**8**). Moreover, in concordance with the NO inhibition results, the five semi-synthetic derivatives, **7a**, **7d**, **7m**, **7r** and **10a**, exhibited a more pronounced inhibitory effect on TNF-α and IL-6, compared to all the other test groups. Among five derivatives, **7a** displayed the strongest anti-inflammatory potential by inhibiting the production of pro-inflammatory cytokines in the cellular model and was much better than the positive control indomethacin (IND) and the parent natural compound (**1**). In addition, other tested groups exhibited moderate activity.

Since the compound **7a** consistently showed the strongest inhibition on NO production as well as the pro-inflammatory cytokines release, TNF-α and IL-6, in LPS-induced macrophages, it was screened for further evaluation of its anti-inflammatory potential.

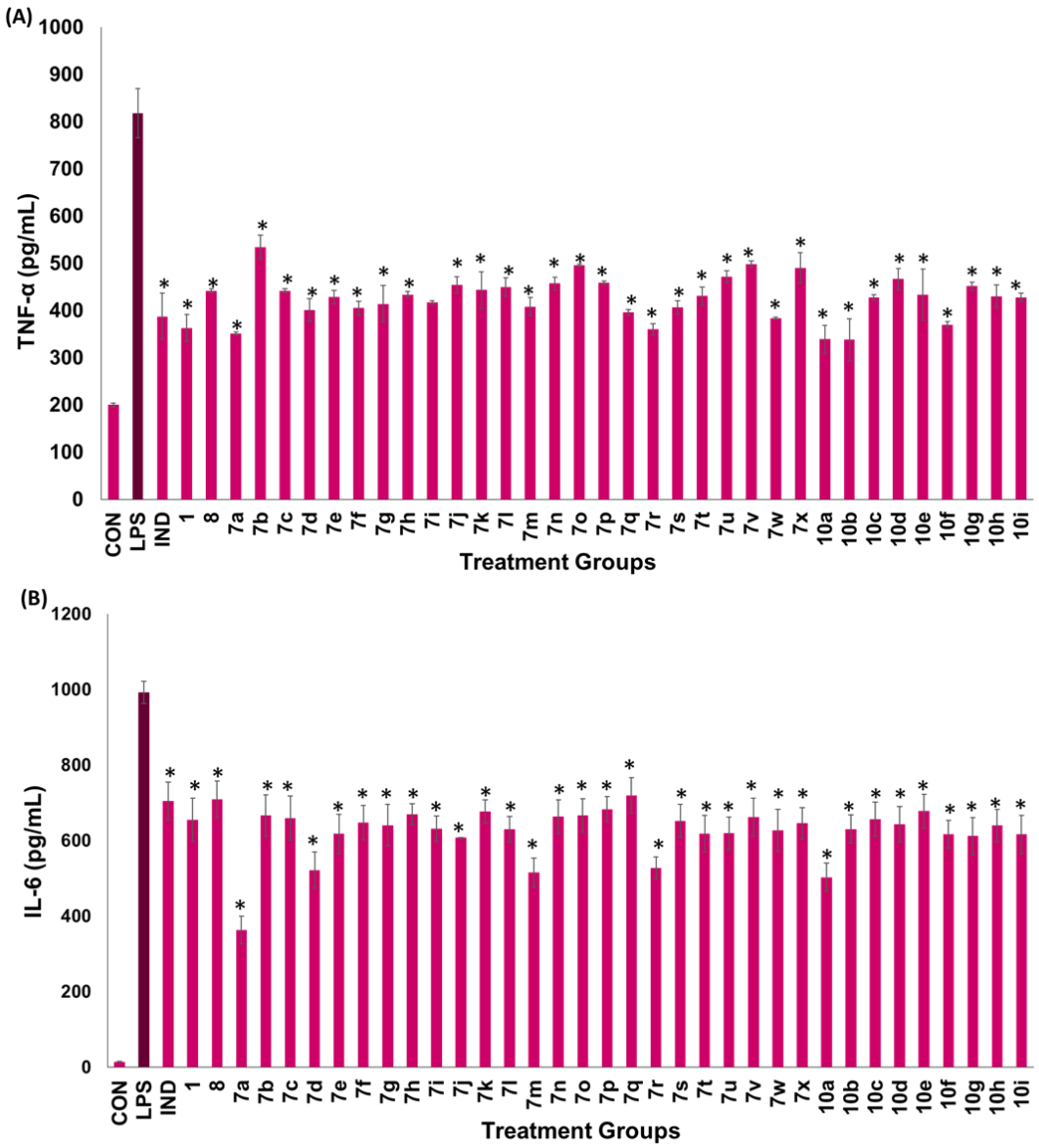

Figure 4.11. Effect of semi-synthetic derivatives of labdane dialdehyde on LPS induced cytokines production **(A)** TNF-α, **(B)** IL-6, in RAW 264.7 cell lines. Cells were pretreated with 20 µM concentration of compounds for 1 h, before treatment with 1 µg/mL LPS. After 24 h of incubation, cytokines production was determined by ELISA. Data are expressed as the mean ± SD (n = 3). *$p < 0.001$ vs LPS group.

4.6.6. Dose-response effect of 7a on TNF-α and IL-6

The effect of different concentrations of **7a** (1, 5 and 10 µM) on the key pro-inflammatory cytokines, i.e., TNF-α and IL-6, were evaluated on LPS-induced macrophages along with

indomethacin (20 µM) as the reference drug. **7a** decreased the levels of the pro-inflammatory cytokines in a concentration-dependent manner (**Figure 4.12A, 4.12B**), and was more potent than the positive control drug indomethacin. This again confirms **7a** to be a promising anti-inflammatory agent and further investigations into its mechanism of action were much warranted.

4.6.7. Effect of 7a on anti-inflammatory cytokine IL-10 *in vitro*

IL-10 is an anti-inflammatory cytokine which induces an immunosuppressive effect during prolonged inflammation, thus helping to prevent immunopathology and immune-mediated damage to the host.[10] Therefore, increased levels of IL-10 in LPS-stimulated macrophages can be considered as an indication of the host mechanism to prevent inflammation. Based on the preliminary screening results, the most active labdane derivative **7a** was evaluated for its effect on IL-10 levels at 1, 5 and 10 µM concentrations, in LPS-stimulated RAW264.7 cells. Indomethacin was again used as the reference drug. As witnessed in the previous assays, **7a** significantly increased the levels of IL-10 in a dose-dependent manner in LPS-stimulated RAW264.7 cells and was comparable to indomethacin (**Figure 4.12C**). Since **7a** demonstrated significant anti-inflammatory properties by suppressing the pro-inflammatory mediators NO, TNF-α and IL-6 as well as by increasing the levels of the anti-inflammatory mediator 1L-10, which was at par with the positive control indomethacin, **7a** was selected for the further detailed anti-inflammatory studies.

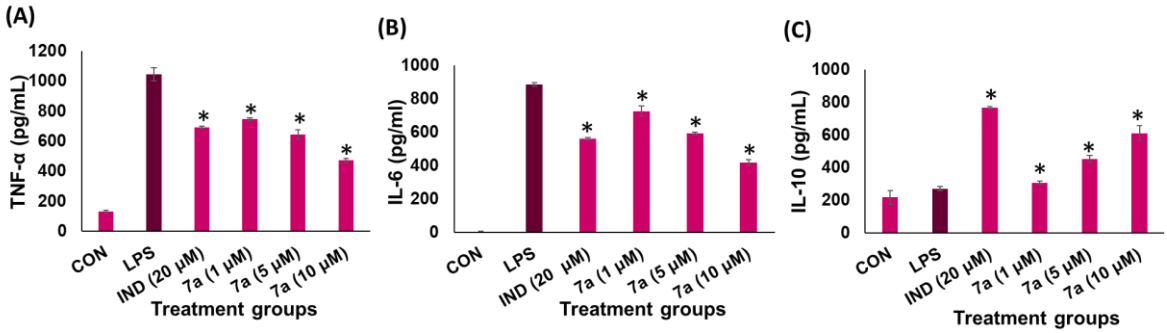

Figure 4.12. Effect of compound **7a** on LPS-induced cytokines production: **(A)** TNF-α **(B)** IL-6 and **(C)** IL-10, in RAW 264.7 cell lines. Cells were pretreated with various concentrations of compound **7a** (1, 5 and 10 µM) and indomethacin (20 µM) for 1 h before treatment with 1 µg/mL LPS. After 24 h of incubation, cytokines production was determined by ELISA. Data are expressed as the mean ± SD (n = 3). *$p < 0.001$ vs LPS group.

4.6.8. Effect of compound 7a on iNOS and COX-2 protein expression

COX-2 and iNOS are the two most critical enzymes convoluted in inflammation. Dysregulated release or overexpression of iNOS leads to the genesis of sepsis, cancer, neurodegenerative diseases, pain etc. NO, a major cell signalling molecule synthesized by iNOS, is the pro-inflammatory mediator responsible for amplifying immune activation and inflammatory responses.[42] COX-2 is an inducible pro-inflammatory enzyme which plays a pivotal role in the biosynthesis of inflammatory prostaglandins such as PGE2 from arachidonic acid, leading to the progression of inflammatory diseases.[45] Therefore, to further explore the molecular mechanism of compound **7a**, its effect on the expression of COX-2 and iNOS enzymes was determined by western blotting, on LPS-stimulated RAW 264.7 cells (at 10 and 20 μM). Indomethacin (20 μM) was again employed as the positive control. As shown in **Figure 4.13A**, LPS stimulation increased the COX-2 and iNOS protein levels significantly. However, there was a dose-dependent decrease in the expression of these enzymes when co-treated with **7a**. Even at 10 μM concentration, compound **7a** inhibited COX-2 in a similar way that indomethacin did at 20 μM. However, at 20 μM compound **7a** inhibited COX-2 more effectively, with a potency greater than that of indomethacin at the same concentration (**Figure 4.13B**). The effect of compound **7a** on iNOS protein was greater than that on COX-2. It is noteworthy that **7a** displayed a higher potency for iNOS suppression than indomethacin even at its lowest tested concentration of 10 μM. However, there was a significantly increased suppression in iNOS level by **7a** at 20 μM, much better than indomethacin (**Figure 4.13C**). The results imply that **7a** exerts its anti-inflammatory activity *via* downregulating COX-2 and iNOS protein expression.

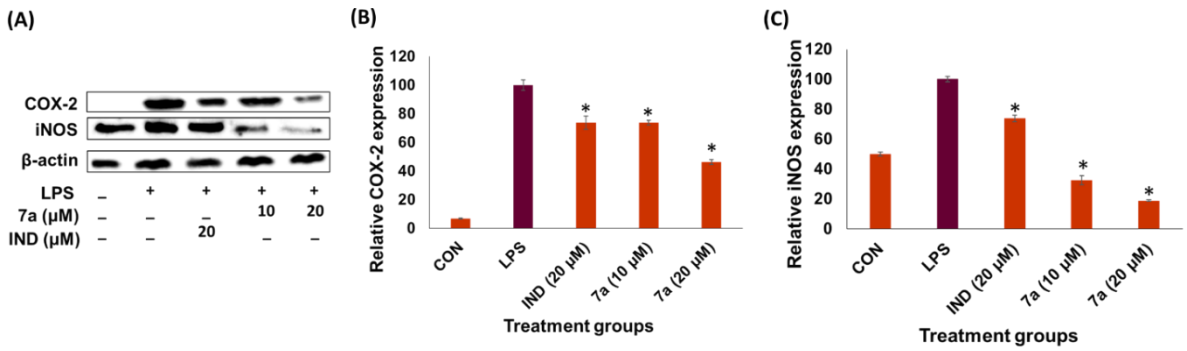

Figure 4.13. Effect of compound **7a** on COX-2 and iNOS expression in LPS-stimulated RAW264.7 cells. Cells were pretreated with different concentrations of compound **7a** (10 and 20 μM) and indomethacin (20 μM) for 1h and then stimulated with or without 1 μg/mL of LPS for 24 h. COX-2 and iNOS expressions were detected by western blotting (**A**, **B** and **C**). *p < 0.001 vs LPS group.

4.6.9. Effect of 7a on NF-κB signalling pathway on LPS-stimulated RAW 264.7 cells by western blotting and immunofluorescence analysis

Extensive studies point to the fact that the activation of NF-κB, a ubiquitous cell transcription factor, is the key regulator in the expression of the pro-inflammatory cytokines such as TNF-α and IL-6 as well as the pro-inflammatory enzymes COX-2 and iNOS.[46–48] To establish the possible intra-cellular anti-inflammatory mechanism of compound **7a**, its effect on the NF-κB signalling pathway was examined by western blotting and immunofluorescence analysis on LPS-stimulated RAW 264.7 cells. Indomethacin at 20 μM was chosen as the positive control. The activation of NF-κB can be attenuated by inhibiting its phosphorylation on p65, which was measured by western blotting. As depicted in **Figure 4.14**, it is clear that the LPS stimulation increased the levels of phosphorylated NF-κB p65 (p-NF-κB p65), while co-treatment with compound **7a** showed a significant reduction in phosphorylation, in a dose-dependent manner, with no effect on the NF-κB p65 protein levels. The compound **7a** showed inhibition on p-NF-κB p65 expression even at 10 μM concentration like that of indomethacin tested at 20 μM. However, at 20 μM, **7a** demonstrated better inhibition on p-NF-κBp65 than indomethacin. To further verify the effect of **7a** on NF-κB pathway, the nuclear translocation of NF-κB was examined by immunofluorescence, in LPS-stimulated RAW 264.7 cells. As depicted in **Figure 4.15**, LPS stimulation significantly increased the distribution of NF-κB in

the cell nuclei. However, co-treatment with **7a** markedly decreased the distribution of NF-κB inside the nuclei in a concentration-dependent manner.

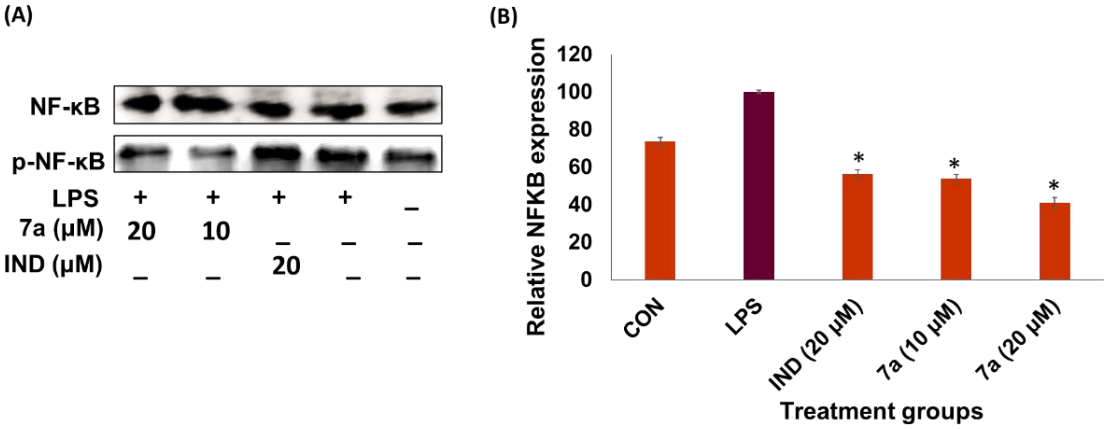

Figure 4.14. Effect of **7a** on NF-κB signalling pathway on LPS-stimulated RAW 264.7. Cells were pre-treated with different concentrations of compound **7a** (10 and 20 μM) and indomethacin (20 μM) for 1h and then stimulated with or without 1 μg/mL of LPS for 24 h. Phospho-p65 and p-65 expressions were detected by western blotting (**A** and **B**). *$p < 0.001$ vs LPS group.

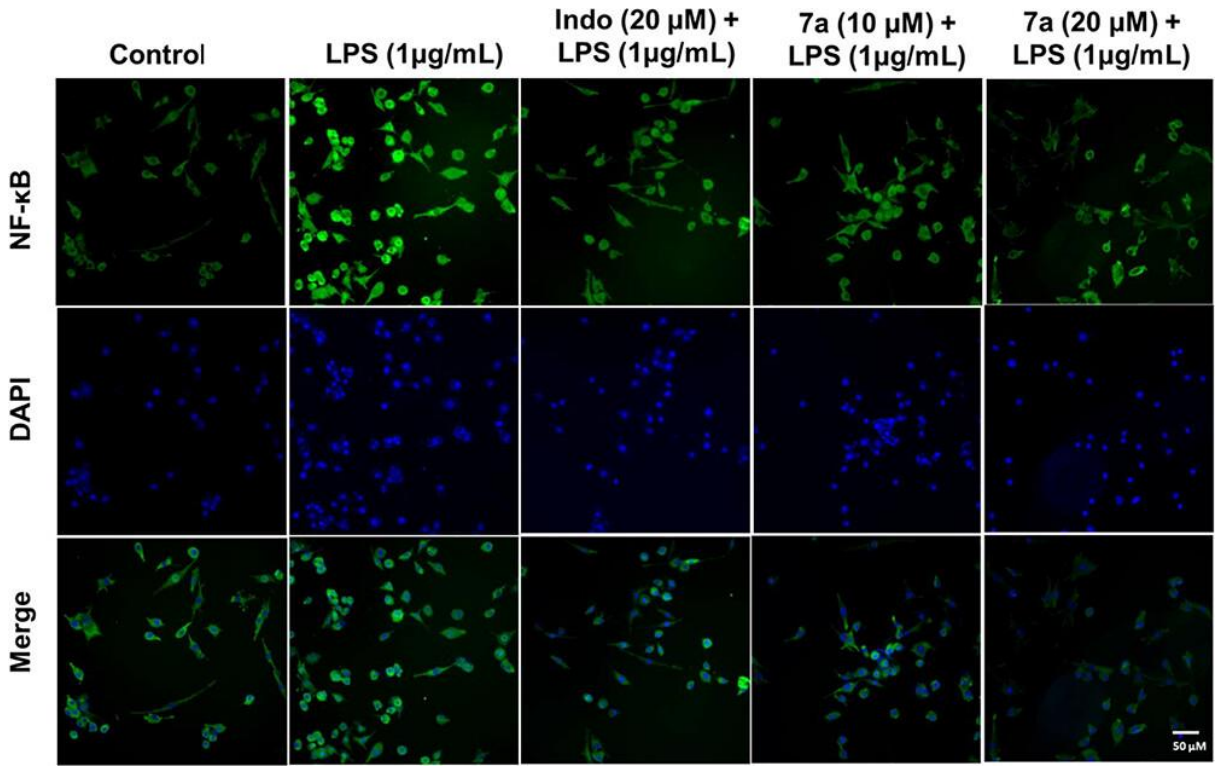

Figure 4.15. Effect of **7a** on NF-κB signalling pathway via immunofluorescence

Immunofluorescence staining detected the distribution of NF-κB-p65 in both the nuclei and cytoplasm by some colocalization of receptors (p65, Alexa Fluor 488, green) with the nuclei (DAPI, blue). Images were captured by fluorescent microscope (OLYMPUS, Japan). Scale = 50 µm.

4.6.10. *In silico* molecular modelling studies of compound 7a on NF-κB

To better understand the structural and molecular mode of physical interaction, relative binding affinity and possible mode of interaction of our synthesized drugs with the NF-κB (monomer), we performed structure-based virtual docking (arbitory docking was performed to over the docking bias) using HADDOCK 2.2 (https://haddock.science.uu.nl/) software and results were analyzed using pymol. Foremost, the structural analysis of NF-κB in apo form or the absence of DNA has shown an available binding pocket of 2013 A2 (**Figure. 4.17**), which could accommodate large compounds ideal for our synthesized compounds (**7a-x**, **10a-i**).

Based on our reference-free and unbiased docking, among the screened compounds **7a-x** and **10a-i**, we found that compound **7a** with the highest binding affinity of dG -8.89±1.3 kcal/mol (**Figure 4.16, Figure 4.17**). As shown in **Figure 4.16,** the structural analysis of h NF-

κB binding with compound **7a**, we notice that compound **7a** could bind the DNA binding site or active site of h NF-κB in two different binding modes (**Figure 4.16A-D**) with a relatively similar binding affinity. LigPlot views show compound **7a** bound to h NF-κB in two distinct conformations, where some of the key interacting residues remained conserved (**Figure 4.16D-E**). This binding affinity was also consistent in our binding assay experiments. We next compared the binding orientation of bound compound **7a** with the apo-form and dsDNA bound (PDB:1NFK) form structure of hNF-κB (homo-dimer) *via* superimposing the structures to see how our compounds can intercalate or inhibit in the DNA recognition. As shown in **Figure 4.16H**, compound **7a** shares some of the dsDNA binding region making the dsDNA deallocate or inhibit the binding of dsDNA. Subsequently, we conducted simple simulation studies to examine how compound **7a** binding influences dsDNA disassembly. As depicted in **Figure 4.16I** and **Figure 4.17**, our simulated model revealed the displacement of bound dsDNA from hNF-κB and the eventual inhibition of dsDNA binding in the presence of compound **7a**.

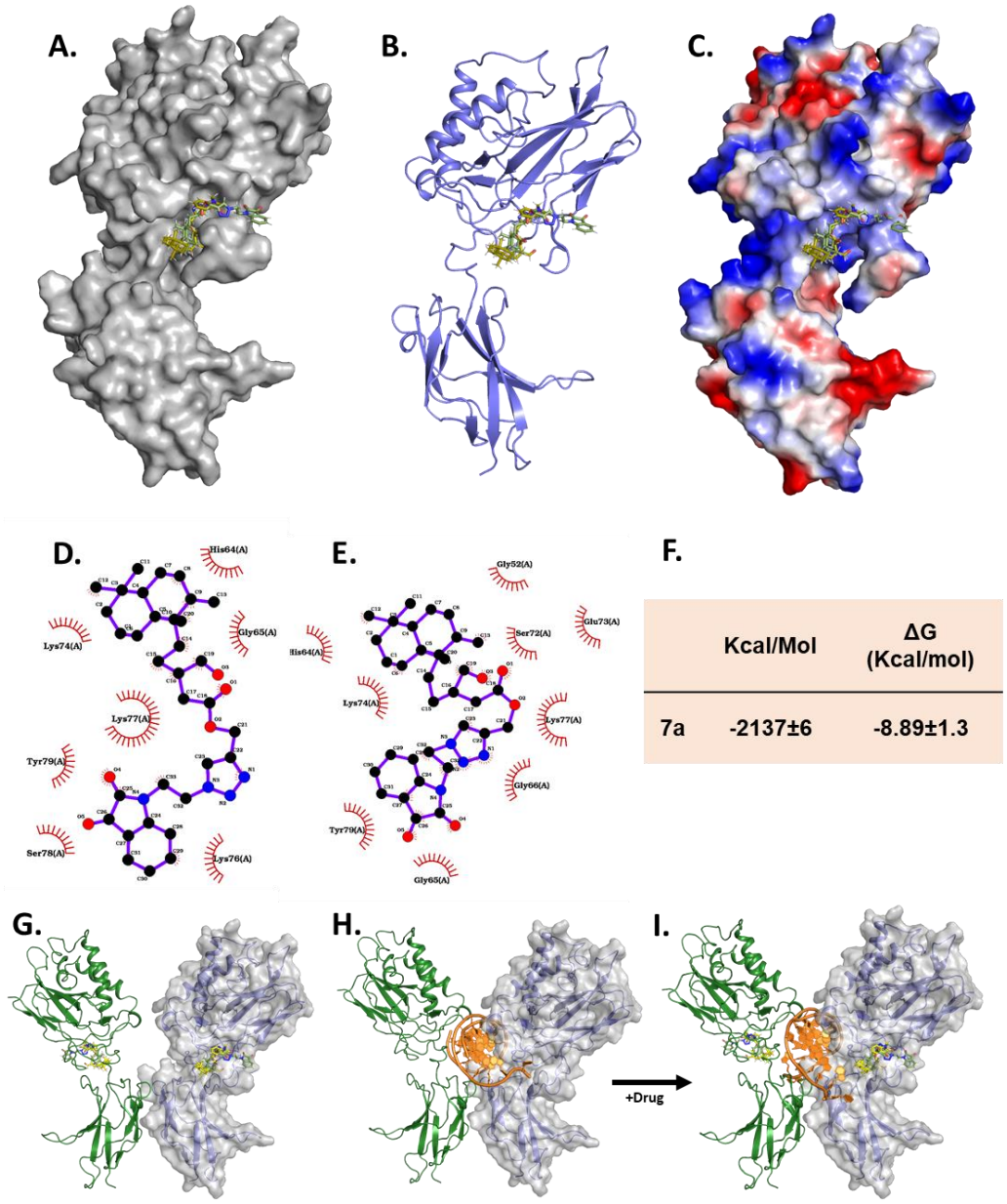

	Kcal/Mol	ΔG (Kcal/mol)
7a	-2137±6	-8.89±1.3

Figure 4.16. Molecular docking studies of **7a** on NF-kB (**A**) Surface (**B**) Cartoon (**C**) electrostatic potential representation of hNF-kB (monomer) with bound **7a** compound in different conformations. (**D-E**) LigPlot view of compound **7a** bound to hNF-KB in two different conformations. Compounds are shown in sticks with numbering Cα and respective interacting amino acids in the hNF-kB are shown with the compound. (**F**) Table showing the relative binding kinetics of NFkB with our **7a** compound. (**G**) Structure of hNF-kB (homo-dimer) in complex with docked **7a** in different conformations. (**H**) and in complex with dsDNA (PDB: 1NFK) (front view). (**I**) Structural simulation of 1NFK in the presence of our proposed compound **7a** resulting in the displacement of bound dsDNA and eventual inhibition of dsDNA binding. For clarity, individual hNF-kB in the homo-dimer is coloured in green and slate with or without surface representation.

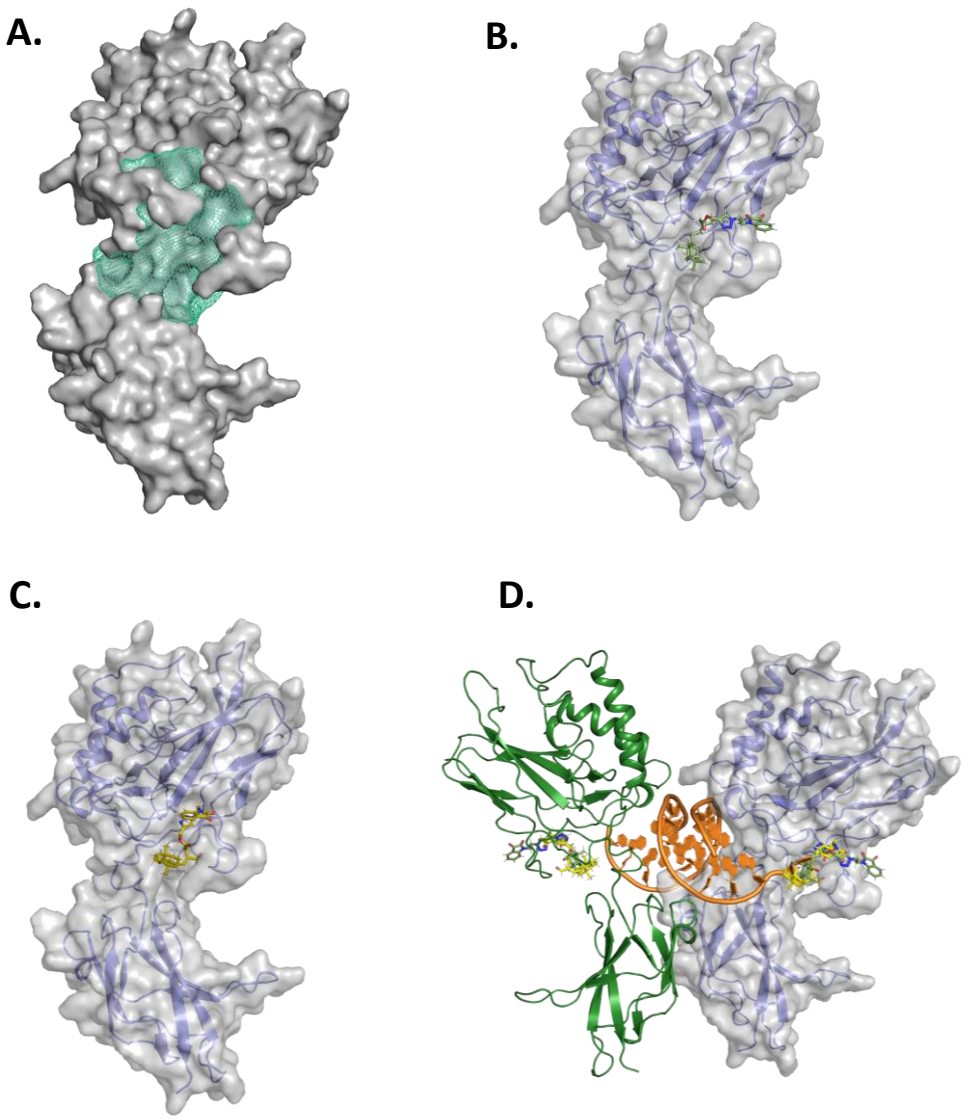

Figure 4.17. Representations of hNF-kB (**A**) Semi-surface representation of hNF-kB (monomer) showing the available space or pocket (teal mesh) (volume 2013 A^2) for ligand interaction. (**B-C**) hNF-kB bound with **7a** compounds in different conformations. (**D**) Superimposed or overly structure of hNF-kB complex with dsDNA (PDB: 1NFK) was shown with hN-FkB bound drugs as derived in our complex structure. The steric clash between the DNA and bound **7a** compound in the hNF-kB is noticeable. Suggesting the eventual displacement bound DNA of inhibition of hNF-kB binding to DNA. For clarity, Individual hNF-kBs in the homo-dimer are coloured in green and slate, and with or without surface representation.

4.7. Conclusions

In conclusion, we have synthesized a library of thirty-three novel labdane-conjugated mono/bis-triazolyl isatins with the goal of discovering new anti-inflammatory agents. Among the synthesized compounds, **7a** exhibited superior anti-inflammatory activity compared to both the commercial drug indomethacin and the parent natural compound (*E*)-labda-8(17),12-diene-15,16-dial (**1**). It effectively inhibited the release of pro-inflammatory mediators—NO, TNF-α, and IL-6—and enhanced the levels of the anti-inflammatory cytokine IL-10 in a dose-dependent manner in LPS-induced RAW 264.7 cells. Further mechanistic investigation revealed that compound **7a** regulates the NF-κB signaling pathway, leading to the downregulation of COX-2 and iNOS expression. These findings suggest that compound 7a is a promising candidate for anti-inflammatory therapy, and ongoing studies in our laboratory will explore its full potential.

4.8. Experimental section

4.8.1. Procedure for the synthesis of *(E)*-2-(2-((1S,4aS,8aS)-5,5,8a-trimethyl-2-methylenedecahydronaphthalen-1-yl)ethylidene)succinic acid (8)

To a stirred solution of compound **1** (1.5g, 1 equiv.) in ^{t}BuOH: H_2O, 2-methyl-2-butene (1.5 equiv.) was added. A mixture of sodium chlorite (10 equiv.) and sodium dihydrogen phosphate (10 equiv.) in water, were added dropwise to the reaction mixture over a period of 10 minutes and stirred at room temperature overnight. Volatile components were removed under vacuum, the residue was dissolved in water, extracted in ethyl acetate, dried over Na_2SO_4 and concentrated under reduced pressure to yield a pure product. Yield: 42 % (661 mg)

4.8.2. Procedure for the synthesis of di(prop-2-yn-1-yl) *(E)*-2-(2-((1S,4aS,8aS)-5,5,8a-trimethyl-2-methylenedecahydronaphthalen-1-yl)ethylidene)succinate (9)

Propargyl bromide (600 mg, 2 equiv.) was added dropwise to a solution of labdane diacid **8** (1 g, 1 equiv.) in DMF at 0 ^{o}C. K_2CO_3 (1.5 equiv.) was added and allowed to stir continuously at room temperature until the completion of the reaction monitored by TLC. The compound was extracted with ethyl acetate, dried over anhydrous Na_2SO_4 and the solvent was removed under reduced pressure afforded the compound **9**. Yield: 48% (353 mg).

4.8.3. General procedure for the synthesis of substituted N-alkyl bromo-isatins (5a-x)

Isatin (1 equiv.) was added to a stirred solution of NaH (1.5 equiv.) in dry DMF, resulting in the formation of a purple-coloured anion. When the H_2 evolution ceased, a solution of dibromoalkane (1.1 equiv.) in DMF was added to this mixture dropwise. The reaction mixture was stirred at 60 ^oC for two hours. After the completion of the reaction, confirmed by TLC, the reaction was quenched by adding H_2O dropwise and was then extracted with ethyl acetate. The combined organic layer was washed with brine, dried over anhydrous Na_2SO_4, and concentrated under reduced pressure. The product was purified by column chromatography using ethyl acetate and hexane.

4.8.4. General procedure for the synthesis of substituted N-alkyl azido-isatins (6a-x)

NaN_3 (1.5 equiv.) was added to a stirred suspension of N-alkyl bromo-isatin (1 equiv.) in dry DMF and stirred at 60 ^oC for two hours. The reaction mixture was diluted with water, extracted in ethyl acetate, dried over anhydrous Na_2SO_4 and the solvent was removed under reduced pressure to furnish the product.

4.8.5. General procedure for the synthesis of triazole appended labdane derivatives (7a-x, 10a-i)

To a stirred mixture of compound **3** or compound **9** and N-alky azido-isatin (**6**) (1 equiv. for **3** and 2 equiv. for **9**), in ^{t}Butanol: H_2O mixture (3:1), $CuSO_4.5H_2O$ (0.1 equiv.) and sodium-ascorbate (0.25 equiv.) were added and stirred at room temperature. The progress of the reaction was monitored by TLC. After the reaction was complete, the combined organic layer was washed with brine, dried over anhydrous Na_2SO_4, and concentrated under reduced pressure. The product was purified by column chromatography using ethyl acetate and hexane.

4.8.6. Synthesis and characterization of labdane conjugates

Characterization of *(E)*-2-(2-((1S,4aS,8aS)-5,5,8a-trimethyl-2-methylenedecahydronaphthalen-1-yl)ethylidene)succinic acid (8)

^{1}H NMR (500 MHz, $CDCl_3$) δ: 6.97 (t, *J* = 6.5 Hz, 1H), 4.76 (s, 1H), 4.31 (s, 1H), 3.31

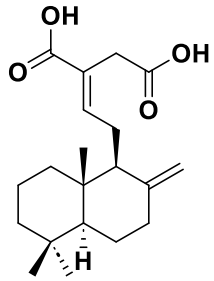

(s, 2H), 2.37-0.97 (m, 14 H), 0.81 (s, 3H), 0.75 (s, 3H), 0.65 (s, 3H)

^{13}C NMR (125 MHz, $CDCl_3$) δ: 177.13, 172.32, 150.29, 148.05, 124.07, 107.94, 56.34, 55.33, 42.02, 39.49, 39.24, 37.85, 33.60, 33.57, 32.38, 24.38, 24.10, 21.76, 19.31, 14.43

HRMS (ESI) m/z : $[M+Na]^+$ calcd for $C_{20}H_{30}O_4Na$ is 357.2042, found 357.2048

Characterization of di(prop-2-yn-1-yl) *(E)*-2-(2-((1S,4aS,8aS)-5,5,8a-trimethyl-2-methylenedecahydronaphthalen-1-yl)ethylidene)succinate (9)

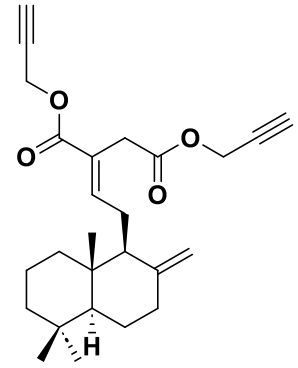

^{1}H NMR (500 MHz, $CDCl_3$) δ: 6.92 (t, J = 6.5 Hz, 1H), 4.77 (s, 1H), 4.67-4.63 (m, 4H), 4.32 (s, 1H), 3.40-3.33 (dd, J_1 = 17 Hz, J_2 = 20 Hz, 2H), 2.40-0.96 (m, 16 H), 0.81 (s, 3H), 0.75 (s, 3H), 0.65 (s, 3H)

^{13}C NMR (125 MHz, $CDCl_3$) δ: 169.80, 165.89, 149.13, 148.07, 123.87, 107.91, 77.82, 77.53, 74.98, 74.76, 56.32, 55.34, 52.39, 52.30, 42.02, 39.51, 39.20, 37.86, 33.60, 33.57, 32.33, 24.36, 24.09, 21.75, 19.31, 14.41

HRMS (ESI) m/z : $[M+Na]^+$ calcd for $C_{26}H_{34}O_4Na$ is 433.2355, found 433.2363.

Synthesis of (1-(2-(2,3-dioxoindolin-1-yl)ethyl)-1H-1,2,3-triazol-4-yl)methyl *(E)*-3-formyl-5-((1S,4aS,8aS)-5,5,8a-trimethyl-2-methylenedecahydronaphthalen-1-yl)pent-3-enoate (7a)

Compound **7a** was prepared by the reaction of compound **3** (22 mg) with 1-(2-azidoethyl)indoline-2,3-dione in ^{t}BuOH: H_2O mixture according to the procedure described in **4.8.5.** Yield: 44% (20 mg)

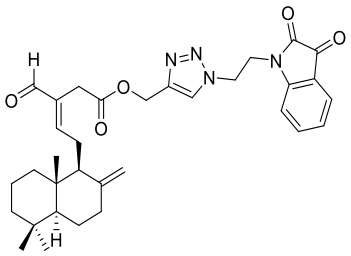

^{1}H NMR (500 MHz, $CDCl_3$) δ: 9.22 (s, 1H), 7.58 (s, 1H), 7.50 (d, *J* = 7Hz, 1H), 7.42 (t, *J* = 7.5 Hz, 1H), 7.02 (t, *J* = 7.5 Hz, 1H), 6.59 (t, *J* = 6.5 Hz, 1H), 6.48 (d, *J* = 8.0 Hz, 1H), 5.09 (s, 2H), 4.77 (s, 1H), 4.63 (t, *J* = 5.5 Hz, 2H), 4.29 (s, 1H), 4.18 (t, *J* = 6.0 Hz, 2H), 3.19 (s, 2H), 2.47-0.96 (m, 14H), 0.82 (s, 3H), 0.75 (s, 3H), 0.65 (s, 3H)

^{13}C NMR (125 MHz, $CDCl_3$) δ: 193.54, 182.31, 169.96, 159.14, 158.59, 149.99, 148.09, 138.62, 135.98, 125.61, 124.75, 124.18, 117.52, 109.47, 107.90, 58.07, 56.41, 55.37, 47.84, 41.98, 40.70, 39.57, 39.24, 37.84, 33.58, 29.76, 24.59, 24.09, 21.73, 19.30, 14.42

HRMS (ESI) m/z : $[M+H]^+$ calcd for $C_{33}H_{41}N_4O_5$ is 573.3077, found 573.3070

Synthesis of (1-(2-(5-methyl-2,3-dioxoindolin-1-yl)ethyl)-1H-1,2,3-triazol-4-yl)methyl *(E)*-3-formyl-5-((1S,4aS,8aS)-5,5,8a-trimethyl-2-methylenedecahydronaphthalen-1-yl)pent-3-enoate (7b)

Compound **7b** was prepared by the reaction of compound **3** (40 mg) with 1-(2-azidoethyl)-5-methylindoline-2,3-dione in ^{t}BuOH: H_2O mixture according to the procedure described in **4.8.5.** Yield: 53% (35 mg).

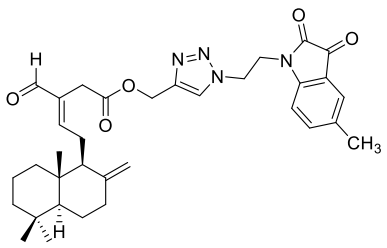

^{1}H NMR (500 MHz, $CDCl_3$) δ: 9.22 (s, 1H), 7.60 (s, 1H), 7.30 (s, 1H), 7.22 (d, *J* = 8 Hz, 1H), 6.59 (t, *J* = 6.5 Hz, 1H), 6.39 (d, *J* = 8.0 Hz, 1H), 5.09 (s, 2H), 4.76 (s, 1H), 4.62 (t, *J* = 5.5 Hz, 2H), 4.28 (s, 1H), 4.14 (t, *J* = 5.5 Hz, 2H), 3.20 (s, 2H), 2.48-2.31 (m, 3H), 2.23 (s, 3H), 1.97-0.96 (m, 11H), 0.82 (s, 3H), 0.75 (s, 3H), 0.65 (s, 3H)

^{13}C NMR (125 MHz, $CDCl_3$) δ: 193.53, 182.63, 169.95, 159.17, 158.71, 148.08, 147.84, 143.37, 139.01, 135.96, 134.05, 125.94, 124.76, 117.51, 109.34, 107.90, 58.08, 56.39, 55.35, 47.81, 41.97, 40.66, 39.56, 39.22, 37.83, 33.58, 33.57, 29.72, 24.59, 24.08, 21.74, 20.64, 19.30, 14.42
HRMS (ESI) m/z : $[M+Na]^+$ calcd for $C_{34}H_{42}N_4O_5$ Na is 609.3053, found 609.3062

Synthesis of (1-(2-(5-methoxy-2,3-dioxoindolin-1-yl)ethyl)-1H-1,2,3-triazol-4-yl)methyl *(E)*-3-formyl-5-((1S,4aS,8aS)-5,5,8a-trimethyl-2-methylenedecahydronaphthalen -1-yl)pent-3-enoate (7c)

Compound **7c** was prepared by the reaction of compound **3** (40 mg) with 1-(2-azidoethyl)-5-methoxyindoline-2,3-dione in ^{t}BuOH: H_2O mixture according to the procedure described in **4.8.5.** Yield: 34% (23 mg).

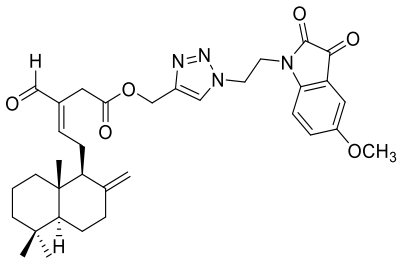

^{1}H NMR (500 MHz, $CDCl_3$) δ: 9.21 (s, 1H), 7.61 (s, 1H), 7.02 (s, 1H), 6.97 (dd, J_1 = 1.5 Hz, J_2 = 8.5 Hz, 1H), 6.59 (t, J = 6.5 Hz, 1H), 6.39 (d, J = 8.5 Hz, 1H), 5.08 (s, 2H), 4.77 (s, 1H), 4.62 (t, J = 6.0 Hz, 2H), 4.28 (s, 1H), 4.14 (t, J = 6.0 Hz, 2H), 3.71 (s, 3H), 3.19 (s, 2H), 2.48-0.96 (m, 14H), 0.82 (s, 3H), 0.75 (s, 3H), 0.65 (s, 3H)

^{13}C NMR (125 MHz, $CDCl_3$) δ: 193.65, 182.70, 169.99, 159.32, 158.74, 156.69, 148.09, 143.82, 143.41, 135.95, 124.86, 117.93, 110.54, 109.78, 107.90, 57.97, 56.40, 55.95, 55.36, 47.93, 41.97, 40.69, 39.56, 39.23, 37.83, 33.58, 29.74, 24.60, 24.08, 21.73, 19.29, 14.41

HRMS (ESI) m/z : $[M+Na]^+$ calcd for $C_{34}H_{42}N_4O_6Na$ is 625.3002, found 625.3002

Synthesis of (1-(2-(2,3-dioxo-5-(trifluoromethoxy)indolin-1-yl)ethyl)-1H-1,2,3-triazol-4-yl)methyl *(E)*-3-formyl-5-((1S,4aS,8aS)-5,5,8a-trimethyl-2-methylenedecahydronaphthalen-1-yl)pent-3-enoate (7d)

Compound **7d** was prepared by the reaction of compound **3** (31 mg) with 1-(2-azidoethyl)-5-(trifluoromethoxy)indoline-2,3-dione in ^{t}BuOH: H_2O mixture according to the procedure described in **4.8.5.** Yield: 42% (24mg).

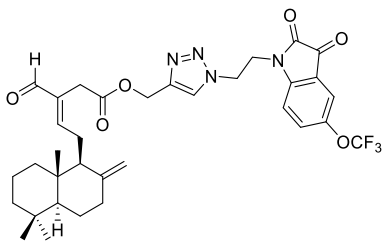

^{1}H NMR (500 MHz, $CDCl_3$) δ: 9.17 (s, 1H), 7.60 (s, 1H), 7.34(s, 1H), 7.27 (d, *J* = 8.5 Hz, 1H), 6.59 (t, *J* = 6.5Hz, 1H), 6.48 (d, *J* = 8.5 Hz, 1H), 5.10 (s, 2H), 4.77 (s, 1H), 4.64 (t, *J* = 5.5 Hz, 2H), 4.29 (s, 1H), 4.19 (t, *J* = 5.5 Hz, 2H), 3.16 (s, 2H), 2.48-0.97 (m, 14H), 0.82 (s, 3H), 0.75 (s, 3H), 0.66 (s, 3H)

^{13}C NMR (125 MHz, $CDCl_3$) δ: 193.65, 181.36, 169.98, 159.22, 158.34, 148.35, 148.06, 145.45, 143.81, 136.02, 131.17, 124.85, 118.40, 118.09, 110.77, 107.90, 58.09, 56.42, 55.37, 47.90, 41.97, 41.01, 39.57, 39.25, 37.83, 33.57, 29.83, 24.58, 24.09, 21.73, 19.29, 14.41

HRMS (ESI) m/z : $[M+Na]^+$ calcd for $C_{34}H_{39}F_3N_4O_6Na$ is 679.2719, found 679.2716

Synthesis of (1-(2-(5-fluoro-2,3-dioxoindolin-1-yl)ethyl)-1H-1,2,3-triazol-4-yl)methyl *(E)*-3-formyl-5-((1S,4aS,8aS)-5,5,8a-trimethyl-2-methylenedecahydronaphthalen-1-yl)pent-3-enoate (7e)

Compound **7e** was prepared by the reaction of compound **3** (50 mg) with 1-(2-azidoethyl)-5-fluoroindoline-2,3-dione in ^{t}BuOH: H_2O mixture according to the procedure described in **4.8.5.** Yield: 36% (30 mg).

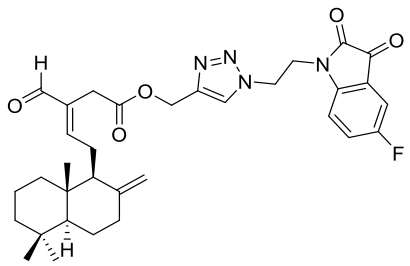

^{1}H NMR (500 MHz, $CDCl_3$) δ: 9.19 (s, 1H), 7.62(s, 1H), 7.18-7.11 (m, 2H), 6.59 (t, J = 6.5 Hz, 1H), 6.41 (dd, J_1= 2.5 Hz, J_2= 8.5 Hz, 1H), 5.09 (s, 2H), 4.77 (s, 1H), 4.63 (t, J = 5.5 Hz, 2H), 4.29 (s, 1H), 4.17 (t, J = 5 Hz, 2H), 3.18 (s, 2H), 2.48-0.97 (m, 14H), 0.82 (s, 3H), 0.75 (s, 3H), 0.66 (s, 3H)

^{13}C NMR (125 MHz, $CDCl_3$) δ: 193.64, 181.82, 169.97, 160.33, 159.27, 158.43, 148.07, 146.10, 143.63, 135.99, 125.00, 124.88, 118.10, 112.37, 110.85, 107.92, 58.07, 56.41, 55.36, 47.93, 41.97, 40.90, 39.57, 39.24, 37.83, 33.57, 29.81, 29.69, 24.59, 24.08, 21.73, 19.30, 14.42

HRMS (ESI) m/z : $[M+Na]^+$ calcd for $C_{33}H_{39}FN_4O_5$ Na is 613.2802, found 613.2810

Synthesis of (1-(2-(5-chloro-2,3-dioxoindolin-1-yl)ethyl)-1H-1,2,3-triazol-4-yl)methyl *(E)*-3-formyl-5-((1S,4aS,8aS)-5,5,8a-trimethyl-2-methylenedecahydronaphthalen-1-yl)pent-3-enoate (7f)

Compound **7f** was prepared by the reaction of compound **3** (50 mg) with 1-(2-azidoethyl)-5-chloroindoline-2,3-dione in ^{t}BuOH: H_2O mixture according to the procedure described in **4.8.5.** Yield: 35% (30 mg).

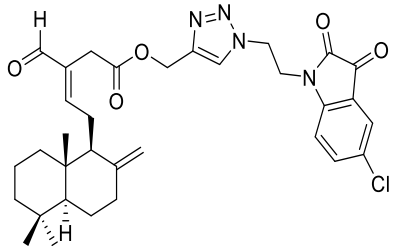

^{1}H NMR (500 MHz, $CDCl_3$) δ: 9.19 (s, 1H), 7.61 (s, 1H), 7.43(s, 1H), 7.37 (d, *J* = 8.5 Hz, 1H), 6.59 (t, *J* = 6.5Hz, 1H), 6.39 (d, *J* = 8 Hz, 1H), 5.10 (s, 2H), 4.78 (s, 1H), 4.63 (t, *J* = 5 Hz, 2H), 4.29 (s, 1H), 4.17 (t, *J* = 5 Hz, 2H), 3.18 (s, 2H), 2.48-0.97 (m, 14H), 0.82 (s, 3H), 0.75 (s, 3H), 0.66 (s, 3H)

^{13}C NMR (125 MHz, $CDCl_3$) δ: 193.61, 181.40, 169.97, 159.21, 158.12, 148.34, 148.07, 143.68, 137.90, 136.01, 129.91, 125.35, 124.85, 118.35, 110.87, 107.93, 58.09, 56.42, 55.37, 47.92, 41.98, 40.96, 39.58, 39.26, 37.84, 33.58, 29.83, 24.61, 24.09, 21.74, 19.31, 14.43

HRMS (ESI) m/z: $[M+Na]^+$ calcd for $C_{33}H_{39}ClN_4O_5Na$ is 629.2507, found 629.2525

Synthesis of (1-(2-(5-bromo-2,3-dioxoindolin-1-yl)ethyl)-1H-1,2,3-triazol-4-yl)methyl *(E)*-3-formyl-5-((1S,4aS,8aS)-5,5,8a-trimethyl-2-methylenedecahydronaphthalen-1-yl)pent-3-enoate (7g)

Compound **7g** was prepared by the reaction of compound **3** (51 mg) with 1-(2-azidoethyl)-5-bromoindoline-2,3-dione in ^{t}BuOH: H_2O mixture according to the procedure described in **4.8.5.** Yield:53 % (49 mg).

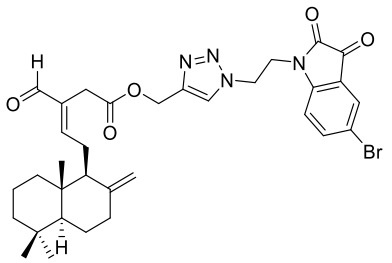

^{1}H NMR (500 MHz, $CDCl_3$) δ: 9.18 (s, 1H), 7.64 (s, 1H), 7.56 (s, 1H), 7.51 (d, *J* = 8.5 Hz, 1H), 6.59 (t, *J* = 6.5 Hz, 1H), 6.35 (d, *J* = 8.0 Hz, 1H), 5.09 (s, 2H), 4.77 (s, 1H), 4.64 (t, *J* = 5.5 Hz, 2H), 4.29 (s, 1H), 4.16 (t, *J* = 5 Hz, 2H), 3.18 (s, 2H), 2.48-0.97 (m, 14H), 0.82 (s, 3H), 0.75 (s, 3H), 0.65 (s, 3H)

^{13}C NMR (125 MHz, $CDCl_3$) δ: 193.62, 181.32, 169.96, 159.28, 157.94, 148.83, 148.07, 143.58, 140.75, 135.99, 128.18, 124.95, 118.67, 116.89, 111.31, 107.94, 58.07, 56.40, 55.35, 47.89, 41.97, 40.93, 39.56, 39.23, 37.83, 33.58, 33.57, 29.82, 24.61, 24.08, 21.74, 19.30, 14.43

HRMS (ESI) m/z: $[M+H]^+$ calcd for $C_{33}H_{40}BrN_4O_5$ is 651.2182, found 651.21783

Synthesis of (1-(2-(5-iodo-2,3-dioxoindolin-1-yl)ethyl)-1H-1,2,3-triazol-4-yl)methyl *(E)*-3-formyl-5-((1S,4aS,8aS)-5,5,8a-trimethyl-2-methylenedecahydronaphthalen-1-yl)pent-3-enoate (7h)

Compound **7h** was prepared by the reaction of compound **3** (35 mg) with 1-(2-azidoethyl)-5-iodoindoline-2,3-dione in ^{t}BuOH: H_2O mixture according to the procedure described in **4.8.5.** Yield: 25% (17 mg).

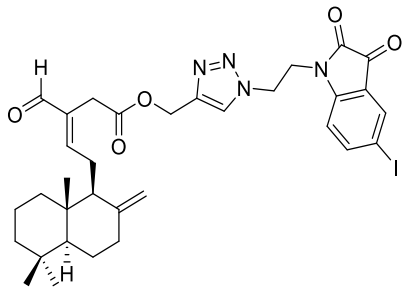

^{1}H NMR (500 MHz, $CDCl_3$) δ: 9.19 (s, 1H), 7.75(s, 1H), 7.71 (d, *J* = 8Hz, 1H), 7.58 (s, 1H), 6.60 (t, *J* = 6.5 Hz, 1H), 6.24 (d, *J* = 8.5 Hz, 1H), 5.11 (s, 2H), 4.78 (s, 1H), 4.62 (t, *J* = 5.5 Hz, 2H), 4.30 (s, 1H), 4.16 (t, *J* = 5.5 Hz, 2H), 3.19 (s, 2H), 2.49-0.98 (m, 14 H), 0.82 (s, 3H), 0.76 (s, 3H), 0.66 (s, 3H)

^{13}C NMR (125 MHz, $CDCl_3$) δ: 193.61, 181.01, 169.99, 159.21, 157.65, 149.38, 148.08, 146.56, 143.71, 136.02, 133.93, 124.81, 119.05, 111.65, 107.97, 86.47, 58.10, 56.43, 55.37, 47.88, 41.98, 40.90, 39.59, 39.27, 37.85, 33.59, 29.90, 24.62, 24.09, 21.75, 19.31, 14.45

HRMS (ESI) m/z : $[M+H]^+$ calcd for $C_{33}H_{40}IN_4O_5$ is 699.2043, found 699.2055

Synthesis of (1-(3-(2,3-dioxoindolin-1-yl)propyl)-1H-1,2,3-triazol-4-yl)methyl *(E)*-3-formyl-5-((1S,4aS,8aS)-5,5,8a-trimethyl-2-methylenedecahydronaphthalen-1-yl)pent-3-enoate (7i)

Compound **7i** was prepared by the reaction of compound **3** (47 mg) with 1-(3-azidopropyl)indoline-2,3-dione in ^{t}BuOH: H_2O mixture according to the procedure described in **4.8.5.** Yield: 52% (40 mg).

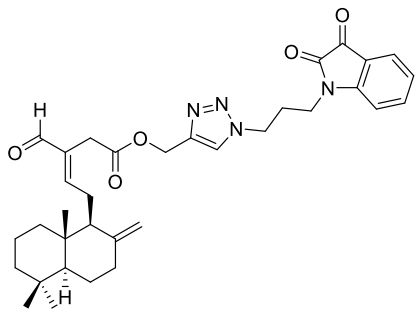

^{1}H NMR (500 MHz, $CDCl_3$) δ: 9.17 (s, 1H), 7.62 (s, 1H), 7.46 (t, *J* = 7.5Hz, 2H), 6.99 (t, *J* = 7.5 Hz, 1H), 6.76 (d, *J* = 8 Hz, 1H), 6.51 (t, *J* = 6.5 Hz, 1H), 5.09 (s, 2H), 4.68 (s, 1H), 4.30 (t, *J* = 6.5 Hz, 2H), 4.21 (s, 1H), 3.67 (t, *J* = 6.5Hz, 2H), 3.18 (s, 2H), 2.40-0.89 (m, 16H), 0.73 (s, 3H), 0.66 (s, 3H), 0.56 (s, 3H)

^{13}C NMR (125 MHz, $CDCl_3$) δ: 193.55, 182.96, 170.03, 159.17, 158.54, 150.26, 148.08, 142.91, 138.69, 135.99, 125.64, 124.48, 124.10, 117.62, 110.19, 107.90, 58.21, 56.38, 55.34, 47.69, 41.96, 39.55, 39.21, 37.83, 37.47, 33.57, 33.56, 29.74, 27.73, 24.60, 24.08, 21.73, 19.29, 14.41

HRMS (ESI) m/z : $[M+Na]^+$ calcd for $C_{34}H_{42}N_4O_5Na$ is 609.3053, found 609.3046

Synthesis of (1-(3-(5-methyl-2,3-dioxoindolin-1-yl)propyl)-1H-1,2,3-triazol-4-yl)methyl *(E)*-3-formyl-5-((1S,4aS,8aS)-5,5,8a-trimethyl-2-methylenedecahydronaphthalen-1-yl)pent-3-enoate (7j)

Compound **7j** was prepared by the reaction of compound **3** (40 mg) with 1-(3-azidopropyl)-5-methylindoline-2,3-dione in ^{t}BuOH: H_2O mixture according to the procedure described in **4.8.5.** Yield: 52% (35mg).

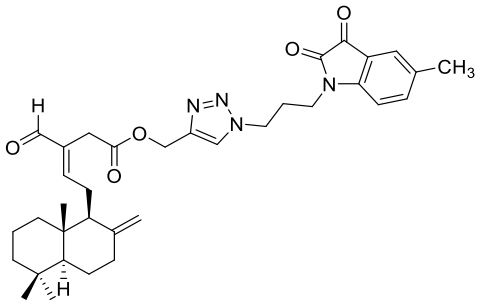

^{1}H NMR (500 MHz, $CDCl_3$) δ: 9.26 (s, 1H), 7.70 (s, 1H), 7.34-7.32 (m, 2H), 6.72 (d, *J* = 7.5 Hz, 1H), 6.59 (t, *J* = 6.5 Hz, 1H), 5.17 (s, 2H), 4.76 (s, 1H), 4.37 (t, *J* = 6 Hz, 2H), 4.29 (s, 1H), 3.72 (t, *J* = 6.5 Hz, 2H), 3.27 (s, 2H), 2.48-2.29 (m, 5H), 2.26 (s, 3H), 1.95-0.96 (m, 11H), 0.81 (s, 3H), 0.74 (s, 3H), 0.64 (s, 3H)

^{13}C NMR (125 MHz, $CDCl_3$) δ: 193.53, 183.22, 170.02, 159.16, 158.66, 148.07, 142.87, 139.03, 135.99, 133.99, 125.99, 124.47, 117.64, 109.99, 107.91, 58.22, 56.37, 55.34, 47.69, 41.96, 39.54, 39.20, 37.83, 37.43, 33.58, 33.56, 29.73, 27.79, 24.60, 24.08, 21.73, 20.68, 19.29, 14.41

HRMS (ESI) m/z : $[M+H]^+$ calcd for $C_{35}H_{45}N_4O_5$ is 601.3390, found 601.3380

Synthesis of (1-(3-(5-methoxy-2,3-dioxoindolin-1-yl)propyl)-1H-1,2,3-triazol-4-yl)methyl *(E)*-3-formyl-5-((1S,4aS,8aS)-5,5,8a-trimethyl-2-methylenedecahydronaphthalen-1-yl)pent-3-enoate (7k)

Compound **7k** was prepared by the reaction of compound 3 (42 mg) with 1-(3-azidopropyl)-5-methoxyindoline-2,3-dione in ^{t}BuOH: H_2O mixture according to the procedure described in **4.8.5.** Yield: 52% (38 mg).

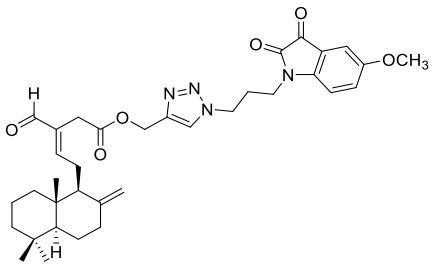

^{1}H NMR (500 MHz, $CDCl_3$) δ: 9.34 (s, 1H), 7.76 (s, 1H), 7.17-7.16 (m, 2H), 6.84-6.82 (m, 1H), 6.68 (t, *J* = 6.5 Hz, 1H), 5.26 (s, 2H), 4.85 (s, 1H), 4.45 (t, *J* = 6.5 Hz, 2H), 4.38 (s, 1H), 3.82 (s, 3H), 3.79 (t, *J* = 6.5 Hz, 2H), 3.35 (s, 2H), 2.57-1.04 (m, 16H), 0.90 (s, 3H), 0.83 (s, 3H), 0.73 (s, 3H)

^{13}C NMR (125 MHz, $CDCl_3$) δ: 193.52, 183.30, 170.02, 159.11, 158.63, 156.73, 148.08, 144.07, 142.94, 136.01, 124.85, 124.44, 118.09, 111.18, 109.94, 107.89, 58.22, 56.40, 56.01, 55.36, 47.68, 41.98, 39.56, 39.23, 37.84, 37.47, 33.57, 29.75, 27.74, 24.60, 24.09, 21.72, 19.29, 14.41

HRMS (ESI) m/z : $[M+Na]^+$ calcd for $C_{35}H_{44}N_4O_6Na$ is 639.3159, found 639.3170

Synthesis of (1-(3-(2,3-dioxo-5-(trifluoromethoxy)indolin-1-yl)propyl)-1H-1,2,3-triazol-4-yl)methyl *(E)*-3-formyl-5-((1S,4aS,8aS)-5,5,8a-trimethyl-2-methylenedecahydronaphthalen-1-yl)pent-3-enoate (7l)

Compound **7l** was prepared by the reaction of compound **3** (33 mg) with 1-(3-azidopropyl)-5-trifluoromethoxyindoline-2,3-dione in ^{t}BuOH: H_2O mixture according to the procedure described in **4.8.5.** Yield: 42% (26 mg).

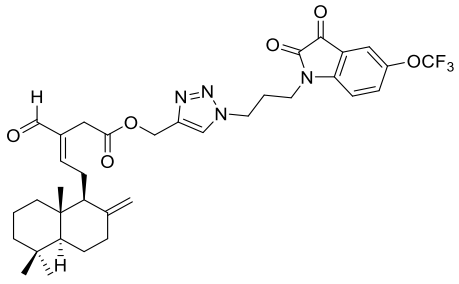

^{1}H NMR (500 MHz, $CDCl_3$) δ: 9.24 (s, 1H), 7.67 (s, 1H), 7.42-7.40 (m, 2H), 6.91 (d, *J* = 8.5 Hz, 1H), 6.60 (t, *J* = 6.5Hz, 1H), 5.19 (s, 2H), 4.77 (s, 1H), 4.38 (t, *J* = 6.5 Hz, 2H), 4.30 (s, 1H), 3.76 (t, *J* = 6.5 Hz, 2H), 3.26 (s, 2H), 2.49-0.97 (m, 16H), 0.82 (s, 3H), 0.75 (s, 3H), 0.66 (s, 3H)

^{13}C NMR (125 MHz, $CDCl_3$) δ: 193.58, 181.96, 170.08, 159.17, 158.18, 148.62, 148.09, 145.50, 136.00, 131.39, 124.48, 118.69, 118.14, 111.48, 107.89, 58.17, 56.41, 55.37, 47.61, 41.97, 39.57, 39.24, 37.83, 37.74, 33.57, 29.81, 27.51, 24.61, 24.09, 21.72, 19.30, 14.42

HRMS (ESI) m/z : $[M+Na]^+$ calcd for $C_{35}H_{41}F_3N_4O_6Na$ is 693.2876, found 693.2868

Synthesis (1-(3-(5-fluoro-2,3-dioxoindolin-1-yl)propyl)-1H-1,2,3-triazol-4-yl)methyl *(E)*-3-formyl-5-((1S,4aS,8aS)-5,5,8a-trimethyl-2-methylenedecahydronaphthalen-1-yl)pent-3-enoate (7m)

Compound **7m** was prepared by the reaction of compound **3** (45 mg) with 1-(3-azidopropyl)-5-fluoroindoline-2,3-dione in ^{t}BuOH: H_2O mixture according to the procedure described in **4.8.5.** Yield: 58% (44 mg).

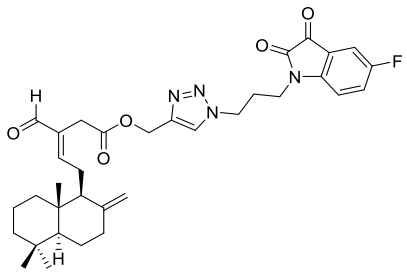

^{1}H NMR (500 MHz, $CDCl_3$) δ: 9.25 (s, 1H), 7.68(s, 1H), 7.27-7.24 (m, 2H), 6.84-6.82 (m, 1H), 6.60 (t, *J* = 6.5 Hz, 1H), 5.17 (s, 2H), 4.77 (s, 1H), 4.38 (t, *J* = 6.5 Hz, 2H), 4.30 (s, 1H), 3.74 (t, *J* = 7 Hz, 2H), 3.26 (s, 2H), 2.49-0.96 (m, 16H), 0.82 (s, 3H), 0.75 (s, 3H), 0.65 (s, 3H)

^{13}C NMR (125 MHz, $CDCl_3$) δ: 193.58, 182.40, 170.06, 160.42, 159.20, 158.30, 148.09, 146.32, 143.04, 135.99, 125.08, 124.47, 118.27, 112.76, 111.54, 107.90, 58.20, 56.39, 55.35, 47.63, 41.97, 39.56, 39.23, 37.83, 37.65, 33.57, 29.78, 29.69, 27.52, 24.61, 24.08, 21.72, 19.29, 14.41

HRMS (ESI) m/z : $[M+Na]^+$ calcd for $C_{34}H_{41}FN_4O_5$ Na is 627.2959, found 627.2964

Synthesis (1-(3-(5-chloro-2,3-dioxoindolin-1-yl)propyl)-1H-1,2,3-triazol-4-yl)methyl *(E)*-3-formyl-5-((1S,4aS,8aS)-5,5,8a-trimethyl-2-methylenedecahydronaphthalen-1-yl)pent-3-enoate (7n)

Compound **7n** was prepared by the reaction of compound **3** (52 mg) with 1-(3-azidopropyl)-5-chloroindoline-2,3-dione in ^{t}BuOH: H_2O mixture according to the procedure described in **4.8.5.** Yield: 55% (50 mg).

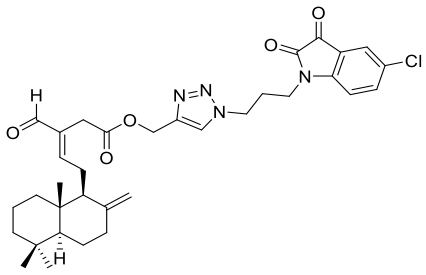

^{1}H NMR (500 MHz, $CDCl_3$) δ: 9.24 (s, 1H), 7.67 (s, 1H), 7.50-7.49 (m, 2H), 6.81 (d, *J* = 9 Hz, 1H), 6.60 (t, *J* = 6.5 Hz, 1H), 5.17 (s, 2H), 4.77 (s, 1H), 4.37 (t, *J* = 6.5 Hz, 2H), 4.30 (s, 1H), 3.74 (t, *J* = 7Hz, 2H), 3.26 (s, 2H), 2.49-0.96 (m, 16H), 0.82 (s, 3H), 0.75 (s, 3H), 0.65 (s, 3H)

^{13}C NMR (125 MHz, $CDCl_3$) δ: 193.56, 181.98, 170.05, 159.17, 157.99, 148.56, 148.09, 143.08, 138.03, 136.00, 129.92, 125.49, 124.42, 118.44, 111.59, 107.90, 58.21, 56.40, 55.36, 47.59, 41.97, 39.56, 39.24, 37.84, 37.69, 33.57, 29.79, 27.53, 24.61, 24.09, 21.72, 19.30, 14.41

HRMS (ESI) m/z : $[M+Na]^+$ calcd for $C_{34}H_{41}ClN_4O_5Na$ is 643.2663, found 643.26807

Synthesis of (1-(3-(5-bromo-2,3-dioxoindolin-1-yl)propyl)-1H-1,2,3-triazol-4-yl)methyl *(E)*-3-formyl-5-((1S,4aS,8aS)-5,5,8a-trimethyl-2-methylenedecahydronaphthalen-1-yl)pent-3-enoate (7o)

Compound **7o** was prepared by the reaction of compound **3** (44 mg) with 1-(3-azidopropyl)-5-bromoindoline-2,3-dione in ^{t}BuOH: H_2O mixture according to the procedure described in **4.8.5.** Yield: 35% (29 mg).

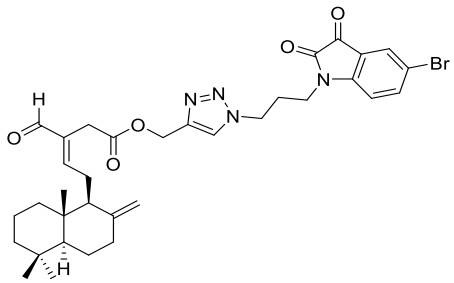

^{1}H NMR (500 MHz, $CDCl_3$) δ: 9.16 (s, 1H), 7.59-7.55 (m, 3H), 6.69 (d, *J* = 8.5 Hz, 1H), 6.52 (t, *J* = 6.5 Hz, 1H), 5.09 (s, 2H), 4.68 (s, 1H), 4.29 (t, *J* = 6.5 Hz, 2H), 4.21 (s, 1H), 3.65 (t, *J* = 7 Hz, 2H), 3.18 (s, 2H), 2.41-0.88 (m, 16H), 0.73 (s, 3H), 0.66 (s, 3H), 0.57 (s, 3H)

^{13}C NMR (125 MHz, $CDCl_3$) δ: 193.57, 181.83, 170.06, 159.18, 157.81, 149.00, 148.09, 143.08, 140.89, 136.00, 128.35, 124.43, 118.78, 116.93, 111.99, 107.90, 58.21, 56.40, 55.36, 47.59, 41.97, 39.56, 39.23, 37.84, 37.67, 33.57, 29.79, 27.53, 24.61, 24.08, 21.73, 19.30, 14.42

HRMS (ESI) m/z : $[M+Na]^+$ calcd for $C_{34}H_{41}BrN_4O_5$ Na is 687.2158, found 687.2184

Synthesis of (1-(3-(5-iodo-2,3-dioxoindolin-1-yl)propyl)-1H-1,2,3-triazol-4-yl)methyl *(E)*-3-formyl-5-((1S,4aS,8aS)-5,5,8a-trimethyl-2-methylenedecahydronaphthalen-1-yl)pent-3-enoate (7p)

Compound **7p** was prepared by the reaction of compound **3** (39 mg) with 1-(3-azidopropyl)-5-iodoindoline-2,3-dione in ^{t}BuOH: H_2O mixture according to the procedure described in **4.8.5.** Yield: 30% (23 mg).

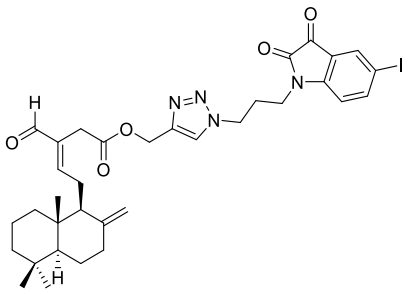

^{1}H NMR (500 MHz, $CDCl_3$) δ: 9.25 (s, 1H), 7.84-7.82 (m, 2H), 7.66 (s, 1H), 6.65 (d, *J* = 8Hz, 1H), 6.60 (t, *J* = 6.5 Hz, 1H), 5.18 (s, 2H), 4.77 (s, 1H), 4.36 (t, *J* = 6.5 Hz, 2H), 4.30 (s, 1H), 3.73 (t, *J* = 7 Hz, 2H), 3.26 (s, 2H), 2.49-0.97 (m, 16 H), 0.82 (s, 3H), 0.75 (s, 3H), 0.65 (s, 3H)

^{13}C NMR (125 MHz, $CDCl_3$) δ: 193.57, 181.62, 170.07, 159.17, 157.52, 149.60, 148.09, 146.72, 143.10, 136.01, 134.06, 124.41, 119.13, 112.38, 107.92, 86.37, 58.22, 56.40, 55.36, 47.58, 41.97, 39.57, 39.24, 37.85, 37.62, 33.58, 30.36, 29.80, 27.55, 24.61, 24.09, 21.74, 19.31, 14.43

HRMS (ESI) m/z : $[M+H]^+$ cald for $C_{34}H_{42}IN_4O_5$ is 713.2200, found 713.2224

Synthesis of (1-(4-(2,3-dioxoindolin-1-yl)butyl)-1H-1,2,3-triazol-4-yl)methyl *(E)*-3-formyl-5-((1S,4aS,8aS)-5,5,8a-trimethyl-2-methylenedecahydronaphthalen-1-yl)pent-3-enoate (7q)

Compound **7q** was prepared by the reaction of compound **3** (57 mg) with 1-(4-azidobutyl)indoline-2,3-dione in ^{t}BuOH: H_2O mixture according to the procedure described in **4.8.5.** Yield: 55% (53 mg).

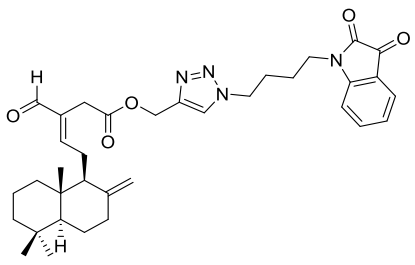

^{1}H NMR (500 MHz, $CDCl_3$) δ: 9.25 (s, 1H), 7.55-7.51 (m, 3H), 7.06 (t, *J* = 7.5Hz, 1H), 6.83 (d, *J* = 8 Hz, 1H), 6.59 (t, *J* = 6.5 Hz, 1H), 5.15 (s, 2H), 4.76 (s, 1H), 4.37 (t, *J* = 7 Hz, 2H), 4.29 (s, 1H), 3.70 (t, *J* = 7 Hz, 2H), 3.24 (s, 2H), 2.48-0.96 (m, 18H), 0.82 (s, 3H), 0.75 (s, 3H), 0.65 (s, 3H)

^{13}C NMR (125 MHz, $CDCl_3$) δ: 193.60, 183.24, 170.07, 159.21, 158.38, 150.52, 148.08, 138.56, 135.98, 125.60, 123.92, 123.78, 117.60, 110.14, 107.90, 58.22, 56.39, 55.35, 49.41, 41.97, 39.56, 39.22, 39.20, 37.83, 33.57, 29.75, 27.35, 24.60, 24.08, 21.73, 19.29, 14.41

HRMS (ESI) m/z: $[M+Na]^+$ calcd for $C_{35}H_{44}N_4O_5Na$ is 623.3209, found 623.3215

Synthesis of (1-(4-(5-methyl-2,3-dioxoindolin-1-yl)butyl)-1H-1,2,3-triazol-4-yl)methyl *(E)*-3-formyl-5-((1S,4aS,8aS)-5,5,8a-trimethyl-2-methylenedecahydronaphthalen-1-yl)pent-3-enoate (7r)

Compound **7r** was prepared by the reaction of compound **3** (32 mg) with 1-(4-azidobutyl)-5-methylindoline-2,3-dione in ^{t}BuOH: H_2O mixture according to the procedure described in **4.8.5.** Yield: 50% (27 mg).

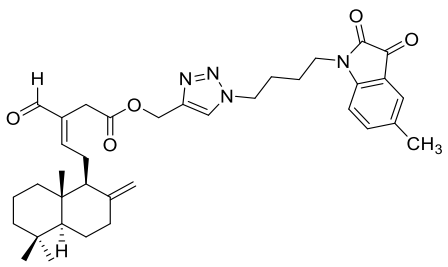

^{1}H NMR (500 MHz, $CDCl_3$) δ: 9.26 (s, 1H), 7.54 (s, 1H), 7.34-7.32 (m, 2H), 6.71 (d, *J* = 7.5 Hz, 1H), 6.59 (t, *J* = 6.5 Hz, 1H), 5.16 (s, 2H), 4.77 (s, 1H), 4.36 (t, *J* = 6.5 Hz, 2H), 4.29 (s, 1H), 3.68 (t, *J* = 7 Hz, 2H), 3.25 (s, 2H), 2.48-2.32 (m, 3H), 2.26 (s, 3H), 1.97-0.97 (m, 15H), 0.82 (s, 3H), 0.75 (s, 3H), 0.65 (s, 3H)

^{13}C NMR (125 MHz, $CDCl_3$) δ: 193.56, 183.49, 170.06, 159.14, 158.49, 148.33, 148.08, 142.99, 138.89, 136.01, 133.78, 125.95, 123.76, 117.64, 109.93, 107.90, 58.22, 56.40, 55.36, 49.46, 41.98, 39.56, 39.23, 39.16, 37.84, 33.58, 29.76, 27.34, 24.60, 24.09, 21.74, 20.66, 19.30, 14.42

HRMS (ESI) m/z : $[M+Na]^+$ calcd for $C_{36}H_{46}N_4O_5Na$ is 637.3366, found 637.3365

Synthesis of (1-(4-(5-methoxy-2,3-dioxoindolin-1-yl)butyl)-1H-1,2,3-triazol-4-yl)methyl *(E)*-3-formyl-5-((1S,4aS,8aS)-5,5,8a-trimethyl-2-methylenedecahydronaphthalen-1-yl)pent-3-enoate (7s)

Compound **7s** was prepared by the reaction of compound **3** (38 mg) with 1-(4-azidobutyl)-5-methoxyindoline-2,3-dione in ^{t}BuOH: H_2O mixture according to the procedure described in **4.8.5.** Yield: 42% (28mg).

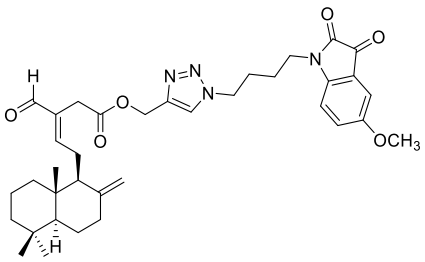

^{1}H NMR (500 MHz, $CDCl_3$) δ: 9.26 (s, 1H), 7.57 (s, 1H), 7.08 (s, 2H), 6.74 (d, *J* = 9 Hz, 1H), 6.59 (t, *J* = 6.5 Hz, 1H), 5.16 (s, 2H), 4.77 (s, 1H), 4.37 (t, *J* = 6.0 Hz, 2H), 4.29 (s, 1H), 3.74 (s, 3H), 3.69 (t, *J* = 6.5 Hz, 2H), 3.25 (s, 2H), 2.48-0.97 (m, 18H), 0.82 (s, 3H), 0.75 (s, 3H), 0.65 (s, 3H)

^{13}C NMR (125 MHz, $CDCl_3$) δ: 193.56, 183.61, 170.06, 159.16, 158.44, 156.59, 148.08, 144.34, 136.01, 124.77, 118.05, 111.13, 109.87, 107.90, 58.23, 56.39, 56.01, 55.36, 49.46, 41.97, 39.56, 39.23, 39.17, 37.84, 33.58, 32.54, 30.94, 29.76, 27.33, 24.60, 24.09, 21.74, 19.30, 14.42

HRMS (ESI) m/z : $[M+Na]^+$ calcd for $C_{36}H_{46}N_4O_6Na$ is 653.3315, found 653.3327

Synthesis of (1-(4-(2,3-dioxo-5-(trifluoromethoxy)indolin-1-yl)butyl)-1H-1,2,3-triazol-4-yl)methyl *(E)*-3-formyl-5-((1S,4aS,8aS)-5,5,8a-trimethyl-2-methylenedecahydronaphthalen-1-yl)pent-3-enoate (7t)

Compound **7t** was prepared by the reaction of compound **3** (27 mg) with 1-(4-azidobutyl)-5-trifluoromethoxyindoline-2,3-dione in ^{t}BuOH: H_2O mixture according to the procedure described in **4.8.5.** Yield: 60% (31 mg).

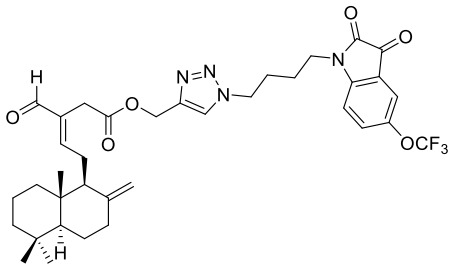

^{1}H NMR (500 MHz, $CDCl_3$) δ: 9.24 (s, 1H), 7.56 (s, 1H), 7.41-7.39 (m, 2H), 6.90 (d, *J* = 9 Hz, 1H), 6.59 (t, *J* = 6.5 Hz, 1H), 5.17 (s, 2H), 4.77 (s, 1H), 4.37 (t, *J* = 7.0 Hz, 2H), 4.29 (s, 1H), 3.71 (t, *J* = 7Hz, 2H), 3.24 (s, 2H), 2.48-0.97 (m, 18H), 0.82 (s, 3H), 0.75 (s, 3H), 0.65 (s, 3H)

^{13}C NMR (125 MHz, $CDCl_3$) δ: 193.59, 182.24, 170.08, 159.20, 158.02, 148.87, 148.08, 135.99, 131.26, 130.90, 128.81, 123.83, 118.66, 118.11, 111.33, 107.89, 58.22, 56.40, 55.36, 49.31, 41.97, 39.56, 39.43, 39.24, 37.83, 33.57, 29.78, 27.29, 24.59, 24.09, 23.95, 21.73, 19.30, 14.42

HRMS (ESI) m/z : $[M+Na]^+$ calcd for $C_{36}H_{43}F_3N_4O_6Na$ is 707.3032, found 707.3026

Synthesis of (1-(4-(5-fluoro-2,3-dioxoindolin-1-yl)butyl)-1H-1,2,3-triazol-4-yl)methyl *(E)*-3-formyl-5-((1S,4aS,8aS)-5,5,8a-trimethyl-2-methylenedecahydronaphthalen-1-yl)pent-3-enoate (7u)

Compound **7u** was prepared by the reaction of compound **3** (45 mg) with 1-(4-azidobutyl)-5-fluoroindoline-2,3-dione in ^{t}BuOH: H_2O mixture according to the procedure described in **4.8.5.** Yield: 41% (32 mg).

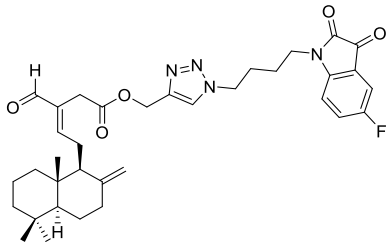

^{1}H NMR (500 MHz, $CDCl_3$) δ: 9.24 (s, 1H), 7.55(s, 1H), 7.27-7.23 (m, 2H), 6.82-6.80 (m, 1H), 6.59 (t, *J* = 6.5 Hz, 1H), 5.16 (s, 2H), 4.77 (s, 1H), 4.37 (t, *J* = 6.5 Hz, 2H), 4.29 (s, 1H), 3.69 (t, *J* = 7 Hz, 2H), 3.24 (s, 2H), 2.48-0.96 (m, 18H), 0.82 (s, 3H), 0.75 (s, 3H), 0.65 (s, 3H)

^{13}C NMR (125 MHz, $CDCl_3$) δ: 193.58, 182.68, 170.07, 160.33, 159.19, 158.11, 148.08, 146.56, 135.99, 124.94, 124.75, 123.76, 118.19, 112.73, 111.35, 107.90, 58.27, 56.39, 55.35, 49.31, 41.97, 39.56, 39.33, 39.23, 37.83, 33.58, 29.77, 27.31, 24.59, 24.08, 23.94, 21.73, 19.30, 14.42

HRMS (ESI) m/z : $[M+Na]^+$ calcd for $C_{35}H_{43}FN_4O_5Na$ is 641.3115, found 641.3125

Synthesis of (1-(4-(5-chloro-2,3-dioxoindolin-1-yl)butyl)-1H-1,2,3-triazol-4-yl)methyl *(E)*-3-formyl-5-((1S,4aS,8aS)-5,5,8a-trimethyl-2-methylenedecahydronaphthalen-1-yl)pent-3-enoate (7v)

Compound **7v** was prepared by the reaction of compound **3** (50 mg) with 1-(4-azidobutyl)-5-chloroindoline-2,3-dione in ^{t}BuOH: H_2O mixture according to the procedure described in **4.8.5.** Yield: 31% (28 mg).

^{1}H NMR (500 MHz, $CDCl_3$) δ: 9.24 (s, 1H), 7.54 (s, 1H), 7.49 (s, 2H), 6.81 (d, *J* = 9 Hz, 1H), 6.60 (t, *J* = 6.5 Hz, 1H), 5.16 (s, 2H), 4.77 (s, 1H), 4.36 (t, *J* = 6.5 Hz, 2H), 4.29 (s, 1H), 3.69 (t, *J* = 7Hz, 2H), 3.24 (s, 2H), 2.49-0.97 (m, 18H), 0.82 (s, 3H), 0.75 (s, 3H), 0.65 (s, 3H)

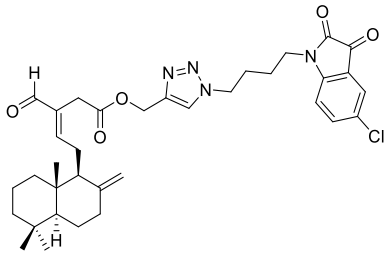

^{13}C NMR (125 MHz, $CDCl_3$) δ: 193.62, 182.24, 170.09, 159.25, 157.82, 148.77, 148.09, 143.16, 137.91, 135.99, 129.76, 125.49, 123.78, 118.43, 111.48, 107.91, 58.24, 56.40, 55.36, 49.31, 41.97, 39.57, 39.37, 39.24, 37.84, 33.58, 29.78, 27.29, 24.60, 24.09, 23.94, 21.74, 19.30, 14.42

HRMS (ESI) m/z : $[M+Na]^+$ calcd for $C_{35}H_{43}ClN_4O_5Na$ is 657.2820, found 657.2825

Synthesis of (1-(4-(5-bromo-2,3-dioxoindolin-1-yl)butyl)-1H-1,2,3-triazol-4-yl)methyl *(E)*-3-formyl-5-((1S,4aS,8aS)-5,5,8a-trimethyl-2-methylenedecahydronaphthalen-1-yl)pent-3-enoate (7w)

Compound **7w** was prepared by the reaction of compound **3** (40 mg) with 1-(4-azidobutyl)-5-bromoindoline-2,3-dione in ^{t}BuOH: H_2O mixture according to the procedure described in 1.5. Yield: 55% (42 mg).

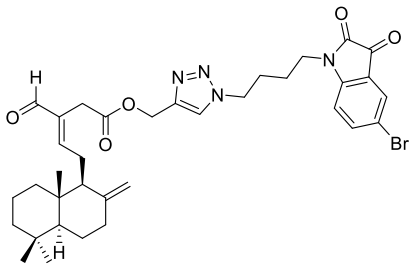

^{1}H NMR (500 MHz, $CDCl_3$) δ: 9.23 (s, 1H), 7.65-7.63 (m, 2H), 7.55 (s, 1H), 6.76 (d, *J* = 8 Hz, 1H), 6.60 (t, *J* = 6.5 Hz, 1H), 5.16 (s, 2H), 4.77 (s, 1H), 4.36 (t, *J* = 6.5 Hz, 2H), 4.29 (s, 1H), 3.68 (t, *J* = 7 Hz, 2H), 3.24 (s, 2H), 2.48-0.97 (m, 18H), 0.82 (s, 3H), 0.75 (s, 3H), 0.65 (s, 3H)

^{13}C NMR (125 MHz, $CDCl_3$) δ: 193.58, 182.10, 170.07, 159.21, 157.63, 149.23, 148.08, 140.75, 135.99, 130.91, 128.81, 128.30, 118.76, 116.72, 111.92, 107.92, 58.27, 56.39, 55.35, 49.29, 41.97, 39.56, 39.36, 39.23, 37.84, 33.58, 30.35, 29.78,

27.29, 24.60, 24.08, 23.93, 21.74, 19.30, 14.43

HRMS (ESI) m/z : $[M+H]^+$ calcd for $C_{35}H_{44}BrN_4O_5$ is 679.2495, found 679.2490

Synthesis of (1-(4-(5-iodo-2,3-dioxoindolin-1-yl)butyl)-1H-1,2,3-triazol-4-yl)methyl *(E)*-3-formyl-5-((1S,4aS,8aS)-5,5,8a-trimethyl-2-methylenedecahydronaphthalen-1-yl)pent-3-enoate (7x)

Compound **7x** was prepared by the reaction of compound **3** (37 mg) with 1-(4-azidobutyl)-5-iodoindoline-2,3-dione in ^{t}BuOH: H_2O mixture according to the procedure described in **4.8.5.** Yield: 32% (24 mg).

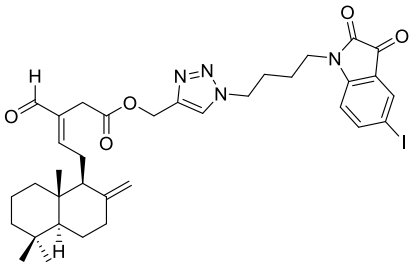

^{1}H NMR (500 MHz, $CDCl_3$) δ: 9.24 (s, 1H), 7.84-7.80 (m, 2H), 7.54 (s, 1H), 6.66 (d, *J* = 8Hz, 1H), 6.60 (t, *J* = 6 Hz, 1H), 5.16 (s, 2H), 4.77 (s, 1H), 4.36 (t, *J* = 6.5 Hz, 2H), 4.30 (s, 1H), 3.68 (t, *J* = 7 Hz, 2H), 3.24 (s, 2H), 2.49-0.97 (m, 18 H), 0.82 (s, 3H), 0.75 (s, 3H), 0.65 (s, 3H)

^{13}C NMR (125 MHz, $CDCl_3$) δ: 193.59, 181.91, 170.08, 159.21, 157.35, 149.84, 148.08, 146.57, 143.15, 135.99, 133.99, 123.76, 119.13, 112.33, 107.93, 86.14, 58.28, 56.39, 55.36, 49.29, 41.97, 39.56, 39.31, 39.24, 37.84, 33.58, 29.79, 27.29, 24.60, 24.09, 23.94, 21.74, 19.31, 14.43

HRMS (ESI) m/z : $[M+Na]^+$ cald for $C_{35}H_{43}IN_4O_5Na$ is 749.2176, found 749.2179

Synthesis of bis((1-(2-(2,3-dioxoindolin-1-yl)ethyl)-1H-1,2,3-triazol-4-yl)methyl) *(E)*-2-(2-((4aS,8aS)-5,5,8a-trimethyl-2-methylenedecahydronaphthalen-1-yl)ethylidene)succinate (10a)

Compound **10a** was prepared by the reaction of compound 3 (22 mg) with 1-(2-azidoethyl)indoline-2,3-dione in ^{t}BuOH: H_2O mixture according to the procedure described in **4.8.5.** Yield: 44% (20 mg).

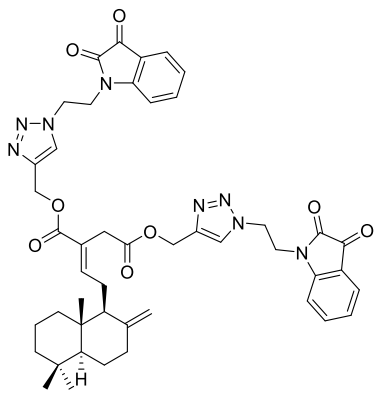

^{1}H NMR (500 MHz, $CDCl_3$) δ: 7.68-7.67 (m, 2H), 7.50-7.38 (m, 4H), 7.03-6.97 (m, 2H), 6.78 (t, *J* = 6.5Hz, 1H), 6.50 (d, *J* = 8Hz, 1H), 6.47 (d, *J* = 8Hz, 1H), 5.07-5.02 (m, 4H), 4.72 (s, 1H), 4.68 (q, *J* = 6Hz, 4H), 4.25 (s, 1H), 4.19 (s, 4H), 3.17 (s, 2H), 2.32-0.93 (m, 14 H), 0.81 (s, 3H), 0.74 (s, 3H), 0.62 (s, 3H)

^{13}C NMR (125 MHz, $CDCl_3$) δ: 182.64, 170.47, 166.41, 158.63, 150.15, 148.63, 148.15, 138.69, 125.57, 125.50, 125.29, 125.21, 124.12, 124.07, 117.45, 109.58, 107.80, 57.93, 57.78, 56.36, 55.32, 47.87, 41.98, 40.69, 39.50, 39.21, 37.84, 33.59, 33.56, 32.43, 24.19, 24.07, 21.74, 19.30, 14.41

HRMS (ESI) m/z : $[M+Na]^+$ cald for $C_{46}H_{50}N_8O_8$ Na is 865.3649, found 865.3649

Synthesis of bis((1-(2-(5-methyl-2,3-dioxoindolin-1-yl)ethyl)-1H-1,2,3-triazol-4-yl)methyl) *(E)*-2-(2-((4aS,8aS)-5,5,8a-trimethyl-2-methylenedecahydronaphthalen-1-yl)ethylidene)succinate (10b)

Compound **10b** was prepared by the reaction of compound **3** (34 mg) with 1-(2-azidoethyl)-5-methylindoline-2,3-dione in ^{t}BuOH: H_2O mixture according to the procedure described in **4.8.5.** Yield: 71% (51 mg).

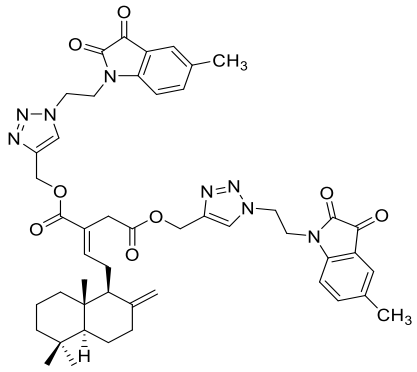

^{1}H NMR (500 MHz, $CDCl_3$) δ: 7.78 (s, 1H), 7.75 (s, 1H), 7.36 (d, *J* = 7.5 Hz, 2H), 7.31-7.28 (m, 2H), 6.87 (t, *J* = 6.5Hz, 1H), 6.49 (t, *J* = 6.5 Hz, 2H), 5.14-5.10 (m, 4H), 4.79 (s, 1H), 4.76-4.72 (m, 4H), 4.32 (s, 1H), 4.24-4.23 (m, 4H), 3.28 (s, 2H), 2.38-1.00 (m, 20 H), 0.88 (s, 3H), 0.81 (s, 3H), 0.70 (s, 3H)

^{13}C NMR (125 MHz, $CDCl_3$) δ: 182.90, 170.45, 166.42, 158.72, 148.60, 148.11, 147.99, 143.44, 143.23, 139.07, 133.98, 133.94, 125.86, 125.15, 124.14, 117.46, 117.44, 109.48, 107.80, 57.94, 57.85, 56.34, 55.30, 47.78, 41.97, 40.63, 39.48, 39.19, 37.83, 33.58, 33.54, 32.40, 24.18, 24.06, 21.73, 20.64, 19.29, 14.40

HRMS (ESI) m/z : $[M+Na]^+$ calcd for $C_{48}H_{54}N_8O_8$ Na is 893.3962, found 893.3973

Synthesis of bis((1-(3-(5-methoxy-2,3-dioxoindolin-1-yl)propyl)-1H-1,2,3-triazol-4-yl)methyl) *(E)*-2-(2-((4aS,8aS)-5,5,8a-trimethyl-2-methylenedecahydronaphthalen-1-yl)ethylidene)succinate (10c)

Compound **10c** was prepared by the reaction of compound **3** (30 mg) with 1-(2-azidoethyl)-5-methoxyindoline-2,3-dione in ^{t}BuOH: H_2O mixture according to the procedure described in **4.8.5.** Yield: 58% (38mg).

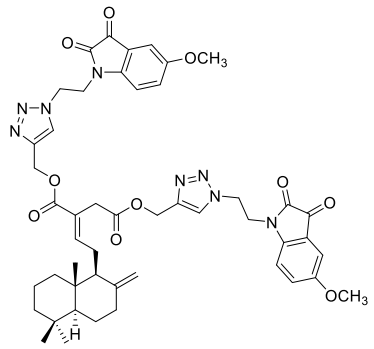

^{1}H NMR (500 MHz, $CDCl_3$) δ: 7.69-7.68 (m, 2H), 7.00-6.93 (m, 4H), 6.79 (t, *J* = 6.5Hz, 1H), 6.41 (t, *J* = 9 Hz, 2H), 5.09-5.03 (m, 4H), 4.71 (s, 1H), 4.68-4.64 (m, 4H), 4.25 (s, 1H), 4.15(s, 4H), 3.70 (s, 6H), 3.18 (s, 2H), 2.31-0.93 (m, 14 H), 0.80 (s, 3H), 0.73 (s, 3H), 0.62 (s, 3H)

^{13}C NMR (125 MHz, $CDCl_3$) δ: 183.00, 170.45, 166.41, 158.72, 156.61, 156.57, 148.63, 148.13, 144.00, 143.48, 143.30, 125.22, 125.19, 124.84, 124.12, 117.86, 110.67, 109.73, 107.79, 57.92, 57.80, 56.33, 55.95, 55.31, 47.89, 41.98, 40.71, 39.48, 39.18, 37.83, 33.58, 33.55, 32.39, 24.17, 24.07, 21.74, 19.30, 14.40

HRMS (ESI) m/z : $[M+Na]^+$ calcd for $C_{48}H_{54}N_8O_{10}$ Na is 925.3861, found 925.3875

Synthesis of bis((1-(2-(5-fluoro-2,3-dioxoindolin-1-yl)ethyl)-1H-1,2,3-triazol-4-yl)methyl) *(E)*-2-(2-((4aS,8aS)-5,5,8a-trimethyl-2-methylenedecahydronaphthalen-1-yl)ethylidene)succinate (10d)

Compound **10d** was prepared by the reaction of compound **3** (40 mg) with 1-(2-azidoethyl)-5-fluoroindoline-2,3-dione in ^{t}BuOH: H_2O mixture according to the procedure described in **4.8.5.** Yield: 68% (58 mg).

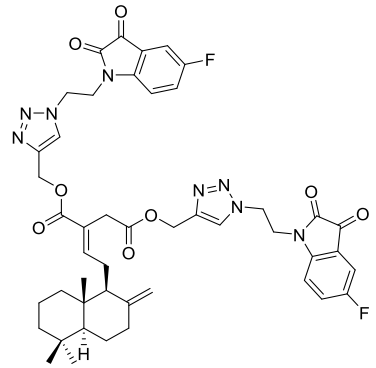

^{1}H NMR (500 MHz, $CDCl_3$) δ: 7.68-7.67 (m, 2H), 7.16-7.07 (m, 4H), 6.78 (t, J = 6.5Hz, 1H), 6.44-6.35 (m, 2H), 5.08-5.01 (m, 4H), 4.72 (s, 1H), 4.69-4.66 (m, 4H), 4.25 (s, 1H), 4.20-4.16 (m, 4H), 3.16 (dd, J_1 = 17Hz, J_2 = 20.5 Hz, 2H), 2.32-0.93 (m, 14 H), 0.81 (s, 3H), 0.74 (s, 3H), 0.63 (s, 3H)

^{13}C NMR (125 MHz, $CDCl_3$) δ: 182.22, 170.45, 166.39, 158.47, 148.68, 148.15, 146.28, 143.57, 143.45, 130.90, 128.79, 125.55, 125.36, 125.10, 124.90, 124.09, 117.99, 112.23, 110.93, 107.78, 57.87, 57.66, 56.33, 55.30, 48.02, 47.91, 41.97, 40.94, 40.88, 39.49, 39.16, 37.82, 33.58, 33.54,

28.91, 24.16, 24.07, 21.73, 19.29, 14.39
HRMS (ESI) m/z : $[M+Na]^+$ calcd for $C_{46}H_{48}F_2N_8O_8$ Na is 901.3461, found 901.3455

Synthesis of bis((1-(2-(5-chloro-2,3-dioxoindolin-1-yl)ethyl)-1H-1,2,3-triazol-4-yl)methyl) *(E)*-2-(2-((4aS,8aS)-5,5,8a-trimethyl-2-methylenedecahydronaphthalen-1-yl)ethylidene)succinate (10e)

Compound **10e** was prepared by the reaction of compound **3** (36 mg) with 1-(2-azidoethyl)-5-chlorolindoline-2,3-dione in ^{t}BuOH: H_2O mixture according to the procedure described in **4.8.5.** Yield: 74% (59 mg).

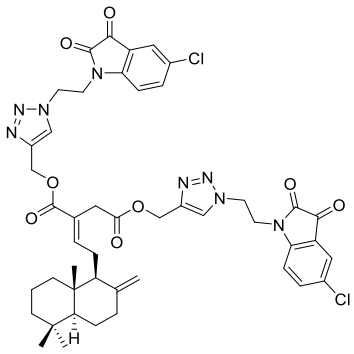

^{1}H NMR (500 MHz, $CDCl_3$) δ: 7.72 (s, 1H), 7.69 (s, 1H), 7.43 (s, 1H), 7.40-7.34 (m, 3H), 6.78 (t, J = 6.5 Hz, 1H), 6.43-6.38 (m, 2H), 5.07-5.02 (m, 4H), 4.71 (s, 1H), 4.70-4.66 (m, 4H), 4.24 (s, 1H), 4.20-4.18 (m, 4H), 3.17 (s, 2H), 2.31-0.94 (m, 14 H), 0.81 (s, 3H), 0.73 (s, 3H), 0.62 (s, 3H)

^{13}C NMR (125 MHz, $CDCl_3$) δ: 181.80, 170.52, 166.42, 158.18, 158.15, 148.69, 148.49, 148.14, 143.63, 143.44, 138.04, 138.01, 129.86, 129.79, 125.45, 125.41, 125.33, 125.27, 124.08, 118.21, 111.02, 110.99, 107.81, 57.86, 57.72, 56.34, 55.30, 47.93, 47.89, 41.97, 40.95, 40.91, 39.50, 39.20, 37.83, 33.55, 32.37, 29.69, 24.20, 24.07, 21.74, 19.30, 14.41

HRMS (ESI) m/z: $[M+Na]^+$ cald for $C_{46}H_{48}Cl_2N_8O_8$ Na is 933.2870, found 933.2894

Synthesis of bis((1-(2-(5-bromo-2,3-dioxoindolin-1-yl)ethyl)-1H-1,2,3-triazol-4-yl)methyl) *(E)*-2-(2-((4aS,8aS)-5,5,8a-trimethyl-2-methylenedecahydronaphthalen-1-yl)ethylidene)succinate (10f)

Compound **10f** was prepared by the reaction of compound **3** (25 mg) with 1-(2-azidoethyl)-5-bromoindoline-2,3-dione in ^{t}BuOH: H_2O mixture according to the procedure described in **4.8.5.** Yield: 46% (28 mg).

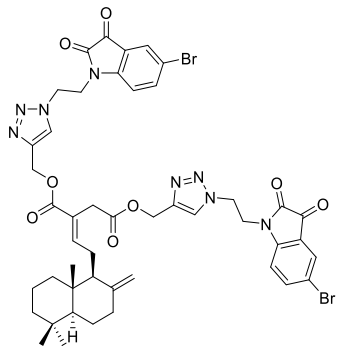

^{1}H NMR (500 MHz, $CDCl_3$) δ: 7.70 (s, 1H), 7.67 (s, 1H), 7.58-7.49 (m, 4H), 6.79 (t, *J* = 6.5Hz, 1H), 6.38-6.34 (m, 2H), 5.06-5.02 (m, 4H), 4.72 (s, 1H), 4.69-4.65 (m, 4H), 4.25 (s, 1H), 4.19-4.18 (m, 4H), 3.18 (s, 2H), 2.31-0.93 (m, 14 H), 0.81 (s, 3H), 0.74 (s, 3H), 0.63 (s, 3H)

^{13}C NMR (125 MHz, $CDCl_3$) δ: 181.59, 170.53, 166.43, 157.97, 148.92, 148.71, 148.15, 143.69, 143.48, 140.88, 128.22, 128.17, 125.41, 124.07, 118.60, 116.90, 111.38, 107.83, 57.87, 57.75, 56.36, 55.32, 47.89, 41.99, 40.91, 39.51, 39.23, 37.84, 33.59, 33.56, 32.40, 24.22, 24.07, 22.35, 21.74, 19.30, 14.42

HRMS (ESI) m/z : $[M+H]^+$ calcd for $C_{46}H_{49}Br_2N_8O_8$ is 999.2040, found 999.2053

Synthesis of bis((1-(2-(5-iodo-2,3-dioxoindolin-1-yl)ethyl)-1H-1,2,3-triazol-4-yl)methyl) *(E)*-2-(2-((4aS,8aS)-5,5,8a-trimethyl-2-methylenedecahydronaphthalen-1-yl)ethylidene)succinate (10g)

Compound **10g** was prepared by the reaction of compound 3 (32mg) with 1-(2-azidoethyl)-5-iodoindoline-2,3-dione in ^{t}BuOH: H_2O mixture according to the procedure described in **4.8.5.** Yield: 65% (55 mg).

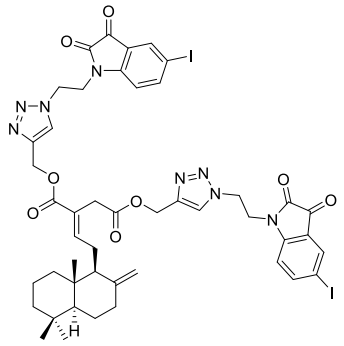

^{1}H NMR (500 MHz, $CDCl_3$) δ: 7.74-7.67 (m, 6H), 6.80 (t, *J* = 6.5Hz, 1H), 6.28 (t, *J* = 8Hz, 2H), 5.08-5.01 (m, 4H), 4.72 (s, 1H), 4.68-4.64 (m, 4H), 4.26 (s, 1H), 4.18-4.15 (m, 4H), 3.19 (s, 2H), 2.31-0.94 (m, 14 H), 0.81 (s, 3H), 0.74 (s, 3H), 0.63 (s, 3H)

^{13}C NMR (125 MHz, $CDCl_3$) δ: 181.39, 181.36, 170.48, 166.41, 157.68, 157.66, 149.55, 148.63, 148.15, 146.66, 143.67, 143.45, 133.87, 133.84, 125.32, 125.28, 124.13, 118.99, 118.97, 111.81, 107.85, 86.40, 57.88, 57.79, 56.38, 55.34, 47.82, 42.01, 40.84, 39.54, 39.26, 37.86, 33.58, 33.55, 32.48, 24.25, 24.09, 21.74, 19.31, 14.43

HRMS (ESI) m/z : $[M+Na]^+$ cald for $C_{46}H_{48}I_2N_8O_8$ Na is 1117.1582, found 1117.1526

Synthesis of bis((1-(3-(5-methoxy-2,3-dioxoindolin-1-yl)propyl)-1H-1,2,3-triazol-4-yl)methyl) *(E)*-2-(2-((4aS,8aS)-5,5,8a-trimethyl-2-methylenedecahydronaphthalen-1-yl)ethylidene)succinate (10h)

Compound **10h** was prepared by the reaction of compound 3 (44 mg) with 1-(3-azidopropyl)-5-methoxyindoline-2,3-dione in ^{t}BuOH: H_2O mixture according to the procedure described in **4.8.5.** Yield: 57% (57 mg).

^{1}H NMR (500 MHz, $CDCl_3$) δ: 7.72 (s, 1H), 7.69(s, 1H), 7.09-7.05 (m, 4H), 6.84 (t, *J* = 6.5Hz, 1H), 6.79-6.76 (m, 2H), 5.17-5.11 (m, 4H), 4.70 (s, 1H), 4.42-4.38 (m, 4H), 4.25 (s, 1H), 3.73(s, 6H), 3.71-3.70 (m, 4H), 3.31 (s,

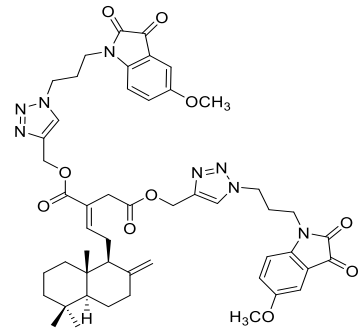

2H), 2.33-0.93 (m, 18 H), 0.80 (s, 3H), 0.73 (s, 3H), 0.61 (s, 3H)

^{13}C NMR (125 MHz, $CDCl_3$) δ: 183.41, 183.37, 170.59, 166.57, 158.65, 156.68, 148.59, 148.11, 144.11, 144.07, 143.08, 142.80, 124.79, 124.75, 124.66, 124.64, 124.26, 118.09, 111.22, 109.89, 107.81, 58.09, 57.97, 56.34, 56.01, 55.30, 47.67, 41.98, 39.48, 39.19, 37.83, 37.45, 33.57, 33.54, 32.56, 27.83, 24.21, 24.06, 21.73, 19.29, 14.12

HRMS (ESI) m/z : $[M+Na]^+$ cald for $C_{50}H_{58}N_8O_{10}Na$ is 953.4174, found 953.4196

Synthesis of bis((1-(3-(5-chloro-2,3-dioxoindolin-1-yl)propyl)-1H-1,2,3-triazol-4-yl)methyl) *(E)*-2-(2-((4aS,8aS)-5,5,8a-trimethyl-2-methylenedecahydronaphthalen-1-yl)ethylidene)succinate (10i)

Compound **10i** was prepared by the reaction of compound **3** (31 mg) with 1-(3-azidopropyl)-5-chloroindoline-2,3-dione in ^{t}BuOH: H_2O mixture according to the procedure described in **4.8.5.** Yield: 49% (35 mg).

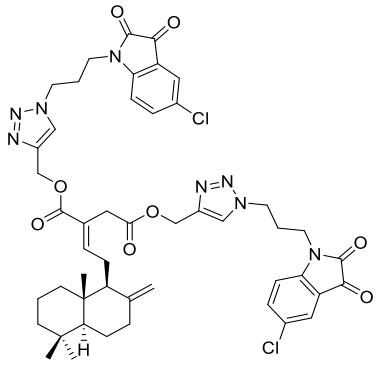

^{1}H NMR (500 MHz, $CDCl_3$) δ: 7.68 (s, 1H), 7.65 (s, 1H), 7.51-7.48 (m, 2H), 7.47 (s, 2H), 6.86-6.83 (m, 3H), 5.12-5.08 (m, 4H), 4.70 (s, 1H), 4.42-4.38 (m, 4H), 4.25 (s, 1H), 3.76-3.73 (m, 4H), 3.30 (s, 2H), 2.34-0.92 (m, 18 H), 0.80 (s, 3H), 0.73 (s, 3H), 0.62 (s, 3H)

^{13}C NMR (125 MHz, $CDCl_3$) δ: 181.08, 181.05, 169.59, 165.55, 157.04, 147.62, 147.57, 147.54, 147.12, 142.12, 141.85, 136.98, 136.96, 128.87, 128.85, 124.39, 123.61, 123.22, 117.44, 110.60, 106.77,

57.03, 56.89, 55.33, 54.29, 46.61, 46.58, 40.95, 38.46, 38.18, 36.81, 36.63, 32.55, 32.52, 31.54, 28.67, 23.19, 23.04, 20.71, 18.27, 13.38

HRMS (ESI) m/z: $[M+Na]^+$ cald for $C_{48}H_{52}Cl_2N_8O_8$ Na is 961.3183, found 961.3191

4.9. References

(1) Ghosh, S.; Hayden, M. S. New Regulators of NF-KB in Inflammation. *Nat. Rev. Immunol.* **2008**, *8* (11), 837–848. https://doi.org/10.1038/nri2423.

(2) Aggarwal, B. B. Nuclear Factor-KB: The Enemy Within. *Cancer Cell*. 2004, pp 203–208. https://doi.org/10.1016/j.ccr.2004.09.003.

(3) Grigalunas, M.; Brakmann, S.; Waldmann, H. Chemical Evolution of Natural Product Structure. *J. Am. Chem. Soc.* **2022**, *144* (8), 3314–3329. https://doi.org/10.1021/jacs.1c11270.

(4) Newman, D. J.; Cragg, G. M. Natural Products as Sources of New Drugs over the Nearly Four Decades from 01/1981 to 09/2019. *J. Nat. Prod.* **2020**, *83* (3), 770–803. https://doi.org/10.1021/acs.jnatprod.9b01285.

(5) Kumar, K.; Waldmann, H. Nature Inspired Small Molecules for Chemical Biology. *Isr. J. Chem.* **2019**, *59* (1), 41–51. https://doi.org/10.1002/ijch.201800105.

(6) Nath, R.; Pathania, S.; Grover, G. Highlights : *J. Mol. Struct.* **2020**, 128900. https://doi.org/10.1016/j.molstruc.2020.128900.

(7) Cheke, R. S.; Patil, V. M.; Firke, S. D.; Ambhore, J. P.; Ansari, I. A.; Patel, H. M.; Shinde, S. D.; Pasupuleti, V. R.; Hassan, M. I.; Adnan, M.; Kadri, A.; Snoussi, M. Therapeutic Outcomes of Isatin and Its Derivatives against Multiple Diseases: Recent Developments in Drug Discovery. *Pharmaceuticals* **2022**, *15* (3). https://doi.org/10.3390/ph15030272.

(8) Varun; Sonam; Kakkar, R. Isatin and Its Derivatives: A Survey of Recent Syntheses, Reactions, and Applications. *Medchemcomm* **2019**, *10* (3), 351–368. https://doi.org/10.1039/c8md00585k.

(9) Thirumurugan, P.; Matosiuk, D.; Jozwiak, K. Click Chemistry for Drug Development and Diverse Chemical-Biology Applications. *Chemical Reviews*. 2013, pp 4905–4979. https://doi.org/10.1021/cr200409f.

(10) Ferroni, C.; Pepe, A.; Kim, Y. S.; Lee, S.; Guerrini, A.; Parenti, M. D.; Tesei, A.; Zamagni, A.; Cortesi, M.; Zaffaroni, N.; De Cesare, M.; Beretta, G. L.; Trepel, J. B.; Malhotra, S. V.; Varchi, G. 1,4-Substituted Triazoles as Nonsteroidal Anti-Androgens for Prostate Cancer Treatment. *J. Med. Chem.* **2017**, *60* (7), 3082–3093. https://doi.org/10.1021/acs.jmedchem.7b00105.

(11) Angeli, A.; Supuran, C. T. Click Chemistry Approaches for Developing Carbonic Anhydrase Inhibitors and Their Applications. *J. Enzyme Inhib. Med. Chem.* **2023**, *38* (1). https://doi.org/10.1080/14756366.2023.2166503.

(12) -H. Zhou, C.; Wang, Y. Recent Researches in Triazole Compounds as Medicinal Drugs. *Curr. Med. Chem.* **2012**, *19* (2), 239–280. https://doi.org/10.2174/092986712803414213.

(13) da S. M. Forezi, L.; Lima, C. G. S.; Amaral, A. A. P.; Ferreira, P. G.; de Souza, M. C. B. V.; Cunha, A. C.; de C. da Silva, F.; Ferreira, V. F. Bioactive 1,2,3-Triazoles: An Account on Their Synthesis, Structural Diversity and Biological Applications. *Chem. Rec.* **2021**, *21* (10), 2782–2807. https://doi.org/10.1002/tcr.202000185.

(14) Jalaja, R.; Leela, S. G.; Valmiki, P. K.; Salfeena, C. T. F.; Ashitha, K. T.; Krishna Rao, V. R. D.; Nair, M. S.; Gopalan, R. K.; Somappa, S. B. Discovery of Natural Product Derived Labdane Appended Triazoles as Potent Pancreatic Lipase Inhibitors. *ACS Med. Chem. Lett.* **2018**, *9* (7), 662–666. https://doi.org/10.1021/acsmedchemlett.8b00109.

(15) Jalaja, R.; Leela, S. G.; Mohan, S.; Nair, M. S.; Gopalan, R. K.; Somappa, S. B. Anti-Hyperlipidemic Potential of Natural Product Based Labdane-Pyrroles via Inhibition of Cholesterol and Triglycerides Synthesis. *Bioorg. Chem.* **2021**, *108*, 104664. https://doi.org/https://doi.org/10.1016/j.bioorg.2021.104664.

(16) Kumar, A.; Rohila, Y.; Kumar, V.; Lal, K. A Mini Review on Pharmacological Significance of Isatin-1,2,3-Triazole Hybrids. *Curr. Top. Med. Chem.* **2023**, *23* (10), 833–847. https://doi.org/10.2174/1568026623666230202160925.

(17) Ferraz de Paiva, R. E.; Vieira, E. G.; Rodrigues da Silva, D.; Wegermann, C. A.; Costa Ferreira, A. M. Anticancer Compounds Based on Isatin-Derivatives: Strategies to Ameliorate Selectivity and Efficiency. *Front. Mol. Biosci.* **2021**, *7* (February), 1–24. https://doi.org/10.3389/fmolb.2020.627272.

(18) Gao, F.; Yang, H.; Lu, T.; Chen, Z.; Ma, L.; Xu, Z.; Schaffer, P.; Lu, G. Design, Synthesis and Anti-Mycobacterial Activity Evaluation of Benzofuran-Isatin Hybrids. *Eur. J. Med. Chem.* **2018**, *159*, 277–281. https://doi.org/10.1016/j.ejmech.2018.09.049.

(19) Boshra, A. N.; Abdu-Allah, H. H. M.; Mohammed, A. F.; Hayallah, A. M. *Click Chemistry Synthesis, Biological Evaluation and Docking Study of Some Novel 2'-Hydroxychalcone-Triazole Hybrids as Potent Anti-Inflammatory Agents*; Elsevier Inc.,

2020; Vol. 95. https://doi.org/10.1016/j.bioorg.2019.103505.

(20) Sharma, P. K.; Balwani, S.; Mathur, D.; Malhotra, S.; Singh, B. K.; Prasad, A. K.; Len, C.; Van der Eycken, E. V.; Ghosh, B.; Richards, N. G. J.; Parmar, V. S. Synthesis and Anti-Inflammatory Activity Evaluation of Novel Triazolyl-Isatin Hybrids. *J. Enzyme Inhib. Med. Chem.* **2016**, *31* (6), 1520–1526. https://doi.org/10.3109/14756366.2016.1151015.

(21) Kim, T. W.; Yong, Y.; Shin, S. Y.; Jung, H.; Park, K. H.; Lee, Y. H.; Lim, Y.; Jung, K. Y. Synthesis and Biological Evaluation of Phenyl-1H-1,2,3-Triazole Derivatives as Anti-Inflammatory Agents. *Bioorg. Chem.* **2015**, *59*, 1–11. https://doi.org/10.1016/j.bioorg.2015.01.003.

(22) Assali, M.; Abualhasan, M.; Sawaftah, H.; Hawash, M.; Mousa, A. Synthesis, Biological Activity, and Molecular Modeling Studies of Pyrazole and Triazole Derivatives as Selective COX-2 Inhibitors. *J. Chem.* **2020**, *2020*. https://doi.org/10.1155/2020/6393428.

(23) Sujith, K. V.; Rao, J. N.; Shetty, P.; Kalluraya, B. Regioselective Reaction: Synthesis and Pharmacological Study of Mannich Bases Containing Ibuprofen Moiety. *Eur. J. Med. Chem.* **2009**, *44* (9), 3697–3702. https://doi.org/10.1016/j.ejmech.2009.03.044.

(24) Jiang, B.; Zeng, Y.; Li, M. J.; Xu, J. Y.; Zhang, Y. N.; Wang, Q. J.; Sun, N. Y.; Lu, T.; Wu, X. M. Design, Synthesis, and Biological Evaluation of 1,5-Diaryl-1,2,4-Triazole Derivatives as Selective Cyclooxygenase-2 Inhibitors. *Arch. Pharm. (Weinheim).* **2010**, *343* (9), 500–508. https://doi.org/10.1002/ardp.200900227.

(25) Lamie, P. F.; Ali, W. A. M.; Bazgier, V.; Rárová, L. Novel N-Substituted Indole Schiff Bases as Dual Inhibitors of Cyclooxygenase-2 and 5-Lipoxygenase Enzymes: Synthesis, Biological Activities in Vitro and Docking Study. *Eur. J. Med. Chem.* **2016**, *123*, 803–813. https://doi.org/10.1016/j.ejmech.2016.08.013.

(26) Claudio Viegas-Junior; Eliezer J. Barreiro; Carlos Alberto Manssour Fraga. Molecular Hybridization: A Useful Tool in the Design of New Drug Prototypes. *Curr. Med. Chem.* **2007**, *14* (17), 1829–1852. https://doi.org/10.2174/092986707781058805.

(27) De Oliveira Pedrosa, M.; Marques Duarte Da Cruz, R.; De Oliveira Viana, J.; Olímpio De Moura, R.; Ishiki, H. M.; Filho, M. B.; Diniz, M. F. F. M.; Tullius Scotti, M.; Scotti, L.; Bezerra, F. J.; Junior, M. Current Topics in Medicinal Chemistry The International

Journal for In-Depth Reviews on Current Topics in Medicinal Chemistry Send Orders for Reprints to Reprints@benthamscience.Ae Hybrid Compounds as Direct Multitarget Ligands: A Review. *Curr. Top. Med. Chem.* **2017**, *17*, 1044–1079. https://doi.org/10.2174/1568026616666160927.

(28) Bird, R. E.; Lemmel, S. A.; Yu, X.; Zhou, Q. A. Bioorthogonal Chemistry and Its Applications. *Bioconjug. Chem.* **2021**, *32* (12), 2457–2479. https://doi.org/10.1021/acs.bioconjchem.1c00461.

(29) Zhang, X.; Zhang, S.; Zhao, S.; Wang, X.; Liu, B.; Xu, H. Click Chemistry in Natural Product Modification. *Front. Chem.* **2021**, *9* (November), 1–29. https://doi.org/10.3389/fchem.2021.774977.

(30) Bogdan, C. Nitric Oxide and the Immune Response - Nature Immunology. *Nat. Immunol.* **2001**, *2* (10), 907–916.

(31) Bryan, N. S.; Grisham, M. B. Methods to Detect Nitric Oxide and Its Metabolites in Biological Samples. *Free Radic. Biol. Med.* **2007**, *43* (5), 645–657. https://doi.org/https://doi.org/10.1016/j.freeradbiomed.2007.04.026.

(32) Mosser, D. M.; Edwards, J. P. Exploring the Full Spectrum of Macrophage Activation. *Nat. Rev. Immunol.* **2008**, *8* (12), 958–969. https://doi.org/10.1038/nri2448.

(33) Howes, A.; Gabryšová, L.; O'Garra, A. Role of IL-10 and the IL-10 Receptor in Immune Responses. *Ref. Modul. Biomed. Sci.* **2014**, *1*, 1–11. https://doi.org/10.1016/b978-0-12-801238-3.00014-3.

(34) Saraiva, M.; O'Garra, A. The Regulation of IL-10 Production by Immune Cells. *Nat. Rev. Immunol.* **2010**, *10* (3), 170–181. https://doi.org/10.1038/nri2711.

(35) Cinelli, M. A.; Do, H. T.; Miley, G. P.; Silverman, R. B. Inducible Nitric Oxide Synthase: Regulation, Structure, and Inhibition. *Med. Res. Rev.* **2020**, *40* (1), 158–189. https://doi.org/10.1002/med.21599.

(36) Simmons, D. L.; Botting, R. M.; Hla, T. Cyclooxygenase Isozymes: The Biology of Prostaglandin Synthesis and Inhibition. *Pharmacol. Rev.* **2004**, *56* (3), 387–437. https://doi.org/10.1124/pr.56.3.3.

(37) Karin, M.; Ben-neriah, Y. Phosporilation Meets the Ubiquitination: The Control of NF-Kapp B Activity. *Annu. Rev. Immunol.* **2000**, *18*, 621–663.

Chapter 5

Lead Optimization of Labdane Conjugates into Novel Therapeutics for Inflammation Modulation

5.1. Abstract

As part of the lead optimization process, we have modified the existing lead compound **7a** by incorporating various heterocyclic amides derived from pharmacologically active cyclic amines into the labdane framework. This strategy was aimed to enhance the biological properties of the abundant bioactive compound. Among the synthesized derivatives, **9b** demonstrated notable improvements, with an IC_{50} for NO inhibition of 1.46 μM, nearly twice as potent as both indomethacin and the existing lead compound **7a** (IC_{50} 3.13 μM). Compound **9b** effectively decreased the levels of the pro-inflammatory cytokines TNF-α and IL-6, while significantly increasing the levels of the anti-inflammatory cytokine IL-10. Mechanistic studies revealed that **9b** downregulated the expression of COX-2 and iNOS through inhibition of the NF-κB signaling pathway. Furthermore, molecular modeling studies of NF-κB proteins supported these findings, indicating strong interactions that corroborate the compound's potent anti-inflammatory activity. These results highlight **9b** as a promising candidate for further development as a powerful anti-inflammatory agent.

5.2. Introduction

Design and synthesis of novel drug candidates based on the chemical structures of natural products is a promising strategy that holds great promise for drug discovery and development. The modification of lead natural products through semi-synthetic approaches represents a highly successful approach for optimizing their pharmacological properties and exploring their intricate modes of action.[1]

Building on our prior research, strategic modifications to the labdane dialdehyde, isolated from the medicinally and nutritionally valuable rhizomes of *Curcuma amada*, have proven effective in enhancing its biological activity.[2,3] Labdane dialdehyde, known for its moderate anti-inflammatory properties, has spurred our interest in exploring further structural modifications to enhance its efficacy and druggability. To this end, we designed and synthesized novel phytochemical entities (NPCEs) by incorporating aromatic and hetero-aromatic fragments into the labdane dialdehyde scaffold using a linker-based molecular hybridization strategy.[4] Additionally, we reported a series of semisynthetic labdane-appended mono- and di-isatin triazoles employing the same approach.[5] These NPCEs exhibited a superior anti-inflammatory effect compared to the standard drug indomethacin, effectively suppressing pro-inflammatory markers such as cytokines (TNF-α, IL-6) and enzymes (COX-2, iNOS). These findings underscore the potential of semi-synthetic modifications to further enhance the therapeutic profile of labdane-derived compounds. Among the derivatives, we have identified the lead compound **7a** (1-(2-(2,3-dioxoindolin-1-yl)ethyl)-1H-1,2,3-triazol-4-yl)methyl (*E*)-3-formyl-5-((4aS,8aS)-5,5,8a-trimethyl-2-methylenedecahydronaphthalen-1-yl)pent-3-enoate, with an attractive skeleton from our in house database of labdane dialdehyde.

Scaffold hopping can be adopted as a rational approach to optimise the structure and properties of a lead natural compound to discover new bioactive molecules.[6] In our current study, as part of the lead optimization process, we have modified the existing lead compound **7a** by incorporating different heterocyclic amides into the labdane template. Saturated cyclic amines are widely recognized as significant bioactive motifs present in numerous natural products and medicinal compounds **(Figure 5.4)**. Numerous pharmacologically active cyclic amines, morpholine, thiomorpholine, piperidine, pyrazole and piperazines, both natural and synthetic, are extensively used in clinical practice. In particular, piperazines containing dual nitrogen atoms enhance the pharmacokinetic characteristics of drug candidates by their suitable pKa values. Consequently, they serve as valuable templates and molecular building blocks in the rational design of pharmaceuticals.

There have been extensive reports on the natural product-piperazine hybrid compounds with varied biological activities.[7,8]

The amide functional group is of extreme interest to both medicinal chemists and chemical biologists. The amide functionality plays a crucial role in the composition of many synthetic and naturally derived drug molecules. The salient features of amides include their unique ability to form hydrogen bonding interactions and resonating structures, which result in high stability.[9] Additionally, many currently used anti-inflammatory drugs, such as piroxicam and indomethacin, contain amide groups in their structures. Therefore, we have designed and synthesized a new series of labdane conjugates linked to heterocyclic amides of various pharmacologically active cyclic amines, intending to enhance the anti-inflammatory properties of the existing lead molecule.

Bioisosteric replacement, a technique that involves replacing a selected fragment within a compound with another fragment that closely mimics its properties, is frequently employed in hit-to-lead and lead optimization processes. Bioisosteric replacement can yield several benefits, such as increased potency, enhanced selectivity, reduced toxicity, improved pharmacokinetic and pharmacodynamic properties, and the facilitation of access to novel chemical space for patent protection.[10] Thus, we adopted this strategy to derivatize the labdane dialdehyde with various anti-inflammatory relevant heterocyclic amides to design and synthesise the target compounds **7a-i**. As observed from our previous studies labdane-triazole hybrids are promising anti-inflammatory agents, prompting the design and synthesis of compounds **8a-j** with a triazole linker in addition. Some of these compounds were converted into the corresponding acid derivatives **9a-d** to have a comparative study.

5.3. Review of literature

To enhance the anti-inflammatory and antimicrobial properties of chrysin and wogonin, natural flavonoids, Kamble and colleagues proposed that hybrid compounds combining a flavonoid core with an amine linkage within a single molecular framework could yield novel, potent agents. Remarkably, the introduction of highly electron-rich groups such as methoxy, pyrimidyl, and morpholine on the piperazine ring, along with the homologation of the chromone and piperazine moieties, showed significant relevance to anti-inflammatory activity (**Figure 5.1)**.[11]

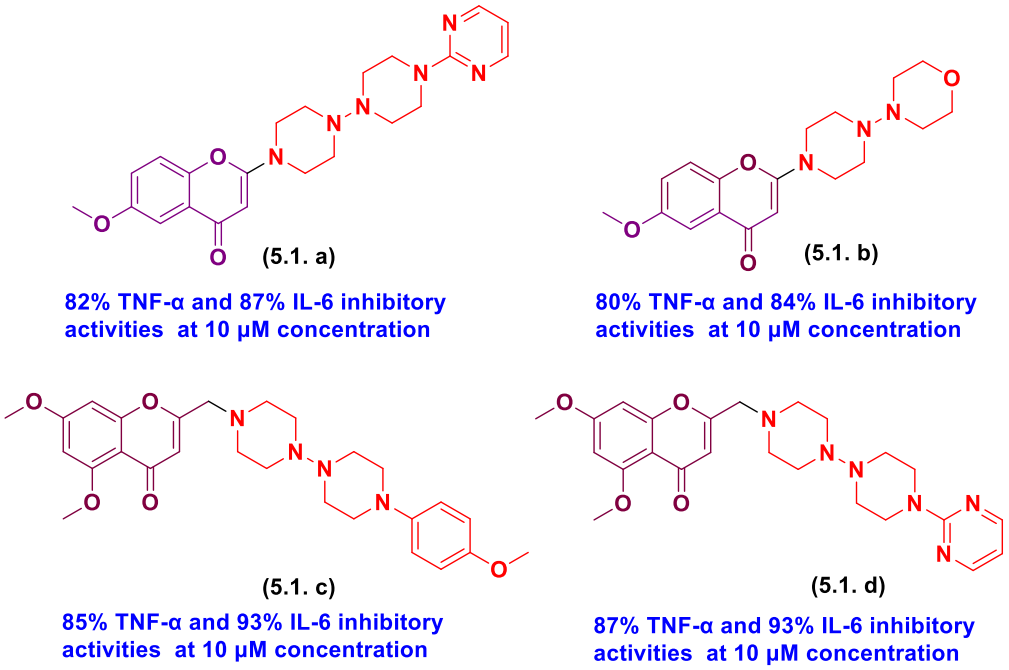

Figure 5.1. Representative cyclic amine appended anti-inflammatory agents

Chalcone, a member of the flavonoid family, is abundant in plants such as vegetables, fruits, tea, and spices. N-aryl piperazine moieties are a prominent class of organic compounds widely utilized in medicinal chemistry. In 2017, Wu et al. synthesized novel chalcone-N-aryl piperazine hybrids, building on the natural anti-inflammatory properties of chalcone derivatives. These hybrid molecules were evaluated for their anti-inflammatory potential using the para-xylene-induced ear-swelling model in mice. Both *in vivo* and *in vitro* anti-inflammatory activities were assessed through this model and ELISA assays. The *in vivo* results showed that most of the synthesized compounds exhibited significant anti-inflammatory effects. Preliminary structure-activity relationship (SAR) analysis and molecular docking studies indicated that incorporating electron-withdrawing groups into aryl-piperazine or aryl sulfonyl-piperazine moieties enhanced anti-inflammatory activity compared to electron-donating groups (**Figure 5.2)**.[12]

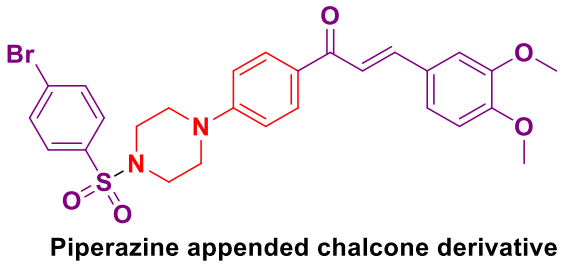

Figure 5.2. The chemical structure of piperazine appended chalcone derivative

Licorice, derived from the roots and rhizomes of *Glycyrrhiza* species, has been widely used in traditional Chinese medicine for its antibacterial, antiviral, anti-inflammatory, and other therapeutic properties. 18β-glycyrrhetic acid (18β-GA, glycyrrhetin), the primary active component, exhibits a range of pharmacological activities, including anti-inflammatory, antioxidant, antibacterial, antiviral, and hepatoprotective effects. In a structural modification study by Li et al., piperazine-conjugated 18β-glycyrrhetic acid demonstrated the most potent inhibitory activity against nitric oxide (NO) and IL-6. Additionally, these compounds significantly suppressed lipopolysaccharide (LPS)-induced expression of inducible nitric oxide synthase (iNOS) and cyclooxygenase (COX)-2, as well as IL-6 production, by modulating the MAPK and NF-κB signaling pathways (**Figure 5.3)**.[13]

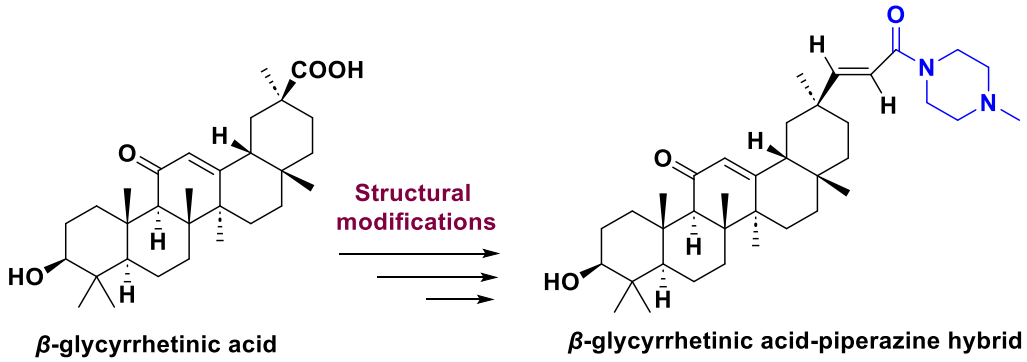

Figure 5.3. Structure of piperazine appended 18β-glycyrrhetic acid derivative

In light of the aforementioned findings and our increasing interest in the exploration of natural product-derived novel chemical entities, we have undertaken the design and synthesis of innovative heterocyclic amide-conjugated labdanes, with broad spectrum of anti-inflammatory activities.

5.4. Aim and scope of the present study

In our previous studies, the marker compound, (*E*)-labda-8(17), 12-diene-15, 16-dial, isolated from the rhizomes of *C. amada* was synthetically transformed into various heterocyclic appended labdane molecules *via* molecular hybridisation strategy. These isolates and synthetic derivatives were screened against multifaceted inflammatory targets. From this work, we identified a lead compound, **7a**, 1-[(2-(2,3-dioxoindolin-1-yl)ethyl)-1H-1,2,3-triazol-4-yl]methyl (E)-3-formyl-5-[(4aS,8aS)-5,5,8a-trimethyl-2-methylenedecahydronaphthalen-1-yl]pent-3-enoate, with an attractive skeleton from our in-house database of labdane dialdehydes. As part of the lead optimization process, our objective was to modify **7a** by incorporating heterocyclic amides derived from various

pharmacologically active cyclic amines into the labdane template to enhance its anti-inflammatory efficacy and druggability. Accordingly, we synthesized a library of 23 novel heterocyclic amide-appended labdane conjugates through strategic structural modifications. The synthesized compounds were evaluated against multifaceted inflammatory targets, including nitric oxide (NO), cytokines, and pro-inflammatory enzymes involved in the NF-κB signaling pathway.

5.5. Design strategy for synthesis of heterocyclic appended labdane conjugates

In our current study, as part of the lead optimization process, we have modified the existing lead compound, a triazole linked labdane conjugate (**7a**), by incorporating different heterocyclic amides to the labdane template. We have synthesised a series of compounds **8a-j** by maintaining the fragments 1 and 2 from the previous lead (**7a**), and introducing variations in fragment 3 with diverse heterocyclic amides. Compounds **7a-i** represent simplified versions of **8**, wherein the intermediate triazole linker (fragment 2) has been eliminated, resulting in the direct conjugation of the labdane core to various heterocyclic amides. Furthermore, we have successfully synthesized a limited number of acid derivatives (**9a-d**) of compound **8**, in which the aldehyde group has been selectively oxidized to acid (**Figure 5.4.)**.

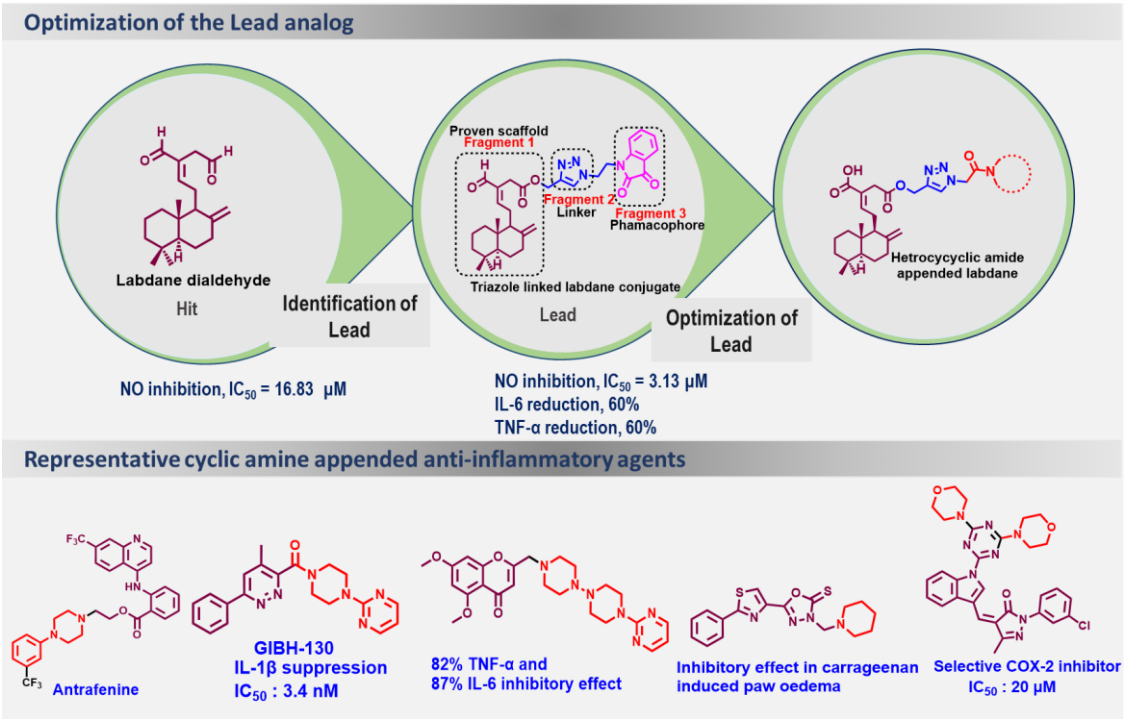

Figure 5.4. Rationale for the design and synthesis of heterocyclic amide appended labdane conjugates

5.6. Results and discussion

In our present work, we have modified the labdane dialdehyde by bringing in a heterocyclic amide to enhance the pharmacological outcome. **Scheme 5.1**, describes the synthesis of heterocyclic amide appended labdane derivatives. One of the aldehyde groups of the labdane dialdehyde (**1**) was selectively oxidised using oxone to give zerumin A (**2**) which was further converted into its alkyne intermediate (**3**) by treating it with propargyl bromide. Chloroacetyl morpholine, chloroacetyl thiomorpholine, chloroacetyl piperidine, chloroacetyl pyrazole and chloroacetyl *N*-substituted piperazines (**5a-i**) were synthesized by the reaction of chloroacetyl chloride with morpholine, thiomorpholine, piperidine, pyrazole and *N*-substituted piperazines (**4**) in the presence of DCM using triethylamine as a base. Compounds **6a-j** were obtained by reacting the corresponding chloroacetyl amides with NaN_3. Zerumin A (**2**) was then reacted with chloroacetyl amides (**5a-i**) in the presence of K_2CO_3 in DMF as solvent at room temperature, *via* a simple nucleophilic substitution, to give heterocyclic amide appended labdane derivatives (**7a-i**) in excellent yields (90–93%). Compounds **8a-j** were obtained by the reaction of compound **3** with azides (**6**) through click chemistry. Compounds **9a-d** were obtained by converting the aldehyde group of **8** into carboxylic acid by pinnick oxidation reaction. The application of spectroscopic methods confirmed the products. **Table 5.1** presents the compounds synthesized using the aforementioned scheme.

Scheme 5.1. Synthesis of heterocyclic amide appended labdane derivatives (**7a-i, 8a-j, and 9a-d**)

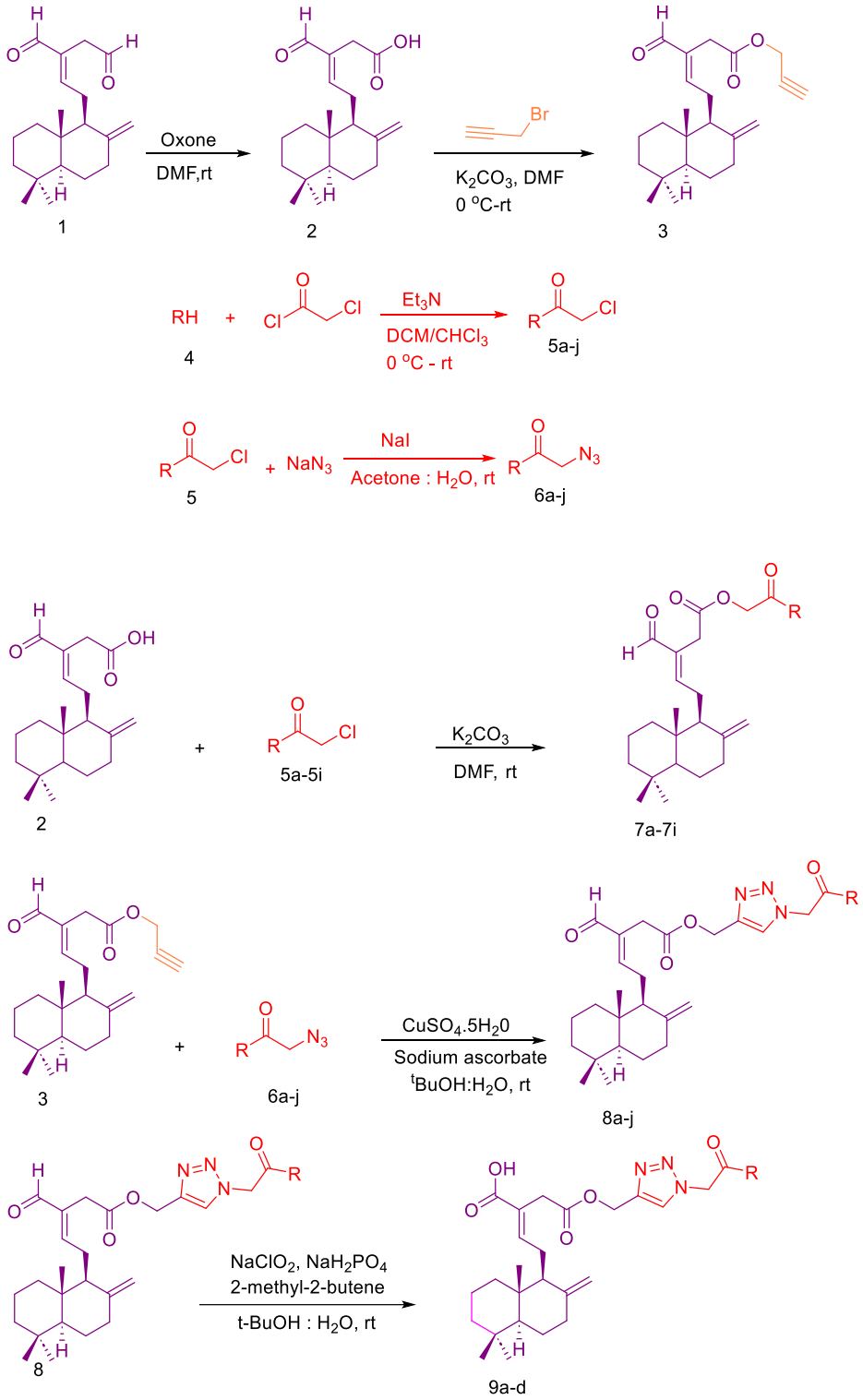

Table 5.1. Synthesized library of heterocyclic amide appended labdane derivatives

Compound	R =	Compound	R =
7a	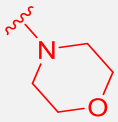	8d	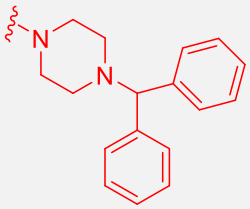
7b	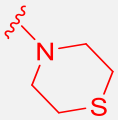	8e	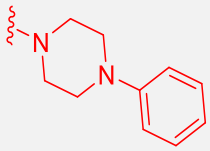
7c	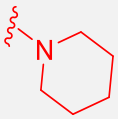	8f	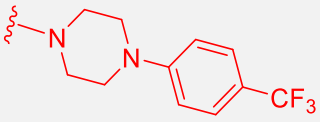
7d		8g	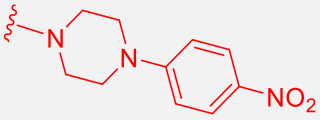
7e	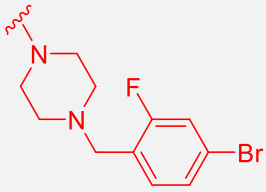	8h	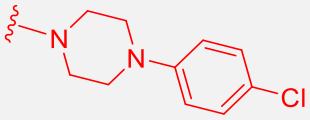
7f	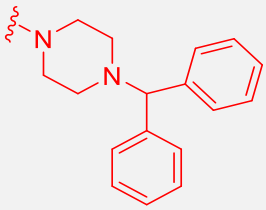	8i	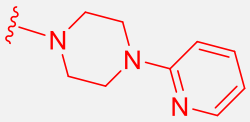
7g	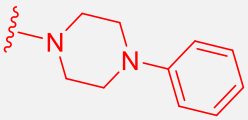	8j	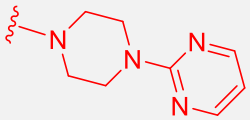
7h	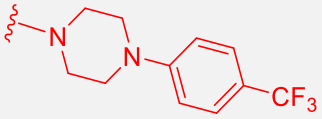	9a	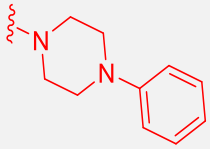
7i	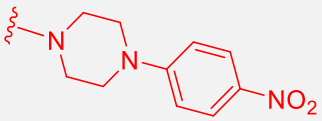	9b	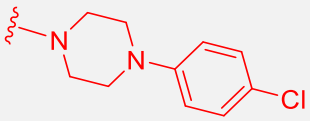
8a	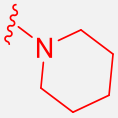	9c	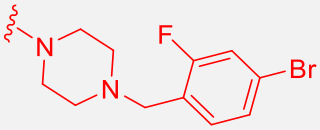

8b 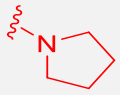

8c 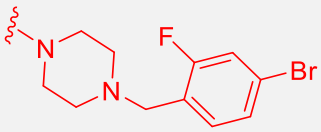

9d 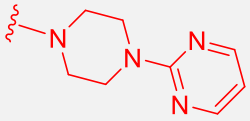

5.6.1. Spectral characterization of heterocyclic amide appended labdane conjugates

5.6.1.1. Spectral characterization of simple heterocyclic amide appended labdane conjugates

Spectral data leading to the structural characterization of heterocyclic amide appended labdane conjugates **(7a-7i)** is exemplified using compound **7g** (**Figure 5.5**). The peak at δ 9.31 in the ^{1}H NMR spectrum (**Figure 5.6**) indicated the presence of aldehyde proton. The two singlets at δ 4.78 and 4.33 attributed to the presence of exo-methylene group. The peaks between δ 7.22-6.84 integrating for five protons corresponds to that of the phenyl ring. A singlet at δ 4.70 integrating for two protons corresponds to that of the methylene group attached to the oxygen atom. The multiplets between δ 3.71-3.68, δ 3.48-3.47 and δ 3.12-3.10 integrating eight protons indicated the protons of the piperazine core. The presence of aldehyde and ester carbonyl groups was confirmed by peaks at δ 193.5 and 169.8 in the ^{13}C NMR spectrum (**Figure 5.7**). The peak at δ 164.7 corresponds to that of the amide carbon. The peaks between δ 150.8-107.9 confirmed the presence of aromatic and aliphatic double bonds. The mass spectrum of the compound showed the molecular ion peak at m/z 543.3195, which is $(M+Na)^{+}$ peak. From these data, along with DEPT-135 and 2D spectra, the structure of the compound **7c** was confirmed as shown below.

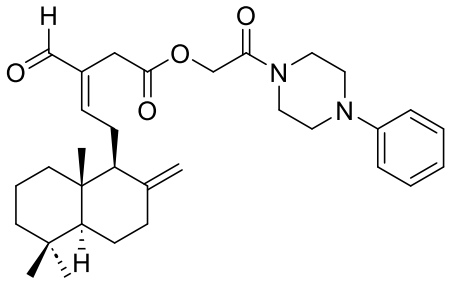

Figure 5.5. Compound **7g**

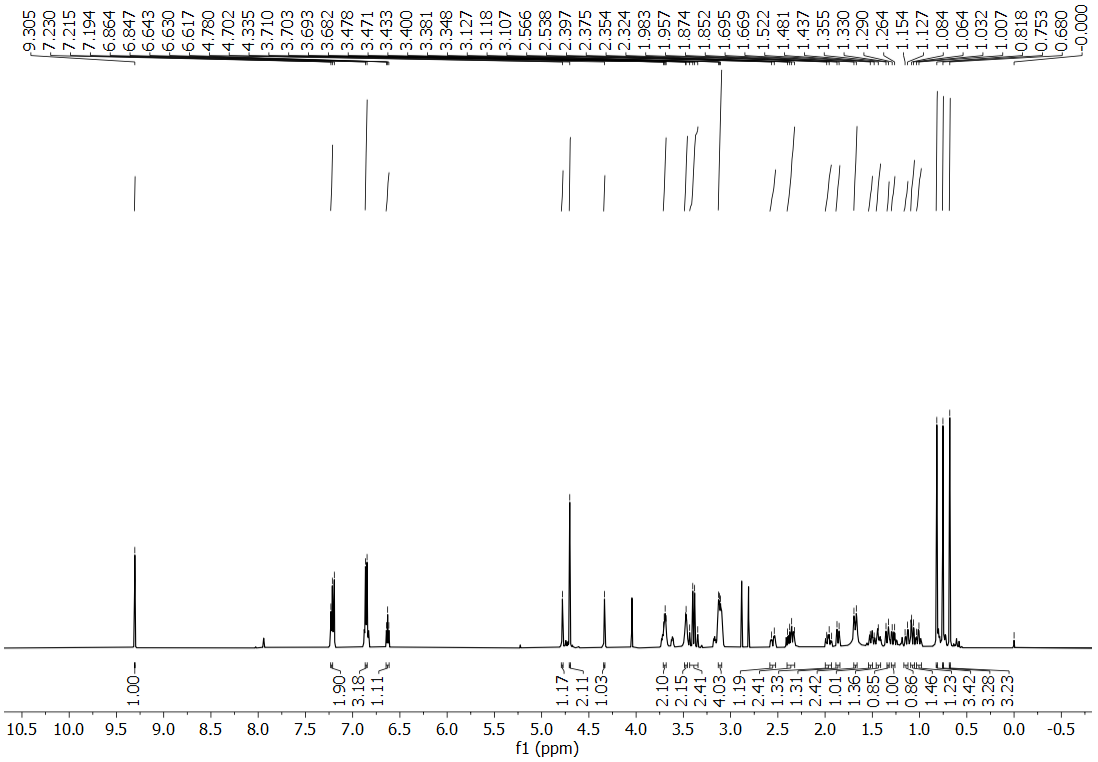

Figure 5.6. ^{1}H NMR spectrum of compound **7g** (500 MHz, $CDCl_3$)

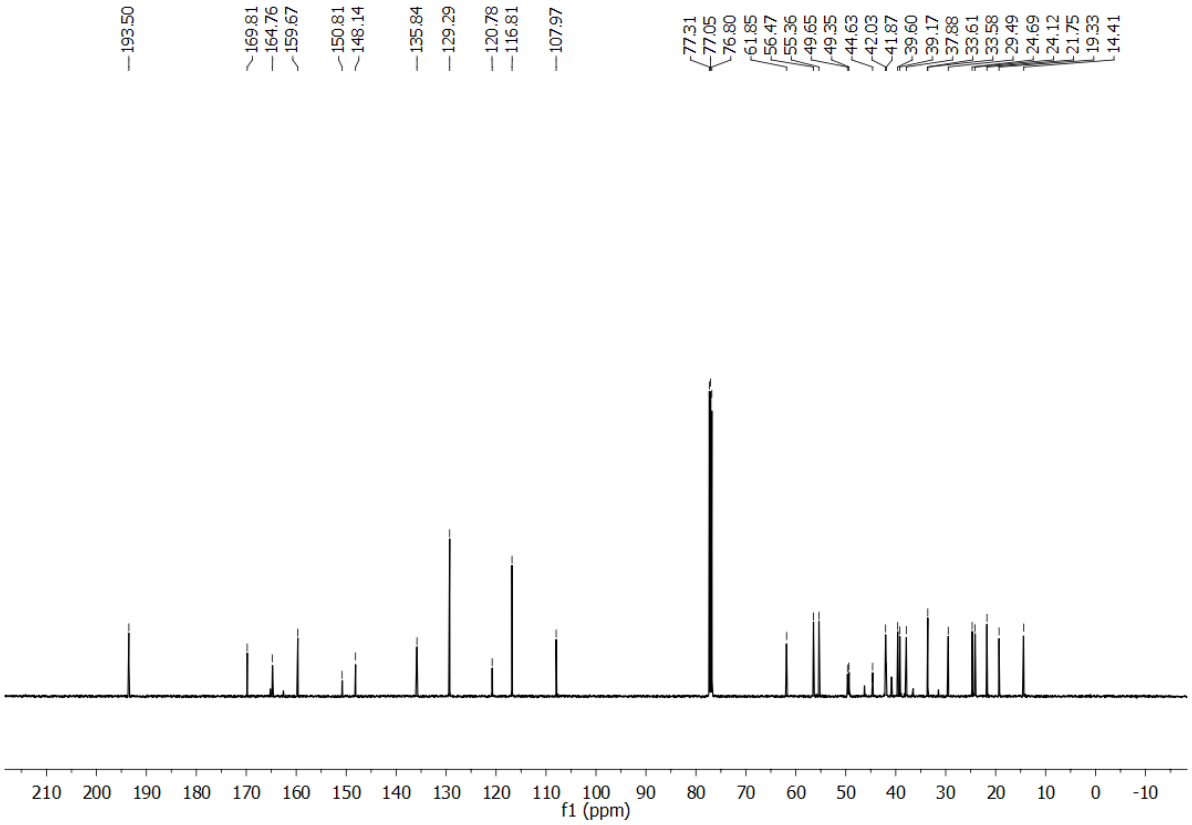

Figure 5.7. ^{13}C NMR spectrum of compound **7g** (125 MHz, $CDCl_3$)

5.6.1.2. Spectral characterization of triazole linked heterocyclic amide appended labdane conjugates

Spectral data leading to the structural characterization of triazole linked heterocyclic amide appended labdane conjugates is exemplified using compound **8e** (**Figure 5.8**). The peak at δ 9.26 in the ^{1}H NMR spectrum (**Figure 5.9**) indicated the presence of aldehyde proton. The two singlets at δ 4.77 and 4.30 attributed to the presence of exo-methylene group. The aromatic proton of the triazole ring resonated at δ 7.74. The peaks between δ 7.23-6.88 integrating for five protons corresponds to that of the phenyl ring. A singlets observed at δ 5.19, integrating two protons, indicated the protons of the methylene group that connects the triazole ring and the amide carbon attached to the piperazine core. Whereas, the singlet at δ 5.02 integrating for two protons attributed to that of the methylene group attached to the oxygen atom of the ester group. The singlets at δ 3.74 and δ 3.67, each corresponding to two protons, along with the multiplet observed between δ 3.15-3.13, integrating for four protons, are indicative of the protons of the piperazine core. The presence of aldehyde and ester carbonyl groups was confirmed by peaks at δ 193.5 and 169.9, in the ^{13}C NMR spectrum (**Figure 5.10**). The peak at δ 163.2 corresponds to that of the amide carbon. The peaks between δ 159.2-107.9 confirmed the presence of aromatic and aliphatic double bonds. The mass spectrum of the compound showed the molecular ion peak at m/z 624.3530, which is $(M+Na)^{+}$ peak. From these data, along with DEPT-135 and 2D spectra, the structure of the compound **8e** was confirmed as shown below.

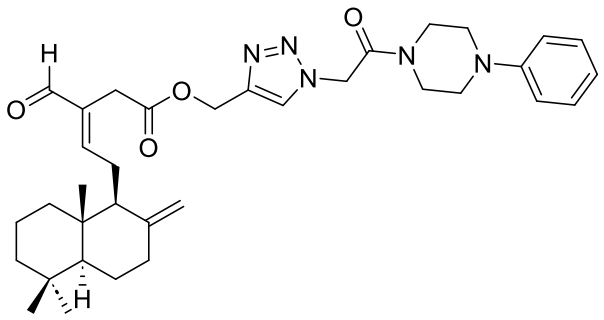

Figure 5.8. Compound **8e**

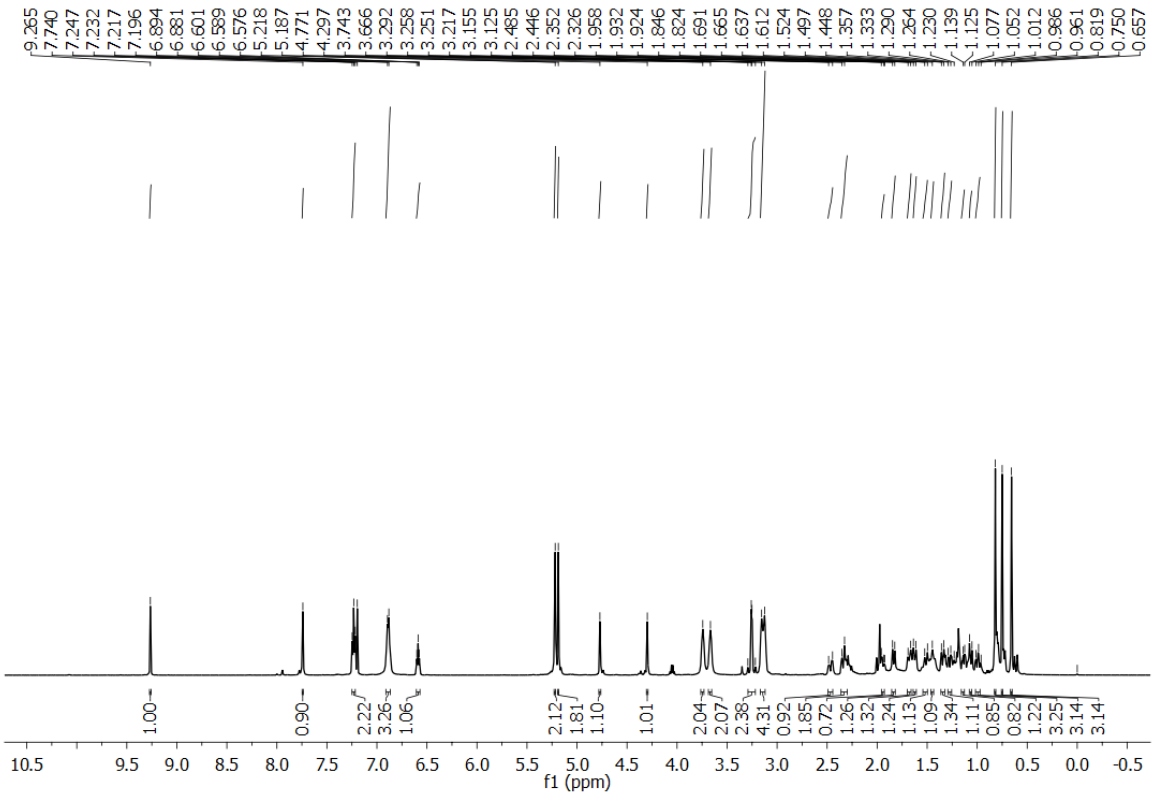

Figure 5.9. ^{1}H NMR spectrum of compound **8e** (500 MHz, $CDCl_3$)

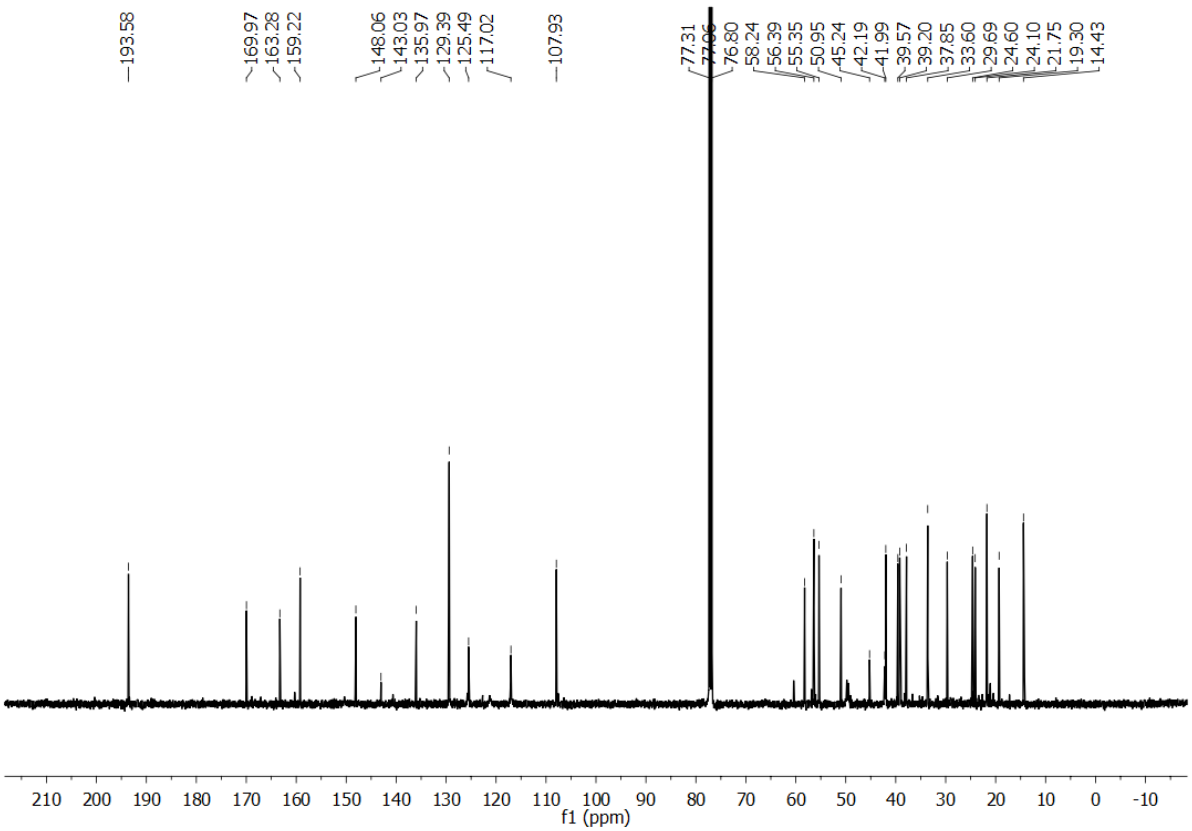

Figure 5.10. ^{13}C NMR spectrum of compound **8e** (125 MHz, $CDCl_3$)

5.6.2. Determination of *in vitro* cell viability by MTT assay

The cytotoxicity of all the target compounds was determined by MTT assay at test concentrations 1, 10 and 20 µM in RAW264.7 cell lines, before evaluating its anti-inflammatory potential (Figure S1, Supporting information). A concentration of 10 µM, was found to be the highest concentration at which most of the compounds were non-toxic to RAW264.7 cell lines. Compounds **7b-h**, **8a-b**, **8e-i**, **9b** and **9d** exhibited no obvious cytotoxic effect at 1 and 10 µM concentrations. However, the compounds **7a**, **7i**, **8c**, **8d**, **8j**, **9a** and **9c** demonstrated increased cytotoxicity at all the tested concentrations and were further excluded from all the cell-based anti-inflammatory tests. Thus, compounds **7b-h**, **8a-b**, **8e-i**, **9b** and **9d** were considered safe for the cell-based anti-inflammatory studies till 10 µM concentrations (**Figure 5.11)**.

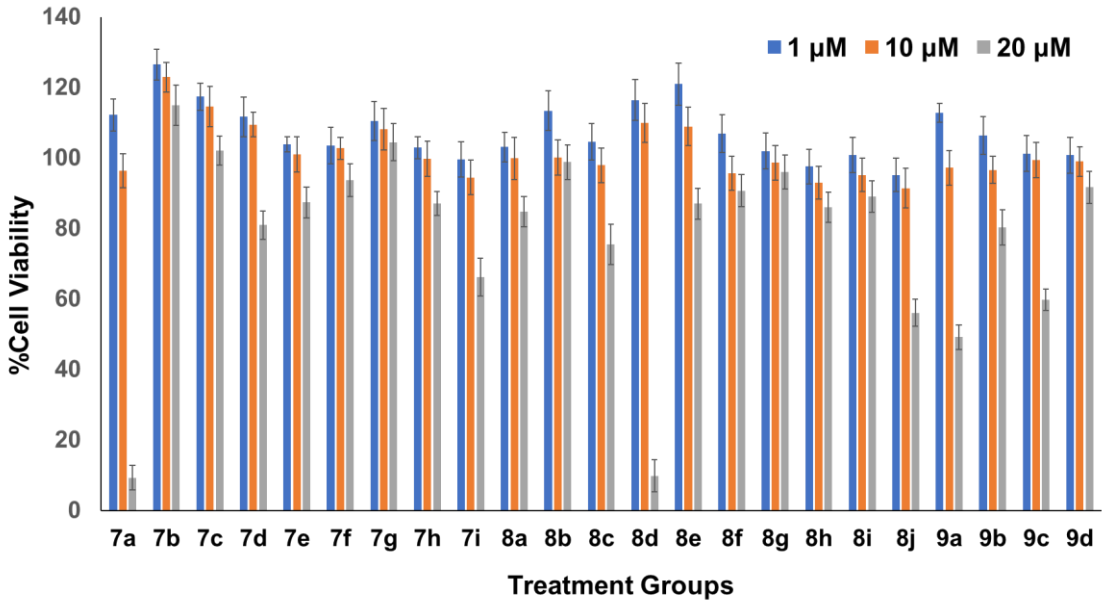

Figure 5.11. Effect of labdane derivatives (**7a-i**, **8a-j and 9a-d**) on cell viability in RAW264.7 cells. The viability of cells after pre-treatment with different concentrations of compounds (1, 10 and 20 µM concentrations) for a period of 24 h, was determined by MTT assay.

5.6.3. Effect of compounds on nitric oxide (NO) production *in vitro*

Excessive release of NO is considered to be the root cause of the progression of many inflammatory diseases. Therefore, the suppression of NO production by the target compounds can be regarded as the initial approach for evaluating their potential anti-inflammatory properties.[14] Based on the MTT assay, 16 heterocyclic amide-labdane

conjugates (**7b-h**, **8a-b**, **8e-i**, **9b**, **9d)** as well as the parent natural compound (**1**) were evaluated for their effect on NO inhibition in LPS induced RAW264.7 cells, by Griess method.[15] Indomethacin (IND, 10 μM) was chosen as the positive control. As observed from **Table 5.2**, it is evident that three compounds, namely **7e**, **8a** and **9b**, demonstrated a significant suppression of NO production, surpassing both the positive control indomethacin and the natural compound labdane dialdehyde (**1**). However, **9b** displayed the most notable NO inhibitory effect among all the compounds tested, with an IC_{50} value of 1.46 ± 0.07 μM, surpassing the positive control indomethacin (IC_{50} = 8.16 ± 0.4 μM).

Table 5.2. Effect of Labdane Derivatives on NO Inhibition (IC_{50}) [a]

Compounds	IC_{50}
IND	8.16 ± 0.4
1	16.83 ± 0.84
7b	12.06 ± 0.60
7c	9.68 ± 0.48
7d	8.10 ± 0.40
7e	5.68 ± 0.28
7f	7.97 ± 0.39
7g	10.27 ± 0.51
7h	7.70 ± 0.38
8a	7.57 ± 0.37
8b	7.71 ± 0.38
8e	12.84 ± 0.64
8f	14.00 ± 0.70
8g	15.28 ± 0.76
8h	15.21 ± 0.76
8i	12.28 ± 0.61
9b	1.46 ± 0.07
9d	24.05 ± 1.20

[a] Half maximal inhibitory concentration (IC_{50}) values for NO inhibition of labdane derivatives and the positive control indomethacin (IND). Data are expressed as the mean ± SD (n= 3).

5.6.4. Structural activity relationship based on the effect of compounds on NO inhibition

A probable structural activity relationship (SAR) was established based on the effects of the synthesized compounds on NO inhibition. Among the simple heterocyclic amide appended labdane derivatives (**7b-h**), piperazine derivatives displayed a higher NO inhibitory effect than the other derivatives with morpholine, thiomorpholine, piperidine and pyrrolidine cores. Among the triazole derivatives **(8a-b**, **8e-i**, **9b** and **9d)** compound **9b,** a p-chlorophenyl piperazine derivative of labdane, demonstrated the strongest NO inhibitory effect. . Derivatives **8a** and **8b**, incorporating piperidine and pyrrolidine cores respectively, also exhibited potent NO inhibitory effects. . The remaining compounds displayed moderate NO inhibitory activity. Notably, while compound **8h** showed moderate inhibition, modifying its aldehyde group into a carboxylic acid to yield compound **9b** resulted in a nearly 10-fold increase in activity. Compound **9b** demonstrated approximately a 2-fold higher activity than the existing lead compound **7a** and a 5-fold increase in activity compared to indomethacin. Interestingly, no consistent SAR pattern was observed regarding the type of cyclic amine or specific substitutions on the piperazine core. This suggests that factors other than the nature of the cyclic amine might contribute significantly to the observed activity.

5.6.5. Effect of compounds on TNF-α and IL-6 production *in vitro*

TNF-α and IL-6 constitute the classical pro-inflammatory cytokines that mediate various inflammatory pathways that compromise organ integrity.[16] Therefore the effect of the 16 compounds on TNF-α and IL-6 inhibition was evaluated on LPS-induced RAW264.7 cells at 10 μM concentration. As depicted in **Figure 5.12**, LPS stimulation increased the levels of the cytokines, whereas there was a marked reduction in cytokines level on pre-treatment with labdane dialdehyde (**1**) and its semi-synthesised derivatives. The three semi-synthetic derivatives, **9b, 7e** and **8a**, exhibited a more pronounced inhibitory effect on TNF-α and IL-6, compared to all the other test groups which was in concordance with the NO inhibition results. Compound **9a** demonstrated the strongest inhibitory effect on TNF-α and IL-6 in comparison to the other test groups and the positive control indomethacin, which is consistent with the NO inhibition results. Other tested groups exhibited moderate activity.

Since compound **9b** consistently showed the strongest inhibition on NO production as well as the release of the pro-inflammatory cytokines, TNF-α and IL-6, in LPS-induced macrophages, it was screened for further evaluation of its anti-inflammatory potential.

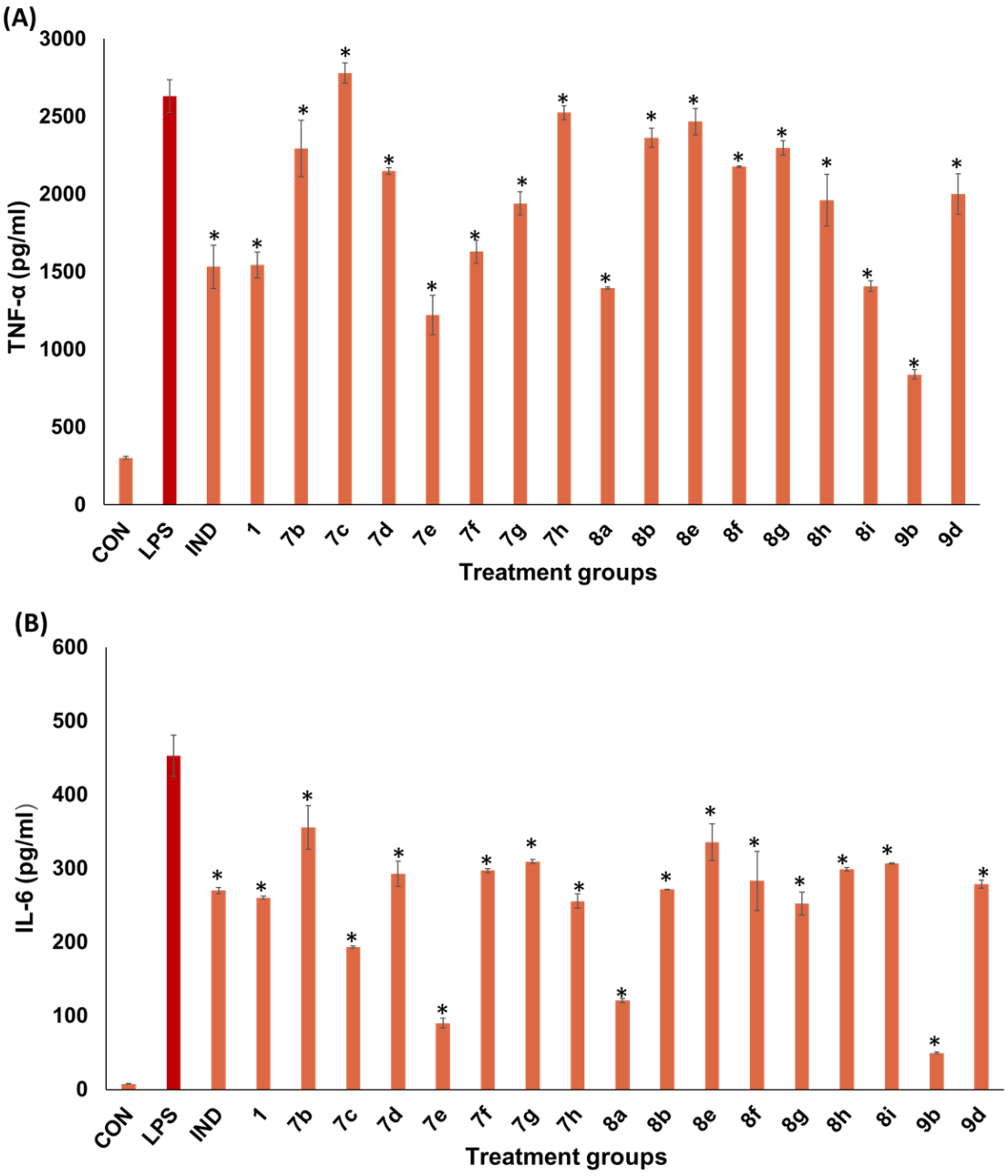

Figure 5.12. Effect of semi-synthetic derivatives of labdane dialdehyde on LPS induced cytokines production (**A**) TNF-α, (**B**) IL-6, in RAW 264.7 cell lines. Cells were pretreated with10 µM concentration of compounds for 1 h, before treatment with 1 µg/mL LPS. After 24 h of incubation, cytokines production was determined by ELISA. Data are expressed as the mean ± SD (n = 3). *p < 0.001 vs LPS group.

5.6.6. Dose-response effect of 9b on TNF-α and IL-6

The effect of different concentrations of **9a** (1, 2.5 and 5 µM) on pro-inflammatory cytokines, i.e., TNF-α and IL-6 were evaluated on LPS-induced macrophages along with

indomethacin (10 µM) as the reference drug. As observed from the **Figures 5.13A and 5.13B**, the compound **9b** decreased the levels of TNF-α and IL-6 in a concentration-dependent manner and was more potent than the positive control indomethacin. Thus, **9b** can be considered to be a promising anti-inflammatory agent and further investigations into its mechanism of action was much warranted.

5.6.7. Effect of compounds on anti-inflammatory cytokine IL-10 *in vitro*

Interleukin-10 (IL-10) serves as an anti-inflammatory cytokine and plays a critical role in the prevention of inflammatory and autoimmune pathologies. [17,18] As a result, elevated IL-10 levels in LPS-stimulated macrophages can be interpreted as an indication of the host's mechanism to mitigate inflammation. Based on the preliminary screening results, the most active labdane derivative **9b** was evaluated for its effect on IL-10 levels at 1, 2.5 and 5 µM concentrations, in LPS-stimulated RAW264.7 cells. Indomethacin was again used as the reference drug. As witnessed in the previous assays, **9a** significantly increased the levels of IL-10 in a dose-dependent manner in LPS-stimulated RAW264.7 cells and was comparable to indomethacin (**Figure 5.13C**). As **9b** demonstrated strong anti-inflammatory properties by suppressing the pro-inflammatory mediators NO, TNF-α and IL-6 as well as by raising the levels of the anti-inflammatory mediator 1L-10, which was at par with the positive control indomethacin, **9b** was selected for the further comprehensive anti-inflammatory studies.

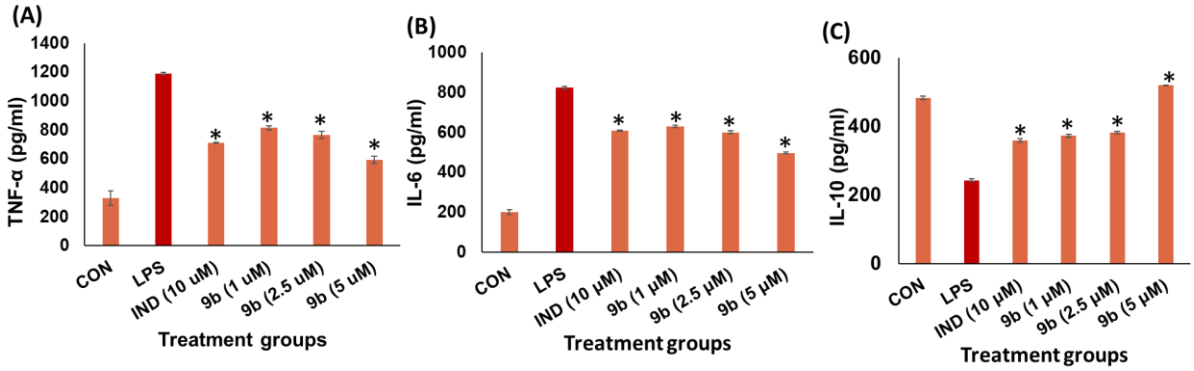

Figure 5.13. Effect of compound 9b on LPS-induced cytokines production. (**A**) TNF-α (**B**) IL-6 and (**C**) IL-10, in RAW 264.7 cell lines. Cells were pretreated with various concentrations of compound **9b** (1, 2.5 and 5 µM) and indomethacin (10 µM) for 1 h before treatment with 1 µg/mL LPS. After 24 h of incubation, cytokines production was determined by ELISA. Data are expressed as the mean ± SD (n = 3). *$p < 0.001$ vs LPS group.

5.6.8. Effect of compound 9a on iNOS and COX-2 protein expression

COX-2 and iNOS are the two most persistent pro-inflammatory proteins convoluted in inflammation.[14,19] To investigate the molecular mechanistic action of compound **9b**, the impact of this compound on the expression of COX-2 and iNOS enzymes was determined using western blotting on LPS-stimulated RAW 264.7 cells (at 5 and 10 µM). Indomethacin (10 µM) was again employed as the positive control. LPS stimulation increased the expression of COX-2 and iNOS proteins significantly. However, when co-treated with **9b** there was a dose-dependent decrease in the expression of these proteins. It was observed that at a concentration of 10 µM, compound **9b** demonstrated a significantly more pronounced inhibitory effect on the expression of iNOS and COX-2 in comparison to indomethacin (**Figure 5.14**). These outcomes suggest that the anti-inflammatory properties of compound **9a** could potentially stem from its ability to downregulate the expression of iNOS and COX-2.

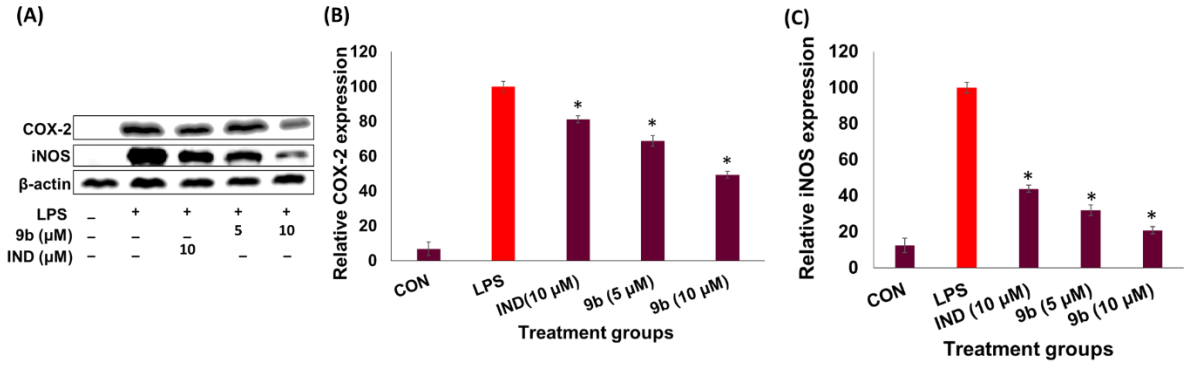

Figure 5.14. Effect of compound **9b** on COX-2 and iNOS expression in LPS-stimulated RAW264.7 cells. Cells were pretreated with different concentrations of compound **9b** (5 and 10 µM) and indomethacin (10 µM) for 1h and then stimulated with or without 1 µg/mL of LPS for 24 h. COX-2 and iNOS expressions were detected by western blotting (**A**, **B** and **C**). *$p < 0.001$ vs LPS group

5.6.9. Effect of 9b on NF-κB signalling pathway on LPS-stimulated RAW 264.7 cells by western blotting and immunofluorescence analysis

Numerous comprehensive studies indicate that the activation of NF-κB, a prevalent cellular transcription factor, is the principal regulator in the expression of pro-inflammatory cytokines, such as TNF-α and IL-6, as well as pro-inflammatory enzymes like COX-2 and iNOS.[20–22] Therefore, we investigated the potential intra-cellular anti-inflammatory

mechanism of **9b** by analyzing its influence on the NF-κB signalling pathway through western blotting and immunofluorescence analysis on LPS-stimulated RAW 264.7 cells. Indomethacin at 10 μM was used as the positive control. Inhibiting the phosphorylation of NF-κB on p65 can reduce its activation, which was measured through western blotting. As depicted in **Figure 5.15**, LPS stimulation increased the levels of phosphorylated NF-κB p65 (p-NF-κB p65), while co-treatment with Compound **9b** significantly reduced phosphorylation in a dose-dependent manner. At 10 μM, **9b** demonstrated better inhibition on p-NF-κB p65 than Indomethacin.

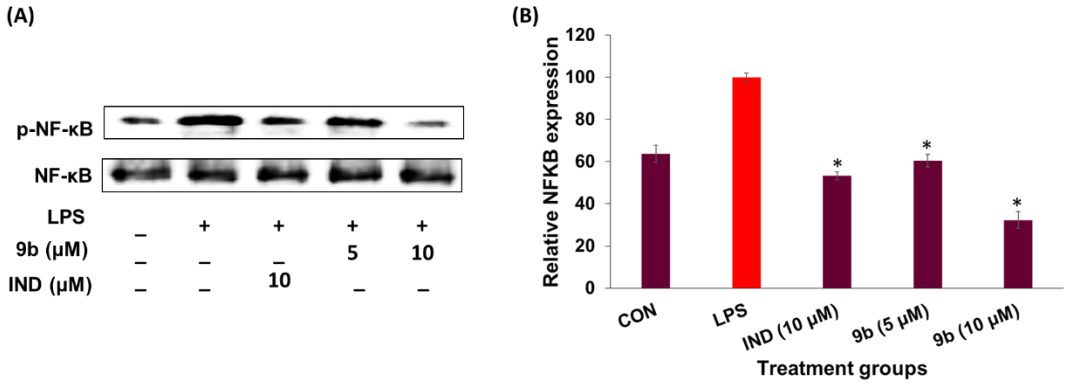

Figure 5.15. Effect of 9b on NF-κB signalling pathway on LPS-stimulated RAW 264.7. Cells were pre-treated with different concentrations of compound **9b** (5 and 10 μM) and indomethacin (10 μM) for 1h and then stimulated with or without 1 μg/mL of LPS for 24 h. NF-κB expression was detected by western blotting (**A** and **B**). *p < 0.001 vs LPS group.

Immunofluorescence was used to investigate the nuclear translocation of NF-κB in LPS-stimulated RAW 264.7 cells to confirm the impact of **9b** on the NF-κB pathway. The distribution of NF-κB in the cell nucleus was greatly enhanced by LPS stimulation, as shown in **Figure 5.16**. On the other hand, co-treatment with **9b** significantly and concentration-dependently diminished the distribution of NF-κB inside the nucleus. Our results revealed that **9b** exerts an anti-inflammatory effect *by* suppressing the NF-κB signaling cascade.

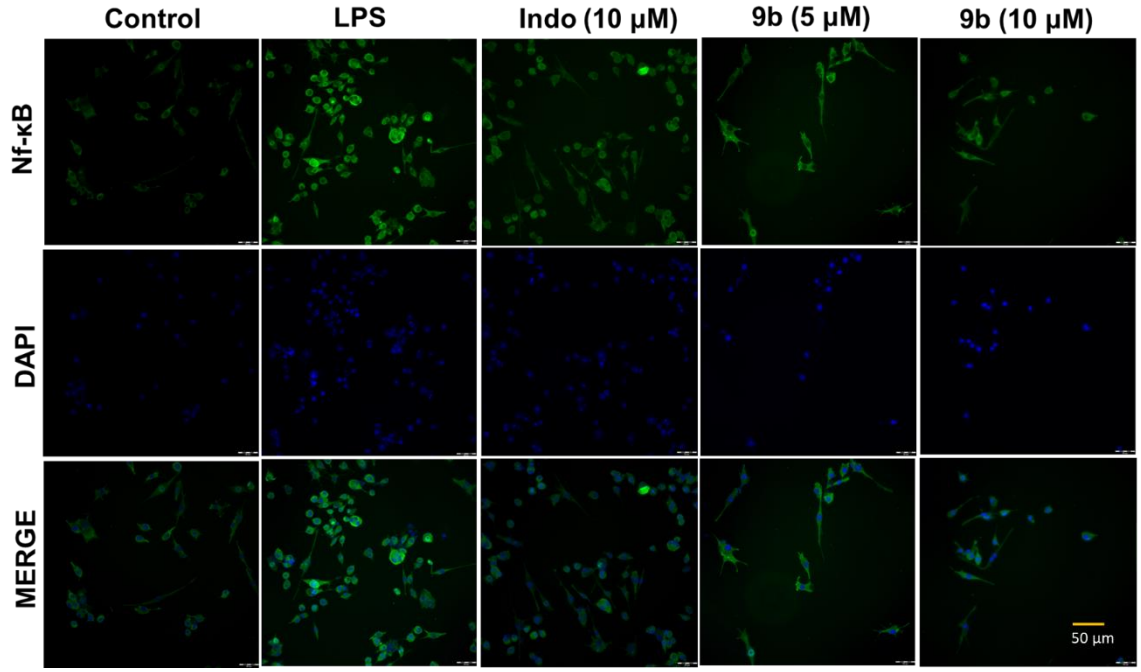

Figure 5.16. Effect of **9b** on NF-κB signalling pathway *via* immunofluorescence. Immunofluorescence staining detected the distribution of NF-κB-p65 in both the nuclei and cytoplasm by some colocalization of receptors (p65, Alexa Fluor 488, green) with the nuclei DAPI, blue). Images were captured by fluorescent microscope (OLYMPUS, Japan). Scale = 50 µm

5.6.10. *In silico* molecular modelling studies of compound 9b on NF-κB;

Using the HADDOCK 2.2 (https://haddock.science.uu.nl/) software, we conducted structure-based virtual docking (arbitrary docking was performed over the docking bias) to better understand the structural and molecular mode of physical interaction, relative binding affinity, and potential mode of interaction of our synthesized drugs with the NF-κB (monomer). The results were analyzed using Pymol. First and foremost, NF-κB's structural study in apo form or without DNA has revealed an accessible binding pocket of 2013 A2, which may hold big molecules that are perfect for our synthetic compounds (**7b-h**, **8a-b**, **8e-i**, **9b**, **9d**). Among the screened compounds, we discovered that compound **9b** had the highest binding affinity of dG -9.48±1.2 kcal/mol based on our reference-free and objective docking. **Figure 5.17 A-I** displays the structural analysis of h NF-κB binding, indicating that dG -9.48±1.2 kcal/mol is the maximum binding affinity. Compound **9b** can bind the active site or DNA binding site of h NF-κB in two distinct binding modes with a comparatively equal binding affinity, as demonstrated by the structural analysis of h NF-

κB binding with compound **9b** in **Figure 5.17**. Compound **9b** is shown coupled to h NF-κB in two different conformations in LigPlot images, with certain important interaction residues remaining conserved (**Figure 5.17 D-E**). Our binding assay experiments confirmed this binding affinity as well. The binding orientation of bound compound **9b** was then examined by superimposing the structures to see if our compounds might intercalate or inhibit DNA recognition, using the apo-form and dsDNA bound (PDB:1NFK) form structure of hNF-κB (homo-dimer) as models. Compound **9b**, as seen in **Figure 5.17 H**, shares a portion of the dsDNA binding site, causing the dsDNA to deallocate or inhibit the binding of dsDNA. We then performed simple simulation tests to investigate how compound **9b** binding influences dsDNA disassembly. Our simulated model demonstrated, the displacement of bound dsDNA from hNF-κB and the eventual inhibition of dsDNA binding in the presence of compound **9b** (**Figure 5.17 H-I)**.

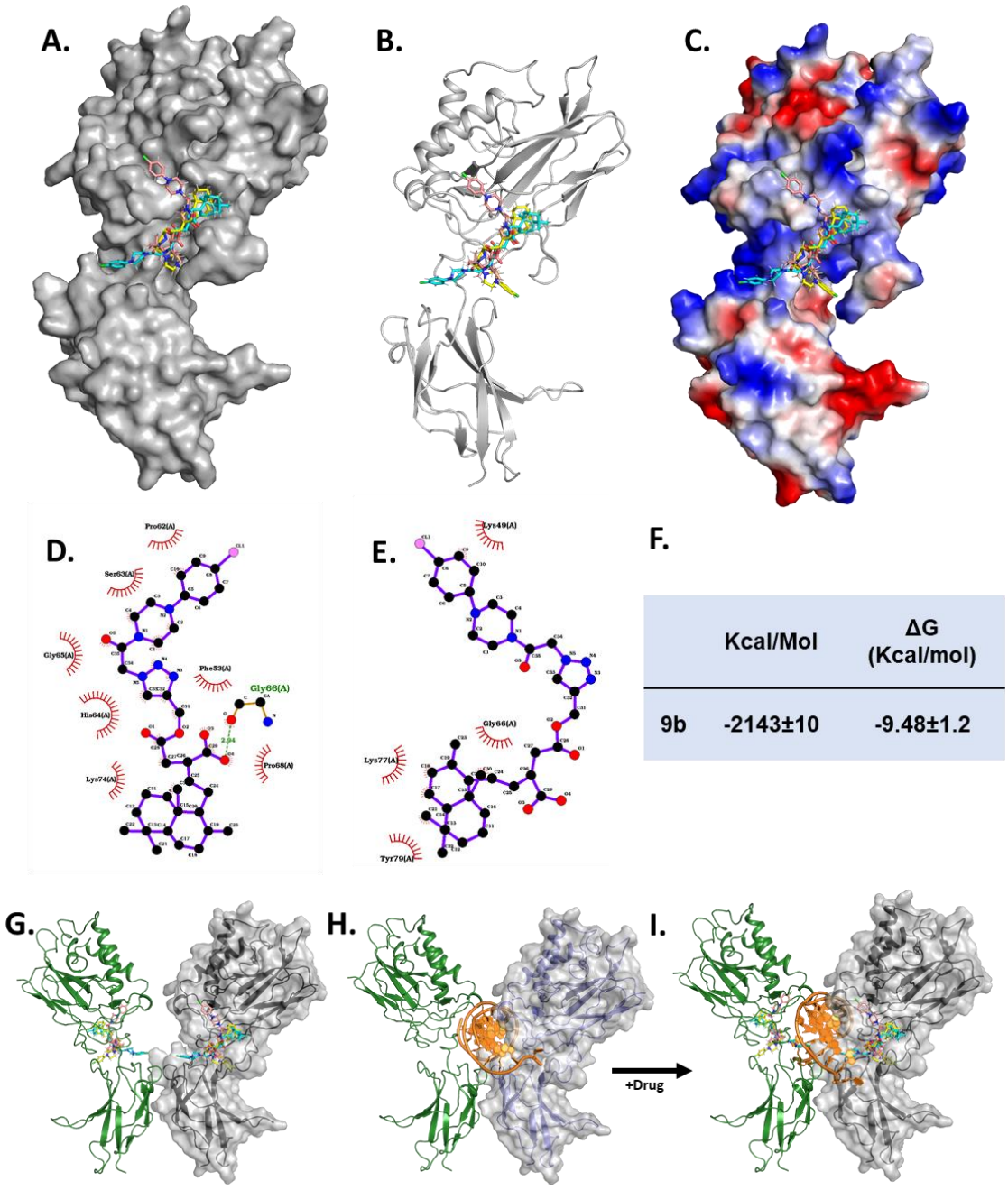

	Kcal/Mol	ΔG (Kcal/mol)
9b	-2143±10	-9.48±1.2

Figure 5.17. Molecular docking studies of **9b** on NF-kB (**A**) Surface (**B**) Cartoon (**C**) electrostatic potential representation of hNF-kB (monomer) with bound **9b** compound in different conformations. (**D-E**) LigPlot view of compound **9b** bound to hNF-KB in two different conformations. Compounds are shown in sticks with numbering Cα and respective interacting amino acids in the hNF-kB are shown with the compound. (**F**) Table showing the relative binding kinetics of NFkB with our **9b** compound. (**G**) Structure of hNF-kB (homo-dimer) in complex with docked **9b** in different conformations. (**H**) and in complex with dsDNA (PDB: 1NFK) (front view). (**I**) Structural simulation of 1NFK in the presence of our proposed compound **9b** resulting in the displacement of bound dsDNA and eventual inhibition of dsDNA binding. For clarity, individual hNF-kB in the homo-dimer are colouredcoloured in green and slate with or without surface representation. .

5.7. Conclusions

From our internal database of labdane analogues, we identified the lead compound **7a** with an attractive skeleton. Building on this lead, we designed and synthesized 23 novel derivatives, leading to the identification of a more effective compound, **9b**, with an IC50 value of 1.45 μM for NO inhibition in LPS-induced RAW 264.7 cells. This represents an 11-fold improvement over the parent compound, labdane dialdehyde, a 2-fold increase in activity over the existing lead 7a, and a 5-fold enhancement compared to the commercial drug indomethacin. At a dose of 1 μM, compound 9b also demonstrated significant inhibitory effects on the primary pro-inflammatory cytokines TNF-α and IL-6, highlighting its superior potency relative to compound **7a**. Mechanistic studies further revealed that **9b** suppresses the expression of COX-2 and iNOS by modulating the NF-κB signaling pathway. These results suggest that the optimized lead, **9b**, is a promising candidate as an anti-inflammatory agent. However, advanced studies are currently underway in our laboratory to further evaluate its therapeutic potential and drug-like properties.

5.8. Experimental Section

5.8.1. Procedure for the synthesis of chloroacetyl amides (5a-j)

Chloroacetyl chloride (1.2 equiv.) was added dropwise to a stirred solution of amines (**4**) and triethyl amine in anhydrous dichloromethane or chloroform at 0 ^{o}C. The reaction mixture was removed from the ice bath and stirred at room temperature until the completion of the reaction by monitoring the TLC. 5% HCl was added to the reaction mixture and the product was extracted in dichloromethane or chloroform, dried over anhydrous Na_2SO_4 and the solvent was removed under reduced pressure to afford the product.

5.8.2. General procedure for the synthesis of chloroacetyl azides (6a-j)

Chloroacetyl amides (**5**) (1.0 equiv.) were dissolved in a mixture of acetone and ice-cold water and cooled to 0 °C. Sodium iodide (NaI) was added to the reaction mixture, which was then stirred for 5–10 minutes. Sodium azide (NaN_3, 1.5 equiv.) was carefully added in portions, and the mixture was stirred overnight to ensure complete conversion of the acyl chloride to the corresponding azide. Upon reaction completion, acetone was removed using a rotary evaporator. The product was then extracted with ethyl acetate, dried over anhydrous Na_2SO_4, and concentrated under reduced pressure to yield the final product.

5.8.3. Procedure for the synthesis of heterocyclic amide appended labdanes (7a-i)

A stirred solution of Zerumin A (**2**) (1 equiv.) in DMF was treated with K_2CO_3 (1.2 equiv.) and chloroacetyl amide (**5**) (1 equiv.). The reaction mixture was stirred at room temperature, and the progress was monitored by TLC. Upon completion, the mixture was extracted with ethyl acetate, washed with brine, and dried over anhydrous Na_2SO_4. The solvent was removed under reduced pressure, and the product was purified via column chromatography using a mixture of ethyl acetate and hexane as the eluent [38].

5.8.4. Procedure for the synthesis of triazole appended labdane derivatives (8a-j)

To a stirred mixture of compound **3** (1 equiv) and chloroacetyl azide (**6**) (1 equiv.), in ^{t}Butanol: H_2O mixture (3:1), $CuSO_4.5H_2O$ (0.1 equiv.) and sodium-ascorbate (0.25 equiv.) were added and stirred at room temperature. The progress of the reaction was monitored by TLC. After the reaction was complete, the combined organic layer was washed with brine, dried over anhydrous Na_2SO_4, and concentrated under reduced pressure. The product was purified by column chromatography using ethyl acetate and hexane.

5.8.5. Procedure for the synthesis of acid derivatives of triazole appended labdane derivatives (9a-d)

To a stirred solution of triazole-labdane conjugate **8** (1 equiv.) in ^{t}BuOH: H_2O, 2-methyl-2-butene (1.5 equiv.) was added. A mixture of sodium chlorite (10 equiv.) and sodium dihydrogen phosphate (10 equiv.) in water, were added dropwise to the reaction mixture over a period of 10 minutes and stirred at room temperature overnight. Volatile components were removed under vacuum, the residue was dissolved in water, extracted in ethyl acetate, dried over Na_2SO_4 and concentrated under reduced pressure to yield pure product.

5.8.6. Synthesis and characterization of labdane conjugates (7a-i, 8a-j and 9a-d)

Synthesis of 2-morpholino-2-oxoethyl *(E)*-3-formyl-5-((1S,8aS)-5,5,8a-trimethyl-2-methylenedecahydronaphthalen-1-yl)pent-3-enoate (7a)

Compound **7a** was prepared by the reaction of zerumin A (**2)** (52 mg) with 2-chloro-1-morpholinoethan-1-one in DMF according to the procedure described in **5.8.3.** Yield: 56% (41 mg)

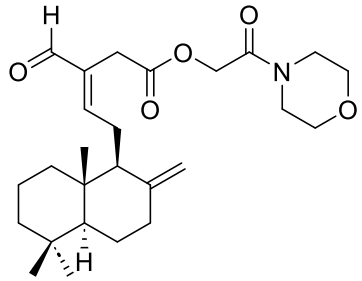

^{1}H NMR (500 MHz, $CDCl_3$) δ: 9.30 (s, 1H), 6.63 (t, *J* = 6.5Hz, 1H), 4.78 (s, 1H), 4.65 (s,2H), 4.33 (s, 1H), 3.63-3.61 (m, 4H), 3.54-3.52 (m, 2H), 3.39-3.32 (m, 4H), 2.56-0.99 (m, 14H), 0.82 (s, 3H), 0.75 (s, 3H), 0.68 (s, 3H)

^{13}C NMR (125 MHz, $CDCl_3$) δ: 193.48, 169.79, 164.92, 159.67, 148.13, 135.81, 107.95, 66.73, 66.37, 61.70, 56.46, 55.36, 45.07, 42.02, 40.59, 39.59, 39.16, 37.87, 33.60, 33.58, 29.46, 24.67, 24.11, 21.74, 19.31, 14.39

HRMS (ESI) m/z : $[M+Na]^+$ calcd for $C_{26}H_{39}NO_5Na$ is 468.2726, found 468.2737

Synthesis of 2-oxo-2-thiomorpholinoethyl *(E)*-3-formyl-5-((1S,8aS)-5,5,8a-trimethyl-2-methylenedecahydronaphthalen-1-yl)pent-3-enoate (7b)

Compound **7b** was prepared by the reaction of zerumin A (**2)** (40 mg) with 2-chloro-1-thiomorpholinoethan-1-one in DMF according to the procedure described in **5.8.3.** Yield: 65% (38 mg)

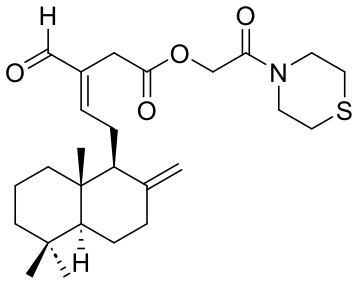

^{1}H NMR (500 MHZ, $CDCl_3$) δ: 9.30(s, 1H), 6.63 (t, *J* = 6.5 Hz, 1H), 4.78 (s, 1H), 4.64 (s, 1H), 3.80-3.78 (m, 2H), 3.58-3.56 (m, 2H), 3.38 (dd, J_1 = 16.5 Hz, J_2 = 27 Hz, 2H), 2.57-2.55 (m, 6H), 2.40-2.33 (m, 2H), 2.41-0.90 (m,12H), 0.82 (s, 3H), 0.753 (s, 3H), 0.680 (s, 3H)

^{13}C NMR (125 MHz, $CDCl_3$) δ: 193.48, 169.80, 164.74, 159.70, 148.14, 135.80, 107.95, 61.90, 56.46, 55.36, 47.49, 44.65, 42.03, 39.59, 39.16, 37.87, 33.60, 33.58,

29.45, 27.74, 27.21, 24.68, 24.11, 21.74, 19.32, 14.39

HRMS (ESI) m/z : $[M+Na]^+$ calcd for $C_{26}H_{39}NO_4SNa$ is 484.2497, found 484.2509

Synthesis of 2-oxo-2-(piperidin-1-yl)ethyl *(E)*-3-formyl-5-((8aS)-5,5,8a-trimethyl-2-methylenedecahydronaphthalen-1-yl)pent-3-enoate (7c)

Compound **7c** was prepared by the reaction of zerumin A (**2)** (59 mg) with 2-chloro-1-(piperidin-1-yl)ethan-1-one in DMF according to the procedure described in **5.8.3.** Yield: 70% (58 mg)

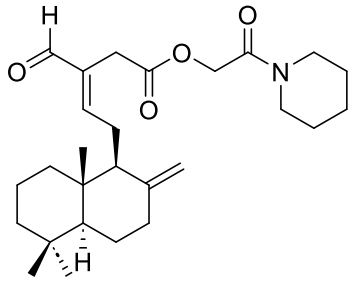

^{1}H NMR (500 MHZ, $CDCl_3$) δ: 9.30(s, 1H), 6.62 (t, *J* = 6.5 Hz, 1H), 4.78 (s, 1H), 4.65(s, 2H), 4.34 (s, 1H), 3.47-3.37 (m, 4H), 3.23-3.22 (m, 2H), 2.57-0.99 (m, 20H), 0.82(s, 3H), 0.75 (s,3H), 0.68(s,3H)

^{13}C NMR (500MHZ, $CDCl_3$) δ: 193.49, 169.85, 164.36, 159.66, 148.13, 135.89, 107.94, 61.93, 56.45, 55.34, 45.63, 43.05, 42.03, 39.57, 39.13, 37.87, 33.60, 33.56, 29.46, 26.23, 25.34, 24.67, 24.39, 24.11, 21.74, 19.30, 14.38

HRMS (ESI) m/z : $[M+Na]^+$ calcd for $C_{27}H_{41}NO_4Na$ is 466.2933, found 466.29318

Synthesis of 2-oxo-2-(pyrrolidin-1-yl)ethyl *(E)*-3-formyl-5-((1S,4aS,8aS)-5,5,8a-trimethyl-2-methylenedecahydronaphthalen-1-yl)pent-3-enoate (7d)

Compound **7d** was prepared by the reaction of zerumin A (**2)** (40 mg) with 2-chloro-1-(pyrrolidin-1-yl)ethan-1-one (mg) in DMF according to the procedure described in **5.8.3.** Yield: 46% (25 mg)

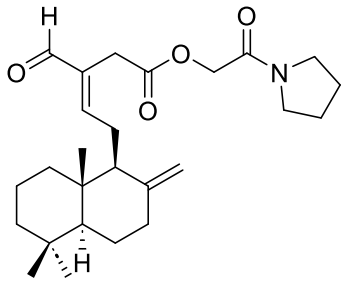

^{1}H NMR (500 MHZ, $CDCl_3$) δ: 9.30 (s, 1H), 6.62 (t, *J* = 6.5 Hz, 1H), 4.78 (s, 1H), 4.57 (s, 2H), 4.34 (s, 1H), 3.47-3.38 (m, 6H), 2.56 - 0.99 (m, 18H), 0.82 (s, 3H), 0.75 (s, 3H), 0.68 (s, 3H)

^{13}C NMR (125 MHz, $CDCl_3$) δ: 193.51, 169.88, 164.74, 159.61, 148.13, 135.91, 107.96, 62.36, 56.49, 55.38, 45.99, 45.29, 42.05, 39.60, 39.17, 37.89, 33.61, 33.58, 29.70, 26.19, 26.15, 24.67, 24.13, 21.75, 19.32, 14.41

HRMS (ESI) m/z: $[M+Na]^+$ calculated for $C_{26}H_{39}NO_4Na$ is 452.2777, found 452.2791

Synthesis of 2-(4-(4-bromo-2-fluorobenzyl)piperazin-1-yl)-2-oxoethyl *(E)*-3-formyl-5-((1S,4aS,8aS)-5,5,8a-trimethyl-2-methylenedecahydronaphthalen-1-yl)pent-3-enoate (7e)

Compound **7e** was prepared by the reaction of zerumin A (**2)** (42 mg) with 1-(4-(4-bromo-2-fluorobenzyl)piperazin-1-yl)-2-chloroethan-1-one in DMF according to the procedure described in **5.8.3.** Yield: 45% (38 mg)

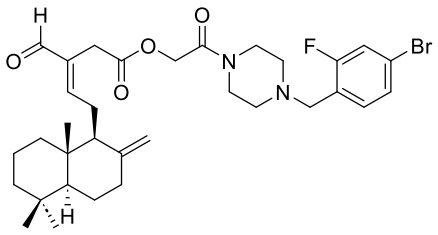

^{1}H NMR (500 MHZ, $CDCl_3$) δ: 9.29 (s, 1H), 7.20-7.15 (m, 3H), 6.62 (t, *J* = 6.5 Hz, 1H), 4.78 (s, 1H), 4.64 (s, 2H), 4.33 (s, 1H), 3.98 (s, 2H), 3.57-3.36 (m, 6H), 2.57 - 0.97 (m, 18H), 0.82 (s, 3H), 0.75 (s, 3H), 0.67 (s, 3H)

^{13}C NMR (126 MHz, $CDCl_3$) δ: 193.41, 169.75, 165.04, 164.61, 162.13, 160.14, 159.54, 148.13, 135.86, 132.50, 127.43, 127.40, 119.19, 118.99, 107.93, 61.79, 56.49, 55.39, 54.61, 52.61, 46.21, 42.05,

40.80, 39.60, 39.18, 37.89, 33.58, 29.47, 24.68, 24.13, 21.74, 19.32, 14.39

HRMS (ESI) m/z: $[M+Na]^+$ calculated for $C_{33}H_{44}BrFN_2O_2Na$ is 653.2366, found 653.2342

5.8.6.6. Synthesis of (1-(2-(4-benzhydrylpiperazin-1-yl)-2-oxoethyl)-1H-1,2,3-triazol-4-yl)methyl *(E)*-3-formyl-5-((1S,4aS,8aS)-5,5,8a-trimethyl-2-methylenedecahydronaphthalen-1-yl)pent-3-enoate (7f)

Compound **7f** was prepared by the reaction of zerumin A (**2)** (46 mg) with 1-(4-benzhydrylpiperazin-1-yl)-2-chloroethan-1-one (mg) in DMF mixture according to the procedure described in **5.8.3.** Yield: 47% (38 mg)

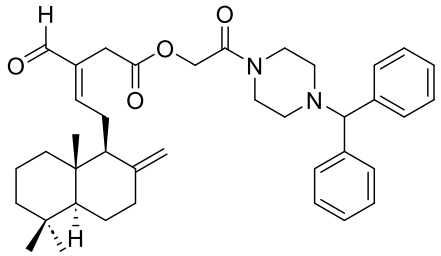

^{1}H NMR (500 MHZ, $CDCl_3$) δ: 9.29 (s, 1H), 7.34-7.32 (m, 4H),7.22-7.21 (m, 4H), 7.12 (t, J = 7.5 Hz, 2H), 6.61 (t, *J* = 6.5 Hz, 1H), 4.77 (s, 1H), 4.61 (s, 2H), 4.32 (s, 1H), 4.17 (s, 1H), 3.52-3.28 (m, 6H), 2.56- 0.96 (m, 18H), 0.81 (s, 3H), 0.74 (s, 3H), 0.66 (s, 3H)

^{13}C NMR (126 MHz, $CDCl_3$) δ:193.40, 169.77, 164.54, 159.52, 148.14, 142.00, 135.88, 128.65, 127.85, 127.23, 107.94, 76.77, 75.90, 61.75, 56.49, 55.39, 51.73, 51.39, 44.75, 42.05, 39.60, 39.17, 37.90, 33.60, 33.58, 29.46, 24.68, 24.14, 21.74, 19.32, 14.39

HRMS (ESI) m/z: $[M+Na]^+$ calculated for $C_{39}H_{50}N_2O_4Na$ is 633.3668, found 633.3673

5.8.6.7. Synthesis of 2-oxo-2-(4-phenylpiperazin-1-yl)ethyl *(E)*-3-formyl-5-((1S,8aS)-5,5,8a-trimethyl-2-methylenedecahydronaphthalen-1-yl)pent-3-enoate (7g)

Compound **7f** was prepared by the reaction of zerumin A (**2)** (51 mg) with 2-chloro-1-(4-phenylpiperazin-1-yl)ethan-1-one in DMF according to the procedure described in **5.8.3.** Yield: 42% (35 mg)

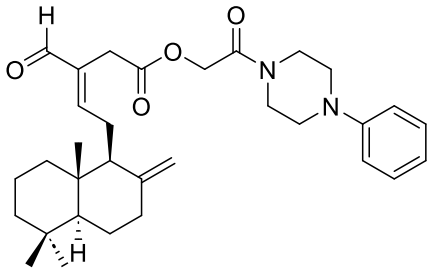

1H NMR (500 MHz, $CDCl_3$) δ: 9.31(s, 1H), 7.22 (m, 2H), 6.86 (m, 3H), 6.63 (t, 1H, *J* = 6.5 Hz), 4.78 (s, 1H), 4.70 (s, 2H), 4.33 (s, 1H), 3.69 (m, 2H), 3.47 (m, 2H), 3.39 (dd, 2H, J_1 = 16.5 Hz, J_2 = 26 Hz), 3.12 (m, 4H), 2.57-1.01 (m, 14H), 0.82 (s, 3H), 0.75 (3H, s), 0.68 (3H, s)

^{13}C NMR (126 MHz, $CDCl_3$) δ: 193.50, 169.81, 164.76, 159.67, 150.81, 148.14, 135.84, 129.29, 120.78, 116.81, 107.97, 61.85, 56.47, 55.36, 49.65, 49.35, 44.63, 42.03, 41.87, 39.60, 39.17, 37.88, 33.61, 33.58, 29.49, 24.69, 24.12, 21.75, 19.33, 14.41

HRMS (ESI) m/z: $[M+Na]^+$ cald for $C_{32}H_{44}N_2O_4$ 543.3199, found 543.3195

5.8.6.8. Synthesis of 2-oxo-2-(4-(4-(trifluoromethyl)phenyl)piperazin-1-yl)ethyl *(E)*-3-formyl-5-((1S,4aS,8aS)-5,5,8a-trimethyl-2-methylenedecahydronaphthalen-1-yl)pent-3-enoate (7h)

Compound **7h** was prepared by the reaction of zerumin A (**3)** (43 mg) with 2-chloro-1-(4-(4-(trifluoromethyl)phenyl)piperazin-1-yl)ethan-1-one in DMF according to the procedure described in **5.8.3.** Yield: 44% (35 mg)

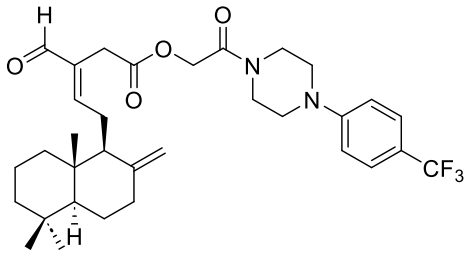

^{1}H NMR (500 MHZ, $CDCl_3$) δ: 9.31 (s, 1H), 7.46 (d, *J* = 8.5Hz, 2H), 6.93 (d, *J* = 8.5 Hz, 2H), 6.64 (t, *J* = 6.5 Hz, 1H), 4.78 (s, 1H), 4.70 (s, 2H), 4.33 (s, 1H), 3.74 (s, 2H), 3.54 (s, 2H), 3.39 (dd, J_1 = 16.5 Hz, J_2 =24 Hz, 2H), 3.27-3.22 (m, 4H), 2.58-0.98 (m, 14H), 0.82 (s, 3H), 0.76 (s, 3H), 0.68 (s, 3H)

^{13}C NMR (126 MHz, $CDCl_3$) δ: 193.52, 169.80, 164.94, 159.69, 148.15, 135.80,

126.68, 126.64, 115.68, 107.96, 77.28, 77.03, 76.77, 61.86, 56.48, 55.38, 44.23, 42.03, 41.41, 39.61, 39.21, 37.88, 33.60, 29.71, 29.52, 24.70, 24.12, 21.75, 19.34, 14.42

HRMS (ESI) m/z: $[M+Na]^+$ calculated for $C_{33}H_{43}F_3N_2O_4Na$ is 611.3073, found 611.7076

5.8.6.9. Synthesis of 2-(4-(4-nitrophenyl)piperazin-1-yl)-2-oxoethyl *(E)*-3-formyl-5-((1S,4aS,8aS)-5,5,8a-trimethyl-2-methylenedecahydronaphthalen-1-yl)pent-3-enoate (7i)

Compound **7i** was prepared by the reaction of zerumin A (**2)** (49 mg) with 2-chloro-1-(4-(4-nitrophenyl)piperazin-1-yl)ethan-1-one in DMF according to the procedure described in **5.8.3.** Yield: 44% (39 mg)

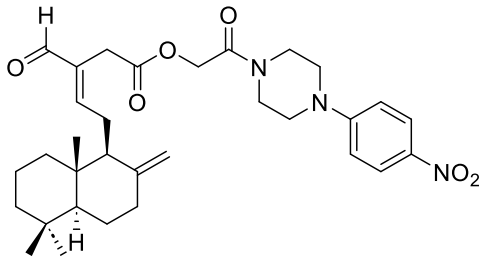

^{1}H NMR (500 MHZ, $CDCl_3$) δ: 9.30 (s, 1H), 8.09 (d, *J* = 9.5Hz, 2H), 6.77 (d, *J* = 7 Hz, 2H), 6.64 (t, *J* = 6.5 Hz, 1H), 4.78 (s, 1H), 4.70 (s, 2H), 4.33 (s, 1H), 3.72 (s, 2H), 3.54 (s, 2H), 3.43-3.38 (m, 6H), 2.56- 0.99 (m, 14H), 0.82 (s, 3H), 0.75 (s, 3H), 0.68 (s, 3H)

^{13}C NMR (126 MHz, $CDCl_3$) δ: 193.51, 169.80, 165.11, 159.70, 154.24, 148.15, 139.39, 135.77, 125.97, 113.26, 107.95, 61.84, 56.47, 55.38, 46.97, 42.02, 41.25, 39.61, 39.21, 37.87, 36.53, 33.58, 29.51, 24.70, 24.12, 21.74, 19.34, 14.42

HRMS (ESI) m/z: $[M+Na]^+$ calculated for $C_{32}H_{43}N_3O_6Na$ is 588.3050, found

5.8.6.10. Synthesis of (1-(2-oxo-2-(piperidin-1-yl)ethyl)-1H-1,2,3-triazol-4-yl)methyl *(E)*-3-formyl-5-((1S,4aS,8aS)-5,5,8a-trimethyl-2-methylenedecahydronaphthalen-1-yl)pent-3-enoate (8a)

Compound **8a** was prepared by the reaction of compound **3** (50 mg) with 2-azido-1-(piperidin-1-yl)ethan-1-one in ^{t}Butanol: H_2O mixture according to the procedure described in **5.8.4.** Yield: 51% (38 mg)

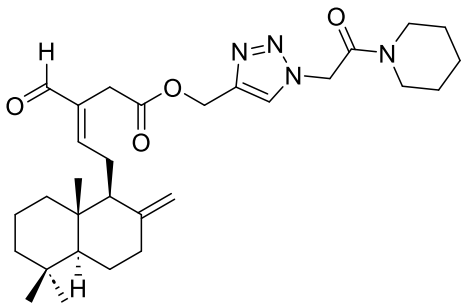

^{1}H NMR (500 MHZ, $CDCl_3$) δ: 9.28 (s, 1H), 7.72 (s, 1H), 6.59 (t, *J* = 6.5 Hz, 1H), 5.19 (s, 2H), 5.15 (s, 2H), 4.77 (s, 1H), 4.30 (s, 1H), 3.51 (t, *J* = 6Hz, 2H), 3.40 (t, *J* = 5.5 Hz, 2H), 3.26 (dd, J_1 = 16.5 Hz, J_2 =2.5 Hz, 2H), 2.49- 0.96 (m, 20H), 0.82 (s, 3H), 0.75 (s, 3H), 0.65(s, 3H)

^{13}C NMR (126 MHz, $CDCl_3$) δ: 193.45, 169.91, 162.83, 159.05, 148.06, 142.84, 136.02, 125.44, 107.90, 77.28, 77.23, 77.03, 76.77, 60.39, 58.27, 56.41, 55.39, 51.02, 46.43, 43.49, 42.02, 39.58, 39.21, 37.86, 33.58, 29.66, 26.30, 25.31, 24.60, 24.22, 24.12, 21.74, 19.30, 14.41

HRMS (ESI) m/z: $[M+Na]^+$ calculated for $C_{30}H_{44}N_4O_4Na$ is 547.3260, found

5.8.6.11. Synthesis of (1-(2-oxo-2-(pyrrolidin-1-yl)ethyl)-1H-1,2,3-triazol-4-yl)methyl *(E)*-3-formyl-5-((1S,4aS,8aS)-5,5,8a-trimethyl-2-methylenedecahydronaphthalen-1-yl)pent-3-enoate (8b)

Compound **8b** was prepared by the reaction of compound **3** (26 mg) with 2-azido-1-(pyrrolidin-1-yl)ethan-1-one in ^{t}Butanol: H_2O mixture according to the procedure described in **5.8.4.** Yield: 45% (17 mg)

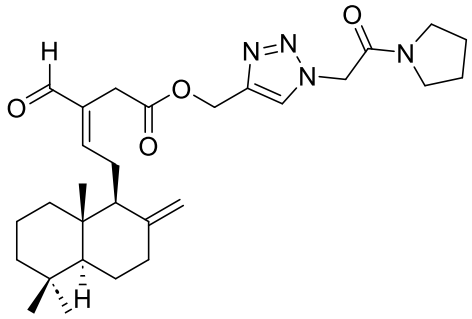

^{1}H NMR (500 MHZ, $CDCl_3$) δ: 9.28 (s, 1H), 7.78 (s, 1H), 6.59 (t, *J* = 6.5 Hz, 1H), 5.19 (s, 2H), 5.07 (s, 2H), 4.77 (s, 1H), 4.30 (s, 1H), 3.49-3.43 (m, 4H), 3.27-3.26 (m, 2H), (2.48 - 0.96 (m, 18H), 0.82 (s, 3H), 0.75 (s, 3H), 0.66 (s, 3H)

^{13}C NMR (126 MHz, $CDCl_3$) δ: 193.43, 169.90, 162.97, 159.02, 148.06, 142.84, 136.02, 125.39, 107.89, 77.28, 77.23, 77.02, 76.77, 58.27, 56.42, 55.39, 51.71, 51.67, 46.41, 46.27, 42.02, 39.58, 39.21, 37.86, 33.57, 29.66, 26.13, 24.60, 24.12, 24.09, 21.73, 19.30, 14.40

HRMS (ESI) m/z: $[M+Na]^+$ calculated for $C_{29}H_{42}N_4O_4Na$ is 533.3104, found 533.3198

5.8.6.12. Synthesis of 2-(4-(4-bromo-2-fluorobenzyl)piperazin-1-yl)-2-oxoethyl *(E)*-3-formyl-5-((1S,4aS,8aS)-5,5,8a-trimethyl-2-methylenedecahydronaphthalen-1-yl)pent-3-enoate (8c)

Compound **8c** was prepared by the reaction of compound **3** (32 mg) with 2-azido-1-(4-(4-bromo-2-fluorobenzyl)piperazin-1-yl)ethan-1-one in ^{t}Butanol: H_2O mixture according to the procedure described in **5.8.4.** Yield: 48% (31 mg)

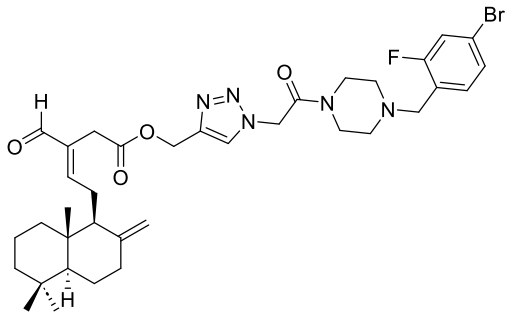

^{1}H NMR (500 MHZ, $CDCl_3$) δ: 9.27 (s, 1H), 7.70 (s, 1H), 7.23-7.17 (m, 3H), 6.59 (t, *J* = 6.5 Hz, 1H), 5.18 (s, 2H), 5.15 (s, 2H), 4.77 (s, 1H), 4.30 (s, 1H), 3.60-3.54 (m, 6H), 3.26-3.25 (m, 2H), 2.49 - 0.96 (m, 18H), 0.82 (s, 3H), 0.75 (s, 3H), 0.66 (s, 3H)

^{13}C NMR (126 MHz, $CDCl_3$) δ: 193.46, 169.91, 163.09, 162.14, 160.14, 159.07, 148.06, 142.98, 136.01, 132.51, 127.48,

125.39, 119.24, 119.03, 107.90, 60.39, 58.25, 56.41, 55.38, 54.55, 52.45, 52.06, 50.85, 42.01, 39.58, 39.22, 37.86, 33.58, 29.68, 24.60, 24.12, 21.74, 19.31, 14.41

HRMS (ESI) m/z: $[M+Na]^+$ calculated for $C_{36}H_{47}BrFN_5O_4Na$ is 734.2693, found 734.2687

5.8.6.13. Synthesis of (1-(2-(4-benzhydrylpiperazin-1-yl)-2-oxoethyl)-1H-1,2,3-triazol-4-yl)methyl *(E)*-3-formyl-5-((1S,4aS,8aS)-5,5,8a-trimethyl-2-methylenedecahydronaphthalen-1-yl)pent-3-enoate (8d)

Compound **8d** was prepared by the reaction of compound **3** (40 mg) with 2-azido-1-(4-benzhydrylpiperazin-1-yl)ethan-1-one in ^{t}Butanol: H_2O mixture according to the procedure described in **5.8.4.** Yield: 50% (39 mg)

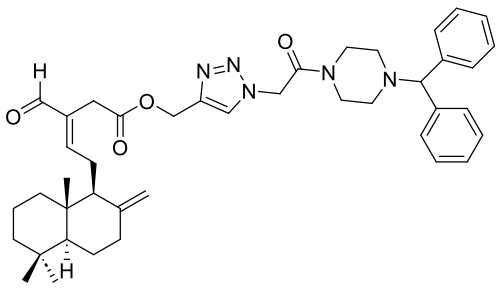

^{1}H NMR (500 MHZ, $CDCl_3$) δ: 9.27 (s, 1H), 7.69 (s, 1H), 7.34 (d, *J* = 7.5 Hz, 4H), 7.23-7.19 (m, 4H), 7.13(t, *J* = 7.5Hz, 2H), 6.58 (t, *J* = 6.5 Hz, 1H), 5.17 (s, 2H), 5.11 (s, 2H), 4.77 (s, 1H), 4.30 (s, 1H), 4.19 (s, 1H), 3.56 (t, *J* = 5Hz, 2H), 3.46 (t, *J* = 5Hz, 2H), 3.26 (dd, J_1 = 16.5 Hz, J_2 = 21 Hz, 2H), 2.48 - 0.95 (m, 16H), 0.82 (s, 3H), 0.75 (s, 3H), 0.66 (s, 3H)

^{13}C NMR (126 MHz, $CDCl_3$) δ: 193.42, 169.89, 163.04, 159.01, 148.06, 142.91, 141.83, 136.02, 128.70, 127.83, 127.31, 125.40, 107.90, 75.78, 58.26, 56.42, 55.39, 51.69, 51.25, 50.82, 45.53, 42.57, 42.02, 39.58, 39.22, 37.87, 33.58, 24.61, 24.12, 21.75, 19.31, 14.41

HRMS (ESI) m/z: $[M+Na]^+$ calculated for $C_{42}H_{53}N_5O_4Na$ is 714.3995, found 714.3987

5.8.6.14. Synthesis of (1-(2-oxo-2-(4-phenylpiperazin-1-yl)ethyl)-1H-1,2,3-triazol-4-yl)methyl *(E)*-3-formyl-5-((1S,4aS,8aS)-5,5,8a-trimethyl-2-methylenedecahydronaphthalen-1-yl)pent-3-enoate (8e)

Compound **8e** was prepared by the reaction of compound **3** (50 mg) with 2-azido-1-(4-phenylpiperazin-1-yl)ethan-1-one in ^{t}Butanol: H_2O mixture according to the procedure described in **5.8.4.** Yield: 47% (41 mg)

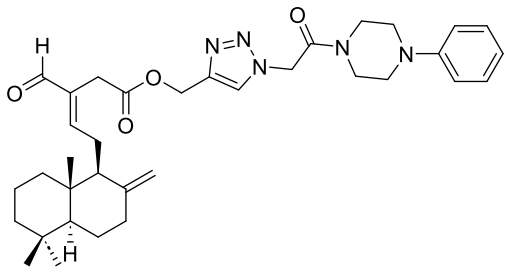

^{1}H NMR (500 MHZ, $CDCl_3$) δ: 9.26(s, 1H), 7.74 (s, 1H), 7.23 (t, *J* = 7.5 Hz, 2H), 6.89-6.88 (m, 3H), 6.59 (t, *J* = 6 Hz, 1H), 5.22 (s, 2H), 5.19 (s, 2H), 4.77 (s, 1H), 4.30 (s, 1H), 3.74 (s, 2H), 3.67 (s, 2H), 3.26 (dd, J_1 = 17 Hz, J_2 = 20.5 Hz, 2H), 3.15-3.13 (m, 4H), 2.49 - 0.96 (m, 14H), 0.82 (s, 3H), 0.75 (s, 3H), 0.66 (s, 3H)

^{13}C NMR (125 MHz, $CDCl_3$) δ: 193.58, 169.97, 163.28, 159.22, 148.06, 143.03, 135.97, 129.39, 125.49, 117.02, 107.93, 58.24, 56.39, 55.35, 50.95, 45.24, 42.19, 41.99, 39.57, 39.20, 37.85, 33.60, 29.69, 24.60, 24.10, 21.75, 19.30, 14.43

HRMS (ESI) m/z: $[M+Na]^+$ calculated for $C_{35}H_{47}N_5O_4Na$ is 624.3526, found 624.3530

5.8.6.15. Synthesis of (1-(2-oxo-2-(4-(4-(trifluoromethyl)phenyl)piperazin-1-yl)ethyl)-1H-1,2,3-triazol-4-yl)methyl *(E)*-3-formyl-5-((1S,4aS,8aS)-5,5,8a-trimethyl-2-methylenedecahydronaphthalen-1-yl)pent-3-enoate (8f)

Compound **8f** was prepared by the reaction of compound **3** (30 mg) with 2-azido-1-(4-(4-(trifluoromethyl)phenyl)piperazin-1-yl)ethan-1-one in ^{t}Butanol: H_2O mixture according to the procedure described in **5.8.4.** Yield: 50% (28 mg)

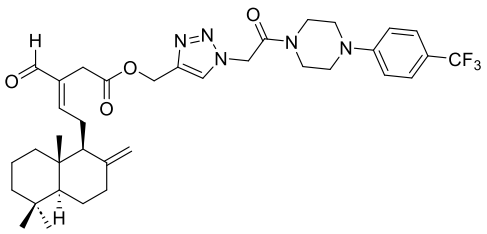

^{1}H NMR (500 MHZ, $CDCl_3$) δ: 9.26(s, 1H), 7.74 (s, 1H), 7.46 (d, *J* = 8 Hz, 2H), 6.92 (d, *J* = 8.5 Hz, 2H), 6.59 (t, *J* = 6.5 Hz, 1H), 5.22 (s, 2H), 5.19 (s, 2H), 4.77 (s, 1H), 4.30 (s, 1H), 3.76 (s, 2H), 3.70 (s, 2H), 3.25-3.24 (m, 6H), 2.49 - 0.97 (m, 14H), 0.82 (s, 3H), 0.75 (s, 3H), 0.66 (s, 3H)

^{13}C NMR (125 MHz, $CDCl_3$) δ: 193.55, 169.96, 163.38, 159.19, 152.25, 148.07, 143.14, 135.97, 126.68, 126.65, 125.40, 115.62, 107.91, 58.21, 56.40, 55.36, 50.96, 48.53, 48.27, 44.91, 41.99, 41.82, 39.57, 39.21, 37.84, 33.58, 29.70, 24.60, 24.10, 21.74, 19.30, 14.42

HRMS (ESI) m/z: $[M+Na]^+$ calculated for $C_{36}H_{46}F_3N_5O_4Na$ is 692.3400, found 692.3411

5.8.6.16. Synthesis of (1-(2-(4-(4-nitrophenyl)piperazin-1-yl)-2-oxoethyl)-1H-1,2,3-triazol-4-yl)methyl *(E)*-3-formyl-5-((1S,4aS,8aS)-5,5,8a-trimethyl-2-methylenedecahydronaphthalen-1-yl)pent-3-enoate (8g)

Compound **8g** was prepared by the reaction of compound **3** (29 mg) with 2-azido-1-(4-(4-nitrophenyl)piperazin-1-yl)ethan-1-one in ^{t}Butanol: H_2O mixture according to the procedure described in **5.8.4.** Yield: 47% (25 mg)

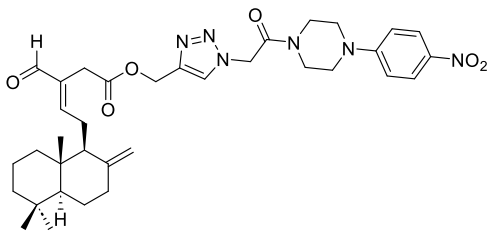

^{1}H NMR (500 MHZ, $CDCl_3$) δ: 9.25(s, 1H), 8.08 (d, *J* = 8.5 Hz, 2H), 7.74 (s, 1H), 6.78 (d, *J* = 8.5 Hz, 2H), 6.59 (t, *J* = 6Hz, 1H), 5.24 (s, 2H), 5.19 (s, 2H), 4.77 (s, 1H), 4.30 (s, 1H), 3.75-3.72 (m, 4H), 3.44-3.40 (m, 4H), 3.25 (s, 2H), 2.49 - 0.97 (m, 14H), 0.82 (s, 3H), 0.75 (s, 3H), 0.66 (s, 3H)

^{13}C NMR (125 MHz, $CDCl_3$) δ: 193.60, 169.98, 163.60, 159.31, 154.15, 148.08, 143.13, 139.39, 135.94, 125.98, 125.47, 113.25, 107.91, 58.17, 56.39, 55.35, 50.99, 46.87, 46.71, 44.63, 41.98, 41.61, 39.57, 39.21, 37.84, 33.58, 29.73, 24.61, 24.09, 21.74, 19.30, 14.43

HRMS (ESI) m/z: $[M+Na]^+$ calculated for $C_{34}H_{46}N_6O_6Na$ is 669.3377, found 669.3389

5.8.6.17. Synthesis of (1-(2-(4-(4-chlorophenyl)piperazin-1-yl)-2-oxoethyl)-1H-1,2,3-triazol-4-yl)methyl *(E)*-3-formyl-5-((1S,4aS,8aS)-5,5,8a-trimethyl-2-methylenedecahydronaphthalen-1-yl)pent-3-enoate (8h)

Compound **8h** was prepared by the reaction of compound **3** (30 mg) with 2-azido-1-(4-(4-chlorophenyl)piperazin-1-yl)ethan-1-one in ^{t}Butanol: H_2O mixture according to the procedure described in **5.8.4.** Yield: 45% (24 mg)

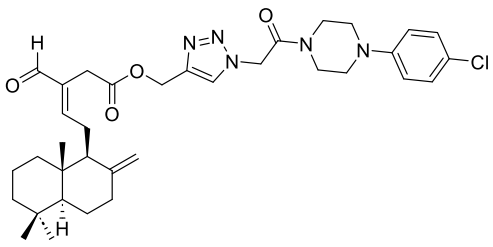

^{1}H NMR (500 MHZ, $CDCl_3$) δ: 9.26 (s, 1H), 7.74 (s, 1H), 7.18-7.17 (m, 2H), 6.82 (d, *J* = 8 Hz, 2H), 6.59 (t, *J* = 6Hz, 1H), 5.21 (s, 2H), 5.19 (s, 2H), 4.77 (s, 1H), 4.30 (s, 1H), 3.74 (t, *J* = 5.5 Hz, 2H), 3.67 (t, *J* = 5Hz , 2H), 3.26 (dd, J_1= 16.6 Hz, J_2= 21Hz, 2H), 3.12-3.09 (m, 4H), (2.49 - 0.97 (m, 14H), 0.82 (s, 3H), 0.75 (s, 3H), 0.66 (s, 3H)

^{13}C NMR (126 MHz, $CDCl_3$) δ: 193.53, 169.95, 163.29, 159.16, 148.07, 143.11, 135.98, 129.29, 125.40, 118.33, 107.92, 58.23, 56.40, 55.37, 50.95, 49.87, 49.54, 45.11, 42.00, 39.58, 39.22, 37.85, 33.58, 29.70, 24.60, 24.10, 21.74, 19.31, 14.42

HRMS (ESI) m/z: $[M+Na]^+$ calculated for $C_{35}H_{46}ClN_5O_4Na$ is 658.3136, found 658.3149

5.8.6.18. Synthesis of (1-(2-oxo-2-(4-(pyridin-2-yl)piperazin-1-yl)ethyl)-1H-1,2,3-triazol-4-yl)methyl *(E)*-3-formyl-5-((1S,4aS,8aS)-5,5,8a-trimethyl-2-methylenedecahydronaphthalen-1-yl)pent-3-enoate (8i)

Compound **8i** was prepared by the reaction of compound **3** (50 mg) with 2-azido-1-(4-(pyridin-2-yl)piperazin-1-yl)ethan-1-one in ^{t}Butanol: H_2O mixture according to the procedure described in **5.8.4.** Yield: 43% (36 mg)

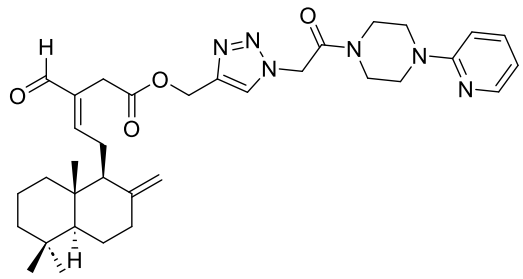

^{1}H NMR (500 MHZ, $CDCl_3$) δ: 9.27(s, 1H), 8.14 (s, 1H), 7.74 (s, 1H), 7.48 (t, J = 8 Hz, 1H), 6.65-6.58 (m, 3H), 5.22 (s, 2H), 5.19 (s, 2H), 4.77 (s, 1H), 4.30 (s, 1H), 3.70 (s, 2H), 3.62 (s, 4H), 3.50 (s, 2H), 3.25 (dd, J_1 = 17 Hz, J_2 = 20.5 Hz, 2H), 2.49 - 0.97 (m, 14H), 0.82 (s, 3H), 0.75 (s, 3H), 0.66 (s, 3H)

^{13}C NMR (125 MHz, $CDCl_3$) δ: 193.55, 169.96, 163.45, 159.20, 148.06, 138.15, 135.98, 125.48, 114.24, 107.92, 107.55, 58.25, 56.39, 55.35, 50.97, 45.10, 45.04, 41.99, 41.90, 39.57, 39.20, 37.85, 33.59, 29.69, 24.60, 24.10, 21.75, 19.30, 14.42

HRMS (ESI) m/z: $[M+H]^+$ calculated for $C_{34}H_{47}N_6O_4$ is 603.3659, found 603.3663

5.8.6.19. Synthesis of (1-(2-oxo-2-(4-(pyrimidin-2-yl)piperazin-1-yl)ethyl)-1H-1,2,3-triazol-4-yl)methyl *(E)*-3-formyl-5-((1S,4aS,8aS)-5,5,8a-trimethyl-2-methylenedecahydronaphthalen-1-yl)pent-3-enoate (8j)

Compound **8j** was prepared by the reaction of compound **3** (34 mg) with 2-azido-1-(4-(pyrimidin-2-yl)piperazin-1-yl)ethan-1-one in ^{t}Butanol: H_2O mixture according to the procedure described in **5.8.4.** Yield: 38% (22 mg)

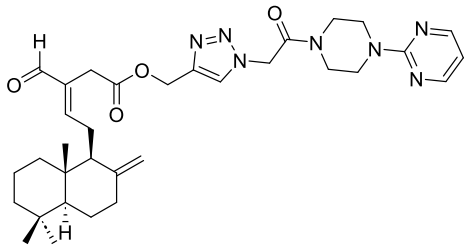

^{1}H NMR (500 MHZ, $CDCl_3$) δ: 9.27 (s, 1H), 8.29 (d, *J* = 4 Hz, 2H), 7.74 (s, 1H), 6.59 (t, *J* = 6.5 Hz, 1H), 6.52 (t, *J* = 4.5 Hz, 1H), 5.22 (s, 2H), 5.19 (s, 2H), 4.77 (s, 1H), 4.30 (s, 1H), 3.86 (s, 2H), 3.81 (s, 2H), 3.66 (s, 2H), 3.57 (s, 2H), 3.27 (dd, J_1 = 16.5 Hz, J_2 = 20.5 Hz, 2H), 2.49 - 0.96 (m, 14H), 0.82 (s, 3H), 0.75 (s, 3H), 0.66 (s, 3H)

^{13}C NMR (125 MHz, $CDCl_3$) δ: 193.52, 169.95, 163.48, 159.13, 157.78, 148.06, 143.03, 135.99, 125.45, 110.76, 107.91, 58.25, 56.40, 55.37, 50.99, 45.14, 43.65, 43.40, 42.13, 42.00, 39.57, 39.21, 37.85, 33.58, 29.69, 24.60, 24.10, 21.74, 19.30, 14.42

HRMS (ESI) m/z: $[M+Na]^+$ calculated for $C_{33}H_{45}N_7O_4Na$ is 626.3431, found 626.3429

5.8.6.20. Synthesis of *(E)*-2-(2-oxo-2-((1-(2-oxo-2-(4-phenylpiperazin-1-yl)ethyl)-1H-1,2,3-triazol-4-yl)methoxy)ethyl)-4-((1S,4aS,8aS)-5,5,8a-trimethyl-2-methylenedecahydronaphthalen-1-yl)but-2-enoic acid (9a)

Compound **9a** was prepared by the reaction of compound **7g** (17 mg) with sodium chlorite (10 equiv.) and sodium dihydrogen phosphate (10 equiv.) in ^{t}Butanol: H_2O mixture according to the procedure described in **5.8.5.** Yield: 57% (10 mg)

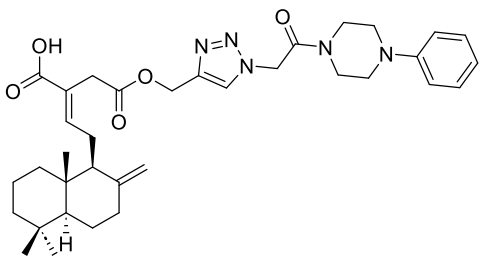

^{1}H NMR (500 MHZ, $CDCl_3$) δ: 7.74 (s, 1H), 7.31 (t, *J* = 7.5 Hz, 2H), 6.88-6.87 (m, 3H), 6.83 (t, *J* = 6 Hz, 1H), 5.26-5.20 (m, 4H), 4.73 (s, 1H), 4.30 (s, 1H), 3.28-3.25 (m, 4H), 3.26 (dd, J_1 = 17 Hz, J_2 = 20.5 Hz, 2H), 3.15-3.13 (m, 4H), 2.49 - 0.96 (m, 14H), 0.82 (s, 3H), 0.75 (s, 3H), 0.66 (s, 3H)

^{13}C NMR (125 MHz, $CDCl_3$) δ: 171.01, 169.98, 163.24, 149.23, 148.05, 143.01, 135.92, 129.39, 125.49, 117.01, 107.92, 58.21, 56.38, 55.36, 50.96, 45.25, 42.17, 41.98, 39.56, 39.21, 37.86, 33.64, 29.68, 24.62, 24.11, 21.76, 19.31, 14.42

HRMS (ESI) m/z: $[M+Na]^+$ calculated for $C_{35}H_{47}N_5O_5Na$ is 640.3475, found 640.3466

5.8.6.21. Synthesis *(E)*-2-(2-((1-(2-(4-(4-chlorophenyl)piperazin-1-yl)-2-oxoethyl)-1H-1,2,3-triazol-4-yl)methoxy)-2-oxoethyl)-4-((1S,4aS,8aS)-5,5,8a-trimethyl-2-methylenedecahydronaphthalen-1-yl)but-2-enoic acid (9b)

Compound **9a** was prepared by the reaction of compound **8h** (22 mg) with sodium chlorite (10 equiv.) and sodium dihydrogen phosphate (10 equiv.) in ^{t}Butanol: H_2O mixture according to the procedure described in **5.8.5.** Yield: 44% (20 mg)

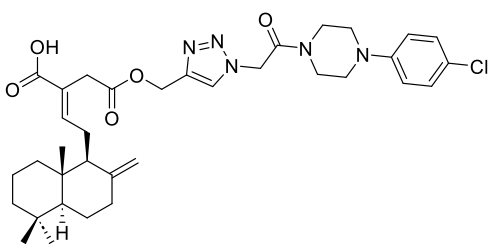

^{1}H NMR (500 MHZ, $CDCl_3$) δ: 7.72 (s, 1H), 7.17 (d, *J* = 8 Hz, 2H), 6.86 (t, *J* = 7Hz, 1H), 6.81 (d, *J* = 8.5 Hz, 2H), 5.22 (s, 2H), 5.20 (s, 2H), 4.73 (s, 1H), 4.29 (s, 1H), 3.70-3.62 (m, 4H), 3.26 (s, 2H), 3.13-3.05 (m, 4H), 2.31 - 0.95 (m, 14H), 0.81 (s, 3H), 0.74 (s, 3H), 0.63 (s, 3H)

^{13}C NMR (126 MHz, $CDCl_3$) δ: 170.82, 169.96, 163.87, 148.94, 148.11, 143.08,

129.24, 125.90, 124.55, 118.26, 107.84, 60.43, 57.96, 56.39, 55.31, 50.88, 45.01, 42.12, 42.00, 39.50, 39.22, 37.85, 33.58, 32.61, 24.27, 24.09, 21.75, 19.31, 14.42

HRMS (ESI) m/z: $[M+Na]^+$ calculated for $C_{35}H_{46}ClN_5O_4Na$ is 674.3085, found 674.3082

5.8.6.22. Synthesis of *(E)*-2-(2-((1-(2-(4-(4-bromo-2-fluorobenzyl)piperazin-1-yl)-2-oxoethyl)-1H-1,2,3-triazol-4-yl)methoxy)-2-oxoethyl)-4-((1S,4aS,8aS)-5,5,8a-trimethyl-2-methylenedecahydronaphthalen-1-yl)but-2-enoic acid (9c)

Compound **9c** was prepared by the reaction of compound **8c** (50 mg) with sodium chlorite (10 equiv.) and sodium dihydrogen phosphate (10 equiv.) in ^{t}Butanol: H_2O mixture according to the procedure described in **5.8.5.** Yield: 49% (25 mg)

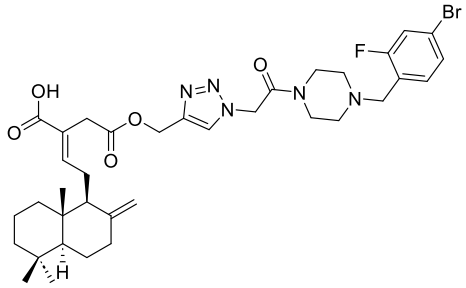

^{1}H NMR (500 MHZ, $CDCl_3$) δ: 7.73 (s, 1H), 7.33-7.18 (m, 3H), 6.81 (t, *J* = 6.5 Hz, 1H), 5.22- 5.19 (m, 4H), 4.73 (s, 1H), 4.30 (s, 1H), 3.70-3.47 (m, 4H), 3.25 (s, 2H), 2.65 - 0.99 (m, 18H), 0.82 (s, 3H), 0.74 (s, 3H), 0.64 (s, 3H)

^{13}C NMR (126 MHz, $CDCl_3$) δ: 170.98, 169.25, 164.05, 148.13, 148.02, 143.26, 127.92, 125.83, 124.91, 119.36, 107.84, 77.28, 77.03, 76.77, 57.82, 56.42, 55.33, 51.64, 51.25, 42.02, 39.51, 39.24, 37.87, 33.83, 33.60, 33.57, 32.81, 31.94, 31.63, 29.71, 24.18, 24.10, 22.70, 21.76, 19.33, 14.44, 14.20, 14.13.

HRMS (ESI) m/z: $[M+H]^+$ calculated for $C_{36}H_{48}BrFN_5O_5$ is 728.2823, found 728.2823

5.8.6.23. Synthesis of *(E)*-2-(2-oxo-2-((1-(2-oxo-2-(4-(pyrimidin-2-yl)piperazin-1-yl)ethyl)-1H-1,2,3-triazol-4-yl)methoxy)ethyl)-4-((1S,4aS,8aS)-5,5,8a-trimethyl-2-methylenedecahydronaphthalen-1-yl)but-2-enoic acid (9d)

Compound **9d** was prepared by the reaction of compound **8j** (29 mg) with sodium chlorite (10 equiv.) and sodium dihydrogen phosphate (10 equiv.) in ^{t}Butanol: H_2O mixture according to the procedure described in **5.8.5.** Yield: 57% (17 mg)

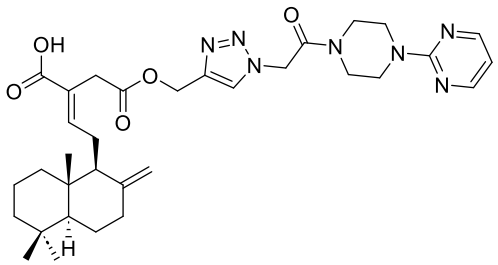

^{1}H NMR (500 MHZ, $CDCl_3$) δ: 8.44 (s, 2H), 7.75 (s, 1H), 6.82 (t, *J* = 6.5 Hz, 1H), 6.73 (s, 1H), 5.30 (s, 2H), 5.21 (s, 2H), 4.74 (s, 1H), 4.30 (s, 1H), 3.95 (s, 4H), 3.71 (s, 2H), 3.60 (s, 2H), 3.27 (s, 2H), 2.29 - 0.95 (m, 14H), 0.83 (s, 3H), 0.74 (s, 3H), 0.64 (s, 3H)

^{13}C NMR (125 MHz, $CDCl_3$) δ: 170.02, 169.92, 163.48, 159.13, 149.78, 148.06, 143.03, 135.99, 125.45, 110.76, 107.92, 58.24, 56.43, 55.37, 50.99, 45.14, 43.65, 43.40, 42.13, 42.00, 39.57, 39.21, 37.85, 33.58, 29.69, 24.60, 24.10, 21.79, 19.30, 14.42

HRMS (ESI) m/z: $[M+Na]^+$ calculated for $C_{33}H_{45}N_7O_5Na$ is 642.3380, found 642.3390

5.9. References

(1) Kumar, K.; Waldmann, H. Nature Inspired Small Molecules for Chemical Biology. *Isr. J. Chem.* **2019**, *59* (1), 41–51. https://doi.org/10.1002/ijch.201800105.

(2) Jalaja, R.; Leela, S. G.; Valmiki, P. K.; Salfeena, C. T. F.; Ashitha, K. T.; Krishna Rao, V. R. D.; Nair, M. S.; Gopalan, R. K.; Somappa, S. B. Discovery of Natural Product Derived Labdane Appended Triazoles as Potent Pancreatic Lipase Inhibitors. *ACS Med. Chem. Lett.* **2018**, *9* (7), 662–666. https://doi.org/10.1021/acsmedchemlett.8b00109.

(3) Jalaja, R.; Leela, S. G.; Mohan, S.; Nair, M. S.; Gopalan, R. K.; Somappa, S. B. Anti-Hyperlipidemic Potential of Natural Product Based Labdane-Pyrroles via Inhibition of Cholesterol and Triglycerides Synthesis. *Bioorg. Chem.* **2021**, *108*, 104664. https://doi.org/https://doi.org/10.1016/j.bioorg.2021.104664.

(4) Mohan, S.; Krishnan, L.; Madhusoodanan, N.; Sobha, A.; Jalaja, R.; Kumaran, A.; Vankadari, N.; Purushothaman, J.; Somappa, S. B. Linker-Based Pharmacophoric Design and Semisynthesis of Labdane Conjugates Active against Multi-Faceted Inflammatory Targets. *J. Agric. Food Chem.* **2024**, *72* (12), 6389–6401. https://doi.org/10.1021/acs.jafc.3c09536.

(5) Mohan, S.; Krishnan, L.; Madhusoodanan, N.; Sobha, A.; Babysulochana, A. D.; Vankadari, N.; Purushothaman, J.; Somappa, S. B. Ligand-Based Pharmacophoric Design and Anti-Inflammatory Evaluation of Triazole Linked Semisynthetic Labdane Conjugates. *ACS Med. Chem. Lett.* **2024**, 1260–1268. https://doi.org/10.1021/acsmedchemlett.4c00141.

(6) Acharya, A.; Yadav, M.; Nagpure, M.; Kumaresan, S.; Guchhait, S. K. Molecular Medicinal Insights into Scaffold Hopping-Based Drug Discovery Success. *Drug Discov. Today* **2024**, *29* (1), 103845. https://doi.org/https://doi.org/10.1016/j.drudis.2023.103845.

(7) Zhang, R. H.; Guo, H. Y.; Deng, H.; Li, J.; Quan, Z. S. Piperazine Skeleton in the Structural Modification of Natural Products: A Review. *J. Enzyme Inhib. Med. Chem.* **2021**, *36* (1), 1165–1197. https://doi.org/10.1080/14756366.2021.1931861.

(8) Jain, A.; Chaudhary, J.; Khaira, H.; Chopra, B.; Dhingra, A. Piperazine: A Promising Scaffold with Analgesic and Anti-Inflammatory Potential. *Drug Res. (Stuttg).* **2021**, *71* (2), 62–72. https://doi.org/10.1055/a-1323-2813.

(9) Kumari, S.; Carmona, A. V.; Tiwari, A. K.; Trippier, P. C. Amide Bond Bioisosteres: Strategies, Synthesis, and Successes. *J. Med. Chem.* **2020**, *63* (21), 12290–12358.

https://doi.org/10.1021/acs.jmedchem.0c00530.

(10) Meanwell, N. A. Applications of Bioisosteres in the Design of Biologically Active Compounds. *J. Agric. Food Chem.* **2023**, *71* (47), 18087–18122. https://doi.org/10.1021/acs.jafc.3c00765.

(11) Hatnapure, G. D.; Keche, A. P.; Rodge, A. H.; Birajdar, S. S.; Tale, R. H.; Kamble, V. M. Synthesis and Biological Evaluation of Novel Piperazine Derivatives of Flavone as Potent Anti-Inflammatory and Antimicrobial Agent. *Bioorganic Med. Chem. Lett.* **2012**, *22* (20), 6385–6390. https://doi.org/10.1016/j.bmcl.2012.08.071.

(12) Li, J.; Li, D.; Xu, Y.; Guo, Z.; Liu, X.; Yang, H.; Wu, L.; Wang, L. Design, Synthesis, Biological Evaluation, and Molecular Docking of Chalcone Derivatives as Anti-Inflammatory Agents. *Bioorganic Med. Chem. Lett.* **2017**, *27* (3), 602–606. https://doi.org/10.1016/j.bmcl.2016.12.008.

(13) Li, B.; Cai, S.; Yang, Y. A.; Chen, S. C.; Chen, R.; Shi, J. B.; Liu, X. H.; Tang, W. J. Novel Unsaturated Glycyrrhetic Acids Derivatives: Design, Synthesis and Anti-Inflammatory Activity. *Eur. J. Med. Chem.* **2017**, *139*, 337–348. https://doi.org/10.1016/j.ejmech.2017.08.002.

(14) Cinelli, M. A.; Do, H. T.; Miley, G. P.; Silverman, R. B. Inducible Nitric Oxide Synthase: Regulation, Structure, and Inhibition. *Med. Res. Rev.* **2020**, *40* (1), 158–189. https://doi.org/10.1002/med.21599.

(15) Bryan, N. S.; Grisham, M. B. Methods to Detect Nitric Oxide and Its Metabolites in Biological Samples. *Free Radic. Biol. Med.* **2007**, *43* (5), 645–657. https://doi.org/https://doi.org/10.1016/j.freeradbiomed.2007.04.026.

(16) Turner, M. D.; Nedjai, B.; Hurst, T.; Pennington, D. J. Cytokines and Chemokines: At the Crossroads of Cell Signalling and Inflammatory Disease. *Biochim. Biophys. Acta - Mol. Cell Res.* **2014**, *1843* (11), 2563–2582. https://doi.org/10.1016/j.bbamcr.2014.05.014.

(17) Howes, A.; Gabryšová, L.; O'Garra, A. Role of IL-10 and the IL-10 Receptor in Immune Responses. *Ref. Modul. Biomed. Sci.* **2014**, *1*, 1–11. https://doi.org/10.1016/b978-0-12-801238-3.00014-3.

(18) Saraiva, M.; O'Garra, A. The Regulation of IL-10 Production by Immune Cells. *Nat. Rev. Immunol.* **2010**, *10* (3), 170–181. https://doi.org/10.1038/nri2711.

(19) Simmons, D. L.; Botting, R. M.; Hla, T. Cyclooxygenase Isozymes: The Biology of Prostaglandin Synthesis and Inhibition. *Pharmacol. Rev.* **2004**, *56* (3), 387–437. https://doi.org/10.1124/pr.56.3.3.

(20) Aggarwal, B. B. Nuclear Factor-KB: The Enemy Within. *Cancer Cell*. 2004, pp 203–208. https://doi.org/10.1016/j.ccr.2004.09.003.

(21) Ghosh, S.; Hayden, M. S. New Regulators of NF-KB in Inflammation. *Nat. Rev. Immunol.* **2008**, *8* (11), 837–848. https://doi.org/10.1038/nri2423.

(22) Karin, M.; Ben-neriah, Y. Phosporilation Meets the Ubiquitination: The Control of NF- Kapp B Activity. *Annu. Rev. Immunol.* **2000**, *18*, 621–663.

ABSTRACT

Name of the Student: **Ms. Sangeetha Mohan**
Registration No.: 10CC19J39004
Faculty of Study: Chemical Sciences
Year of Submission: 2025
AcSIR academic centre/CSIR Lab: CSIR-National Institute for Interdisciplinary Science and Technology (CSIR-NIIST)
Name of the Supervisor: Dr. Sasidhar B. S.

Title of the thesis: **Rational Design and Discovery of Natural Product-Inspired Chemical Entities Active against Multi-Faceted Inflammatory Targets**

Natural products are a vital source for next-generation drugs, with plant-derived compounds well-known for their anti-inflammatory properties due to potent phytoconstituents and semi-synthetic derivatives. *Curcuma amada* (mango ginger), a rhizomatous herb from the *Zingiberaceae* family, has shown significant anti-inflammatory effects. As part of our medicinal chemistry efforts, we isolated a labdane diterpenoid, (*E*)-labda-8(17),12-diene-15,16-dial (**1**), from *C. amada* to explore its anti-inflammatory potential. Limitations of current anti-inflammatory treatments, including high costs and side effects, underscore the need for cost-effective, therapeutically improved drugs. Semi-synthetic modifications of natural leads provide a promising approach to optimize its pharmacological properties.

Chapter 1 delves into the concept of inflammation. A major focus is semisynthesis, a versatile natural product research tool bridging the gap between initial discovery and the development of viable drugs. The chapter also reviews pivotal milestones in semisynthetic drug discovery, showcasing recent examples where modifications of natural products have led to the identification of new anti-inflammatory agents. Additionally, the anti-inflammatory potential of *Curcuma amada* is highlighted. **Chapter 2** outlines the materials and methods employed in the experiments described in the subsequent chapters.

In **Chapter 3,** we present rational designing and synthesis of novel phytochemical entities (NPCEs) through strategic linker-based molecular hybridization of aromatic or hetero-aromatic fragments with the labdane dialdehyde, isolated from the medicinally and nutritionally significant rhizomes of the plant *C. amada*. Among the synthesised novel compounds, **5f** exhibited the highest anti-inflammatory potential by inhibiting the COX-2 enzyme (IC_{50} 17.67 μM), with a four-fold increased activity than the standard drug indomethacin (IC_{50} 67.16 μM). **5f** also significantly reduced the levels of LPS-induced NO and cytokines much better than the positive control. The *in silico* data well supported the *invitro* studies. This infers the labdane derivative **5f** is a promising lead candidate as an anti-inflammatory agent for further exploring the therapeutic landscape.

In **Chapter 4**, a ligand-based pharmacophoric approach was employed to design and synthesize thirty-three novel semi-synthetic labdane-appended triazolyl isatins. The initial screening revealed that compound **7a** exhibited an anti-inflammatory effect (NO inhibition, IC_{50} 3.13 μM), surpassing both the positive control indomethacin (NO inhibition, IC_{50} 7.31 μM) and the parent compound labdane dialdehyde. Mechanistic and *in silico* studies confirmed that **7a** inhibits the NF-κB pathway, reducing COX-2 and iNOS expression, highlighting its potential as a potent anti-inflammatory agent.

In **Chapter 5**, as part of the lead optimization process, we have modified the existing lead compound **7a** by incorporating different heterocyclic amides into the labdane template. Among the synthesised derivatives, **9b** (NO inhibition, IC_{50} 1.46 0.07 μM) exhibited nearly 2-fold increased activity than indomethacin and the existing lead **7a** (NO inhibition, IC_{50} 3.13 μM). The levels of the pro-inflammatory cytokines were reduced by **9b**. Studies investigating mechanisms found that **9b** reduced the expression of COX-2 and iNOS by inhibiting the NF-κB signalling pathway. Molecular modelling studies on NF-κB proteins provided valuable support for these results and indicated that **9b** has the potential as a powerful anti-inflammatory agent.

Details of Publications

List of publications emanating from the thesis

1) **Sangeetha Mohan.**; Krishnan, L.; Madhusoodanan, N.; Sobha, A.; Jalaja, R.; Kumaran, A.; Vankadari, N.; Purushothaman, J.; Somappa, S. B. Linker-Based Pharmacophoric Design and Semisynthesis of Labdane Conjugates Active against Multi-Faceted Inflammatory Targets. *ACS J. Agric. Food Chem.* **2024**, *72* (12), 6389–6401. https://doi.org/10.1021/acs.jafc.3c09536

2) **Sangeetha Mohan.**; Krishnan, L.; Madhusoodanan, N.; Sobha, A.; Babysulochana, A. D.; Vankadari, N.; Purushothaman, J.; Somappa, S. B. Ligand-Based Pharmacophoric Design and Anti-Inflammatory Evaluation of Triazole Linked Semisynthetic Labdane Conjugates. *ACS Med. Chem. Lett.* **2024**, *15* (8), 1260–1268. *Published as part of the special issue on "Natural Products Driven Medicinal Chemistry".* https://doi.org/10.1021/acsmedchemlett.4c00141

3) **Sangeetha Mohan**.; Krishnan, L.; Vankadari, N.; Purushothaman, J.; Somappa, S. B. Lead Optimization of Labdane Conjugates into Novel Therapeutics for Inflammation Modulation. (Manuscript to be communicated)

List of publications not related to the thesis work

4) **Sangeetha Mohan**.; Krishna, M. S. A.; Chandramouli, M.; Keri, R. S.; Patil, S. A.; Ningaiah, S.; Somappa, S. B. Antibacterial Natural Products from Microbial and Fungal Sources : A Decade of Advances. *Mol. Divers.* **2022**, *27*(1), 517–541. https://doi.org/10.1007/s11030-022-10417-5.

5) Krishna, A.[†]; **Sangeetha Mohan**. [†]; Ashitha, K. T.; Chandramouli, M.; Alaganandam, K.; Ningaiah, S.; Babu, S. K.; Somappa, S. B. Marine Based Natural Products: Exploring the Recent Developments in the Identification of Antimicrobial Agents. *Chem. Biodivers.* **2022**, 19 [† Equally Contributed] https://doi.org/10.1002/cbdv.202200513

6) Sobha, A.; **Sangeetha Mohan**.; Madhusoodanan, N.; Krishnana, G. V.; Varughese, S.;Kumar, B .S. D.; Ningaiah, S.; Shridevi, D.; Somappa, S. B. Pyrazole Appended Hetero-Hybrids: Bioisosteric Design, Synthesis, In silico and In Vitro Antibacterial and Anti-inflammatory Evaluations. *J. Mol. Struct.* **2023,** *1289*, 135780. https://doi.org/10.1016/j.molstruc.2023.135780

7) Veedu, K. K.; **Sangeetha Mohan.**; Somappa, S. B.; Gopalan, N. K. Eco-Friendly Anticorrosive Epoxy Coating from Ixora Leaf Extract: A Promising Solution for Steel Protection in Marine Environment. *J. Clean. Prod.* **2022**, *340*, 130750. https://doi.org/10.1016/j.jclepro.2022.130750

8) Jalaja, R.; Leela, S. G.; **Sangeetha Mohan.**; Nair, M. S.; Gopalan, R. K.; Somappa, S. B. Anti-Hyperlipidemic Potential of Natural Product Based Labdane-Pyrroles via Inhibition of Cholesterol and Triglycerides Synthesis. *Bioorg. Chem.* **2021**, *108*, 104664. https://doi.org/10.1016/j.bioorg.2021.104664.

9) Sobha, A.; Ganapathy, A.; **Sangeetha Mohan**.; Madhusoodanan, N.; Babysulochana, A. D.; Alaganandan, K.; Somappa, S. B. Novel Small Molecule-Based Acetylcholinesterase (AChE) Inhibitors: From Biological Perspective to Recent Developments. *Eur. J. Med. Chem. Reports* **2024**, *12*, 100237. https://doi.org/https://doi.org/10.1016/j.ejmcr.2024.100237.

10) Sobha, A.; Krishnan, L.; Doddamani S. V.; Vijayakumar S.; **Sangeetha Mohan**.; Pai S. A.; Ghosh D.; Purushothaman, J.; Somappa, S. B. Exploring Novel Triazole Derivatives as Multi-Target-Directed-Ligands: A Promising Avenue to Attenuate Alzheimer's Disease (Manuscript to be communicated)

11) Sobha, A.; Krishnan, L.; **Sangeetha Mohan**.; Purushothaman, J.; Somappa, S. B. Discovery of Phthalimide Benzylpyridinium Derivatives as Multifunctional Agents against Alzheimer's Disease. (Manuscript under preparation)

Contributions to Academic Conferences

1) Natural Product-based Pharmacophoric Design and Semi-Synthesis of Labdane Conjugates Active against Multi-Faceted Inflammatory Targets. **Sangeetha Mohan**, Lekshmy Krishnan, Naveen Vankadari, Jayamurthy Purushothaman and Sasidhar B. Somappa, ***36th Kerala Science Congress*** at Government College, Kasaragod, Kerala, *9-11 February 2024* [Oral presentation]

Background: Prolonged inflammation leads to the genesis of various inflammatory diseases. Due to the excessive cost and hostile side effects associated with existing therapies for inflammation, there is an unmet medical need to develop new, therapeutically improved and cost-effective drugs to treat inflammation and associated diseases.

Method: We present the rational design and synthesis of novel phytochemical entities (NPCEs) through a linker-based molecular hybridization of aromatic / hetero-aromatic fragments with the labdane dialdehyde, isolated from the rhizomes of *Curcuma amada*. We employed a comprehensive *in-vitro* study assessing its inhibitory effect on COX-2 enzyme and other inflammatory mediators *viz.* NO, TNF-α, IL-6 and IL-1α, in bacterial lipopolysaccharide-stimulated macrophages, as well as *in-silico* molecular modelling studies targeting the inflammation regulator COX-2 enzyme.

Results: Among the synthesized compounds, **5f** exhibited the highest anti-inflammatory potential by inhibiting COX-2 enzyme (IC_{50} 17.67 ± 0.89 μM), with a four-fold increased activity than the standard drug indomethacin (IC_{50} 67.16 ± 0.17 μM). **5f** also significantly reduced the levels of LPS-induced NO, TNF-α, IL-6, and IL-1α. Molecular mechanistic studies revealed that the anti-inflammatory effect of **5f** was associated with the inhibition of NF-κB signalling pathway.

Conclusions: The results suggested that the compound **5f** holds the potential as a novel promising anti-inflammatory agent. The study clearly emphasizes the role of semi-synthetic modifications in the enhancement of the bioactivity of natural products.

Keywords. *Curcuma amada*, labdane-conjugates, TNF-α, IL-6, IL-1α, cytokines, COX-2

2) Mitochondriotropic Oleanolic Acid TPP Conjugates: Isolation, Semi-Synthesis and Antioxidant Evaluation. **Sangeetha Mohan,** Michael G. Ibok, Raghu K. Gopalan, Sasidhar B. Somappa, **National Seminar on Recent Trends in Disease Prevention and Health Management** at CSIR-National Institute for Interdisciplinary Science and Technology, Thiruvananthapuram, Kerala, 14 & 15 December 2022 [Poster presentation]

3) Triphenylphosphine conjugates of oleanolic acid isolated from macrostyla longistyla as potential mitochondrial antioxidants. **Sangeetha Mohan,** Michael G. Ibok, Raghu K. Gopalan, Sasidhar B. Somappa, ***International Seminar on Plant Chemistry, Gene Prospecting and Clinical Biology*** organised by *Kerala Academy of Sciences Thiruvananthapuram, Kerala* 10 & 11, November 2022 [Oral presentation]

   Macrosphyra longistyla is a climbing shrub which belongs to the family Rubiaceae. It is a native of Africa and is found in several tropical countries. Bio-assay guided fractionation of its crude ethyl acetate leaf extract led to the isolation of oleanolic acid (OA), a penta-cyclic triterpenoid, as colourless crystals. Oleanolic acid (3b-hydroxyolean-12-en-28-oic acid) and its derivatives are reported to possess several promising biological properties such as hepatoprotective effects, anti-inflammatory, anti-oxidant and anti-cancer activities.

   Mitochondria are the organelles where reactive oxygen species are released as a result of its oxidative metabolic activities. Rational design of the anti-oxidants that target mitochondria are being developed as a new strategy to reduce oxidative stress in mitochondria. Mitochondriotropic anti-oxidants are usually generated by conjugating a bioactive to a lipophilic triphenyl phosphonium cation (TPP). Hence, we hypothesized that the conjugation of the bioactive oleanolic acid to TPP would lead to the targeted mitochondriotropic action of the lead bioactive and also enhance its bioavalability. Oleanolic acid (OA) was reacted with propyl triphenylphosphonium bromide (TPP) in the presence of triethyl amine, in acetonitrile at room temperature, in order to synthesise TPP conjugated oleanolic acid (OATPP) in good yield. The related chemistry and biology will be presented in the poster, in detail.

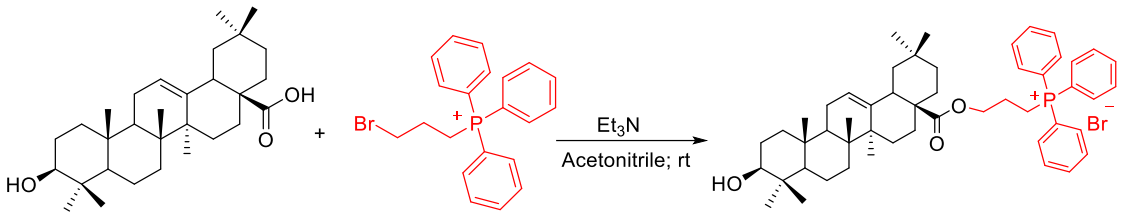

(OA) (TPP) (OATPP)

Keywords: Oleanolic acid, TPP conjugate, *Macrosphyra longistyla*, mitochondrial antioxidant

JOURNAL OF AGRICULTURAL AND FOOD CHEMISTRY

pubs.acs.org/JAFC Article

Linker-Based Pharmacophoric Design and Semisynthesis of Labdane Conjugates Active against Multi-Faceted Inflammatory Targets

Sangeetha Mohan, Lekshmy Krishnan, Nithya Madhusoodanan, Anjali Sobha, Renjitha Jalaja, Alaganandam Kumaran, Naveen Vankadari, Jayamurthy Purushothaman,* and Sasidhar B. Somappa*

Cite This: J. Agric. Food Chem. 2024, 72, 6389−6401 Read Online

ACCESS | Metrics & More | Article Recommendations | Supporting Information

ABSTRACT: Prolonged inflammation leads to the genesis of various inflammatory diseases such as atherosclerosis, cancer, inflammatory bowel disease, Alzheimer's, etc. The uncontrolled inflammatory response is characterized by the excessive release of pro-inflammatory mediators such as nitric oxide (NO), tumor necrosis factor-alpha (TNF-α), interleukin-6 (IL-6), interleukin-1alpha (IL-1α), and inflammatory enzymes such as cyclooxygenase-2 (COX-2). Hence, the downregulation of these inflammatory mediators is an active therapy to control aberrant inflammation and tissue damage. To address this, herein, we present the rational design and synthesis of novel phytochemical entities (NPCEs) through strategic linker-based molecular hybridization of aromatic/heteroaromatic fragments with the labdane dialdehyde, isolated from the medicinally and nutritionally significant rhizomes of the plant *Curcuma amada*. To validate the anti-inflammatory potential, we employed a comprehensive *in vitro* study assessing its inhibitory effect on the COX-2 enzyme and other inflammatory mediators, *viz*., NO, TNF-α, IL-6, and IL-1α, in bacterial lipopolysaccharide-stimulated macrophages, as well as *in-silico* molecular modeling studies targeting the inflammation regulator COX-2 enzyme. Among the synthesized novel compounds, **5f** exhibited the highest anti-inflammatory potential by inhibiting the COX-2 enzyme (IC_{50} = 17.67 ± 0.89 μM), with a 4-fold increased activity relative to the standard drug indomethacin (IC_{50} = 67.16 ± 0.17 μM). **5f** also significantly reduced the levels of LPS-induced NO, TNF-α, IL-6, and IL-1α, much better than the positive control. Molecular mechanistic studies revealed that **5f** suppressed the expression of COX-2 and pro-inflammatory cytokine release dose-dependently, which was associated with the inhibition of the NF-κB signaling pathway. This infers that the labdane derivative **5f** is a promising lead candidate as an anti-inflammatory agent to further explore its therapeutic landscape.

KEYWORDS: *Curcuma amada, labdane-conjugates, TNF-α, IL-6, IL-1α, COX-2, NF-κB*

1. INTRODUCTION

Inflammation is the natural immunological response of the body toward external stimuli such as microbial invasions or tissue injury.[1] However, prolonged inflammation can lead to the pathogenesis of various inflammatory diseases such as atherosclerosis,[2] cancer,[3] Alzheimer's,[4] inflammatory bowel disease,[5] type II diabetes,[6] etc. Steroidal drugs, though effective against inflammation, are often associated with irreversible side effects such as hypertension, osteoporosis, immunosuppression, glucose elevation, etc.[7] Today, inflammation is mainly treated with nonsteroidal anti-inflammatory drugs (NSAIDs) or anticytokine biologics. However, these therapies show clinical inefficacy due to their high cost and unwarranted side effects.[8,9] Therefore, there is an unmet medical need to develop new, therapeutically improved and cost-effective drugs to treat inflammation and associated diseases.[10] The uncontrolled inflammatory response is characterized by the excessive release of pro-inflammatory mediators such as nitric oxide (NO), TNF-α, IL-6, IL-1α, and inflammatory enzymes such as cyclooxygenase-2 (COX-2) etc. Hence, the down-regulation of these inflammatory factors, such as cytokines, chemokines, and enzymes, can be an active therapy to control aberrant inflammation and tissue damage.[11]

Natural products continue to be a major alternative source for the development of next-generation drugs.[12] Plant-based natural products, in particular, have been well documented for their anti-inflammatory properties, owing to their therapeutically potent phytoconstituents and their semisynthetic derivatives.[13,14] *Curcuma amada* (mango ginger), a rhizomatous edible herb, belongs to a medicinally significant plant family called Zingiberaceae. Various extracts, preparations, and bioactives from many species of its genus *Curcuma* have been well explored for their anti-inflammatory properties.[15] The rhizomes of *Curcuma amada* impart a distinctive raw mango flavor, which makes them popular in culinary dishes. Furthermore, the rhizomes, being the storehouse of bioactives, are widely used as coolants, astringents, appetizers, and nutraceuticals.[16−18] Due to its wide popularity in traditional medicine and food preparations, it is the second-largest cultivated *Curcuma* species after *C. longa*.[16,19] The rhizomes of *C. amada* are a rich source of essential oils with remarkable antioxidant, insecticidal, antibacterial, etc. properties.[20] Around 130 phytochemicals are reported to be isolated from the

Received: December 15, 2023
Revised: March 2, 2024
Accepted: March 4, 2024
Published: March 18, 2024

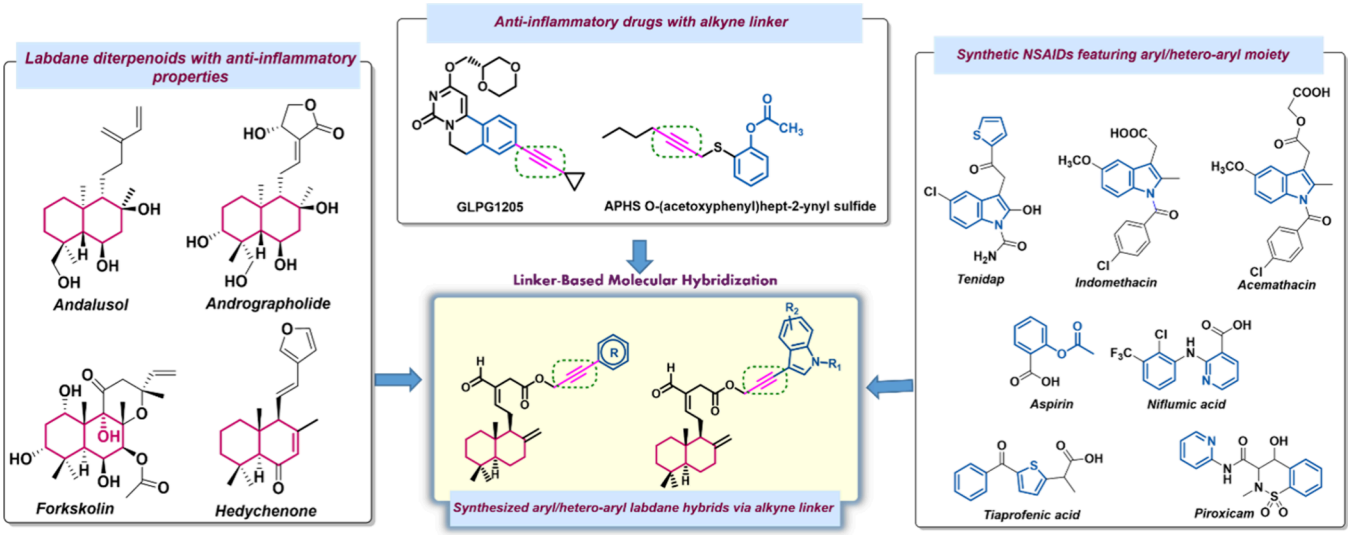

Figure 1. Rationale for the design and synthesis of aryl/heteroaryl appended labdane conjugates.

rhizomes[21] and possess various biological properties such as antimicrobial, hepatoprotective, anticancer, analgesic, etc. properties.[22−24] Moreover, the extracts of *C. amada* rhizomes have been reported to have anti-inflammatory properties at various acute and chronic phases of inflammation.[25,26] In the present work, we have isolated the abundant bioactive marker compound, a labdane diterpenoid, (*E*)-labda-8(17),12-diene-15,16-dial (**1**), from the rhizomes of *C. amada*, to further explore the anti-inflammatory properties of the plant.

Among the plant-based secondary metabolites, labdane diterpenoids have emerged as unique naturally occurring leads for the contemporary drug development process. There has been substantial evidence about the apparent interventions of labdane diterpenoids in inflammatory diseases, over the past decade.[27−30]

Semisynthetic modification of therapeutically proven lead natural products is one of the most successful approaches to optimizing their pharmacological properties and also to explore their vivid mode of action.[31−33] We have previously reported a series of novel labdane-appended scaffolds with very promising antiobesity and antihyperlipidemic properties.[34,35] These encouraging discoveries provided the insights for us to continue our focused efforts on medicinal chemistry,[36−42] in particular natural-product-based semisynthetic modifications for the development of therapeutically improved scaffolds. Therefore, in the present work, we have rationally designed and synthesized a series of 27 new phytochemical entities (NPCEs), by the strategic inclusion of aromatic or heteroaromatic fragments to the labdane template via a linker-based molecular hybridization (Figure 1) and explored their potential toward multifaceted inflammatory targets.

2. MATERIALS AND METHODS

All the chemicals and reagents, used for isolation and semisynthetic modifications, were of commercial reagent grade and were purchased from Sigma-Aldrich and Spectrochem. Solvents were purchased from Merck and were distilled before use. TLC plates (silica gel 60 F254) were used for monitoring the purity of the isolated compounds and the reaction progress. The IR spectra were recorded on a Bruker Alpha-T FT-IR spectrometer. ^{1}H and ^{13}C NMR spectra were recorded at 500 and 125 MHz, respectively, on a Bruker ASCEND spectrometer using $CDCl_3$ as the solvent and tetramethylsilane (TMS) as the internal standard. Chemical shift values are expressed in δ scale and coupling constants in hertz. In ^{1}H NMR, the solvent ($CDCl_3$) peak appeared as a singlet at δ 7.19, and in ^{13}C NMR, the peak appeared as a triplet at δ 77.0. Mass spectra were recorded under HRMS (ESI) using Thermo Scientific Exactive Orbitrap mass spectrometer. The natural compound and its synthesized analogs were purified by column chromatography using silica gel (100−200 mesh), using a mixture of hexane-ethyl acetate as the solvent system. A Heidolph rotary evaporator was used for the removal of solvents. Dulbecco's Modified Eagle's Medium (DMEM-high glucose) and 100 U/L mL penicillin-streptomycin (100 μg/mL) mix were purchased from Himedia Pvt. Ltd. (Mumbai, India). Fetal bovine serum (FBS) was from Gibco (Grand Island, NY). 3-[4,5-Dimethylthiazol-2-yl]-2,5-diphenyl tetrazolium bromide (MTT) and indomethacin were purchased from Sigma-Aldrich (U.S.A.). An IL-1α ELISA kit and COX-2 inhibitor screening kit (fluorometric) were purchased from Abcam (U.K.). TNF-α and IL-6 ELISA kits were purchased from BD Biosciences (U.S.A.). Absorbance and fluorescence were recorded using a microplate reader (BIOTEK- USA). Immunofluorescence images were captured using a fluorescent microscope (OLYMPUS, Japan).

2.1. Chemistry. *Isolation of E-labda 8(17),12-diene-15,16-dial (**1**).* A 1 kg amount of dried and powdered rhizomes of *C. amada* was extracted three times with chloroform. Then, 50 g of crude extract was obtained after solvent removal, which was then subjected to column chromatography on silica gel (100−200 mesh). Different fractions of approximately 100 mL volume were collected by gradient elution using different polarities of hexane and ethyl acetate mixture. The fractions collected in 5% ethyl acetate−hexane were crystallized in hexane to obtain the pure compound **1** (*E*-labda 8(17),12-diene-15,16-dial, 15 g) as a white solid. The structure of compound **1** was confirmed by various spectroscopic and analytical methods, *viz.*, IR, ^{1}H NMR, ^{13}C NMR, and HRMS, as well as by comparing it with the literature.[24,43]

*General Procedure for the Synthesis of Aromatic/Heteroaromatic Labdane Derivatives (**5a**−**5za**).* To a stirred solution of compound **3** and aryl/heteroaryl iodides (**4**, 1.2 equiv) in dry DMF, $Pd(Ph_3P)_2Cl_2$ (0.05 equiv), CuI (0.02 equiv), and triethyl amine (2 equiv) were added. The reaction mixture was stirred at room temperature until completion of the reaction, as indicated by TLC. The reaction mixture was diluted with water, extracted with ethyl acetate, and dried over Na_2SO_4. The solvent was removed under reduced pressure, and the product was purified by silica gel column chromatography, using ethyl acetate and hexane as the solvent system, to afford the pure products in good yields.[44]

2.2. Biology. *Cell Culture.* Murine macrophage cell line RAW264.7 was procured from NCCS (Pune), and the cells were maintained in Dulbecco's Modified Eagle Medium (DMEM)

https://doi.org/10.1021/acs.jafc.3c09536
J. Agric. Food Chem. 2024, 72, 6389−6401

Scheme 1. Synthesis of Aryl/hetero-aryl Appended Labdane Derivatives *via* Sonogashira Coupling (5a−5za)

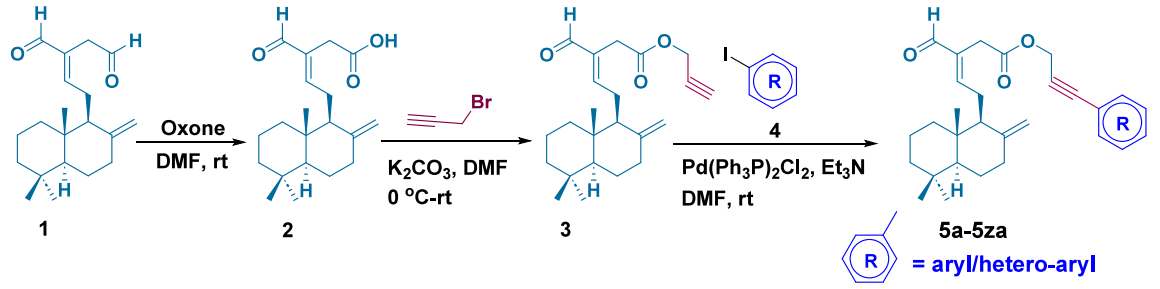

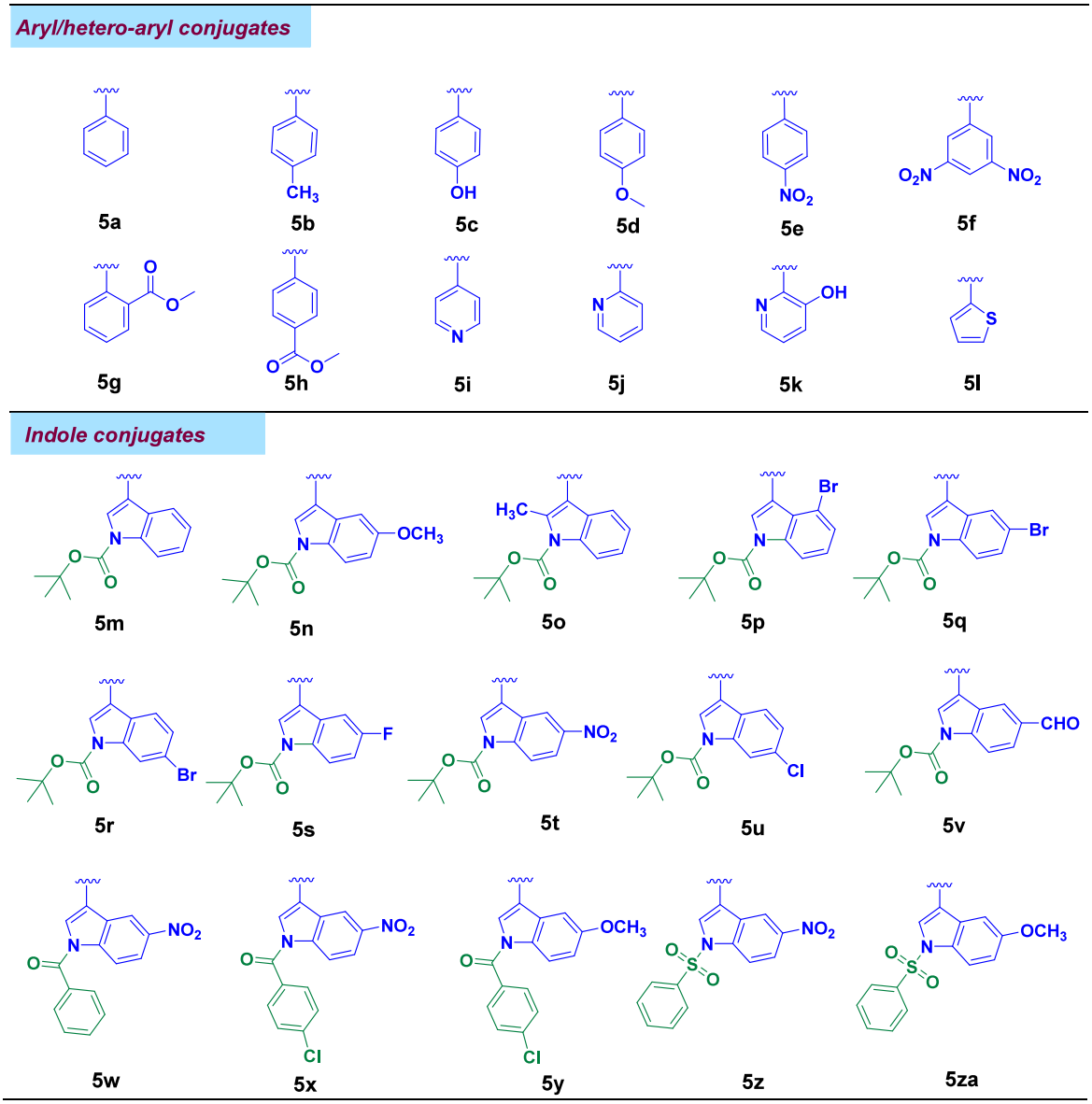

supplemented with 10% fetal bovine serum and 100 units/mL of penicillin streptomycin mix. The cell cultures were maintained at 37 °C in 5% CO_2 in a humidified atmosphere.

MTT Assay. To determine the noncytotoxic concentration in RAW264.7, an MTT assay[45] was performed for 24 h. RAW264.7 cells were cultured in a 96-well plate at a density of 1×10^4 cells/well, and after attaining 70% confluency, the cells were treated with various concentrations of compounds (5 μM, 10 μM, and 20 μM). After 24 h of pretreatment, the pretreated medium was decanted and washed, and 100 μL of MTT (0.5 mg/mL) suspended in plain medium was added and incubated for 4 h at 37 °C in a CO_2 incubator. The supernatant was decanted followed by the addition of dimethyl sulfoxide (DMSO) to each well. The plate was held on for 30 min in a plate shaker and the absorbance was recorded at 570 nm using a microplate reader (BIOTEK- USA). Percentage viability was calculated using the following equation:

$$\text{Percentage of viability} = \frac{[\text{Absorbance of sample}]}{\text{Absorbance of control}} \times 100$$

Determination of Nitric Oxide (NO) Production. Followed by pretreatment with compounds of varying concentrations for 1 h and

https://doi.org/10.1021/acs.jafc.3c09536
J. Agric. Food Chem. 2024, 72, 6389−6401

coincubated with lipopolysaccharide LPS (1 μg/mL) for an additional 23 h, the concentration of nitrite in the culture medium as a sign of nitric oxide production was quantified using the Griess method.[46] Briefly, 50 μL of Griess reagent (1% sulfanilamide and 0.1% naphthylethylenediamine dihydrochloride in 2.5% phosphoric acid) and an equal volume of cell supernatant after pretreatment was conflated, and the plate was incubated for 10 min at room temperature. The absorbance was measured in a microplate reader (BIOTEK, USA) at 540 nm. The concentration of nitrite was quantified based on a sodium nitrite standard curve. Indomethacin was used as a positive control.

COX-2 Inhibitory Assay. The potential of compounds to inhibit the enzyme COX-2 was determined using a COX2 inhibitor screening kit (ABCAM, ab283401, fluorometric) according to the manufacturer's instructions. The IC_{50} value of the compounds was determined from the concentration−inhibition response curve.

Measurement of Proinflammatory Cytokines (TNF-α, IL-6, and IL-1α). RAW264.7 cells, seeded in six-well plates (1×10^6 cells/well), were treated with compounds at 20 μM concentration and LPS (1 μg/mL) for a period of 24 h. The pretreated cell-free culture supernatant was collected, and the concentrations of the cytokine levels (TNF-α, IL-6, and IL-1α) in the culture medium were determined using ELISA kits according to the manufacturer's instructions. Indomethacin was employed as the positive control. The natural compound was also expended for the comparative evaluation of these semisynthetic molecules.

Western Blotting. Raw 264.7 cells were seeded into a six-well plate at a density of 4×10^6 cells per well. The cells were pretreated with the test compounds **5f** (10 and 20 μM) and the positive control indomethacin (20 μM) for 2 h and then coincubated with LPS (1 μg/mL) for a period of 24 h. The cells were harvested, lysed with 200 μL of RIPA cell lysis buffer (Sigma, United States), and incubated at 4 °C for 30 min. The cell lysate was collected and centrifuged for 5 min at 4 °C, and the concentration of total protein was measured using a BCA protein assay kit (Pierce, Thermo Fischer). Protein samples were resolved using 8−10% SDS-polyacrylamide gel electrophoresis and transferred to polyvinylidene difluoride (PVDF) membranes electrophoretically. The membranes were blocked with tris-buffered saline containing 0.1% Tween 20 (TBST) and 5% skim milk for 1 h at room temperature. Each blotted membrane was incubated with the specific primary antibody against COX-2, NF-κB, p-NF-κB, and β-actin (1:1000) overnight at 4 °C. The membranes were washed with TBST three times and incubated with HRP-conjugated secondary antibody (1:2000) for 2 h at room temperature. The membranes were then probed with the ECL substrate (Thermo Fisher Scientific, Massachusetts, USA) in Chemidoc MP Imaging systems (BioRad, USA). Densitometric analysis of the obtained bands was performed using Image lab software version 6.1 (BioRad, USA).

Immunofluorescence Assay. Raw 264.7 cells were seeded at a density of 2×10^5 cells into a 96-black-well clear-bottomed plate. The cells were pretreated with compound **5f** (10 and 20 μM) and the positive control indomethacin (20 μM) for 2 h and then coincubated with LPS (1 μg/mL) for a period of 24 h. After incubation, cells were washed twice with 200 μL of PBS and fixed with 4% paraformaldehyde for 15 min. The cells were permeabilized with 0.5% Triton x-100 for 10 min and then blocked with 5% bovine serum albumin (BSA) in PBS for 1 h at room temperature. The cells were then incubated overnight with a primary antibody specific to NF-κb p65 (1:250) at 4 °C. The cells were washed with PBST and incubated with a secondary antibody labeled with Alexa flour 488 diluted to 1:400 in PBST at 37 °C for 2 h. After washing, the nuclei were stained with 4′,6-diamidino-2-phenylindole (DAPI), and the wells were washed with PBS. A fluorescent microscope (OLYMPUS, Japan) was used to capture the images, with excitation/emission wavelengths of 490/540 nm for Alexa Fluor-488 and 360/450 nm for DAPI.

Statistical Analysis. All the experiments were completed in triplicate, and the data are expressed as mean ± standard deviation (SD). Data were analyzed by GraphPad software: Dotmatics, followed by a two-sample unpaired t test. A P value $P < 0.001$ was considered to be statistically significant.

2.3. Molecular Modeling Studies of Aryl/Heteroaryl Labdane Derivatives with COX-2. We used structure-guided drug-binding analysis to screen our synthesized labdane derivatives for the potential target protein COX-2 (PDB:5KIR). The server SwissDock (http://swissdock.ch/) was primarily used for docking our novel compounds with COX-2 and then further validated using another server HADDOCK2.2 (https://haddock.science.uu.nl/) to obtain unbiased results. Both servers showed consistent docking results, indicating three positions where our compounds could potentially interact with COX-2 (Supporting Information, Figure S2 and Figure S3): a single true site (C1) and two false-positive sites (C2, C3). We assessed and corroborated these sites based on C-score (confidence score), Z-score (clash score), and based on known active site pockets. To select the best docking site and mode/orientation of the bound drug, we considered binding free energies and overall occupancy of the bound drug. The final best-fit model of individual drugs/ligands from Scheme 1, docked in COX-2 (Supporting Information, Figure S2), was visualized in PyMol.

3. RESULTS AND DISCUSSION

3.1. Chemistry. The majority of the traditional anti-inflammatory drugs in the market, such as aspirin, diclofenac, ibuprofen, etc., feature a simple aryl type core (Figure 1). Hence, we hypothesized that the conjugation of an aryl core to the active labdane system, via an alkyne linker, would lead to the generation of new hybrid molecules active against inflammation, prompting the design and syntheses of compounds **5a−5h** (Scheme 1). As per the drug bank data, about 85% of bioactives encompass a heterocyclic system. The presence of heterocycles helps in the improvement of solubility, lipophilicity, polarity, and hydrogen bonding capacity, which in turn results in the optimization of the properties of the drugs.[47] Heterocycles constitute the core structure of many commonly used anti-inflammatory drugs commonly used. Piroxicam, niflumic acid, tinoridine, tiaprofenic acid (Figure 1), etc. are a few anti-inflammatory drugs with a pyridine or thiophene type system. This forms the rationale for the design and synthesis of compounds **5i−5l** (Scheme 1), using the same alkyne linker where the aryl core is replaced by pyridine and thiophene moieties. Indole is a "privileged" nucleus found in many bioactive natural products and synthetic and semisynthetic drugs.[48,49] Indomethacin, etodolac, acemethacin and tenidap (Figure 1) are a few examples of indole-based NSAIDs, which have been proven to be COX-2 inhibitors. The derivatives **5m−5za** (Scheme 1) were synthesized to include an indole core into the labdane system, where the nitrogen atom on the substituted indole rings was protected with *tert*-butyloxycarbonyl (boc), benzoyl, and benzenesulfonyl groups. Indomethacin being a non-selective COX-2 inhibitor is known to cause various gastrointestinal side effects. Recently, there have been significant reports on the synthesis of modified indomethacin-based compounds as inhibitors of COX-2 and other inflammatory mediators such as LOX, NO radical, ROS, interleukins, etc.[50] Studies reveal that the derivatization of the carboxyl group at the third position of indomethacin can improve its selectivity toward COX-2, thus enhancing its anti-inflammatory activity and safety profile.[51−53] In this context, we have specifically synthesized the derivatives **5w−5y**, compounds incorporated with indomethacin kind of fragments, where the third position of the indole ring is substituted with the active labdane moiety by using an alkyne linker.

To begin with, fresh rhizomes of *C. amada* were procured from the CTCRI, Thiruvananthapuram, in January 2022. The marker compound, (*E*)-labda-8(17),12-diene-15,16-dial (**1**),

https://doi.org/10.1021/acs.jafc.3c09536
J. Agric. Food Chem. 2024, 72, 6389−6401

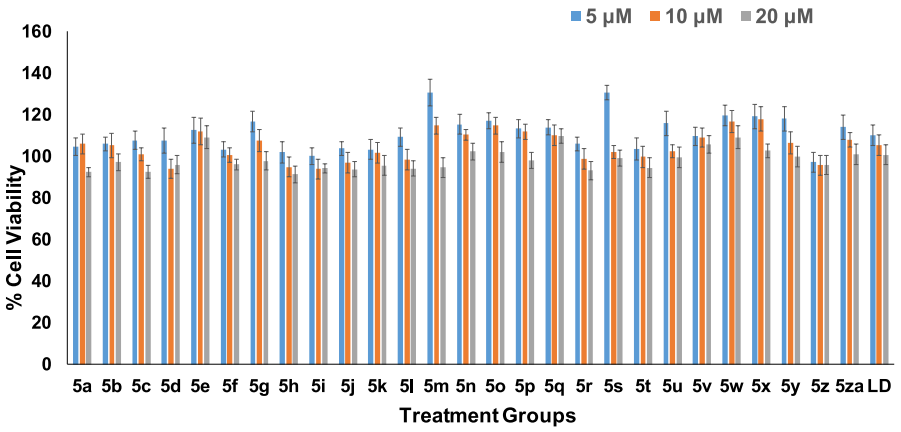

Figure 2. Effect of labdane dialdehyde (LD) and its semisynthetic derivatives (**5a−5za**) on cell viability in RAW264.7 cells. The viability of cells after pretreatment with different concentrations of compounds (5, 10, and 20 μM concentrations) for a period of 24 h was determined by MTT assay.

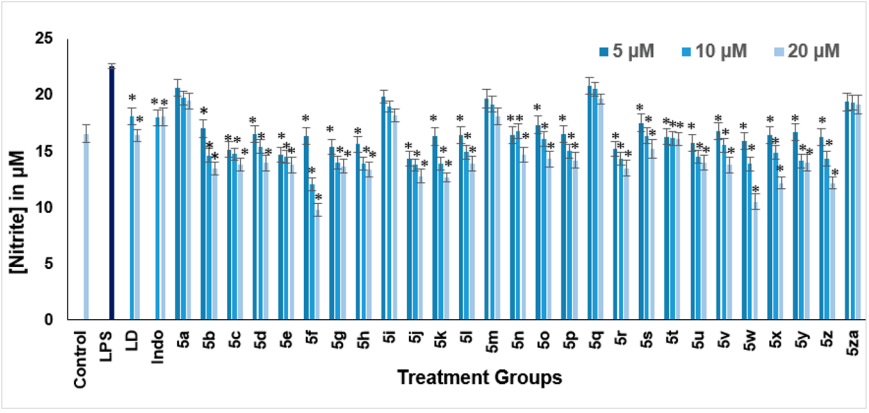

Figure 3. Effect of semisynthetic derivatives of labdane dialdehyde on LPS induced NO production in RAW 264.7 cell lines. Cells were pretreated with 5, 10, and 20 μM concentrations of compounds for 1 h before treatment with 1 μg/mL LPS. After 24 h of incubation, NO production was determined by the Griess test. Data are expressed as the mean ± SD (n = 3). *p < 0.001 vs LPS group.

was isolated from the chloroform extract of the rhizomes by adopting our standard protocol,[34,35] as a colorless solid. The structure of the compound was confirmed by various spectroscopic and analytical data.

One of the aldehyde groups of (*E*)-labda-8(17),12-diene-15,16-dial (**1**) was selectively oxidized to give Zerumin A (**2**), by treating it with oxone in DMF at room temperature.[54] Zerumin A was further converted to the corresponding propargyl ester (**3**) by treatment with propargyl bromide. The structures of compounds **2** and **3** were confirmed by various spectroscopic and analytical data and comparison with the reported literature.[24,34,55] A new series of 27 novel aromatic/heteroaromatic appended analogues of labdane (Scheme 1) were synthesized by the reaction of propargyl ester (**3**) with substituted aryl/heteroaryl iodides (4) by Sonogashira coupling.[44] $Pd(Ph_3P)_2Cl_2$ and CuI were used as the catalyst and cocatalyst, respectively, in dry DMF. All of the synthesized derivatives were well characterized by IR, NMR, and HRMS analyses (Supporting Information).

3.2. Biology. *Determination of in Vitro Cell Viability by MTT Assay.* To determine the utmost effectual dose for an inflammatory response, the cytotoxic effect of all the semisynthetic derivatives of labdane dialdehyde (**5a-5za**) was evaluated via the MTT assay.[45] The cytotoxicity assay showed a dose-dependent decrease in cell viability in RAW 264.7 cell lines upon pretreatment with the semisynthetic derivatives. All the compounds tested at 5, 10, and 20 μM concentrations for 24 h did not show marked cytotoxic effects in RAW 264.7 cell lines (Figure 2). Thus, these concentrations were chosen for the evaluation of their anti-inflammatory potential

Preliminary Screening Based on the Inhibitory Effect of Labdane Conjugates on NO Production. Nitric oxide is a membrane-permeable signaling molecule produced when lipopolysaccharide binds to the TLR-4 receptor and mounts a crucial defense in the contradiction of foreign infiltration. Conversely, the uninhibited generation of NO accelerates various chronic inflammatory ailments.[56] Hence, it is critical to maintain the NO level using various anti-inflammatory mediators.[57] LPS-induced macrophages stimulate unrestricted release of nitric oxide by the degradation of L-arginine.[58] Based on the MTT assay, all the synthesized labdane derivatives were evaluated for their potential to inhibit nitric oxide at 5, 10, and 20 μM concentrations in LPS-induced RAW 264.7 cells. The parent compound labdane dialdehyde (**1**; LD), at 10 and 20 μM concentrations, was also included in the study for a comparative evaluation with the semisynthetic derivatives. The anti-inflammatory drug indomethacin (Indo) at 10 and 20 μM concentrations was used as the positive control. Nitrite concentration was assessed, as an indicator of NO production after 24 h of stimulus, through Griess assay.[46] Relative to the

https://doi.org/10.1021/acs.jafc.3c09536
J. Agric. Food Chem. 2024, 72, 6389−6401

LPS-treated group, the parent compound (LD) exhibited a significant decrease in the production of NO, similar to that of the positive control. Among the 27 tested labdane derivatives, 22 derivatives (**5b**−**5h**, **5j**−**5l**, **5n**−**5p**, **5r**−**5z**) exhibited a significant decrease in NO production when compared to the positive control as well as the parent natural compound, in a dose-dependent manner. The decrease in NO production in the groups treated with these labdane derivatives rather than LD highlights the increased anti-inflammatory potential of the semisynthetic derivatives over its parent natural product in murine macrophages (Figure 3). However, compounds **5a**, **5i**, **5m**, **5q**, and **5za** had no obvious NO inhibitory activity. Thus, the compounds **5b**−**5h**, **5j**−**5l**, **5n**−**5p**, and **5r**−**5z** which demonstrated effective NO inhibition were selected for further evaluation of their anti-inflammatory potential.

Structural Activity Relationship Based on the Inhibitory Effect of Labdane Conjugates on NO Production. Based on the NO inhibitory effect of the labdane conjugates, a probable structural activity relationship is drawn. Among the simple benzene series (**5a**−**5h**), nitro-substituted derivatives (**5e**, **5f**) exhibited the highest NO inhibition. To be more specific, the dinitro substituted conjugate (**5f**), exhibited a higher NO inhibitory effect than the monosubstituted derivative. **5a** with an unsubstituted benzene core exhibited the least NO inhibition. Among the simple heteroaromatic conjugates (**5i**−**5l**), −OH substituted pyridine derivatives (**5k**) demonstrated pronounced effect on NO inhibition. Among the indole derivatives (**5m**−**5za**), *N*-benzoyl or *N*-benzenesulfonyl substituted derivatives exhibited high NO inhibition potential. However, the *N*-boc-protected indole conjugates exhibited only a moderate inhibitory effect for NO. Among the *N*-benzoyl or *N*-benzenesulfonyl substituted conjugates, nitro-substituted derivatives (**5w** and **5x**) were more potent than the other derivatives. Interestingly, there was no particular trend based on the type of substitution on the indole ring, i.e., among halogens, electron-withdrawing, or electron-donating groups. Overall, among both simple aromatic/heteroaromatic conjugates and indole conjugates, the nitro-substituted analogues were found to be more potent candidates of the series.

In Silico Molecular Modeling Studies on the COX-2 Enzyme. COX-2 is an inflammatory mediator and an inducible enzyme that catalyzes the PGE2 synthesis. The activation of one of the mammalian transcription factors NF-κB by LPS and other cytokines is mediated by COX-2.[59] The inhibition of COX-2 regulates the inflammatory homeostasis, and hence, it is identified as a molecular target in the prevention and treatment of inflammatory diseases. To understand the binding mode and mechanism of action of the selected compounds (**5b**−**5h**, **5j**−**5l**, **5n**−**5p**, **5r**−**5z**), interacting with the target protein COX-2, we mapped the amino acid residues of COX-2 most likely involved in establishing the interaction with drugs (Figure S2, Supporting Information). We found that the catalytic pocket or active site of COX-2 is well conserved, having a deep hydrophobic pocket (Figure S3, Supporting Information). Structural interactions showed that the amino acid residues A199, A202, T206, H207, F210, T212, L294, L295, Q383, H386, W387, H388, M391, L408, I444, H446, D450, and E454 make up the COX-2 active site. Furthermore, docking analysis revealed that the large catalytic pocket of COX-2 could accommodate both simple aromatic and heteroaromatic derivatives. The head or labdane core of the compounds faces inward to the active site pocket and mostly occupies the inner pocket area made of amino acids A199, A202, Q203, T206, H207, F210, and W387 in COX-2. We calculated the overall buried interface and pocket volume between the COX-2 active site and labdane derivatives to be ∼1400 Å^2 as calculated from the D3 pocket server (www.d3pharma.com/D3Pocket/), suggesting the ability of COX-2 to accommodate large targets. In addition, the docking studies of the semisynthetic labdane derivatives to COX-2 showed that the binding affinity (delG) ranged from −10.35 kcal/mol for compound **5f** to −5.82 kcal/mol for compound **5g** among the simple aromatic/heteroaromatic conjugates, while among the indole conjugates, the binding affinity (delG) ranged from −10.61 kcal/mol for compound **5x** to −5.78 kcal/mol for compound **5o** (Table 1).

Table 1. Estimated Free Energy of Binding of the Labdane Conjugates with COX-2 *in Silico*

compound code	Del G, kcal/mol
aryl/heteroaryl conjugates	
5f	−10.35
5k	−9.28
5e	−8.78
5h	−8.47
5j	−7.65
5l	−7.43
5b	−6.80
5c	−6.61
5d	−6.45
5g	−5.82
indole conjugates	
5x	−10.61
5w	−9.81
5z	−9.47
5y	−9.14
5t	−8.64
5s	−8.31
5p	−8.27
5r	−8.05
5u	−7.93
5v	−6.91
5n	−6.73
5o	−5.78
ROX	−8.2

The ligand in protein COX-2 (PDB: 5KIR) is rofecoxib (ROX).[60] Hence, the binding affinities of compounds were compared to that of ROX. For ROX, the binding affinity is about −8.2 kcal/mol, whereas for **5x**, the binding affinity is about −10.61 kcal/mol, followed by **5f** with a binding affinity of −10.35 kcal/mol. The compounds **5x** and **5f** can compete with the porphyrin and effectively bind into the catalytic pocket of COX-2. Whereas in the crystal structure, ROX binds to an allosteric site. **5x**/**5f** can bind and compete for both allosteric and catalytic sites with good affinity (Figure 4).

Among the examined compounds, **5e**, **5f**, **5k**, and **5w**−**5z** exhibited excellent binding affinity for the COX-2 enzyme (Table 1). These findings further corroborate the high binding affinity of synthesized labdane conjugates targeting COX-2 as potential inhibitors.

Effect of Compounds on COX-2 Enzyme Inhibition. Based on the *in silico* molecular docking results on the COX-2 enzyme, the seven most promising active compounds **5e**, **5f**, **5k**, and **5w**−**5z** were then investigated for the *in vitro* COX-2

https://doi.org/10.1021/acs.jafc.3c09536
J. Agric. Food Chem. 2024, 72, 6389−6401

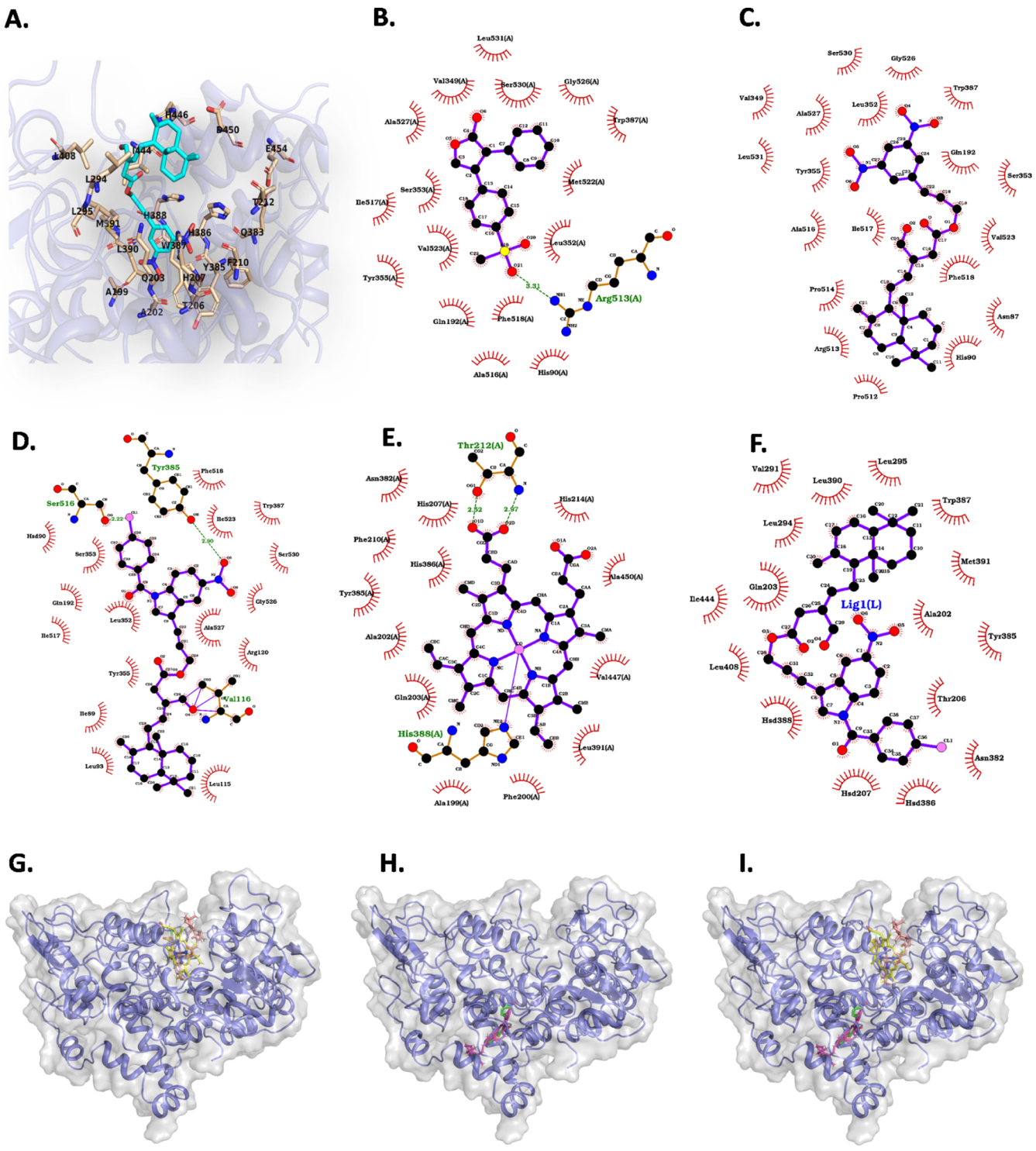

Figure 4. (A) The bound/docked compound **5f** (cyan) in the COX-2 enzyme with the active site or catalytic pocket (shown in amino acid side chains). Ligplot view showing the COX-2 interaction with (B) rofecoxib (ROX) as derived from the crystal structure (PDB: 5KIR), (C) docked compound **5f** in the same ROX binding site, (D) docked compound **5x** in the same ROX binding site. (E) Protoporphyrin IX (COH) in the catalytic pocket (PDB: 5KIR) and (F) docked compound **5x** in the COH binding site or catalytic pocket. (G) Superimposition of COH (yellow) and **5x** (sand), (H) ROX (green) and **5x** (pink), and (I) all three molecules, where COX-2 is shown in a blue representation with a gray surface, showing that the **5x** compound could effectively bind COX-2 in both sites and makes a larger binding interface.

inhibition at 20, 40, and 60 μM concentrations. Indomethacin (at 40 μM and 60 μM) was used as the positive control. The parent compound 1 (**LD**; at 40 and 60 μM) was also included in the study for a comparison with the semisynthetic derivatives. Among the screened derivatives, **5f** displayed the highest inhibition on COX-2, with an IC_{50} value of 17.67 ± 0.89 μM, which was nearly 4-fold more active than the positive control indomethacin (IC_{50} = 67.16 ± 0.17 μM), followed by **5w** (IC_{50} = 34.86 ± 2.32 μM). **5k**, **5x**, and **5z** also exhibited excellent COX-2 inhibition potential better than that of the

https://doi.org/10.1021/acs.jafc.3c09536
J. Agric. Food Chem. 2024, 72, 6389−6401

positive control. Table 2 shows the IC_{50} values of the evaluated compounds. To our delight, the *in silico* results supported the *in vitro* investigations to a great extent. These seven derivatives (**5e**, **5f**, **5k**, and **5w**−**5z**) were again shortlisted for the next level of anti-inflammatory studies (Supporting Information, Figure S1).

Table 2. Effect of Labdane Derivatives on COX-2 Inhibition (IC_{50})[a]

compounds	IC_{50} (μM)
5e	84.27 ± 0.93
5f	17.67 ± 0.89
5k	52.5 ± 3.38
5w	34.86 ± 2.32
5x	50.58 ± 0.25
5y	101.25 ± 3.18
5z	42.68 ± 0.99
Indo	67.16 ± 0.17

[a]Half maximal inhibitory concentration (IC_{50}) values for COX-2 inhibition of selected labdane derivatives and the positive control indomethacin (Indo). Data are expressed as the mean ± SD (n = 3).

Inhibitory Effect of Labdane Conjugates on Pro-Inflammatory Cytokines Production (TNF-α, IL-6, and IL-1α). LPS-stimulated cells secrete excessive inflammatory markers comprising COX-2, a key enzyme involved in the production of PGE2, and pro-inflammatory cytokines like TNF-α, IL-6, and IL-1α. The quantities of these cytokines specify the impact of inflammation in cellular models.[61] Hence, we further studied the effect of the seven selected (**5e**, **5f**, **5k**, **5w**−**5z**) compounds (at 20 μM concentration), on the quantity of TNF-α, IL-6, and IL-1α in the supernatant of LPS-stimulated RAW 264.7 cell lines via enzyme-linked immunosorbent assay (ELISA). LPS-treated groups exhibited remarkable incrementation in all three cytokine concentrations in RAW 264.7 cells when compared to control cells, which implies the successful establishment of the cellular inflammatory model in murine macrophages. The LPS-induced upsurges were reversed by the treatment with natural compound LD and its semisynthetic derivatives as this significantly reduced the level of cytokines. The level of IL-6 was found to be declined in the following order: LD > 5e > 5y > 5k > Indo > 5x > 5z > 5w > 5f. The results also demonstrated a reduction in IL-6 levels similar to the results obtained from COX-2 inhibition results. The levels of TNF-α and IL-1α were found to decline in a similar order to that of IL-6 and COX-2 (Figure 5).

In concordance with COX-2 inhibition results, compound **5f** was observed with the most anti-inflammatory potential by inhibiting the production of pro-inflammatory cytokines in the cellular model. The other derivatives **5w**, **5z**, **5x**, and **5k** also demonstrated a similar pattern of cytokine concentration in LPS cotreated cells better than the positive control indomethacin. The compounds **5e** and **5y** exhibited the release of pro-inflammatory cytokines, which is on par with the positive control, indomethacin, and better than that of the parent compound LD. Hence, this study indicates that the anti-inflammatory potential of the semisynthetic derivatives of LD are superior over that of the parental compound.

*Dose-Dependent Studies of **5f** on Key Pro-Inflammatory Cytokines (TNF-α and IL-6).* The most promising candidate, **5f**, was further assessed for its inhibitory effect on LPS-induced TNF-α and IL-6 release at different concentrations (1, 5, and 10 μM). As illustrated in Figure 6, compound **5f** markedly inhibited the TNF-α and IL-6 release in a dose-dependent manner and hence was confirmed to be a highly potent anti-inflammatory agent, outperforming the effects of the commercial drug indomethacin.

*Effect of **5f** on COX-2 Protein Expression on LPS-Stimulated RAW 264.7 Cell Lines.* To explore the effect of **5f** on COX-2 protein expression, Western blot analysis was performed on LPS-stimulated RAW 264.7 cells at 10 and 20 μM concentrations. Indomethacin at 20 μM concentration was employed as the positive control. LPS stimulation significantly increased the expression of the COX-2 protein, as depicted in Figure 7. However, there was a significant decrease in COX-2 expression when pretreated with compound **5f**, in a dose-dependent manner, and was on par with indomethacin. The results confirm that **5f** exerts its anti-inflammatory effect by inhibiting the release of pro-inflammatory cytokines and nitric oxide via the down-regulation of COX-2 expression.

*Effect of **5f** on NF-κB Signaling Pathway on LPS-Stimulated RAW 264.7 Cells via Western Blotting and Immunofluorescence Analysis.* There have been extensive studies that point to the fact that the expression of the pro-inflammatory cytokines and enzymes such as COX-2 is transcriptionally mediated by the nuclear transcription factor NF-κB.[62−64] NF-κB exists as an inactive dimer along with IκB in the cytoplasm of the cell. However, upon activation by external stimuli, NF-κB phosphorylates and translocates into the nuclei, where it promotes the expression of various pro-

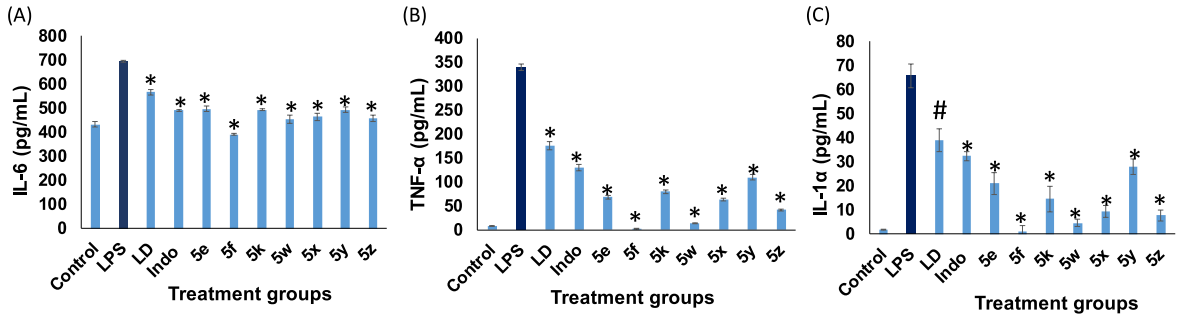

Figure 5. Effect of semisynthetic derivatives of labdane dialdehyde on LPS induced cytokines production: (a) IL-6, (b) TNF-α, (c) IL-1 α, in RAW 264.7 cell lines. Cells were pretreated with 20 μM concentration of compounds for 1 h, before treatment with 1 μg/mL LPS. After 24 h of incubation, cytokine production was determined by ELISA. Data are expressed as the mean ± SD (n = 3). *p < 0.001 vs LPS group, #p < 0.05 vs LPS group.

https://doi.org/10.1021/acs.jafc.3c09536
J. Agric. Food Chem. 2024, 72, 6389−6401

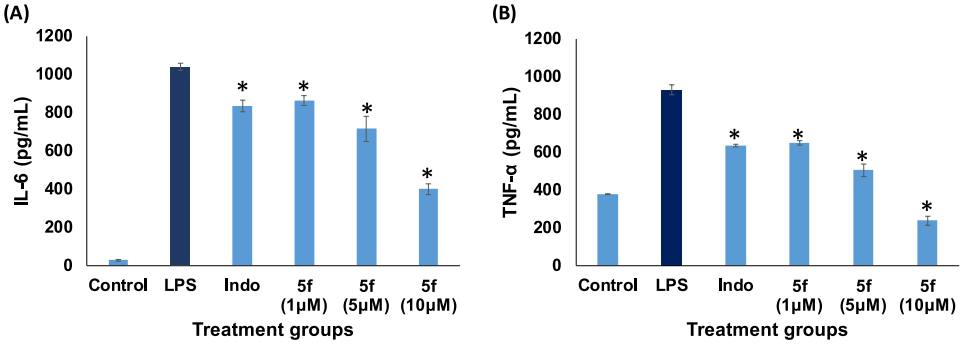

Figure 6. Effect of compound **5f** on LPS induced cytokine production: (a) IL-6 and (b) TNF-α, in RAW 264.7 cell lines. Cells were pretreated with various concentrations of compound **5f** (1, 5, and 10 μM) and indomethacin (10 μM) for 1 h before treatment with 1 μg/mL LPS. After 24 h of incubation, cytokine production was determined by ELISA. Data are expressed as the mean ± SD (n = 3). *p < 0.001 vs LPS group.

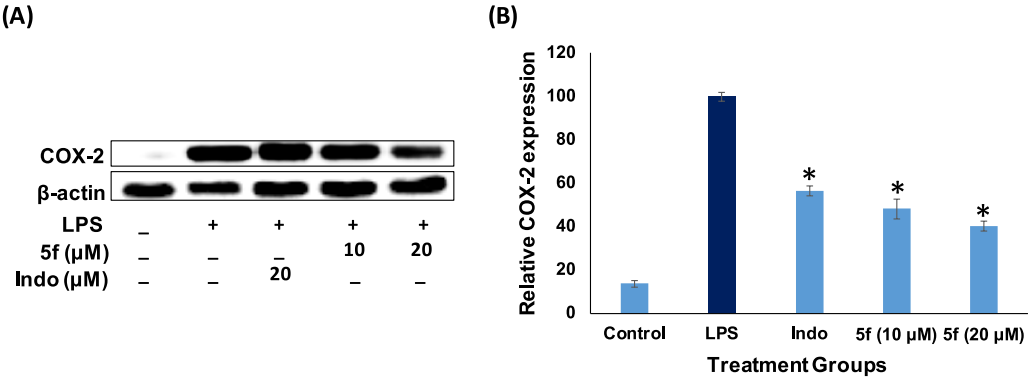

Figure 7. Effect of **5f** on the COX-2 expression in LPS-stimulated RAW264.7 cells. Cells were pretreated with different concentrations of compound **5f** (10 and 20 μM) and indomethacin (20 μM) for 1 h and then stimulated with or without 1 μg/mL of LPS for 24 h. COX-2 expression was detected by Western blotting (A and B). Data are expressed as the mean ± SD (n = 3). *p < 0.001 vs LPS group.

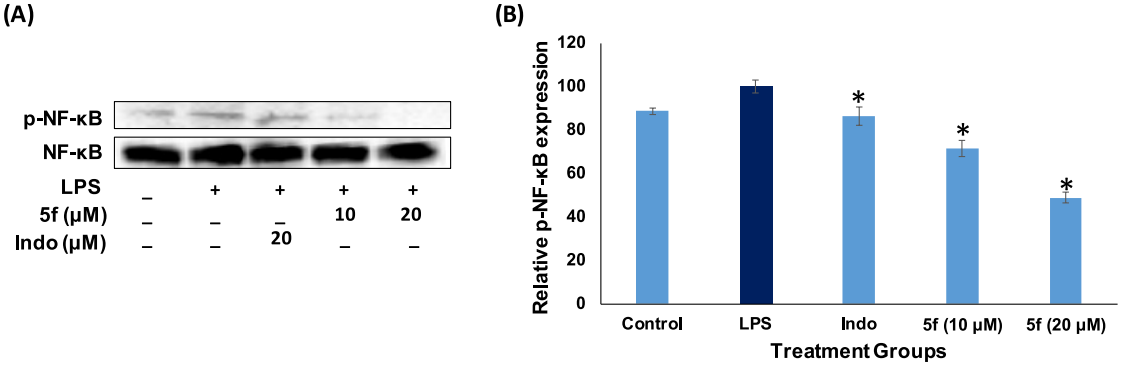

Figure 8. Effect of **5f** on NF-κB expression in LPS-stimulated RAW264.7 cells. Cells were pretreated with different concentrations of compound **5f** (10 and 20 μM) and indomethacin (20 μM) for 1 h and then stimulated with or without 1 μg/mL of LPS for 24 h. NF-κB expression was detected by Western blotting (A and B). Data are expressed as the mean ± SD (n = 3). *p < 0.001 vs LPS group.

inflammatory mediators. Hence, down-regulating the expression of p-NF-κB is one of the effective approaches to preventing inflammation. To establish the anti-inflammatory mechanism of **5f**, the effect on the NF-κB signaling pathway was investigated via Western blotting and immunofluorescence assays. Indomethacin (20 μM) was chosen as the positive control. As depicted in Figure 8, LPS stimulation increased the expression of the p-NF-κB, on LPS-stimulated RAW 264.7 cells. Compound **5f** exhibited a significant reduction in NF-κB phosphorylation in a dose-dependent manner and was comparable to positive control indomethacin. The confirmation of the anti-inflammatory mechanism of **5f** involving inhibition of the NF-κB signaling pathway was demonstrated by analyzing the effect of the compound **5f** on the nuclear translocation of NF-κB by immunofluorescence assay. As shown in Figure 9A, compound **5f** markedly reduced the distribution of NF-κB in the nucleus in a dose-dependent manner, signifying the suppression of phosphorylation and transport of NF-κB from the cytoplasm to the nucleus. The fluorescence intensity histogram extracted using cellSens software (OLYMPUS, Japan) demonstrated a significant increase in nuclear p65 in the cells treated with LPS. However, the cells cotreated with **5f** exhibited a significant reduction in nuclear p65 in a dose-dependent manner and was comparable

https://doi.org/10.1021/acs.jafc.3c09536
J. Agric. Food Chem. 2024, 72, 6389−6401

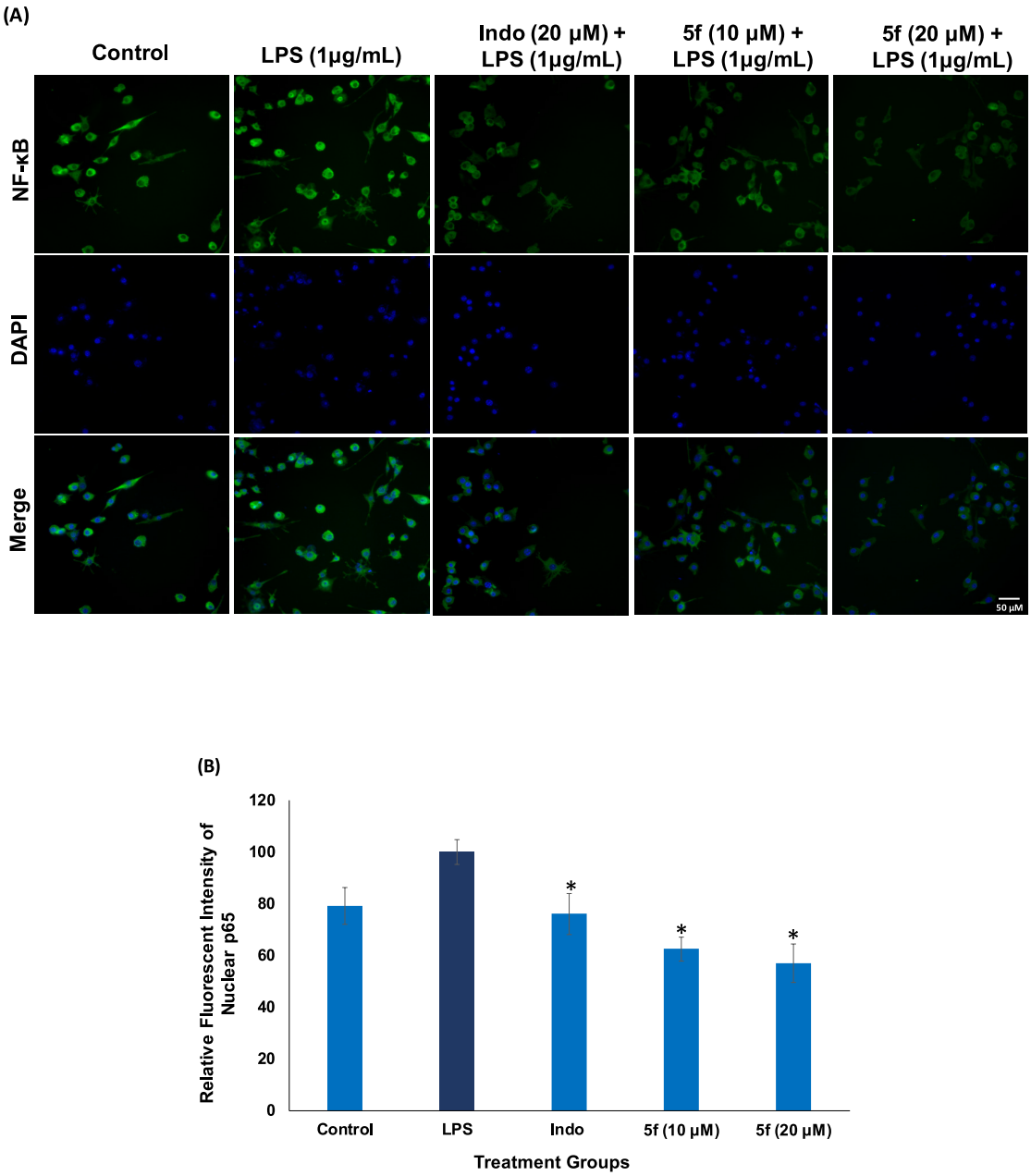

Figure 9. (A) Immunofluorescence staining detected the distribution of NF-κB-p65 in both the nuclei and the cytoplasm by some colocalization of receptors (p65, Alexa Fluor 488, green) with the nuclei (DAPI, blue). Images were captured by fluorescent microscope (OLYMPUS, Japan). Scale = 50 μM. (B) Intensity histogram of NF-κB translocation. The fluorescence intensity was quantified using the cellSens software (OLYMPUS, Japan). Data are expressed as the mean ± SD (n = 3). *p < 0.001 vs LPS group.

to that of the positive control indomethacin (Figure 9B). The results indicated that compound **5f** inhibits the LPS-stimulated overexpression of pro-inflammatory mediators such as cytokines, NO, and COX-2 by down-regulating the expression of the NF-κB signaling pathway.

In summary, the anti-inflammatory potential of the medicinally as well as nutritionally relevant plant *C. amada* was explored. The abundant marker compound, (*E*)-labda-8(17),12-diene-15,16-dial, was isolated from its rhizomes, and a new series of 27 unique rationally designed labdane hybrids were synthesized, using a strategic linker-based molecular hybridization approach which includes the conjugation of aromatic and heteroaromatic fragments into the labdane template, and were evaluated for their anti-inflammatory potential. Among the labdane conjugates, **5f** demonstrated the highest anti-inflammatory potential by inhibiting the COX-2 enzyme, with a 4-fold increased activity compared to the commercial drug indomethacin. The derivative **5f** also inhibited the production of other inflammatory mediators such as NO, TNF-α, IL-6, and IL-1α, much better than the positive control as well as the parent natural compound LD. Molecular mechanistic studies revealed that compound **5f** suppressed the expression of pro-inflammatory cytokines, NO, and COX-2 via the regulation of the NF-κB signaling pathway. The results clearly emphasize the role of semisynthetic modifications in the enhancement of the bioactivity of natural products. The in-silico data supported the study. This is the first report on the anti-inflammatory studies of labdane

https://doi.org/10.1021/acs.jafc.3c09536
J. Agric. Food Chem. 2024, 72, 6389−6401

dialdehyde and its semisynthetic derivatives. The results suggested that the compound **5f** holds the potential as a novel promising anti-inflammatory agent.

Therefore, extensive studies emphasize the medicinal relevance of the plant *C. amada*, which can result in economic value addition to the crop and hence improve its agricultural status. *C. amada* is a common edible plant native to India. The scientific value addition to the crop can boost its export worth and promote it to the category of cash crop, which in turn can contribute to the uplifting of the socio-economic status of the farmers who cultivate it.

■ ASSOCIATED CONTENT

Supporting Information

The Supporting Information is available free of charge at https://pubs.acs.org/doi/10.1021/acs.jafc.3c09536.

Experimental procedures for the synthesis of starting materials and characterization data (chemistry), dose-dependent data for COX-2 inhibition, figures of molecular docking studies of compounds on COX-2, and ^{1}H and ^{13}C NMR spectra of all the newly synthesized compounds (PDF)

■ AUTHOR INFORMATION

Corresponding Authors

Sasidhar B. Somappa − *Chemical Sciences and Technology Division, CSIR-National Institute for Interdisciplinary Science and Technology (CSIR-NIIST), Thiruvananthapuram 695 019 Kerala, India; Academy of Scientific and Innovative Research (AcSIR), Ghaziabad 201 002, India;* orcid.org/0000-0003-1546-2083; Email: drsasidharbs@gmail.com, drsasidharbs@niist.res.in

Jayamurthy Purushothaman − *Agro Processing and Technology Division, CSIR-National Institute for Interdisciplinary Science and Technology (CSIR-NIIST), Thiruvananthapuram 695 019 Kerala, India; Academy of Scientific and Innovative Research (AcSIR), Ghaziabad 201 002, India*; Email: pjayamurthy@niist.res.in

Authors

Sangeetha Mohan − *Chemical Sciences and Technology Division, CSIR-National Institute for Interdisciplinary Science and Technology (CSIR-NIIST), Thiruvananthapuram 695 019 Kerala, India; Academy of Scientific and Innovative Research (AcSIR), Ghaziabad 201 002, India*

Lekshmy Krishnan − *Chemical Sciences and Technology Division, CSIR-National Institute for Interdisciplinary Science and Technology (CSIR-NIIST), Thiruvananthapuram 695 019 Kerala, India*

Nithya Madhusoodanan − *Chemical Sciences and Technology Division, CSIR-National Institute for Interdisciplinary Science and Technology (CSIR-NIIST), Thiruvananthapuram 695 019 Kerala, India; Academy of Scientific and Innovative Research (AcSIR), Ghaziabad 201 002, India*

Anjali Sobha − *Chemical Sciences and Technology Division, CSIR-National Institute for Interdisciplinary Science and Technology (CSIR-NIIST), Thiruvananthapuram 695 019 Kerala, India; Academy of Scientific and Innovative Research (AcSIR), Ghaziabad 201 002, India*

Renjitha Jalaja − *Chemical Sciences and Technology Division, CSIR-National Institute for Interdisciplinary Science and Technology (CSIR-NIIST), Thiruvananthapuram 695 019 Kerala, India*

Alaganandam Kumaran − *Agro Processing and Technology Division, CSIR-National Institute for Interdisciplinary Science and Technology (CSIR-NIIST), Thiruvananthapuram 695 019 Kerala, India; Academy of Scientific and Innovative Research (AcSIR), Ghaziabad 201 002, India*

Naveen Vankadari − *Department of Biochemistry and Pharmacology, Bio21 Institute, The University of Melbourne, Melbourne, Victoria 3052, Australia;* orcid.org/0000-0001-9363-080X

Complete contact information is available at: https://pubs.acs.org/10.1021/acs.jafc.3c09536

Author Contributions

The manuscript was written through the contributions of all authors. All authors have given approval to the final version of the manuscript.

Notes

The authors declare no competing financial interest.

■ ACKNOWLEDGMENTS

Financial support from the Kerala State Council for Science, Technology and Environment (KSCSTE), Govt. of Kerala, via the KSCSTE-Kerala State Young Scientist Award Research Grant (KSCSTE/1096/2020-KSYSA-RG) and the CSIR Young Scientist Award Research Grant (HRDG/YSA-19/02/33(0045)/2020) from the Council of Scientific and Industrial Research (CSIR), Government of India, New Delhi, is gratefully acknowledged. We also thank the DST-Science and Engineering Research Board (SERB), Government of India, New Delhi, India (Grant no. EEQ/2021/000374) for the research grant. S.M. and L.K. thank UGC and DST for research fellowships.

■ ABBREVIATIONS

NO, nitric oxide; COX-2, cyclooxygenase-2; IL-6, interleukin-6; TNF-α, tumor necrosis factor α; IL-1α, interleukin-1α; LPS, lipopolysaccharide; IC_{50}, half maximal inhibitory concentration; LOX, lipoxygenase; ROS, reactive oxygen species

■ REFERENCES

(1) Medzhitov, R. Origin and Physiological Roles of Inflammation. *Nature* **2008**, *454* (7203), 428−435.

(2) Alexander, R. W. Inflammation and Coronary Artery Disease. *N. Engl. J. Med.* **1994**, *331* (7), 468−469.

(3) Crusz, S. M.; Balkwill, F. R. Inflammation and Cancer: Advances and New Agents. *Nat. Rev. Clin. Oncol.* **2015**, *12* (10), 584−596.

(4) Kokiko-Cochran, O. N.; Godbout, J. P. The Inflammatory Continuum of Traumatic Brain Injury and Alzheimer's Disease. *Front. Immunol.* **2018**, *9*, DOI: 10.3389/fimmu.2018.00672.

(5) Bai, R.; Jie, X.; Yao, C.; Xie, Y. Discovery of Small-Molecule Candidates against Inflammatory Bowel Disease. *Eur. J. Med. Chem.* **2020**, *185*, 111805.

(6) Donath, M. Y.; Shoelson, S. E. Type 2 Diabetes as an Inflammatory Disease. *Nat. Rev. Immunol.* **2011**, *11* (2), 98−107.

(7) Cain, D. W.; Cidlowski, J. A. Immune Regulation by Glucocorticoids. *Nat. Rev. Immunol.* **2017**, *17* (4), 233−247.

(8) Bleumink, G. S.; Feenstra, J.; Sturkenboom, M. C. J. M.; Stricker, B. H. C. Nonsteroidal Anti-Inflammatory Drugs and Heart Failure. *Drugs* **2003**, *63* (6), 525−534.

(9) Schmid, A. S.; Neri, D. Advances in Antibody Engineering for Rheumatic Diseases. *Nat. Rev. Rheumatol.* **2019**, *15* (4), 197−207.

(10) Dinarello, C. A. Anti-Inflammatory Agents: Present and Future. *Cell* **2010**, *140* (6), 935−950.
(11) Germolec, D. R.; Shipkowski, K. A.; Frawley, R. P.; Evans, E. Markers of Inflammation. *Methods Mol. Biol.* **2018**, *1803*, 57−79.
(12) Newman, D. J.; Cragg, G. M. Natural Products as Sources of New Drugs over the Nearly Four Decades from 01/1981 to 09/2019. *J. Nat. Prod.* **2020**, *83* (3), 770−803.
(13) Nunes, C. d. R.; Barreto Arantes, M.; Menezes de Faria Pereira, S.; Leandro da Cruz, L.; De Souza Passos, M.; Pereira de Moraes, L.; Vieira, I. J. C.; Barros de Oliveira, D. Plants as Sources of Anti-Inflammatory Agents. *Molecules* **2020**, *25*, 3726.
(14) Recio, M. C.; Andujar, I.; Rios, J. L. Anti-Inflammatory Agents from Plants: Progress and Potential. *Curr. Med. Chem.* **2012**, *19* (14), 2088−2103.
(15) Rahaman, M. M.; Rakib, A.; Mitra, S.; Tareq, A. M.; Emran, T. B.; Shahid-Ud-daula, A. F. M.; Amin, M. N.; Simal-Gandara, J. The Genus Curcuma and Inflammation: Overview of the Pharmacological Perspectives. *Plants* **2021**, *10* (1), 63.
(16) Singh, S.; Singh, R.; Banerjee, S.; Negi, A. S.; Shanker, K. Determination of Anti-Tubercular Agent in Mango Ginger (Curcuma Amada Roxb.) by Reverse Phase HPLC-PDA-MS. *Food Chem.* **2012**, *131* (1), 375−379.
(17) Bhutia, P. H.; Viswavidyalaya, K.; Sharangi, A. B. Promising Curcuma Species Suitable for Hill Regions towards Maintaining Biodiversity. *J. Pharmacogn. Phytochem.* **2017**, *6* (6), 726−731.
(18) Al-Qudah, T. S.; Abu Malloh, S.; Nawaz, A.; Adnan Ayub, M.; Nisar, S.; Idrees Jilani, M.; Said Al-Qudah, T. Mango Ginger (Curcuma Amada Roxb.): A Phytochemical Mini Review. *Int. J. Chem. Biochem. Sci.* **2017**, *11*, 51.
(19) Syamkumar, S.; Sasikumar, B. Molecular Marker Based Genetic Diversity Analysis of Curcuma Species from India. *Sci. Hortic. (Amsterdam).* **2007**, *112* (2), 235−241.
(20) Dosoky, N. S.; Setzer, W. N. Chemical Composition and Biological Activities of Essential Oils of Curcuma Species. *Nutrients.* **2018**, *10*, 1196.
(21) Jatoi, S. A.; Kikuchi, A.; Gilani, S. A.; Watanabe, K. N. Phytochemical, Pharmacological and Ethnobotanical Studies in Mango Ginger (Curcuma Amada Roxb.; Zingiberaceae). *Phyther. Res.* **2007**, *21* (6), 507−516.
(22) Ramachandran, C.; Quirin, K. W.; Escalon, E. A.; Lollett, I. V.; Melnick, S. J. Therapeutic Effect of Supercritical CO2 Extracts of Curcuma Species with Cancer Drugs in Rhabdomyosarcoma Cell Lines. *Phyther. Res.* **2015**, *29* (8), 1152−1160.
(23) Policegoudra, R. S.; Aradhya, S. M.; Singh, L. Mango Ginger (Curcuma Amada Roxb.) - A Promising Spice for Phytochemicals and Biological Activities. *J. Biosci.* **2011**, *36* (4), 739−748.
(24) Singh, S.; Kumar, J. K.; Saikia, D.; Shanker, K.; Thakur, J. P.; Negi, A. S.; Banerjee, S. A Bioactive Labdane Diterpenoid from Curcuma Amada and Its Semisynthetic Analogues as Antitubercular Agents. *Eur. J. Med. Chem.* **2010**, *45* (9), 4379−4382.
(25) Mujumdar, A. M.; Naik, D. G.; Dandge, C. N.; Puntambekar, H. M. Antiinflammatory Activity of Curcuma Amada Roxb. in Albino Rats. *Indian J. Pharmacol.* **2000**, *32* (6), 375−377.
(26) Nagavekar, N.; Singhal, R. S. Supercritical Fluid Extraction of Curcuma Longa and Curcuma Amada Oleoresin: Optimization of Extraction Conditions, Extract Profiling, and Comparison of Bioactivities. *Ind. Crops Prod.* **2019**, *134* (March), 134−145.
(27) Yang, N.; Zou, C.; Luo, W.; Xu, D.; Wang, M.; Wang, Y.; Wu, G.; Shan, P.; Liang, G. Sclareol Attenuates Angiotensin II -induced Cardiac Remodeling and Inflammation via Inhibiting MAPK Signaling. *Phyther. Res.* **2023**, *37*, 578−591.
(28) Chen, H.-W.; Lin, A.-H.; Chu, H.-C.; Li, C.-C.; Tsai, C.-W.; Chao, C.-Y.; Wang, C.-J.; Lii, C.-K.; Liu, K.-L. Inhibition of TNF-α-Induced Inflammation by Andrographolide via Down-Regulation of the PI3K/Akt Signaling Pathway. *J. Nat. Prod.* **2011**, *74* (11), 2408−2413.
(29) De Las Heras, B.; Navarro, A.; Díaz-Guerra, M. J.; Bermejo, P.; Castrillo, A.; Boscá, L.; Villar, A. Inhibition of NOS-2 Expression in Macrophages through the Inactivation of NF-KB by Andalusol. *Br. J. Pharmacol.* **1999**, *128* (3), 605−612.
(30) Tran, Q. T. N.; Wong, W. S. F.; Chai, C. L. L. Labdane Diterpenoids as Potential Anti-Inflammatory Agents. *Pharmacol. Res.* **2017**, *124*, 43−63.
(31) DeCorte, B. L. Underexplored Opportunities for Natural Products in Drug Discovery. *J. Med. Chem.* **2016**, *59* (20), 9295−9304.
(32) Szychowski, J.; Truchon, J.-F.; Bennani, Y. L. Natural Products in Medicine: Transformational Outcome of Synthetic Chemistry. *J. Med. Chem.* **2014**, *57*, 9292−9308.
(33) Guo, Z. The Modification of Natural Products for Medical Use. *Acta Pharmaceutica Sinica B* **2017**, *7*, 119.
(34) Jalaja, R.; Leela, S. G.; Valmiki, P. K.; Salfeena, C. T. F.; Ashitha, K. T.; Krishna Rao, V. R. D.; Nair, M. S.; Gopalan, R. K.; Somappa, S. B. Discovery of Natural Product Derived Labdane Appended Triazoles as Potent Pancreatic Lipase Inhibitors. *ACS Med. Chem. Lett.* **2018**, *9* (7), 662−666.
(35) Jalaja, R.; Leela, S. G.; Mohan, S.; Nair, M. S.; Gopalan, R. K.; Somappa, S. B. Anti-Hyperlipidemic Potential of Natural Product Based Labdane-Pyrroles via Inhibition of Cholesterol and Triglycerides Synthesis. *Bioorg. Chem.* **2021**, *108*, 104664.
(36) Sasidhar, B. S.; Biradar, J. S. Synthesis of Some Bisindolyl Analogs for in Vitro Cytotoxic and DNA Cleavage Studies. *Med. Chem. Res.* **2013**, *22* (7), 3518−3526.
(37) Lakshmi, S.; Renjitha, J.; B. Sasidhar, S.; Priya, S. Epoxyazadiradione Induced Apoptosis/Anoikis in Triple-Negative Breast Cancer Cells, MDA-MB-231, by Modulating Diverse Cellular Effects. *J. Biochem. Mol. Toxicol.* **2021**, *35* (6), 1−17.
(38) Shilpa, G.; Renjitha, J.; Saranga, R.; Sajin, F. K.; Nair, M. S.; Joy, B.; Sasidhar, B. S.; Priya, S. Epoxyazadiradione Purified from the Azadirachta Indica Seed Induced Mitochondrial Apoptosis and Inhibition of NFκB Nuclear Translocation in Human Cervical Cancer Cells. *Phyther. Res.* **2017**, *31* (12), 1892−1902.
(39) Anaga, N.; D, B.; Abraham, B.; Nisha, P.; Varughese, S.; Jayamurthy, P.; Somappa, S. B. Advanced Glycation End-Products (AGE) Trapping Agents: Design and Synthesis of Nature Inspired Indeno[2,1-c]Pyridinones. *Bioorg. Chem.* **2020**, *105*, 104375.
(40) Salfeena, C. T. F.; Jalaja, R.; Davis, R.; Suresh, E.; Somappa, S. B. Synthesis of 1,2,4-Trisubstituted-(1H)-Imidazoles through Cu-(OTf)2-/I2-Catalyzed C-C Bond Cleavage of Chalcones and Benzylamines. *ACS Omega* **2018**, *3* (7), 8074−8082.
(41) Somappa, S. B.; Biradar, J. S.; Rajesab, P.; Rahber, S.; Sundar, M. A One-Pot Synthesis of Indole-Appended Heterocycles as Potent Anti-Inflammatory, Analgesic, and CNS Depressant Agents. *Monatshefte fur Chemie* **2015**, *146* (12), 2067−2078.
(42) V, P. K.; J, R.; C T, F. S.; K T, A.; S. Keri, R.; Varughese, S.; Balappa Somappa, S. Antibacterial and Antitubercular Evaluation of Dihydronaphthalenone-Indole Hybrid Analogs. *Chem. Biol. Drug Des.* **2017**, *90* (5), 703−708.
(43) Facile Isolation of (E)-Labda-8(17),12-Diene-15,16-Dial from Curcuma Amada and Its Conversion to Other Biologically Active Compounds. *Indian J. Chem. Sect. B* **2014**, *53* (3), 319−324.
(44) Sonogashira, K.; Tohda, Y.; Hagihara, N. A Convenient Synthesis of Acetylenes : Catalytic Sutitutions of Acetyleyic Hydrogen With Broa E Es, Iodoare Es. *Tetrahedron Lett.* **1975**, *16* (50), 4467−4470.
(45) Wilson, A. P. Cytotoxicity and Viability Assays. *Anim. cell Cult. a Pract. approach* **2000**, *1*, 175−219.
(46) Bryan, N. S.; Grisham, M. B. Methods to Detect Nitric Oxide and Its Metabolites in Biological Samples. *Free Radic. Biol. Med.* **2007**, *43* (5), 645−657.
(47) Jampilek, J. Heterocycles in Medicinal Chemistry. *Molecules* **2019**, *24* (21), 3839.
(48) Kumari, A.; Singh, R. K. *Medicinal Chemistry of Indole Derivatives: Current to Future Therapeutic Prospectives*; Elsevier Inc., 2019; Vol. *89*. DOI: 10.1016/j.bioorg.2019.103021.
(49) Sravanthi, T. V.; Manju, S. L. Indoles - A Promising Scaffold for Drug Development. *Eur. J. Pharm. Sci.* **2016**, *91*, 1−10.

(50) Nisha, N.; Singh, S.; Sharma, N.; Chandra, R. The Indole Nucleus as a Selective COX-2 Inhibitor and Anti-Inflammatory Agent (2011−2022). *Org. Chem. Front.* **2022**, *9* (13), 3624−3639.
(51) Kalgutkar, A. S.; Crews, B. C.; Rowlinson, S. W.; Marnett, A. B.; Kozak, K. R.; Remmel, R. P.; Marnett, L. J. Biochemically Based Design of Cyclooxygenase-2 (COX-2) Inhibitors: Facile Conversion of Nonsteroidal Antiinflammatory Drugs to Potent and Highly Selective COX-2 Inhibitors. *Proc. Natl. Acad. Sci. U. S. A.* **2000**, *97* (2), 925−930.
(52) Kalgutkar, A. S.; Marnett, A. B.; Crews, B. C.; Remmel, R. P.; Marnett, L. J. Ester and Amide Derivatives of the Nonsteroidal Antiinflammatory Drug, Indomethacin, as Selective Cyclooxygenase-2 Inhibitors. *J. Med. Chem.* **2000**, *43* (15), 2860−2870.
(53) Amir, M.; Kumar, S. Anti-Inflammatory and Gastro Sparing Activity of Some New Indomethacin Derivatives. *Arch. Pharm. (Weinheim).* **2005**, *338* (1), 24−31.
(54) Travis, B. R.; Sivakumar, M.; Hollist, G. O.; Borhan, B. Facile Oxidation of Aldehydes to Acids and Esters with Oxone. *Org. Lett.* **2003**, *5* (7), 1031−1034.
(55) Xu, H. X.; Dong, H.; Sim, K. Y. Labdane Diterpenes from Alpinia Zerumbet. *Phytochemistry* **1996**, *42* (1), 149−151.
(56) Bengmark, S. Curcumin, an Atoxic Antioxidant and Natural NFκB, Cyclooxygenase-2, Lipooxygenase, and Inducible Nitric Oxide Synthase Inhibitor: A Shield against Acute and Chronic Diseases. *J. Parenter. Enter. Nutr.* **2006**, *30* (1), 45−51.
(57) Kim, Y.; Park, W. Anti-Inflammatory Effect of Quercetin on RAW 264.7 Mouse Macrophages Induced with Polyinosinic-Polycytidylic Acid. *Molecules.* **2016**, *21*, 450.
(58) Van Amersfoort, E. S.; Van Berkel, T. J. C.; Kuiper, J. Receptors, Mediators, and Mechanisms Involved in Bacterial Sepsis and Septic Shock. *Clin. Microbiol. Rev.* **2003**, *16* (3), 379−414.
(59) Guan, F.; Wang, H.; Shan, Y.; Chen, Y.; Wang, M.; Wang, Q.; Yin, M.; Zhao, Y.; Feng, X.; Zhang, J. Inhibition of COX-2 and PGE2 in LPS-stimulated RAW264.7 Cells by Lonimacranthoide VI, a Chlorogenic Acid Ester Saponin. *Biomed Rep* **2014**, *2* (5), 760−764.
(60) Orlando, B. J.; Malkowski, M. G. Crystal Structure of Rofecoxib Bound to Human Cyclooxygenase-2. *Acta Crystallogr. Sect. Struct. Biol. Commun.* **2016**, *72* (10), 772−776.
(61) Muniandy, K.; Gothai, S.; Badran, K. M. H.; Suresh Kumar, S.; Esa, N. M.; Arulselvan, P. Suppression of Proinflammatory Cytokines and Mediators in LPS-Induced RAW 264.7 Macrophages by Stem Extract of *Alternanthera Sessilis* via the Inhibition of the NF-κB Pathway. *J. Immunol. Res.* **2018**, *2018*, 3430684.
(62) Aggarwal, B. B. Nuclear Factor-KB: The Enemy Within. *Cancer Cell.* **2004**, *6*, 203−208.
(63) Ghosh, S.; Hayden, M. S. New Regulators of NF-KB in Inflammation. *Nat. Rev. Immunol.* **2008**, *8* (11), 837−848.
(64) Karin, M.; Ben-neriah, Y. Phosporilation Meets the Ubiquitination: The Control of NF- Kapp B Activity. *Annu. Rev. Immunol.* **2000**, *18*, 621−663.

https://doi.org/10.1021/acs.jafc.3c09536
J. Agric. Food Chem. 2024, 72, 6389−6401

ACS Medicinal Chemistry Letters

pubs.acs.org/acsmedchemlett Letter

Ligand-Based Pharmacophoric Design and Anti-inflammatory Evaluation of Triazole Linked Semisynthetic Labdane Conjugates

Published as part of ACS Medicinal Chemistry Letters virtual special issue "Natural Products Driven Medicinal Chemistry".

Sangeetha Mohan, Lekshmy Krishnan, Nithya Madhusoodanan, Anjali Sobha, Alansheeja D. Babysulochana, Naveen Vankadari, Jayamurthy Purushothaman, and Sasidhar B. Somappa*

Cite This: ACS Med. Chem. Lett. 2024, 15, 1260−1268 Read Online

ACCESS | Metrics & More | Article Recommendations | Supporting Information

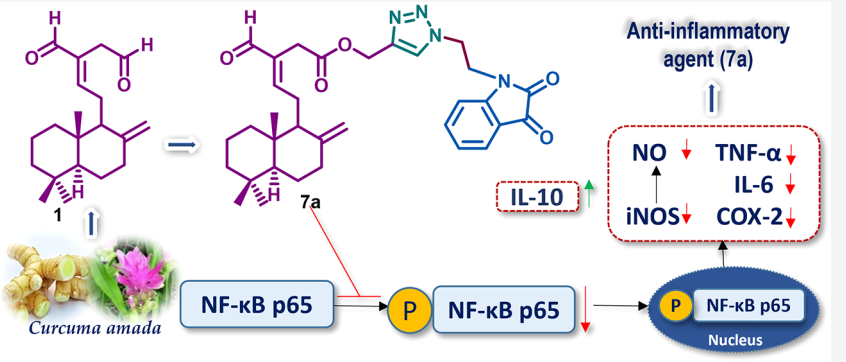

ABSTRACT: This study employed a ligand-based pharmacophoric approach to design and synthesize 33 novel semisynthetic labdane-appended triazolyl isatins to discover potential anti-inflammatory agents. The anti-inflammatory efficacy of the derivatives was evaluated by their ability to inhibit the production of NO, TNF-α, and IL-6, in lipopolysaccharide-induced RAW264.7 macrophages. The initial screening revealed that compound **7a** ((1-(2-(2,3-dioxoindolin-1-yl)ethyl)-1*H*-1,2,3-triazol-4-yl)methyl (*E*)-3-formyl-5-((1*S*,4a*S*,8a*S*)-5,5,8a-trimethyl-2-methylenedecahydronaphthalen-1-yl)pent-3-enoate) exhibited an anti-inflammatory effect (NO inhibition, IC_{50} = 3.13 μM), surpassing both the positive control indomethacin (NO inhibition, IC_{50} = 7.31 μM) and the parent compound labdane dialdehyde. Notably, **7a** reduced the levels of pro-inflammatory cytokines TNF-α and IL-6 while increasing the levels of the anti-inflammatory cytokine IL-10. Mechanistic studies revealed that **7a** downregulated the expression of COX-2 and iNOS by inhibiting the NF-κB signaling pathway. In silico molecular modeling studies on NF-κB proteins support these findings, suggesting that **7a** is a promising candidate for developing into a potent anti-inflammatory clinical agent.

KEYWORDS: *COX-2, Curcuma amada, Cytokines, iNOS, Isatin-triazole hybrids, NF-κB*

Inflammation serves as a protective adaptive response of the body against harmful external stimuli such as infection or injury to maintain tissue homeostasis, and it is characterized by the occurrence of pain, edema, redness, heat, and dysfunction.[1,2] However, the excessive inflammatory response has been implicated in the onset of numerous pathologies such as cancer,[3] Alzheimer's,[4] atherosclerosis,[5] type II diabetes,[6] etc. Steroidal anti-inflammatory drugs (SAIDs) and nonsteroidal anti-inflammatory drugs (NSAIDs) together with anticytokine biologicals constitute the significant clinical therapeutic strategies that are currently used for the treatment of inflammation. Although steroidal drugs are effective against inflammation, they are often associated with irreversible side effects such as hypertension, osteoporosis, immunosuppression, and elevated glucose levels.[7] NSAIDs, on the other hand, are frequently linked to gastrointestinal and cardiovascular complications.[8] Thus, due to the adverse side effects associated with some of these medications, it is extremely desirable to explore novel anti-inflammatory agents with enhanced efficacy and advanced safety profiles.

Received: March 28, 2024
Revised: July 17, 2024
Accepted: July 17, 2024
Published: July 23, 2024

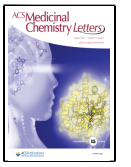

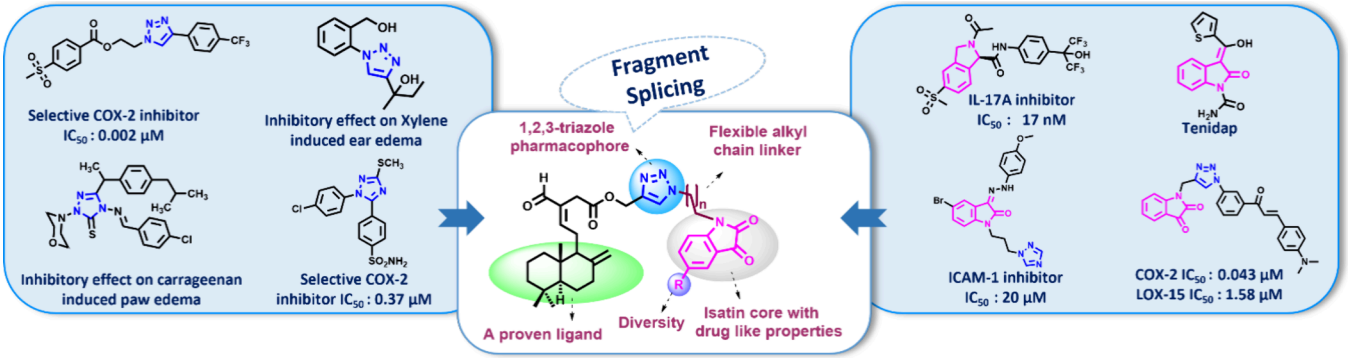

Figure 1. Rationale for the design and synthesis of triazolyl-isatin linked labdane conjugates

Nuclear factor κB (NF-κB) is the key transcription factor that induces the expression of major inflammation-related genes. It exists in the cellular cytoplasm as an inactive dimer with an inhibitor of NF-κB (IκB). However, when activated by inflammatory stimuli, IκB kinase (IKK) phosphorylates and degrades IκB, leading to the phosphorylation and activation of NF-κB. Phosphorylated NF-κB (p-NF-κB) translocates into the nucleus, where it interacts with the gene-promoting region on DNA, leading to the transcription of a variety of pro-inflammatory mediators such as cytokines tumor necrosis factor-α (TNF-α), interleukin-6 (IL-6), and inflammatory enzymes cyclooxygenase-2 (COX-2) and inducible nitric oxide synthase (iNOS). Therefore, the downregulation of the NF-κB signaling pathway can be an effective strategy to combat inflammation and associated complications.[9] Interleukin-10 (IL-10) serves as an anti-inflammatory cytokine and plays a pivotal role in the prevention of inflammatory and autoimmune pathologies. Consequently, elevated IL-10 levels in LPS-stimulated macrophages may be interpreted as a sign of the host's anti-inflammatory defense mechanism.[10]

Natural products are intrinsically biologically relevant and prevalidated by evolution and continue to be the major reservoir for discovering novel drugs. However, due to evolutionary constraints, the diversity of novel scaffolds accessible directly from nature is quite limited.[11] Around 60% of the total small molecule drugs discovered from 1989 to 2019 are natural product-based, with 2% of those being anti-inflammatory agents.[12] Semisynthetic modification of individual metabolites is a versatile tool that can be intended to unravel its potential to interface with variable biomolecular targets with great specificity, thus exploring its new biologically relevant chemical space.[13]

Curcuma amada is a rhizomatous plant that belongs to the medicinally relevant Zingiberaceae family.[14,15] The extracts of its rhizomes have been reported to be effective against various acute and chronic phases of inflammation.[16,17] However, there have not been many reports on the detailed exploration of the anti-inflammatory properties of *C. amada* or its bioactive natural products or semisynthetic derivatives. (*E*)-Labda-8(17),12-diene-15,16-dial (**1**) is the abundant marker compound, a labdane-type diterpenoid, isolated from the chloroform extract of *Curcuma amada* rhizomes. Many labdane diterpenoids and their derivatives, such as angrographolide, sclareol, forskolin, and others, have been proven to have substantial anti-inflammatory effects.[18] Therefore, as part of our ongoing dedicated research program on natural product-based[19−21] semisynthetic modifications to explore the biologically relevant chemical space,[22,23] we have isolated the abundant (*E*)-labda-8(17),12-diene-15,16-dial (**1**) from the chloroform extract of *C. amada* and rationally modified it to generate a library of novel anti-inflammatory scaffolds.

Isatin and its derivatives exhibit a broad range of biological applications, such as anti-inflammatory, anticancer, antimicrobial, antiviral properties, etc. It is an attractive scaffold to medicinal chemists due to its vast scope for chemical modifications and can thus be employed as a precursor in drug synthesis.[24,25] Triazoles are crucial molecular frameworks in medicinal chemistry. They are a key pharmacophore in many natural products as well as in various anticancer, anti-inflammatory, antibacterial, and anti-HIV drugs. Triazole moiety possesses extensive physicochemical properties, such as high hydrogen bonding affinity, increased dipole moment, and π-stacking ability and are also stable bioisoteres for amides. Furthermore, 1,2,3-triazoles, in particular, are resistant to oxidative and reductive conditions as well as hydrolysis, making them exceptionally stable in biological systems compared to amide functionality.[26,27]

Molecular hybridization is a rational drug design strategy that involves combining distinct pharmacophoric subunits to create fewer undesirable side effects.[28] In the past decade, there have been extensive reports on the design and synthesis of various isatin-triazole hybrids, via molecular hybridization techniques, with diversified pharmacological effects[29] such as anticancer,[30] antitubercular,[31] anti-inflammatory properties,[32,33] etc. Considering the aforementioned findings and our growing interest toward the discovery of natural product-based new chemical entities, we have chosen the molecular hybridization approach to generate novel labdane appended 1,2,3-triazole tethered isatin hybrids with a broad spectrum of anti-inflammatory properties[32−36] (Figure 1).

The recent impressive breakthroughs in the field of "Click chemistry"[37,38] as well as the innumerable contribution of natural product-based triazoles[39] to chemical biology and drug design, have inspired us to construct a large library of novel triazolyl-isatin tethered labdanes, via a copper-catalyzed alkyne−azide cycloaddition (CuAAC) reaction.

Fresh rhizomes of *Curcuma amada* were procured from CTCRI, Thiruvananthapuram, Kerala, in January 2023. The abundant and medicinally relevant marker compound (*E*)-labda-8(17),12-diene-15,16-dial (**1**) was isolated from the chloroform extract by our standard protocol.[22,23] A series of labdane appended monotriazolyl-isatins as well as bis-triazolyl-isatins was synthesized using variable alkyl chain linkers, which acts as a spacer between the isatin core and the triazole moiety. Scheme 1 outlines the synthesis of monotriazolyl isatin appended labdane derivatives (**7a−7x**). One of the aldehyde

https://doi.org/10.1021/acsmedchemlett.4c00141
ACS Med. Chem. Lett. 2024, 15, 1260−1268

Scheme 1. Synthesis of Mono-triazolyl Isatin Appended Labdane Derivatives (7a−x)

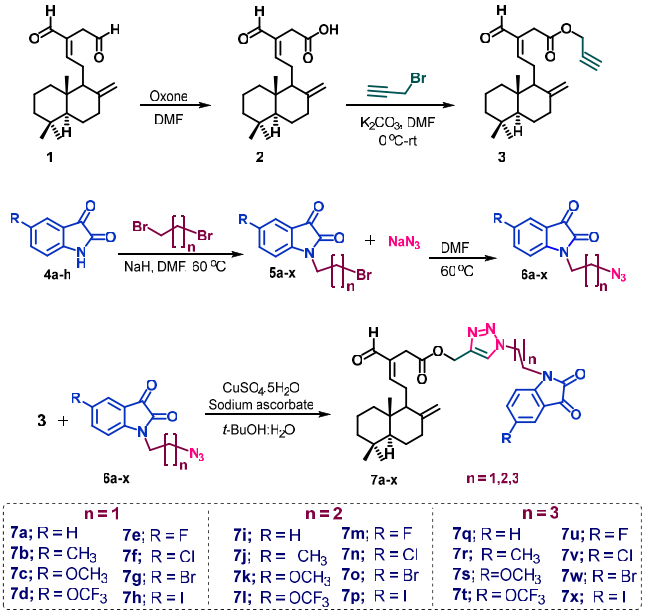

groups of labdane dialdehyde (**1**) was selectively oxidized by using oxone to give Zerumin A (**2**), which was further converted into its alkyne intermediate (**3**) by treating it with propargyl bromide. The structures of compounds **2** and **3** were confirmed by various spectroscopic and analytical data and comparison with the reported literature.[22,40,41] Subsequently, substituted isatins (**4**) were alkylated with dibromoalkanes (with carbon chain length ranging from two to four) to give *N*-alkylated isatins (**5**), which were further treated with sodium azide to synthesize isatin-azides (**6**) with variable alkyl chain length. The propargylated ester of labdane dialdehyde (**3**) was reacted with different isatin-azides (**6**) in the presence of $CuSO_4 \cdot 5H_2O$ and sodium ascorbate, via a highly regioselective CuAAC reaction, to generate exclusively the 1,4-disubstituted triazole appended labdane isatins (**7**), in good to excellent yields. Scheme 2 describes the synthesis of bis-triazolyl isatin appended labdanes (**10a−i**). Here, both aldehyde groups of labdane dialdehyde (**1**) were oxidized to furnish labdane diacid (**8**) by following the Pinnick oxidation protocol (Supporting Information (SI)), which was further converted into the dipropargylated ester derivative (**9**) in good yield. Compound **9** was used as the substrate for the subsequent cycloaddition reaction with selected isatin azides (**6a−c**, **6e−h**, **6k**, and **6n**), via a click reaction, to afford the desired bis-triazolyl isatin appended labdane hybrids (**10a−i**) in good to excellent yields. The structures of all the synthesized derivatives were confirmed by comprehensive analytical and spectroscopic techniques such as HRMS, ^{1}H NMR and ^{13}C NMR analysis (SI).

Scheme 2. Synthesis of Bis-triazolyl Isatin Appended Labdane Derivatives (10a−i)

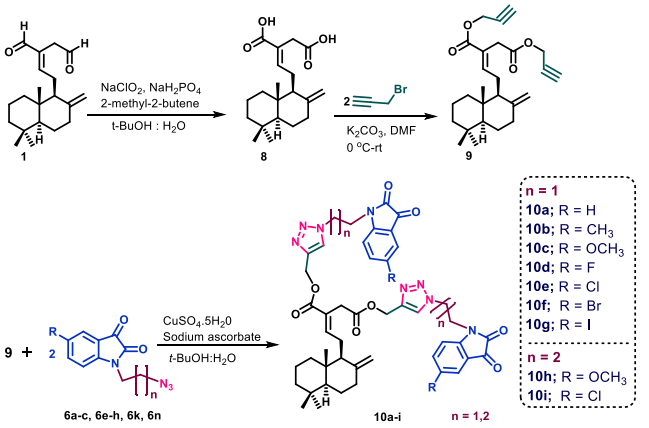

To avoid cytotoxic interference in the anti-inflammatory effect, the intrinsic cytotoxicity of all the target compounds (**1**, **8**, **7a−x**, **10a−i**) was determined by an MTT assay. None of the compounds showed significant cytotoxicity at test concentrations 1, 10, and 20 μM in RAW264.7 cell lines (Figure S1, Supporting Information). Thus, these concentrations were considered to be safe for cell-based anti-inflammatory experiments.

Elevated release of NO by activated macrophages leads to the initiation and progression of many inflammatory diseases.[42] Therefore, inhibition of NO production by the target compounds can be considered the preliminary approach to evaluate its anti-inflammatory properties. All the synthesized 33 triazolyl-isatin derivatives of labdane dialdehyde (**7** and **10**), as well as the parent compound (**1**) and its diacid derivative (**8**), were evaluated for its potential to inhibit the production of NO in LPS-stimulated RAW 264.7 cells at 1, 10, and 20 μM concentrations. Indomethacin (IND) was chosen as the positive control. Griess method[43] was adopted to determine the nitrite concentration, which is an indicator of NO production, after 24 h LPS stimulation in RAW 264.7 cells. As observed in Table S (SI), five compounds specifically **7a**, **7d**, **7m**, **7r**, and **10a**, significantly suppressed the production of NO better than the positive control indomethacin and the parent natural compound, labdane dialdehyde (**1**). Dialdehyde (**1**) exhibited better anti-inflammatory activity compared to that of its diacid derivative (**8**). Among all the tested groups, compound **7a** exhibited the most significant NO inhibitory effect with an IC_{50} value of 3.13 ± 0.03 μM and was much better than the positive control indomethacin (IC_{50} 7.31 ± 0.12).

A probable structural−activity relationship based on the effect of compounds on the NO inhibition was drawn. Among the monotriazolyl isatin labdane conjugates with alkyl chain length n = 1, compound **7a** incorporating a simple unsubstituted isatin core demonstrated a pronounced effect on NO inhibition. In contrast, the halogen substitutions at the fifth position of the isatin core (**7e−h**) resulted in reduced efficacy, among which a −Cl substituted derivative (**7f**) exhibited the least NO inhibition. The derivatives with $-OCF_3$, $-OCH_3$, and $-CH_3$ substitutions on isatin (**7b−d**) showed a moderate NO inhibitory effect. On increasing the alkyl chain length to n = 2, the NO inhibitory potential of the unsubstituted isatin derivative (**7i**) decreased. However, the −F substituted derivative **7m** displayed an improved NO inhibitory effect. Other halogenated derivatives (**7n**, **7o**, **7p**), displayed less inhibitory effect for NO. Derivatives **7j−l** with $-CH_3$, $-OCH_3$, and $-OCF_3$ substitutions showed a moderate effect on NO inhibition. Further increasing the alkyl chain length to n = 3, yet again decreased the activity of the unsubstituted isatin derivative (**7q**). Among the halogenated derivatives, −F and −I substituted derivatives (**7u** and **7x**) displayed a better NO inhibitory effect than −Br and −Cl

https://doi.org/10.1021/acsmedchemlett.4c00141
ACS Med. Chem. Lett. 2024, 15, 1260−1268

substituted derivatives (**7w**, **7v**). Moreover, increasing the chain length increased the NO inhibitory effect of the $-CH_3$ substituted conjugate (**7r**). Among the bis-triazolyl isatin conjugates of labdane, again, a simple unsubstituted isatin derivative (**10a**) demonstrated the highest NO inhibition potential. Overall, among all the mono/bis-triazolyl isatin appended labdane conjugates, analogues with a simple isatin core without any substitution and with the shortest alkyl chain length (**7a** and **10a**) were found to be more potent candidates of the series. Interestingly, there was no particular trend based on the type of substitution on the isatin ring or based on alkyl chain length alone. However, we assume a synergistic effect of the alkyl chain length along with the substitution on the isatin core to be responsible for the NO inhibitory effect.

TNF-α and IL-6 are the crucial cytokines which mediate different inflammatory mechanisms that impair organ integrity.[44] Therefore, we evaluated the potential of our 33 labdane derivatives to inhibit TNF-α and IL-6, using enzyme-linked immunosorbent assay (ELISA) at 20 μM concentration, in LPS induced RAW264.7 cells. As displayed in Figure 2, the

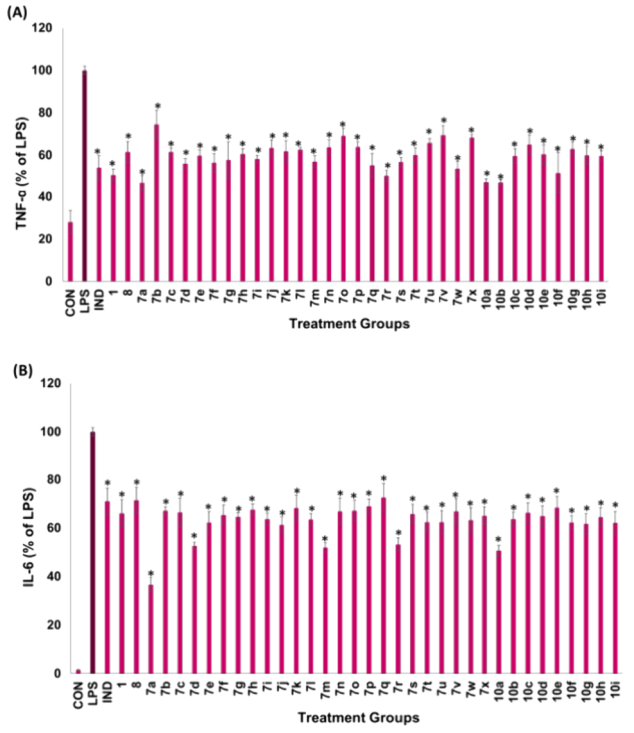

Figure 2. Effect of semisynthetic derivatives of labdane dialdehyde on LPS induced cytokine production (A) TNF-α and (B) IL-6 in RAW 264.7 cell lines. Cells were pretreated with 20 μM concentration of compounds for 1 h before treatment with 1 μg/mL LPS. After 24 h of incubation, cytokines production was determined by ELISA. Data are expressed as the mean ± SD (n = 3). *p < 0.001 vs LPS group.

levels of the cytokines increased markedly with LPS exposure, whereas there was a marked reduction in pretreatment with labdane dialdehyde (**1**) and all its semisynthetic derivatives. Dialdehyde (**1**) exhibited better inhibition on TNF-α and IL-6, compared to that of its diacid derivative (**8**). Moreover, in concordance to the NO inhibition results, the five semisynthetic derivatives, **7a**, **7d**, **7m**, **7r**, and **10a**, exhibited a more pronounced inhibitory effect on TNF-α and IL-6, compared to all the other test groups. Among five derivatives, **7a** displayed the strongest anti-inflammatory potential by inhibiting the production of pro-inflammatory cytokines in the cellular model and was much better than the positive control indomethacin (IND) and the parent natural compound (**1**). In addition, the other tested groups exhibited moderate activity.

Because compound **7a** consistently showed the strongest inhibition on NO production as well as the pro-inflammatory cytokines release, TNF-α and IL-6, in LPS-induced macrophages, it was screened for further evaluation of its anti-inflammatory potential.

The effect of different concentrations of **7a** (1, 5, and 10 μM) on the key pro-inflammatory cytokines, i.e., TNF-α and IL-6, were evaluated on LPS-induced macrophages along with indomethacin (20 μM) as the reference drug. **7a** decreased the levels of the pro-inflammatory cytokines in a concentration-dependent manner (Figure 3A,B) and was more potent than the positive control drug indomethacin. This again confirms **7a** to be a promising anti-inflammatory agent, and further investigations into its mechanism of action were much warranted.

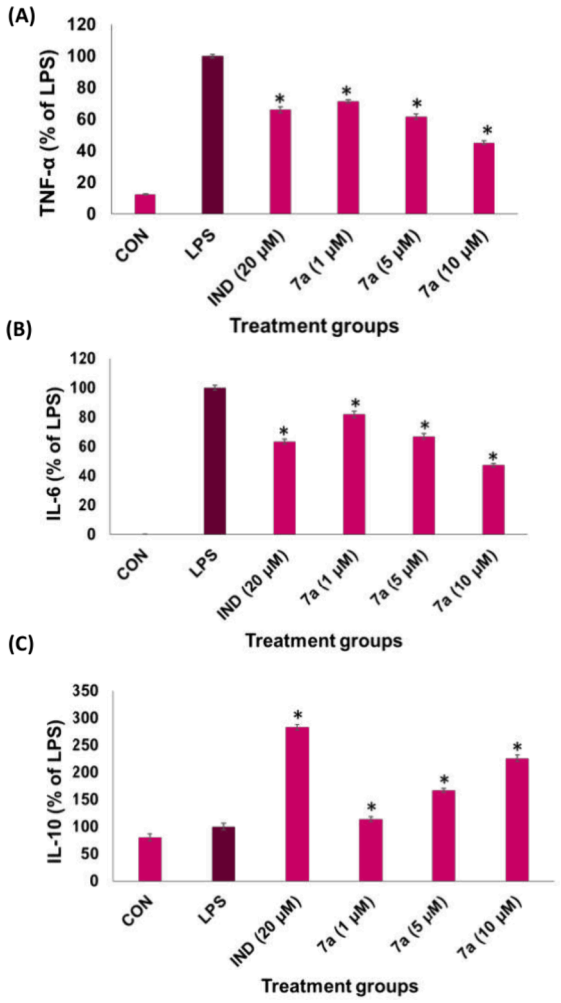

Figure 3. Effect of compound **7a** on LPS-induced cytokine production: (A) TNF-α (B) IL-6, and (C) IL-10, in RAW 264.7 cell lines. Cells were pretreated with various concentrations of compound **7a** (1, 5, and 10 μM) and indomethacin (20 μM) for 1 h before treatment with 1 μg/mL LPS. After 24 h of incubation, cytokines production was determined by ELISA. Data are expressed as the mean ± SD (n = 3). *p < 0.001 vs LPS group.

https://doi.org/10.1021/acsmedchemlett.4c00141
ACS Med. Chem. Lett. 2024, 15, 1260−1268

IL-10 is an anti-inflammatory cytokine which induces an immunosuppressive effect during prolonged inflammation, thus helping to prevent immunopathology and immune-mediated damage to the host.[10] Therefore, increased levels of IL-10 in LPS-stimulated macrophages can be considered as an indication of the host mechanism to prevent inflammation. Based on the preliminary screening results, the most active labdane derivative **7a** was evaluated for its effect on IL-10 levels at 1, 5, and 10 μM concentrations in LPS-stimulated RAW264.7 cells. Indomethacin was again used as the reference drug. As witnessed in the previous assays, **7a** significantly increased the levels of IL-10 in a dose-dependent manner in LPS-stimulated RAW264.7 cells and was comparable to indomethacin (Figure 3C). Because **7a** demonstrated significant anti-inflammatory properties by suppressing the pro-inflammatory mediators NO, TNF-α and IL-6 as well as by increasing the levels of the anti-inflammatory mediator 1L-10, which was at par with the positive control indomethacin, **7a** was selected for further detailed anti-inflammatory studies.

COX-2 and iNOS are the two most critical enzymes that are convoluted in inflammation. Dysregulated release or over-expression of iNOS leads to the genesis of sepsis, cancer, neurodegenerative diseases, pain, etc. NO, a major cell signaling molecule synthesized by iNOS, is the pro-inflammatory mediator responsible for amplifying immune activation and inflammatory responses.[42] COX-2 is an inducible pro-inflammatory enzyme, which plays a pivotal role in the biosynthesis of inflammatory prostaglandins such as PGE2 from arachidonic acid, leading to the progression of inflammatory diseases.[45] Therefore, to further explore the molecular mechanism of compound **7a**, its effect on the expression of COX-2 and iNOS enzymes was determined by Western blotting on LPS-stimulated RAW 264.7 cells (at 10 and 20 μM). Indomethacin (20 μM) was again employed as the positive control. As shown in Figure 4A, LPS stimulation significantly increased the COX-2 and iNOS protein levels significantly. However, there was a dose-dependent decrease in the expression of these enzymes when cotreated with **7a**. Even at 10 μM concentration, compound **7a** inhibited COX-2 in a similar way that indomethacin did at 20 μM. However, at 20 μM, compound **7a** inhibited COX-2 more effectively, with a potency greater than that of indomethacin at the same concentration (Figure 4B). The effect of compound **7a** on the iNOS protein was greater than that on COX-2. It is noteworthy that **7a** displayed a higher potency for iNOS suppression than indomethacin even at its lowest tested concentration of 10 μM. However, there was a significantly increased suppression in the iNOS level by **7a** at 20 μM, much better than indomethacin (Figure 4C). The results imply that **7a** exerts its anti-inflammatory activity via down-regulation of COX-2 and iNOS protein expression.

Extensive studies point to the fact that the activation of NF-κB, a ubiquitous cell transcription factor, is the key regulator in the expression of the pro-inflammatory cytokines such as TNF-α and IL-6 as well as the pro-inflammatory enzymes COX-2 and iNOS.[46−48] To establish the possible intracellular anti-inflammatory mechanism of compound **7a**, its effect on the NF-κB signaling pathway was examined by Western blotting and immunofluorescence analysis on LPS-stimulated RAW 264.7 cells. Indomethacin at 20 μM was chosen as the positive control. The activation of NF-κB can be attenuated by inhibiting its phosphorylation on p65, which was measured by Western blotting. As depicted in Figure 5, it is clear that the

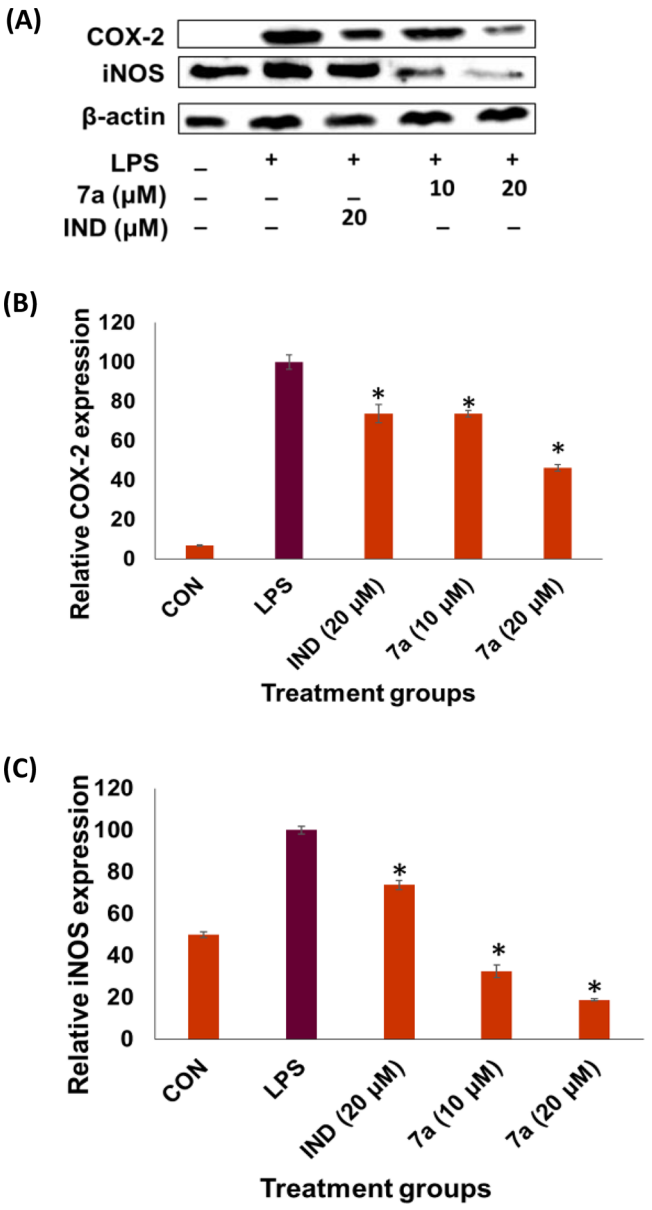

Figure 4. Effect of compound **7a** on COX-2 and iNOS expression in LPS-stimulated RAW264.7 cells. Cells were pretreated with different concentrations of compound **7a** (10 and 20 μM) and indomethacin (20 μM) for 1 h and then stimulated with or without 1 μg/mL of LPS for 24 h. COX-2 and iNOS expressions were detected by Western blotting (A, B, and C). *p < 0.001 vs LPS group.

LPS stimulation increased the levels of phosphorylated NF-κB p65 (p-NF-κB p65), while cotreatment with compound **7a** showed a significant reduction in phosphorylation, in a dose-dependent manner, with no effect on the NF-κB p65 protein levels. The compound **7a** showed inhibition of p-NF-κB p65 expression even at 10 μM concentration, like that of indomethacin tested at 20 μM. However, at 20 μM, **7a** demonstrated better inhibition on p-NF-κB p65 than indomethacin. To further verify the effect of **7a** on NF-κB pathway, the nuclear translocation of NF-κB was examined by immunofluorescence, in LPS-stimulated RAW 264.7 cells. As depicted in Figure 6, LPS stimulation significantly increased the distribution of NF-κB in the cell nuclei. However, cotreatment with **7a** markedly decreased the distribution of NF-κB inside the nuclei in a concentration-dependent manner.

https://doi.org/10.1021/acsmedchemlett.4c00141
ACS Med. Chem. Lett. 2024, 15, 1260−1268

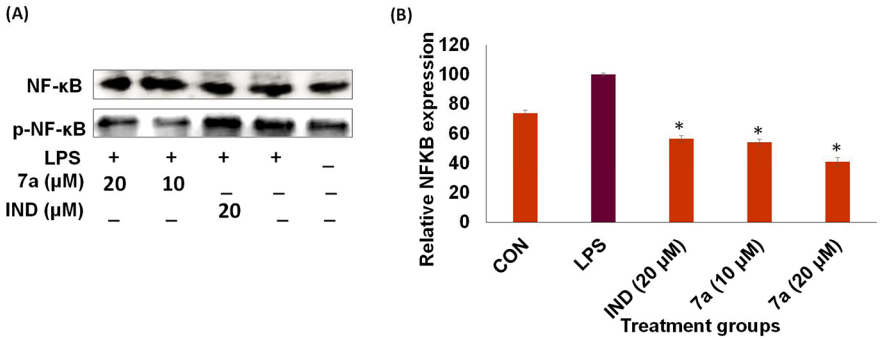

Figure 5. Effect of **7a** on NF-κB signaling pathway on LPS-stimulated RAW 264.7 cells. Cells were pretreated with different concentrations of compound **7a** (10 and 20 μM) and indomethacin (20 μM) for 1 h and then stimulated with or without 1 μg/mL of LPS for 24 h. NF-κB expression was detected by Western blotting (A and B). *$p < 0.001$ vs LPS group.

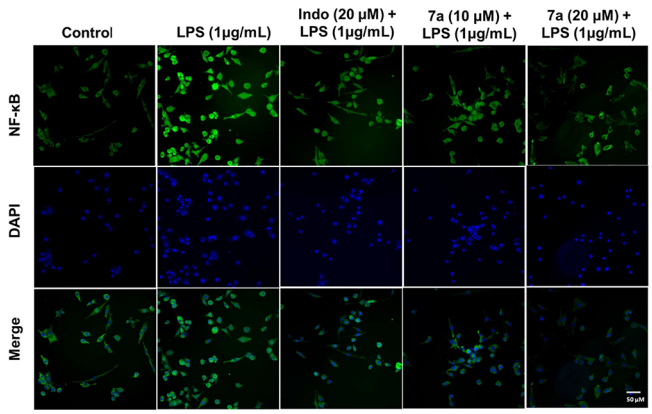

Figure 6. Immunofluorescence staining detected the distribution of NF-κB-p65 in both the nuclei and cytoplasm by some colocalization of receptors (p65, Alexa Fluor 488, green) with the nuclei (DAPI, blue). Images were captured by fluorescent microscope (OLYMPUS, Japan). Scale = 50 μm.

Our findings demonstrate that compound **7a** exerts an anti-inflammatory effect by downregulating the pro-inflammatory mediators via the suppression of the NF-κB signaling cascade. Figure 8, demonstrates the possible anti-inflammatory mechanism of lead analogue **7a**.

In silico molecular modeling studies of compound **7a** on NF-κB; To better understand the structural and molecular mode of physical interaction, relative binding affinity and possible mode of interaction of our synthesized drugs with the NF-κB (monomer), we performed structure-based virtual docking (arbitory docking was performed to over the docking bias) using HADDOCK 2.2 (https://haddock.science.uu.nl/) software, and results were analyzed using Pymol. Foremost, the structural analysis of NF-κB in apo form or in the absence of DNA has shown an available binding pocket of 2013 A2 (Figure. S3, SI), which could accommodate large compounds ideal for our synthesized compounds (**7a**–**x**, **10a**–**i**).

Based on our reference-free and unbiased docking, among the screened compounds **7a**–**x** and **10a**–**i**, we found that compound **7a** with the highest binding affinity of dG −8.89 ± 1.3 kcal/mol (Figure S2 and S3 of SI, and Figure 7C). As shown in Figure 7 the structural analysis of h NF-κB binding with the highest binding affinity of dG −8.89 ± 1.3 kcal/mol (SI, Figure S2 and S3 and Figure 7C). As shown in Figure 7 the structural analysis of h NF-κB binding with compound **7a**, we notice that compound **7a** could bind the DNA binding site or active site of h NF-κB in two different binding modes

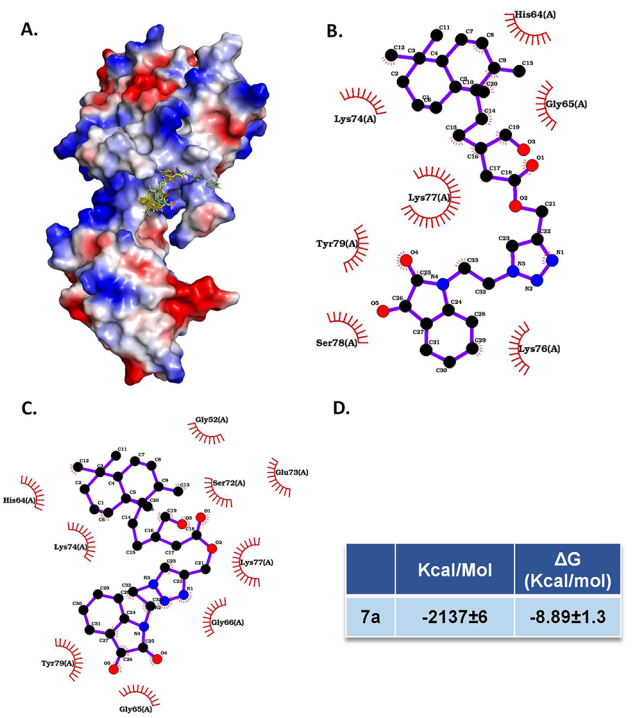

	Kcal/Mol	ΔG (Kcal/mol)
7a	-2137±6	-8.89±1.3

Figure 7. (A) Electrostatic potential representation of hNF-kB (monomer) with the bound **7a** compound in different conformations. (B,C) LigPlot view of compound **7a** bound to hNF-KB in two different conformations. Compounds are shown in sticks with numbering Cα and respective interacting amino acids in the hNF-kB are shown with the compound. (D) Table showing the relative binding kinetics of NFkB with our **7a** compound.

(Figure S3A–D) with a relatively similar binding affinity. LigPlot views show compound **7a** bound to h NF-κB in two distinct conformations, where some of the key interacting residues were remained conserved (SI, Figure 7D,E). This binding affinity was also consistent with our binding assay experiments. We next compared the binding orientation of bound compound **7a** with the apo-form and dsDNA bound (PDB 1NFK) form structure of h NF-κB (homodimer) via superimposing the structures to see how our compounds can intercalate or inhibit in the DNA recognition. As shown in SI, Figure S2(H), compound **7a** shares some of the dsDNA binding region making the dsDNA deallocate or inhibit the binding of dsDNA. Subsequently, we conducted simple simulation studies to examine how compound **7a** binding

https://doi.org/10.1021/acsmedchemlett.4c00141
ACS Med. Chem. Lett. 2024, 15, 1260−1268

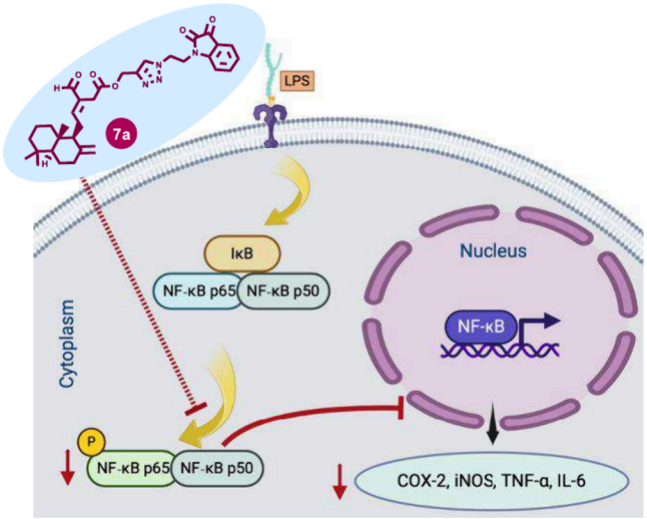

Figure 8. Proposed anti-inflammatory mechanism of compound **7a**.

influences dsDNA disassembly. As depicted in SI, Figure S2(I) and S3, our simulated model revealed the displacement of bound dsDNA from hNF-κB and the eventual inhibition of dsDNA binding in the presence of compound **7a**.

In conclusion, we have synthesized a series of 33 novel labdane conjugated mono/bis-triazolyl isatins in search of new anti-inflammatory agents. Among the synthesized derivatives, compound **7a** outperformed the commercial drug indomethacin and the parent natural compound (*E*)-labda-8(17),12-diene-15,16-dial (**1**) in terms of anti-inflammatory activity by inhibiting the release of pro-inflammatory mediators, NO, TNF-α, and IL-6, as well as by increasing the levels of the anti-inflammatory cytokine IL-10 in a dose-dependent manner, in LPS-induced RAW 264.7 cells. Mechanistic studies revealed that **7a** could downregulate the expression of COX-2 and iNOS by regulating the NF-κB signaling pathway. The results suggested that the lead compound **7a** could serve as a promising anti-inflammatory agent; however, advanced studies are being progressed in our laboratory.

■ ASSOCIATED CONTENT

Supporting Information

The Supporting Information is available free of charge at https://pubs.acs.org/doi/10.1021/acsmedchemlett.4c00141.

Experimental details of synthesis, characterization data, biological assays, and ^{1}H and ^{13}C NMR spectra of all the newly synthesized compounds (PDF)

■ AUTHOR INFORMATION

Corresponding Author

Sasidhar B. Somappa − *Chemical Sciences and Technology Division, CSIR−National Institute for Interdisciplinary Science and Technology (CSIR-NIIST), Thiruvananthapuram 695 019 Kerala, India; Academy of Scientific and Innovative Research (AcSIR), Ghaziabad 201 002, India;* orcid.org/0000-0003-1546-2083; Email: drsasidharbs@gmail.com, drsasidharbs@niist.res.in

Authors

Sangeetha Mohan − *Chemical Sciences and Technology Division, CSIR−National Institute for Interdisciplinary Science and Technology (CSIR-NIIST), Thiruvananthapuram 695 019 Kerala, India; Academy of Scientific and Innovative Research (AcSIR), Ghaziabad 201 002, India*

Lekshmy Krishnan − *Agro Processing and Technology Division, CSIR−National Institute for Interdisciplinary Science and Technology (CSIR-NIIST), Thiruvananthapuram 695 019 Kerala, India*

Nithya Madhusoodanan − *Chemical Sciences and Technology Division, CSIR−National Institute for Interdisciplinary Science and Technology (CSIR-NIIST), Thiruvananthapuram 695 019 Kerala, India; Academy of Scientific and Innovative Research (AcSIR), Ghaziabad 201 002, India*

Anjali Sobha − *Chemical Sciences and Technology Division, CSIR−National Institute for Interdisciplinary Science and Technology (CSIR-NIIST), Thiruvananthapuram 695 019 Kerala, India; Academy of Scientific and Innovative Research (AcSIR), Ghaziabad 201 002, India*

Alansheeja D. Babysulochana − *Chemical Sciences and Technology Division, CSIR−National Institute for Interdisciplinary Science and Technology (CSIR-NIIST), Thiruvananthapuram 695 019 Kerala, India; Department of Chemistry, Government Arts College, Thiruvananthapuram, Kerala 695 014, India*

Naveen Vankadari − *Department of Biochemistry and Pharmacology, Bio21 Institute, The University of Melbourne, Melbourne VIC 3052, Australia;* orcid.org/0000-0001-9363-080X

Jayamurthy Purushothaman − *Agro Processing and Technology Division, CSIR−National Institute for Interdisciplinary Science and Technology (CSIR-NIIST), Thiruvananthapuram 695 019 Kerala, India; Academy of Scientific and Innovative Research (AcSIR), Ghaziabad 201 002, India*

Complete contact information is available at: https://pubs.acs.org/10.1021/acsmedchemlett.4c00141

Author Contributions

The manuscript was written through the contributions of all authors.

Notes

The authors declare no competing financial interest.

■ ACKNOWLEDGMENTS

Financial support from the KSCSTE, Govt. of Kerala, via Kerala State Young Scientist Award Research Grant (KSCSTE/1096/2020-KSYSA-RG) and the CSIR Young Scientist Award Research Grant (HRDG/YSA-19/02/33(0045)/2020) from the CSIR, Government of India, New Delhi, is gratefully acknowledged. We also thank the DST-SERB, Government of India, New Delhi, India (grant no. EEQ/2021/000374), for the research grant. S.M. and L.K. thank UGC and DST for research fellowships.

■ ABBREVIATIONS USED

CON, control; COX-2, cyclooxygenase-2; ELISA, enzyme-linked immunosorbent assay; IND, indomethacin; IκB, inhibitor of NF-κB; IKK, IκB kinase; IL-6, interleukin-6; IL-10, interleukin-10; iNOS, inducible nitric oxide synthase; LPS, lipopolysaccharide; NF-κB, nuclear factor kappa B; NO, nitric oxide; PGE2, prostaglandin E2; p-NF-κB, phosphorylated nuclear factor kappa B; TNF-α, tumor necrosis factor-α

REFERENCES

(1) Zhao, H.; Wu, L.; Yan, G.; Chen, Y.; Zhou, M.; Wu, Y.; Li, Y. Inflammation and Tumor Progression: Signaling Pathways and Targeted Intervention. *Signal Transduct. Target. Ther.* **2021**, *6* (1), 263.

(2) Germolec, D. R.; Shipkowski, K. A.; Frawley, R. P.; Evans, E. Markers of Inflammation. *Methods Mol. Biol.* **2018**, *1803*, 57−79.

(3) Crusz, S. M.; Balkwill, F. R. Inflammation and Cancer: Advances and New Agents. *Nat. Rev. Clin. Oncol.* **2015**, *12* (10), 584−596.

(4) Kokiko-Cochran, O. N.; Godbout, J. P. The Inflammatory Continuum of Traumatic Brain Injury and Alzheimer's Disease. *Front. Immunol.* **2018**, *9*, 672.

(5) Kong, P.; Cui, Z. Y.; Huang, X. F.; Zhang, D. D.; Guo, R. J.; Han, M. Inflammation and Atherosclerosis: Signaling Pathways and Therapeutic Intervention. *Signal Transduct. Target. Ther.* **2022**, *7* (1), 131.

(6) Tsalamandris, S.; Antonopoulos, A. S.; Oikonomou, E.; Papamikroulis, G. A.; Vogiatzi, G.; Papaioannou, S.; Deftereos, S.; Tousoulis, D. The Role of Inflammation in Diabetes: Current Concepts and Future Perspectives. *Eur. Cardiol. Rev.* **2019**, *14* (1), 50−59.

(7) Cain, D. W.; Cidlowski, J. A. Immune Regulation by Glucocorticoids. *Nat. Rev. Immunol.* **2017**, *17* (4), 233−247.

(8) Pereira-Leite, C.; Nunes, C.; Jamal, S. K.; Cuccovia, I. M.; Reis, S. Nonsteroidal Anti-Inflammatory Therapy: A Journey Toward Safety. *Med. Res. Rev.* **2017**, *37* (4), 802−859.

(9) Chen, L.; Liu, Y.; Song, H.; Liu, Y.; Wang, L.; Wang, Q. Expanding Indole Diversity: Direct 1-Step Synthesis of 1,2-Fused Indoles and Spiroindolines from 2-Halo Anilines for Fast SAR Antiviral Elucidation against Tobacco Mosaic Virus (TMV). *Mol. Divers.* **2017**, *21* (1), 61−68.

(10) Howes, A.; Gabryšová, L.; O'Garra, A. Role of IL-10 and the IL-10 Receptor in Immune Responses. *Ref. Modul. Biomed. Sci.* **2014**, *1*, 1−11.

(11) Grigalunas, M.; Brakmann, S.; Waldmann, H. Chemical Evolution of Natural Product Structure. *J. Am. Chem. Soc.* **2022**, *144* (8), 3314−3329.

(12) Newman, D. J.; Cragg, G. M. Natural Products as Sources of New Drugs over the Nearly Four Decades from 01/1981 to 09/2019. *J. Nat. Prod.* **2020**, *83* (3), 770−803.

(13) Kumar, K.; Waldmann, H. Nature Inspired Small Molecules for Chemical Biology. *Isr. J. Chem.* **2019**, *59* (1), 41−51.

(14) Al-Qudah, T. S.; Abu Malloh, S.; Nawaz, A.; Adnan Ayub, M.; Nisar, S.; Idrees Jilani, M.; Said Al-Qudah, T. Mango Ginger (Curcuma Amada Roxb.): A Phytochemical Mini Review. *Ijcbs* **2017**, *11*, 51.

(15) Ewon, K.; Bhagya, A. S. A Review on Golden Species of Zingiberaceae Family around the World: Genus Curcuma. *African J. Agric. Res.* **2019**, *14* (9), 519−531.

(16) Mujumdar, A. M.; Naik, D. G.; Dandge, C. N.; Puntambekar, H. M. Antiinflammatory Activity of Curcuma Amada Roxb. In Albino Rats. *Indian J. Pharmacol.* **2000**, *32* (6), 375−377.

(17) Nagavekar, N.; Singhal, R. S. Supercritical Fluid Extraction of Curcuma Longa and Curcuma Amada Oleoresin: Optimization of Extraction Conditions, Extract Profiling, and Comparison of Bioactivities. *Ind. Crops Prod.* **2019**, *134* (March), 134−145.

(18) Tran, Q. T. N.; Wong, W. S. F.; Chai, C. L. L. Labdane Diterpenoids as Potential Anti-Inflammatory Agents. *Pharmacol. Res.* **2017**, *124*, 43−63.

(19) Lakshmi, S.; Renjitha, J.; Sasidhar, S. B.; Priya, S. Epoxyazadiradione Induced Apoptosis/Anoikis in Triple-Negative Breast Cancer Cells, MDA-MB-231, by Modulating Diverse Cellular Effects. *J. Biochem. Mol. Toxicol.* **2021**, *35* (6), 1−17.

(20) Shilpa, G.; Renjitha, J.; Saranga, R.; Sajin, F. K.; Nair, M. S.; Joy, B.; Sasidhar, B. S.; Priya, S. Epoxyazadiradione Purified from the Azadirachta Indica Seed Induced Mitochondrial Apoptosis and Inhibition of NFκB Nuclear Translocation in Human Cervical Cancer Cells. *Phyther. Res.* **2017**, *31* (12), 1892−1902.

(21) Anaga, N.; D, B.; Abraham, B.; Nisha, P.; Varughese, S.; Jayamurthy, P.; Somappa, S. B. Advanced Glycation End-Products (AGE) Trapping Agents: Design and Synthesis of Nature Inspired Indeno[2,1-c]Pyridinones. *Bioorg. Chem.* **2020**, *105*, 104375.

(22) Jalaja, R.; Leela, S. G.; Valmiki, P. K.; Salfeena, C. T. F.; Ashitha, K. T.; Krishna Rao, V. R. D.; Nair, M. S.; Gopalan, R. K.; Somappa, S. B. Discovery of Natural Product Derived Labdane Appended Triazoles as Potent Pancreatic Lipase Inhibitors. *ACS Med. Chem. Lett.* **2018**, *9* (7), 662−666.

(23) Jalaja, R.; Leela, S. G.; Mohan, S.; Nair, M. S.; Gopalan, R. K.; Somappa, S. B. Anti-Hyperlipidemic Potential of Natural Product-Based Labdane-Pyrroles via Inhibition of Cholesterol and Triglycerides Synthesis. *Bioorg. Chem.* **2021**, *108*, 104664.

(24) Cheke, R. S.; Patil, V. M.; Firke, S. D.; Ambhore, J. P.; Ansari, I. A.; Patel, H. M.; Shinde, S. D.; Pasupuleti, V. R.; Hassan, M. I.; Adnan, M.; Kadri, A.; Snoussi, M. Therapeutic Outcomes of Isatin and Its Derivatives against Multiple Diseases: Recent Developments in Drug Discovery. *Pharmaceuticals* **2022**, *15* (3), 272.

(25) Varun; Sonam; Kakkar, R. Isatin and Its Derivatives: A Survey of Recent Syntheses, Reactions, and Applications. *Medchemcomm* **2019**, *10* (3), 351−368.

(26) Angeli, A.; Supuran, C. T. Click Chemistry Approaches for Developing Carbonic Anhydrase Inhibitors and Their Applications. *J. Enzyme Inhib. Med. Chem.* **2023**, *38* (1), 2166503.

(27) da S. M. Forezi, L.; Lima, C. G. S.; Amaral, A. A. P.; Ferreira, P. G.; de Souza, M. C. B. V.; Cunha, A. C.; de C. da Silva, F.; Ferreira, V. F. Bioactive 1,2,3-Triazoles: An Account on Their Synthesis, Structural Diversity and Biological Applications. *Chem. Rec.* **2021**, *21*, 2782−2807.

(28) De Oliveira Pedrosa, M.; Marques Duarte Da Cruz, R.; De Oliveira Viana, J.; Olímpio De Moura, R.; Ishiki, H. M.; Filho, M. B.; Diniz, M. F. F. M.; Tullius Scotti, M.; Scotti, L.; Bezerra, F. J.; Junior, M. Hybrid Compounds as Direct Multitarget Ligands: A Review. *Curr. Top. Med. Chem.* **2017**, *17*, 1044−1079.

(29) Kumar, A.; Rohila, Y.; Kumar, V.; Lal, K. A Mini Review on Pharmacological Significance of Isatin-1,2,3-Triazole Hybrids. *Curr. Top. Med. Chem.* **2023**, *23* (10), 833−847.

(30) Ferraz de Paiva, R. E.; Guimarães Vieira, E. G.; Rodrigues da Silva, D.; Anchau Wegermann, C.; Costa Ferreira, A. M. Anticancer Compounds Based on Isatin-Derivatives: Strategies to Ameliorate Selectivity and Efficiency. *Front. Mol. Biosci.* **2021**, *7*, 627272.

(31) Gao, F.; Yang, H.; Lu, T.; Chen, Z.; Ma, L.; Xu, Z.; Schaffer, P.; Lu, G. Design, Synthesis and Anti-Mycobacterial Activity Evaluation of Benzofuran-Isatin Hybrids. *Eur. J. Med. Chem.* **2018**, *159*, 277−281.

(32) Boshra, A. N.; Abdu-Allah, H. H. M.; Mohammed, A. F.; Hayallah, A. M. *Click Chemistry Synthesis, Biological Evaluation and Docking Study of Some Novel 2′-Hydroxychalcone-Triazole Hybrids as Potent Anti-Inflammatory Agents*; Elsevier, 2020; Vol. *95*. .

(33) Sharma, P. K.; Balwani, S.; Mathur, D.; Malhotra, S.; Singh, B. K.; Prasad, A. K.; Len, C.; Van der Eycken, E. V.; Ghosh, B.; Richards, N. G. J.; Parmar, V. S. Synthesis and Anti-Inflammatory Activity Evaluation of Novel Triazolyl-Isatin Hybrids. *J. Enzyme Inhib. Med. Chem.* **2016**, *31* (6), 1520−1526.

(34) Kim, T. W.; Yong, Y.; Shin, S. Y.; Jung, H.; Park, K. H.; Lee, Y. H.; Lim, Y.; Jung, K. Y. Synthesis and Biological Evaluation of Phenyl-1H-1,2,3-Triazole Derivatives as Anti-Inflammatory Agents. *Bioorg. Chem.* **2015**, *59*, 1−11.

(35) Assali, M.; Abualhasan, M.; Sawaftah, H.; Hawash, M.; Mousa, A. Synthesis, Biological Activity, and Molecular Modeling Studies of Pyrazole and Triazole Derivatives as Selective COX-2 Inhibitors. *J. Chem.* **2020**, *2020*, 6393428.

(36) Lamie, P. F.; Ali, W. A. M.; Bazgier, V.; Rárová, L. Novel N-Substituted Indole Schiff Bases as Dual Inhibitors of Cyclooxygenase-2 and 5-Lipoxygenase Enzymes: Synthesis, Biological Activities in Vitro and Docking Study. *Eur. J. Med. Chem.* **2016**, *123*, 803−813.

(37) Thirumurugan, P.; Matosiuk, D.; Jozwiak, K. Click Chemistry for Drug Development and Diverse Chemical-Biology Applications. *Chem. Rev.* **2013**, *113*, 4905−4979.

https://doi.org/10.1021/acsmedchemlett.4c00141
ACS Med. Chem. Lett. 2024, 15, 1260−1268

(38) Bird, R. E.; Lemmel, S. A.; Yu, X.; Zhou, Q. A. Bioorthogonal Chemistry and Its Applications. *Bioconjugate Chem.* **2021**, *32* (12), 2457−2479.
(39) Zhang, X.; Zhang, S.; Zhao, S.; Wang, X.; Liu, B.; Xu, H. Click Chemistry in Natural Product Modification. *Front. Chem.* **2021**, *9*, 774977.
(40) Xu, H. X.; Dong, H.; Sim, K. Y. Labdane Diterpenes from Alpinia Zerumbet. *Phytochemistry* **1996**, *42*, 149−151.
(41) Singh, S.; Kumar, J. K.; Saikia, D.; Shanker, K.; Thakur, J. P.; Negi, A. S.; Banerjee, S. A Bioactive Labdane Diterpenoid from Curcuma Amada and Its Semisynthetic Analogues as Antitubercular Agents. *Eur. J. Med. Chem.* **2010**, *45* (9), 4379−4382.
(42) Cinelli, M. A.; Do, H. T.; Miley, G. P.; Silverman, R. B. Inducible Nitric Oxide Synthase: Regulation, Structure, and Inhibition. *Med. Res. Rev.* **2020**, *40* (1), 158−189.
(43) Bryan, N. S.; Grisham, M. B. Methods to Detect Nitric Oxide and Its Metabolites in Biological Samples. *Free Radic. Biol. Med.* **2007**, *43* (5), 645−657.
(44) Turner, M. D.; Nedjai, B.; Hurst, T.; Pennington, D. J. Cytokines and Chemokines: At the Crossroads of Cell Signalling and Inflammatory Disease. *Biochim. Biophys. Acta - Mol. Cell Res.* **2014**, *1843* (11), 2563−2582.
(45) Jin, K.; Qian, C.; Lin, J.; Liu, B. Cyclooxygenase-2-Prostaglandin E2 Pathway: A Key Player in Tumor-Associated Immune Cells. *Front. Oncol.* **2023**, *13*, 1099811.
(46) Liu, T.; Zhang, L.; Joo, D.; Sun, S. C. NF-KB Signaling in Inflammation. *Signal Transduct. Target. Ther.* **2017**, *2*, 17023.
(47) MedComm, 2021, Zhang - NF-κB Signaling in Inflammation and Cancer.pdf.
(48) Yu, H.; Lin, L.; Zhang, Z.; Zhang, H.; Hu, H. Targeting NF-KB Pathway for the Therapy of Diseases: Mechanism and Clinical Study. *Signal Transduct. Target. Ther.* **2020**, *5* (1), 209.

https://doi.org/10.1021/acsmedchemlett.4c00141
ACS Med. Chem. Lett. 2024, 15, 1260−1268